

NOAA Technical Memorandum NWS SR-112

1985 NWS SOUTHERN REGION QPF WORKSHOP

San Antonio, Texas  
January 28-30, 1985

Scientific Services Division  
Southern Region  
Fort Worth, Texas  
April 1985

UNITED STATES  
DEPARTMENT OF COMMERCE  
Malcolm Baldrige, Secretary

National Oceanic and  
Atmospheric Administration  
John V. Byrne, Administrator

National Weather  
Service  
Richard E. Hallgren, Director





## TABLE OF CONTENTS

Preface.....	i
Abstracts.....	ii-vi
Papers	
A Proposed Rainfall Classification System.....	1-7
Heavy Rain Associated with Northwest Flow Aloft.....	8-14
Climatology of Heavy Rain Producing Synoptic Patterns in North Florida.....	15-24
The Diurnal Distribution of Summertime Heavy Precipitation in the Eastern and Central United States.....	25-30
The Tulsa Flood of 27 May 1984. Part I: Synoptic and Mesoscale Overview.....	31-37
Synoptic Pattern Types Associated with Heavy Snowfall Events in Oklahoma.....	38-46
An Investigation of LFM Derived Fields.....	47-52
Omega Diagnostics as a Supplement to LFM/MOS Guidance in a Weekly-Forced Convective Situation.....	53-60
Operational Satellite Precipitation Estimates.....	61-66
Satellite Convective Cloud Categories Associated with Heavy Rainfall.....	67-74
West Gulf River Forecast Center Operations Using Satellite Estimations of Rainfall.....	75-81
Meteorology Associated with Water Resources.....	82-86
Computer Analyses of Hourly Recording Rain Gage Data for the U.S. Gulf Coast.....	87-89
Integrated Hydrometeorological Forecast System - Design and Tests.....	90-98
A Probabilistic Approach to Flash Flood Forecasting.....	99-106
QPF Workshop Panel Discussion.....	107-109



## PREFACE

This Technical Memorandum and the workshop it summarizes, marks a milestone in Quantitative Precipitation Forecasting (QPF). Although a national QPF program has existed for many years, field forecasters in the late 1970's recognized the need to develop localized QPF techniques to enhance national products and improve local forecast and warning services. The initial emphasis appears to have begun at WSFO Lubbock because of unique terrain, data void problems, and hydrological and meteorological responsibilities along the international river boundary, the Rio Grande. The success of the program and the relocation of some of the originators of the Lubbock QPF program opened opportunities to expand the effort. WSFO Station Managers and Southern Region Headquarters support permitted the first field coordinated QPF workshop in January 1982 in Fort Worth. Workshops in 1983 (again, Fort Worth), and 1984 (New Orleans) attested to the desire of field forecasters to share findings and techniques with their peers. Interest in QPF-related issues grew throughout the Region, and several other forecasters initiated case studies and synoptic climatologies in support of local QPF needs. Field participation at recent AMS Hydrometeorology Conferences blossomed as local efforts increased.

At the same time, NESDIS was continuing to refine its satellite rainfall estimation program, and ERL, under the leadership of Dr. Robert Maddox, was examining heavy rainfall events from a diagnostic meteorological perspective. Maddox' meso- and synoptic-scale evaluations provided important clues for understanding frequently occurring subtle events. WSFO Oklahoma City was also refining warning skills using RADAP, an interactive radar digitizing system, and compiling a synoptic climatology for heavy snow in Oklahoma.

River Forecast Centers (RFCs) were also involved in hydrometeorological activities. Early RFC efforts included the study and use of automatic digitized radar precipitation estimates into river forecasts, a forerunner of today's RADAP program. Later, when manually digitized radar products (MDR) became routinely available, Southern Region RFC's, again took the lead in utilizing the data in objective techniques supporting river forecasting. Today, the Fort Worth RFC is involved in developing methods of incorporating real-time satellite/radar rainfall estimates into river flood forecasting.

Collectively, these and other independent and related efforts brought together researchers and "practitioners", hydrologists and meteorologists, all interested in solving a common goal - the accurate and

timely prediction of heavy rain- and snow- fall, and ultimately the issuance of timely and site-specific flash flood watches and warnings, and river forecasts. But QPF goes beyond major storm events. The management of surface and groundwater resources, especially in the semi-arid southwest, demands more accurate forecasts of rainfall, including amount, distribution, and timing.

Those involved in QPF efforts will be the first to admit that what has been accomplished in a few years is only the tip of the iceberg. Success stories, though many, are still overwhelmed by numerous inaccurate predictions. Some miss the mark because of data limitations; others fail because forecasters lack the necessary training in numerical model or satellite interpretation, mesoscale analysis, or radar evaluation. Storm patterns and signatures, terrain, moisture variations and other factors vary significantly from one part of the country to another, further compounding a national solution. Our understanding of scale interactions and internal storm dynamics / thermodynamics is limited. Development of synoptic climatologies has been completed at only some offices; and the personnel resources needed to complete the initial effort, and tailor it seasonally and geographically within a state, are diminishing. Limited training efforts, focused at the NWSTC, have been successfully supplemented Region-wide by visiting lecturers from NESDIS, ERL, and NMC. Even so, training still falls short of what is needed.

Meteorologists from the NWS Eastern Region (ER), NMC, NWSH, ERL, NESDIS, TDL, and several representatives from the university community attended this workshop. The ER attendees plan to share workshop information throughout their region. Hopefully such participation will broaden the QPF effort within the NWS and between forecasters and university-based researchers across the nation.

All the more reason to share the efforts of dedicated NWS field employees and others in the satellite and research arms of NOAA. These papers, and others included in recent AMS Conference Preprints, set the stage for continued scientific advances in the QPF Program. I urge ALL Southern Region forecasters to consider contributing to the state of the science in QPF or in other forecast program/problem areas. I can personally attest that not only will the NWS benefit directly, but you, too, will become much richer for the effort and experience.

  
Ray E. Jensen

Director,  
NWS Southern Region



## ABSTRACTS

### A Proposed Rainfall Classification System

James D. Belville  
and  
Gary K. Grice

Classifying meteorological events is not a new concept. Methods for classifying both tornadoes and hurricanes were developed during the 1970s; however, during the past decade, floods and flash floods have become the major cause of weather related deaths (excluding lightning), and produce an average of two billion dollars in property losses annually. A rainfall classification system is needed. A system is proposed (using data from 376 storms) which classifies rainfall events based on maximum storm rainfall, average storm rainfall, area covered and duration. The latter three factors are combined into one element called the Heavy Rain Factor. A few notable heavy rain events are presented in light of this proposed system.

### Heavy Rains Associated with Northwest Flow Aloft

Bill Reed

Summer season heavy rain events in North Texas occur under three basic synoptic settings: tropical disturbances, split in the subtropical high, and northwest flow aloft. This study investigates heavy rains with northwest flow aloft. Nine excessive rainfall events occurring with 500 mb winds from a northwest direction are examined. Temporal and spatial features at standard levels are compared for similarities and differences. Several important similarities were noted. In seven of the nine cases, onset of heavy rain occurred nocturnally. In six of the events, heavy rain occurred east of a subsynoptic surface low/wave on a weak frontal boundary. This subsynoptic feature appeared to be an important trigger mechanism as no discernable upper level dynamics were present. One of the nine cases is presented in detail to illustrate some of the results.

### Climatology of Heavy Rain Producing Synoptic Patterns in North Florida

Raymond E. Biedinger

Heavy rainfall is one of the most important forecast parameters that forecasters are challenged to predict because of the disruptive nature and life threatening characteristics of this phenomenon. The occurrence of heavy rains in north Florida is not uncommon and can occur in any month of the year. While this is true, it is the winter rainfall that usually has the most adverse effect on north Florida, aside from the tropical system related heavy rains. River and small stream flooding is the main property threatening and sometimes life threatening result of the heavy rains. Generally, December through April is the

period when this occurs. The winter heavy rains are caused primarily by large scale or synoptic scale weather systems. Recognition by forecasters of the synoptic patterns that have the potential of producing heavy rain in the winter is the first step in making a heavy rain forecast. That is the intent of this paper--to provide forecasters with a climatology of the types of synoptic patterns that have produced the heavy rains in the past and are likely to be responsible for those in the future. The two most widely used levels, surface and 500 mb, were chosen for this study.

The Tulsa Flood of 27 May 1984. Part I:  
Synoptic and Mesoscale Overview

Michael L. Branick

Synoptic and mesoscale conditions accompanying excessive rainfall and disastrous flash flooding in Tulsa, Oklahoma, on 27 May 1984 are presented and discussed. The heavy rains occurred in a region of strong low-level warm advection north of a quasistationary surface front. The analyses suggest that the event was focused by complex scale interactions between the subsynoptic environment and intense convection that was in progress prior to the flooding in Tulsa. Specifically, the subsynoptic flow was modified by the convection resulting in enhanced upper-tropospheric divergence, as well as subsynoptic-scale height falls and ageostrophic flow at middle levels over northeastern Oklahoma. A mesoscale surface trough, arising from the combined effects of convective modification and low-level warm advection, enhanced surface convergence over northeastern Oklahoma during the period of heaviest rainfall.

Synoptic Pattern Types Associated with Heavy  
Snowfall Events in Oklahoma

Michael L. Branick

A climatological study of 137 heavy snowfall events in Oklahoma during the period 1951-1984 has been completed. Seasonal variations indicate a slight preference for late winter versus early winter, with greatest frequencies in February and March. Geographic variations are strongly governed by orography; greatest frequencies are found in high-elevation areas where a prevailing northeasterly surface wind produces upslope flow. Synoptic flow patterns were identified for 79 of the events. These events were classified into 6 pattern types based on the prevailing 500 mb longwave pattern. Subsynoptic characteristics of the surface and 500 mb flow patterns associated with each type are presented and discussed. The results, when used in conjunction with operational objective forecast output, are intended to improve the forecaster's ability to detect and forecast an impending heavy snow event.

An Analysis of LFM Derived Fields During the  
Oklahoma Floods of May 27-28, 1984

Gifford F. Ely, Jr.

Output from gridded LFM forecast fields were examined for the heavy rain event in Oklahoma on May 27 and 28, 1984. These fields provide additional information of LFM output than is traditionally available to the WSFO field forecaster. Since the LFM provided reasonably good guidance for the May 27 flood event in Oklahoma, an examination of these fields could be indicative of potential utility. Other cases are also presented.

Omega Diagnostics as a Supplement to LFM/MOS Guidance  
in a Weakly-Forced Convective Situation,  
Their Accuracy, and Application to  
LFM Forecast Height Fields

Stanley L. Barnes

Using reported height data at mandatory pressure levels, a version of Hoskins' Q-vector diagnosis is computed for two layers, producing contoured patterns of vertical motion and other diagnostics at two levels. The scheme is applied to a severe convective episode (25-26 June 1982) in eastern Colorado that resulted in the development of a mesoscale convective complex. Convection developed in association with a polar air mass overlying the high plains and a weak short wave in the westerlies. LFM/MOS and quantitative precipitation guidance all indicated Wyoming as the most threatened area, whereas the actual convection was most intense in Colorado, and the resulting convective system propagated southeastward into the Texas panhandle. While the computed omega patterns are qualitative and reflect only the geostrophic forcing that is ongoing at observation time, when viewed in light of concurrent information such as satellite images and surface maps they suggest how NMC and NSSFC guidance could have been modified in this case.

Temporal changes in omega diagnostics computed from 3-hourly soundings (AVE-SESAME V, 20 May 1979) indicate the ageostrophic adjustment patterns changed relatively slowly over a period of 6 to 12 h, thus lending some justification to their use as a forecasting tool.

The accuracy of the diagnostic computations is investigated for hypothetical analytically determined height fields. Provided one has observations outside the domain of the computation grid, the accuracy of the diagnostic results is acceptable with the exception of gridpoints just interior to the grid boundary. If the grid domain is larger than the area for which observations are available, as in the tested example, the area of useful results is further limited.

Application of the diagnostic scheme to LFM predicted height fields yields vertical motion information that, for the 1982 case studied, is more meaningful than the LFM predicted vertical motion fields.

Further experience and development are necessary to determine the scheme's value under a variety of synoptic conditions. However, the fact that it currently runs on a microcomputer in only 13 min indicates that it may have potential as a real-time operational diagnostic aid for short range forecasting.

### Operational Satellite Precipitation Estimates

Charles Kadin  
and  
Dane Clark

Precipitation estimates are routinely produced for excessive rainfall by the Synoptic Analysis Branch of NESDIS. These estimates are disseminated to NWS forecasters using the AFOS PIL header SPE. A new interactive computer system, referred to as IFFA, has recently completed one year of service as the primary tool used to calculate the satellite derived precipitation estimates. This man-machine interactive system was used in more than 6000 hours of estimates since the summer of 1983. Recent verification studies have substantiated the reliability of calculated estimates as a primary source of guidance for flash flood watches and warnings, especially during night-time hours when other sources of rainfall data are at a minimum.

### Satellite Convective Cloud Categories Associated with Heavy Rainfall

Roderick A. Scofield

Seven convective categories were developed based on satellite, radar, rainfall characteristics and surface and upper air data. The categories include: I<sub>A</sub> - Synoptic Scale Tropical, I<sub>B</sub> - Mesoscale Convective Complex, II<sub>A</sub> - Large Scale Wedge, II<sub>B</sub> - Squall Line, III - Single Clustered, IV<sub>A</sub> - Multi-clustered Circular, IV<sub>B</sub> - Multi-Clustered Linear, V - Synoptic Scale Cyclonic Circulation, VI - Overrunning and VII - Regenerative. Satellite meteorologists do their best work in estimating rainfall from categories I and II; their most difficult work is with categories III, VI, and VII. Flash floods occurred most frequently from multi-clustered thunderstorms with warm tops (Category IV).

### West Gulf River Forecast Center Operations Using Satellite Estimations of Rainfall

David G. Morris

The West Gulf River Forecast Center (WGRFC) utilizes a dense grid (subset of the LFM) over the State of Texas to position rainfall reports or remote sensed point estimates. The grid is roughly 6 miles by 6 miles for a total of 10,000 intersections (grid points) across the state. In cooperation with NESDIS, 360/195

software was written to allow near real-time 3 hourly sums of satellite estimated precipitation to be written into a WGRFC hydrologic precipitation file. The storm precipitation data may be used for river forecasting purposes. This report illustrates the operational procedures employed at the RFC when utilizing satellite derived data, and describes future development work required to make better use of such information.

#### Meteorology Associated with Water Resources

Jimmy D. Ward

Available useable water resources will likely be one of the major topics in society's planning over the next few decades. The National Weather Service will be intimately involved in water management. Involvement will range from long range seasonal outlooks to short-term flood warnings. From situations of water shortages such as widespread drought to situations of too much water such as heavy rain events, the National Weather Service must have the skills to advise water supply managers or alert local authorities of flooding.

#### Computer Analyses of Hourly Recording Rain Gage Data for the U.S. Gulf Coast

Jerry R. Rogers

Seven recording rain gages in-and-around Harris County, Texas measured hourly rainfall data which was acquired on computer tapes from the U.S. National Climatic Center, Asheville, North Carolina. Statistical analyses and intensity-frequency-duration curves for 15-100 year periods are developed for the Harris County Flood Control District. Harris County is a flat, coastal region near the Gulf of Mexico and is noted for high intensity rainfalls from weather fronts, tropical storms, and hurricanes. Tropical Storm Claudette in July, 1979 produced the record 24-hour U.S. rainfall near Alvin, Texas.

#### Integrated Hydrometeorological Forecast System--Design and Tests

Konstantine P. Georgakakos  
and  
Michael D. Hudlow

The Integrated Hydrometeorological Forecast System (IHFS) is based on the idea of coupling meteorological and hydrological models for the purpose of real-time flash-flood forecasting. Its mathematical form consists of a one-dimensional precipitation model coupled to a lumped drainage response model. Real-time updating procedures monitor the errors in the model forecasts and correct the model state-variables in real-time. The system is suitable for use in mini- and micro-computers and is transportable. System performance is examined in an operational environment.



## A PROPOSED RAINFALL CLASSIFICATION SYSTEM

James D. Belville  
Office of Meteorology  
NWSH  
Silver Spring, Maryland

Gary K. Grice  
National Weather Service  
Forecast Office  
San Antonio, Texas

### 1. INTRODUCTION

Classifying meteorological events is not a new concept. Methods for classifying both tornadoes and hurricanes have been developed during the past 20 years; however, during the past decade, floods and flash floods have become the major cause of weather related deaths (excluding lightning), and produce an average of two billion dollars in property losses annually. A rainfall classification system is needed (especially for heavy rainfall events) in order to compare different storms (by the operational community) and as a research tool (for researching heavy rains).

Operationally, a classification system could be used for the comparison of forecast heavy rainfall events (or those in progress) to past events within similar geographical areas. Meteorologists and hydrologists could relate the expected rainfall to the flood potential in qualitative, and in some cases, quantitative terms. This would help forecasters word statements and warnings to correspond with the event.

Many local studies relate intensities of heavy rainfall events to maximum storm rainfall. However, total depth, area covered, and storm duration are also important parameters in describing an event. A classification scheme using these parameters would be helpful in verifying quantitative precipitation forecasts (QPF) as well as flash flood watches and warnings. Comparison of heavy rain (HR) events produced by different scale features would be useful for research purposes (i.e., meso-alpha versus meso-beta forcing mechanisms). Lastly, a quantitative

description of HR events would be valuable for historical record keeping purposes such as inclusion in the NOAA publication STORM DATA.

### 2. OBJECTIVES

The primary objective in developing the rainfall classification system was to describe rainfall events in quantitative terms yet be simple to apply. The scheme should also relate the rainfall to subsequent flooding. This can be difficult since flooding is also dependent on a large number of variables such as antecedent soil moisture conditions, topography, soil type, vegetation, etc. The proposed system relates rainfall to flooding in only general terms.

### 3. DATA AND ANALYSIS PROCEDURES

A total of 376 storms were used in developing the proposed rainfall classification system. Much of the rainfall data were in the form of depth-area-duration studies provided by the U.S. Corps of Engineers and the National Weather Service. Many of the events contained in these studies occurred in the late 1800s to the mid 1950s with a significant reduction of cases from the mid 1950s to the present. An example of the data is shown in Fig. 1.

Geographically, the 376 storms occurred over most of the Country (Fig. 2). Although most of the events were associated with mid-latitude cold core systems, 30 cases occurred with tropical cyclones.

Rainfall characteristics varied greatly within the storm sample. Table 1 shows the ranges.

TABLE 1

- 1. Average depth 0.7 in - 15.5 in
- 2. Areal coverage 8 mi<sup>2</sup> - 306,000 mi<sup>2</sup>
- 3. Duration 2 h - 126h
- 4. Maximum 1.5 in - 45.0 in

4. DEVELOPMENT OF THE PROPOSED CLASSIFICATION SYSTEM

A large number of parameters exists which can be used to describe a rainfall event. Table 2 lists a few of the more common possibilities.

TABLE 2

- 1. Maximum 24 h rainfall
- 2. Maximum storm total rainfall
- 3. Average depth of rainfall
- 4. Areal coverage
- 5. Duration
- 6. Volume of rainfall
- 7. Latent heat energy as a function of measured rainfall

Selected parameters should not only describe the rainfall event as completely as possible but also be simple to calculate.

One of the most common methods of displaying storm rainfall is through isohyetal analyses. From an isohyetal map the areal coverage and average storm rainfall is available. The NWS River Forecast Centers (RFC) receive daily rainfall reports which are used to produce computerized rainfall charts. By using one of several methods, the average rainfall (in) can be computed from an RFC produced isohyetal analysis. Multiplying the average rainfall by the area (mi<sup>2</sup>) covered by the storm will result in the volume (mi<sup>2</sup>-in) of water produced by the storm. Rain volume can also be expressed in other units such as m<sup>3</sup>, acre-ft, degrees<sup>2</sup>-in, and mi<sup>2</sup>-in. Using the volume as a portion of the classification system is operationally significant since the QPF is essentially a forecast of rainfall volume.

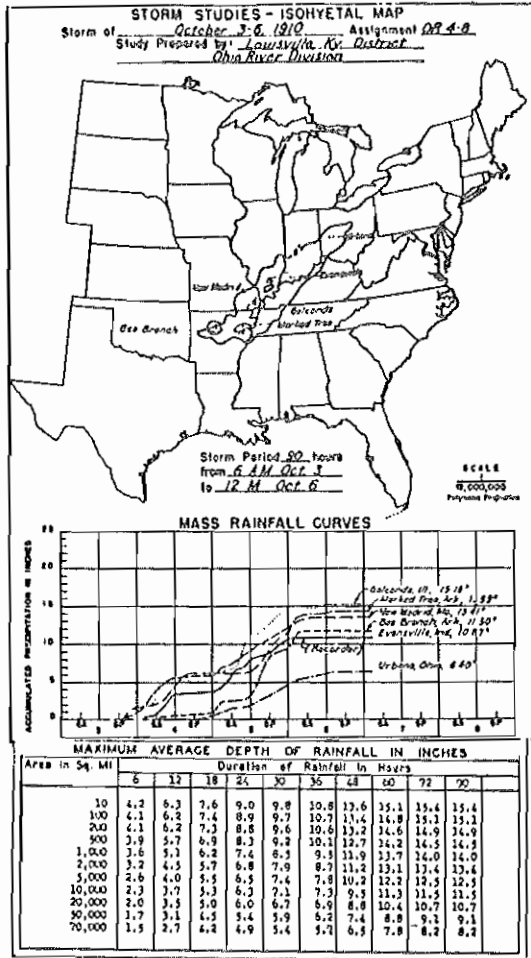


Figure 1. Example of data used in the study.

The vast majority of events were associated with 24 h rainfall amounts of 5 in or greater although cases with lesser amounts were also available. Events used in this study were defined by the following spatial and temporal guidelines:

- 1. The spatial extent of an event was defined as the area enclosed within the 2 in isohyets (see Fig. 3a).
- 2. The temporal extent of an event was the time period from the beginning to end of the storm rainfall as determined from mass diagrams. Two periods of rainfall over the same area but separated by more than 24 h were considered separate events (see Fig. 3b).

Rainfall volume alone does not accurately describe a rainfall event and is not directly related to the character of the resulting flood. Rainfall duration also plays a large role in the runoff rate (Fig. 4).

To accommodate the time factor the volume of rainfall was divided by the time (h) during which the rain fell. This time was calculated using mass rainfall analyses of data from recording rain gauges in the storm area (see Fig. 3b). The resultant units of the depth-area (volume)-duration factor are mi<sup>2</sup>-in per hour and represent the average volumetric rainfall rate of a rainfall event. Dividing by the duration normalizes the events so that a direct comparison is available. In this classification system this term (depth-area-duration) is labeled the heavy rain factor (HR factor). Numerically, the HR factor

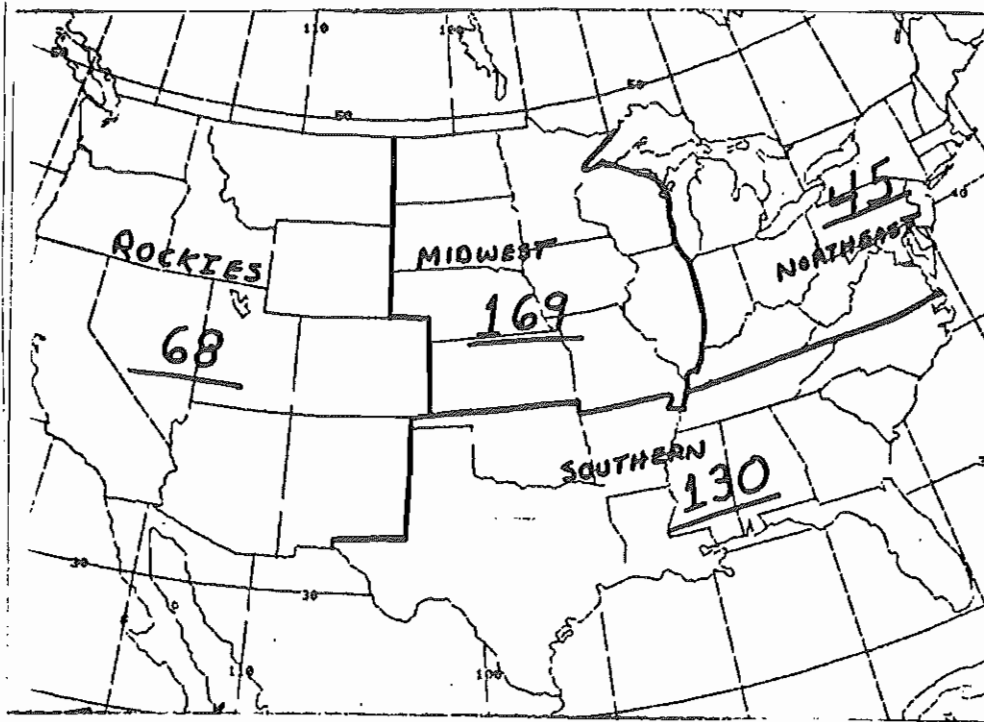


Figure 2. Geographic distribution of rainfall events.

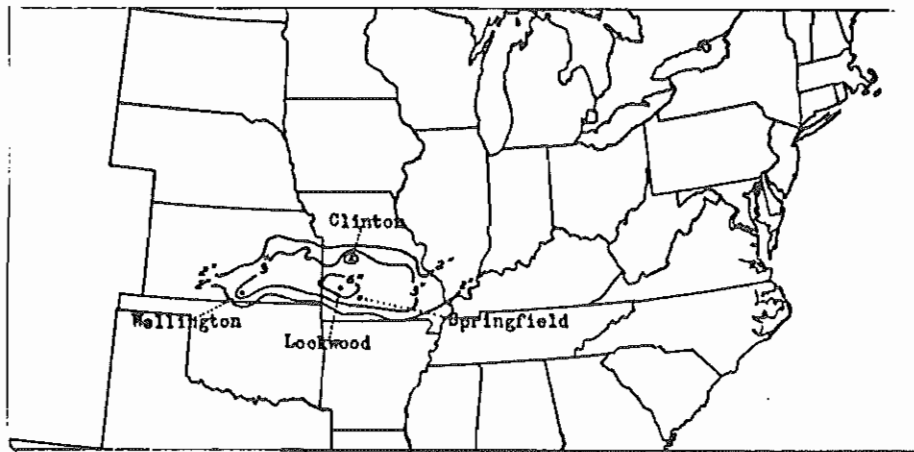


Figure 3a. Example of isohyetal analysis used in the study for determining the spatial extent of an event.

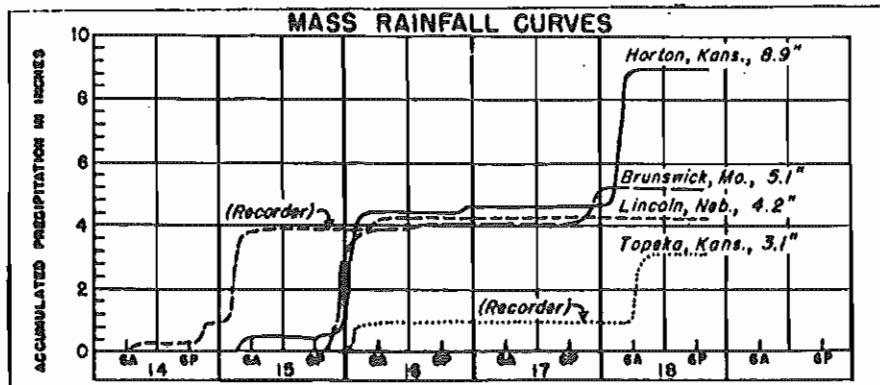


Figure 3b. Example of mass rainfall curves of selected stations for a heavy rain event.

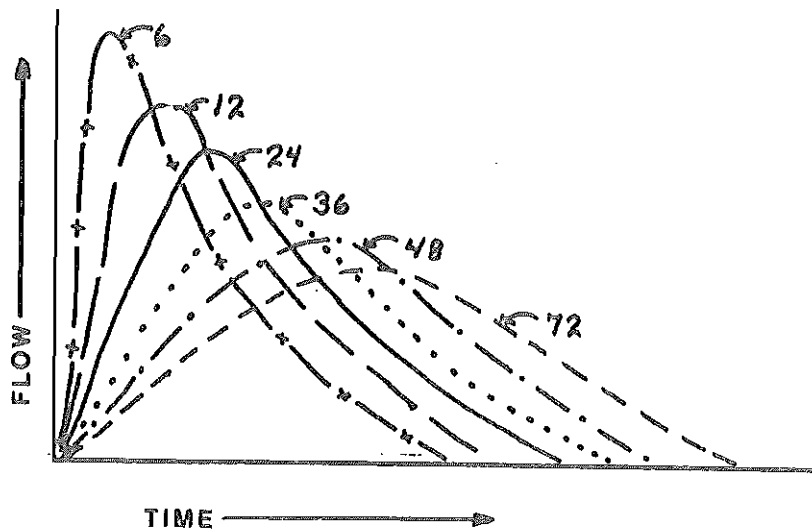


Figure 4. Hydrographs for storm durations of 6 to 72 h. Peak flows are higher for shorter durations although the runoff volumes for the different time periods are equal.

ranged from under 100 to slightly above 12,000 in the 376 study cases.

Unfortunately, the HR factor was not related to maximum storm rainfall of the 376 events (correlation coefficient of  $-0.25$ ). This is consistent with recent studies which indicate storms with high maximum storm rainfall are generally quite small with low rainfall volumes.

To adequately describe a rainfall event, maximum storm rainfall must be included. A two digit system can be utilized with both maximum storm rainfall and HR factor although this approach is not inclusive.

##### 5. DEVELOPING CATEGORIES

A set of categories could have been developed for both the HR factor and maximum storm rainfall using the entire sample of storms. However, there were many types of meteorological phenomena contained within the sample. These ranged from individual thunderstorms to situations where multiple baroclinic waves produced an event. In fact, a large scale event consists of several smaller scale events. Figure 5 shows the isohyetal pattern for a large rainfall event of 72 h duration. Yet, this event was comprised of several smaller meso-scale events each of which occurred at a different time. In order to meet the objective of having a flexible classification system; a categorical system must be able to handle this type of situation.

Considering the various scales of rainfall events is important in a rainfall classification system. Figures 6 and 7 show the spatial and temporal relationships of the different rainfall producing phenomena.

The initial separation of the rainfall events into groups for classification purposes was by stratifying the events with respect to duration (Table 3)

TABLE 3

Group	Duration (h)
A	0 - 12
B	12 - 36
C	36 - 60
D	60 - 84
E	>84

Next, the events in the sample were put into one of the five groups. Then categories were determined for each group by using the frequency distribution of HR factor and maximum rainfall within the group. Tables 4 - 8 show the categories for each group.

##### 6. USING THE PROPOSED CLASSIFICATION SYSTEM

In this section a few significant rainfall events are classified in order to show how the use of this system is envisioned.

New Orleans urban flood event June 30, 1984  
 Duration - 2 h, Max Rainfall - 3.5 in  
 HR Factor 100 mi<sup>2</sup> - in/h, **A,3,3**

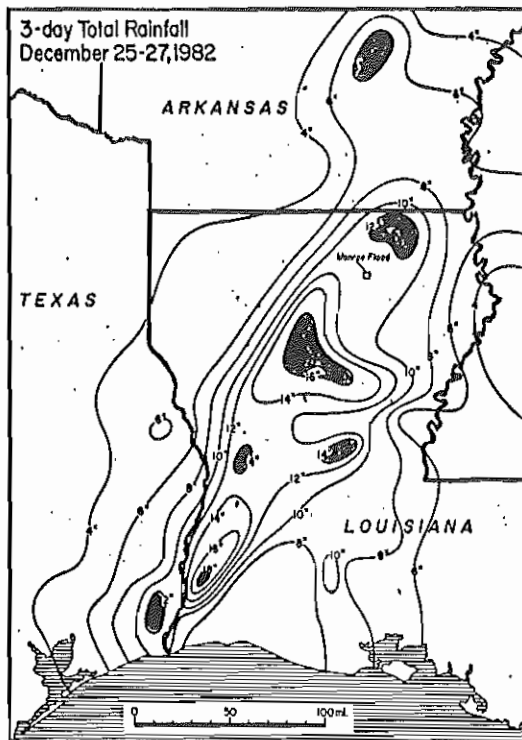


Figure 5. Isohyetal pattern for a prolonged heavy rain event.

MESO $\gamma$	MESO $\beta$	MESO $\alpha$
2 - 20 km	20 - 200 km	200 - 2000 km
TSTM C.A.T. URBAN EFFECTS	SQUALL LINE CLOUD CLUSTERS MOUNTAIN WAVE	FRONT HURRICANE MCC
MACRO $\beta$	MACRO $\alpha$	
2000 - 10,000 km	> 10,000 km	
BAROCLINIC WAVE	STANDING WAVE ULTRA LONG WAVE	

Figure 6. Part of scale definitions and different meteorological phenomena with characteristic horizontal spatial scales (after Orlanski, 1975).

Palo Duro Canyon flash flood May 26, 1978  
Duration - 2 h, Max Rainfall - 11.5 in  
HR Factor 450 mi<sup>2</sup> - in/h, A,5,3

Albany, Texas flash flood August, 1978  
Duration - 18 h, Max Rainfall - 35 in  
HR Factor 1500 mi<sup>2</sup> - in/h, B,7,3

South Texas flood September, 1967  
Duration - 96 h, Max Rainfall - 37.5 in  
HR Factor - 12,000 mi<sup>2</sup> - in/h, E,6,6

## 7. USE OF THE CLASSIFICATION SYSTEM

A rainfall classification system benefits both the operational and research arenas. Presently, a classification system does not exist for grouping rainfall events for a study. Consider the flash flood types described by Maddox *et al.* (1979). The following questions cannot be answered without a quantitative way of grouping storms.

1. Which of the flash flood types will most likely produce the most significant heavy rain event?
2. Are the rainfall characteristics the same or different for each type?
3. Do the rainfall patterns with the different types vary across the Country?

A rainfall classification system would assist in answering these and other questions.

This proposed system is one of several which can be used to classify rainfall events. Acceptance of this particular scheme is secondary. Of primary importance is that the meteorological community adopt some quantitative method of stratifying rainfall events. Within the past five years considerable progress has been made towards understanding heavy rain events; however, to advance significantly farther, some method must be accepted for classifying rainfall events.

## REFERENCES

- Maddox, R.A., C.F. Chappell, and L.R. Hoxit, 1979: Synoptic and meso-alpha scale aspects of flash flood events. *Bull. Amer. Soc.*, **60**, 115-123.
- Orlanski, I., 1975: A rational subdivision of scales for atmospheric processes. *Bull. Amer. Meteor. Soc.*, **56**, 527-530.

0 to 12	12 to 36	36 to 60	60 to 84	greater than 84
meso $\gamma$ meso $\beta$	meso $\alpha$ meso $\beta$	meso $\alpha$ synoptic scale	synoptic scale	long waves
TSTMS TSTM CLUSTERS SQUALL LINE SEA BREEZE	MCC's TROPICAL STORMS FRONTAL RAIN	BAROCLINIC WAVE TROPICAL STORMS	BAROCLINIC WAVE	MULTIPLE BAROCLINIC WAVES

Figure 7. Part of scale definitions and different meteorological phenomena with characteristic temporal scales (after Orlandi, 1975).

TABLE 4

STORM DURATION

0 to 12 HOURS

CAT.	MAX RAINFALL (INCHES)	CAT.	HR FACTOR (MI <sup>2</sup> - INCHES/HOUR)
1	0 - 1	1	0 - 10
2	1 - 3	2	10 - 100
3	3 - 5	3	100 - 500
4	5 - 10	4	500 - 1000
5	10 - 15	5	1000 - 3000
6	$\geq$ 15	6	3000 - 5000
		7	$\geq$ 5000

TABLE 5

STORM DURATION

12 to 36 hours

CAT.	MAX RAINFALL (INCHES)	CAT.	HR FACTOR (MI <sup>2</sup> - INCHES/HOUR)
1	0 - 1	1	0 - 500
2	1 - 3	2	500 - 1000
3	3 - 5	3	1000 - 2000
4	5 - 10	4	2000 - 4000
5	10 - 15	5	4000 - 6000
6	15 - 20	6	6000 - 8000
7	$\geq$ 20	7	$\geq$ 8000

TABLE 6

## STORM DURATION

36 to 60 HOURS

CAT.	MAX RAINFALL (INCHES)	CAT.	HR FACTOR (MI <sup>2</sup> - INCHES/HOUR)
1	0 - 5	1	0 - 1000
2	5 - 10	2	1000 - 2000
3	10 - 15	3	2000 - 4000
4	15 - 20	4	4000 - 6000
5	20 - 30	5	6000 - 8000
6	≥ 30	6	8000 - 10000
		7	≥ 10000

TABLE 7

## STORM DURATION

60 to 84 HOURS

CAT.	MAX RAINFALL (INCHES)	CAT.	HR FACTOR (MI <sup>2</sup> - INCHES/HOUR)
1	0 - 5	1	0 - 2000
2	5 - 10	2	2000 - 4000
3	10 - 15	3	4000 - 6000
4	15 - 20	4	6000 - 8000
5	20 - 30	5	8000 - 10000
6	≥ 30	6	≥ 10000

TABLE 8

## STORM DURATION

84 HOURS OR GREATER

CAT.	MAX RAINFALL (INCHES)	CAT.	HR FACTOR (MI <sup>2</sup> - INCHES/HOUR)
1	0 - 5	1	0 - 2000
2	5 - 10	2	2000 - 4000
3	10 - 15	3	4000 - 6000
4	15 - 20	4	6000 - 8000
5	20 - 30	5	8000 - 10000
6	≥ 30	6	≥ 10000



## HEAVY RAIN ASSOCIATED WITH NORTHWEST FLOW ALOFT

William L. Read

National Weather Service Forecast Office  
Fort Worth, Texas 76102

### 1. INTRODUCTION

The summer season in North Texas is characteristically dry. The airmass is generally too stable to support airmass type thunderstorms common to Gulf coast areas. North Texas is a bit too far north to benefit from waves in the tropical easterlies. On the other hand, the westerlies have migrated too far north to provide significant dynamics for rainfall in North Texas.

There are three basic anomalies to the above mentioned scenario that can provide significant summertime rains in North Texas. Tropical cyclones, or more typically their remnants, may move inland and cross North Texas. The 30 plus inches at Albany, Texas from T.S. Amelia in 1978 is a recent example. A second condition which can lead to excessive rain during the summer is when a split develops between the 500 mb subtropical high over the southeastern United States and the high pressure ridge over the Rocky Mountain plateau area. Convection develops within the favorable cyclonic shear zone with daytime heating. The pattern may persist for days, thus yielding widespread heavy rain. The third pattern that can produce significant rainfall occurs when North Texas is under northwest flow at 500 mb, which allow the dynamics of the westerlies to move southward into Texas.

Figure 1 shows the mean 500 mb pattern for the month of July. Note the tendency for a ridge over the western U. S. and a trough to the east. Also note the lack of gradient over North Texas. The northwest flow pattern develops when there is an amplification of this mean pattern. Again, the importance of the northwest flow is that it allows frontal systems in the westerlies to reach into Texas.

Northwest flow patterns associated with severe thunderstorm outbreaks have been well documented (Johns, (1984). As Johns points out, it is important to recognize patterns favorable for the development of organized convection if one is to forecast these events. Keeter (1982) found that 11% of all flash flood events over a 10 year period in North Texas occurred when a northwest flow

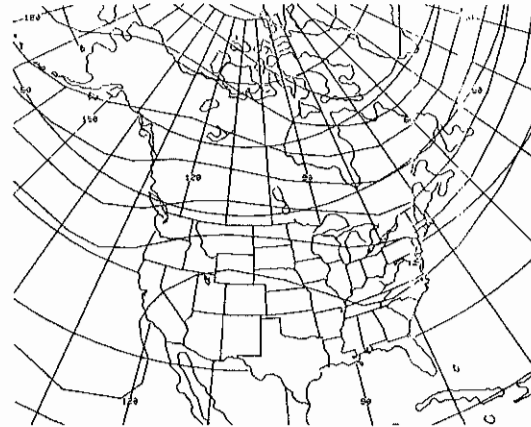


Figure 1. Mean 500 mb height field for July.

pattern existed. The purpose of this study was to examine northwest flow (NWF) heavy rain events to try to develop techniques for forecasting these events.

### 2. DATA

Rainfall records for North Texas climatological stations were examined over a 10 year period (1974-1984) for all days in which five or more inches of rain fell in a 24 hour period. These data were categorized according to 500mb flow patterns, one of which was NWF. During the ten year period, 8 NWF heavy rain events occurred in North Texas. A ninth event (August 20, 1984), which occurred in southern Arkansas and northern Louisiana, was included in the study for comparison purposes and because a more detailed data set was available. For each event the climatological data was further examined to try to determine the time of onset of heavy rain. Map sets were assembled for the synoptic time just prior to onset of heavy rain. The data included standard level charts from 850 mb through 200 mb and three hourly surface synoptic charts. Hourly data, radar and satellite imagery were available for the two 1984 events.

### 3. RESULTS

Each case was analyzed for various parameters commonly associated with

heavy rain events. Table 1 shows results of this analysis. As stated earlier, time of onset was established for each event. From Table 1, it appears that NWF heavy rain events are predominantly nocturnal onset. This was somewhat surprising since Johns (1984) study of severe outbreaks under NWF indicated that the southern plains events were distinctly daytime onset. The two events that occurred during the daytime had aspects that set them apart from the nocturnal events. The August 1984 event was the only event in which 850 mb flow was southerly, The airmass was quite unstable (LI=-6). With the mean environmental flow being northwest, developing thunderstorms would tend to move to the southeast. If a supercell were to develop and tend to move to the right, it would be moving more to the south. With 850 mb winds from the south at 20 knots, a south moving thunderstorm would experience greatly enhanced inflow and could become a very efficient rainmaker. The limited rainfall reports for this day point to possibly one supercell thunderstorm produced the five inch rains. The other daytime event, September 1976, was the only case associated with strong upper level dynamics. A very intense short wave was approaching North Texas at 12z and it appears several intense thunderstorms developed along the front and merged, evolving into a large mesohigh. Severe weather also occurred with this event.

Forecasters are in the habit of examining 500mb charts for important short waves. Only one event in this study occurred with a significant short wave. Five other cases exhibited more subtle impulses upstream from North Texas. For three cases there was no evidence of a short wave at 500 mb.

Upper tropospheric diffluence is frequently noticed in areas of intense organized convection. For 7 of the 9 events, diffluence was analyzed prior to onset. For most events the pattern was subtle, as winds aloft were rather light. With the limited data set, it could not be determined whether or not the diffluence resulted from earlier convection.

The last four features in Table 1 relate to lower tropospheric conditions. All nine cases occurred on the cool side of a front or significant outflow boundary. The boundary in all cases was generally east-west oriented at the time of heavy rain. Five of the events exhibited a well defined sub-synoptic low or wave along the front, with the heavy rain occurring to the northeast of the low. However, four of the events exhibited no such feature. All but one event evolved into a well defined mesohigh. The August 1977 event was unique in that a very strong front ( for August ) had moved into central Texas. The pressure and temperature gradients were such that with three hourly data it was not possible to analyse a mesohigh. The heavy rain was localized for this event as in all the events. The predominance of mesohigh development and the localized nature of the rainfall point the importance of sub-synoptic scale focussing mechanisms for NWF heavy rain events.

An unusual feature noticed during analysis of the data was the occurrence of a moist west wind. With the exception of the August 1974 event discussed above, all NWF events occurred with a west wind at 850 mb where the dewpoint was 12 degrees C or greater. Normally, west wind at 850 mb over Texas is associated with dry, warm air. Johns (1984) noticed the same tendency with NWF severe weather outbreaks.

ITEM	AUG 5 1974	JUN 19 1976	JUL 4 1976	SEP 3 1976	AUG 20 1977	JUL 5 1981	AUG 1 1982	JUN 30 1984	AUG 20 1984	SUMMARY
NOCTURNAL ONSET	NO	YES	YES	NO	YES	YES	YES	YES	YES	7/9 NOCTURNAL
500 MB S/W	MOD	WK	MOD	STG	NO	MOD	MOD	NO	NO	6/9 WITH 500MB S/W
U/L DIFFLUENCE	WK	WK	MOD	STG	MOD	MOD	MOD	NO	NO	7/9 WITH U/L DIFFLUENCE
SBL/WAVE	NO	YES	NO	NO	YES	NO	YES	YES	YES	NO DEFINITE PATTERN
MESOHIGH	YES	YES	YES	YES	NO	YES	YES	YES	YES	8/9 MESOHIGH
WEST WIND 850MB TD>12	NO	YES	YES	YES	YES	YES	YES	YES	YES	8/9 WEST WIND 850MB TD>12
850 MB WARM ADV	WK	WK	WK	WK	STG	WK	WK	MOD	STG	ALL 9 850 MB WARM ADV

Table 1. Comparison of events with respect to selected parameters.

Last but not least, warm advection at 850 mb has been found to be important for producing vertical motion. In all 9 cases warm advection was evident. Most were classified as weak due to light wind speeds coupled with weak temperature gradients.

Since the NWF heavy rain event was essentially a mesohigh type event, comparison to the composite mesohigh sounding prepared by Maddox, et al, (1979) seemed appropriate. As expected, many similarities existed. These included deep moisture, weak shear and a high degree of instability. In the NWF composite, relatively warm mid-tropospheric conditions were offset by very warm lower tropospheric conditions.

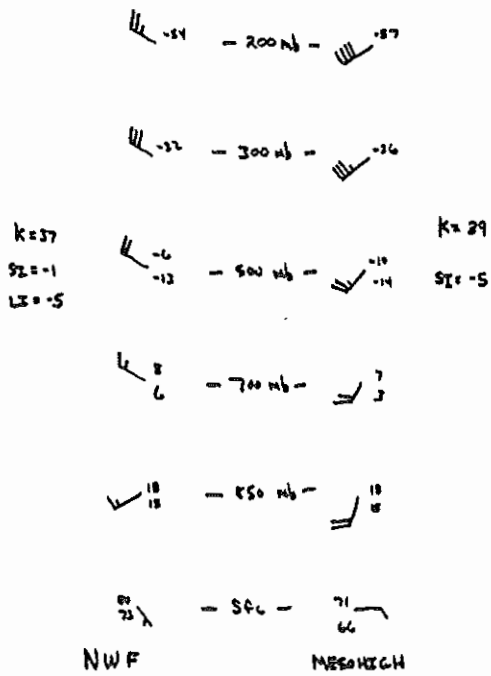


Figure 2. Composite sounding for NWF and Maddox mesohigh.

4. DISCUSSION OF NOCTURNAL NATURE OF EVENT

A surprising finding from this study was the primarily nocturnal nature of NWF heavy rain events. Johns (1984) found no cases of Southern Plains NWF severe weather outbreaks with initial development during the night. Apparently the rather weak dynamics associated with NWF heavy rain events sets them apart from the severe outbreak.

There are several theories currently in vogue concerning the nocturnal onset of thunderstorms. Forbes, et al, (1984) summarizes these ideas and present yet another. These various theories include: 1. radiational cooling of cloud tops destabilize the atmosphere sufficiently to initiate convection, 2. differential cooling between cloudy and clear areas set up solenoidal conditions such that upward vertical motion exists in the cloudy area, 3. the nocturnal low-level jet develops and acts to either enhance warm advection or upslope conditions.

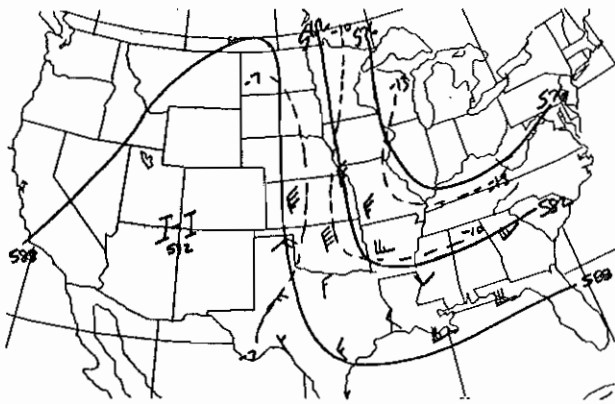
The mechanism as proposed by Forbes, et al, (1984) is that, given a surface boundary oriented such that air from the warm sector flows toward the boundary, the diurnal heating cycle dictates onset at night in many cases. During the morning, air in the boundary layer is at its most stable condition due to overnight radiational cooling. This air, even when lifted over a boundary, may not be unstable enough for convection to develop. By nightfall, the air in the boundary layer is at its most unstable condition due to insolation. This air, when lifted over the boundary, would be more likely to develop into convection. With relatively light wind and shallow boundary, the time required for boundary layer air to be lifted could be rather long, thus onset times well after dark can be expected.

This mechanism appears to describe North Texas NWF nocturnal onset quite well. In all 7 nocturnal cases there was a boundary to the south of where heavy rain fell. Warm sector air was flowing toward the boundary, in most cases nearly normal to the boundary. The other mechanisms may also play a role. The surface data indicated clear air in the warm sector and cloud cover over the eventual rain area prior to onset. Also, the nocturnal increase in boundary layer winds act to enhance lifting over the boundary.

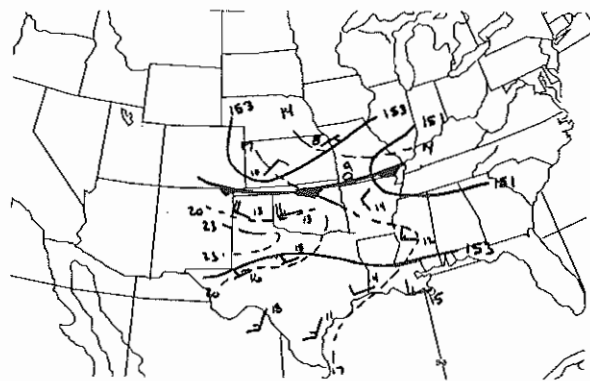
5. EXAMPLE

The June 30, 1984 case was used to illustrate the NWF heavy rain event mainly due to the fact that satellite imagery was readily available and the author was working shift during the event. This was a nocturnal event, with initial convection developing around 03z. Most of East Texas received 1 to 3 inches of rain overnight, with a small area east of Waco reporting 5 to 7 inches.

Figure 3 shows the surface, 850 and 500 mb analyses and corresponding satellite imagery for 12z June 29, 1984. The 500 mb flow was a high amplitude version of NWF, with the major ridge



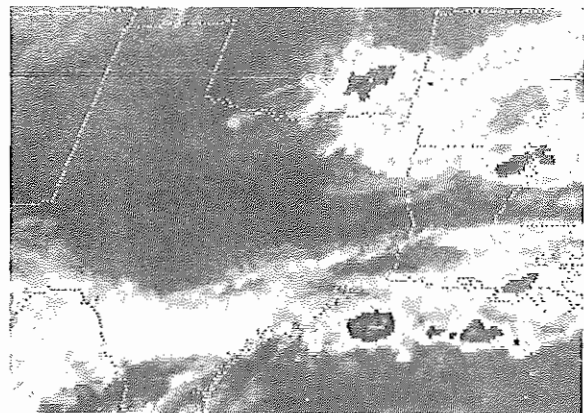
a. 500 mb height, temperature and selected wind observations.



b. 850 mb height, temperature and selected wind observations. Dewpoint (C) plotted adjacent wind barb.



c. Selected surface observations and important boundaries.



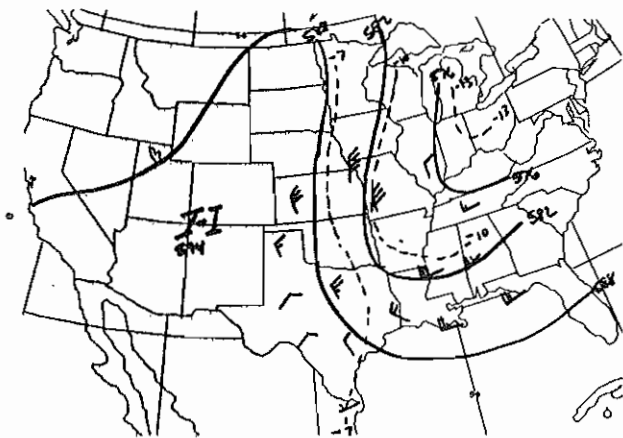
d. Infrared satellite imagery.

Figure 3. Selected synoptic conditions for 12z June 29, 1984.

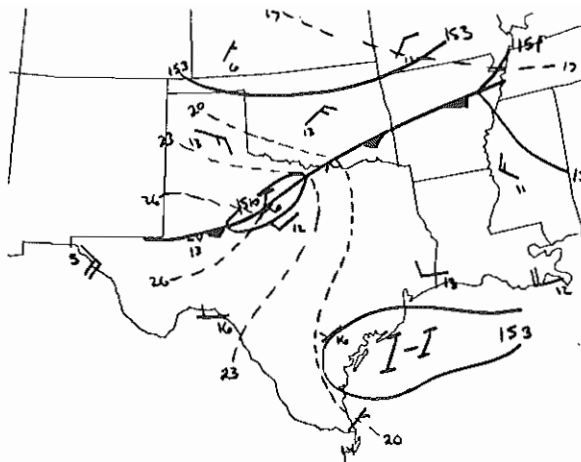
over the Rockies and the corresponding downstream trough over the eastern U.S. A significant short wave was moving into the base of the trough through central Arkansas and Texas. At 850 mb, the significant trough was located in Oklahoma. Note the strong west wind ahead of the trough and the corresponding convection as indicated by satellite. The 850mb moisture and thermal fields also fit well with observed convection. Surface features of interest at 12z included the sub-synoptic low (SSL) near Childress on a frontal boundary through west Texas and central Oklahoma. Note also the outflow boundary from the southeastern Oklahoma thunderstorm complex. These features had been moving steadily southward during the night.

During the day the surface features discussed above maintained basically the same pattern while moving steadily southward. Isolated intense convection developed near the intersection of the SSL and outflow boundary, prompting SELS to issue a Severe Thunderstorm Watch. Some large hail occurred southwest of Fort Worth. By 00z, however, all convection was rapidly dissipating.

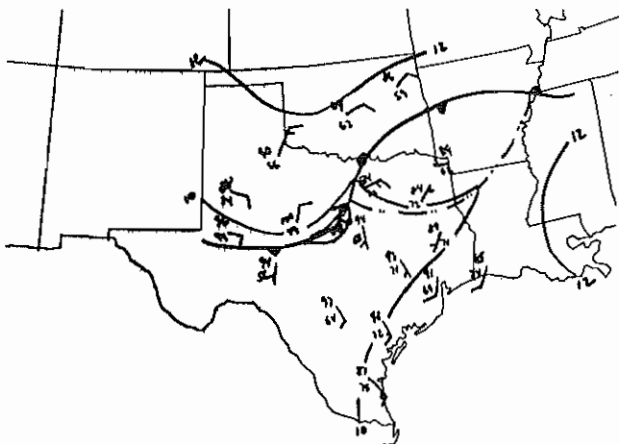
Figure 4 shows surface, 850 and 500 mb analyses and corresponding satellite imagery for 00z, June 30, 1984. At 500 mb the short wave had progressed further southeastward while the major ridge and trough remained essentially unchanged. The 850 mb trough had advanced southward into North Texas. Note the well defined temperature and dewpoint ridges



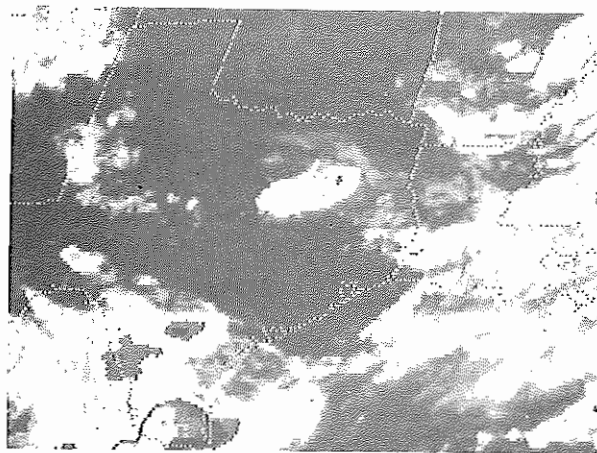
a. 500 mb



b. 850 mb



c. Surface



d. Satellite

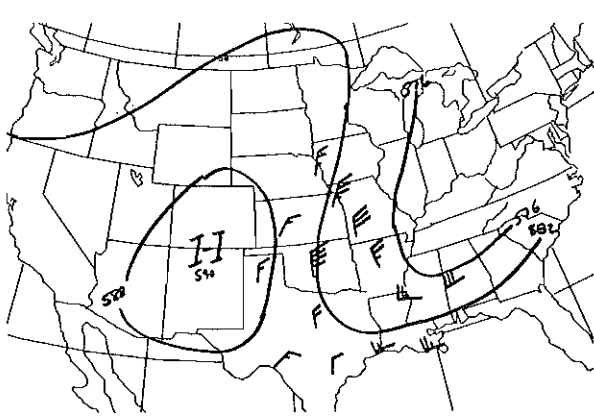
Figure 4. Same as Figure 3, except for 00z June 30 1984.

extending into East Texas. Wind flow at this time was quite light. At the surface, the SSL had progressed southward to just west of Waco with the attendant front moving with it. The outflow boundary had maintained its thermal contrast due to considerable cloud cover on the cool side. The area that was to receive the heavy rain was to the east of the SSL and north of the outflow boundary.

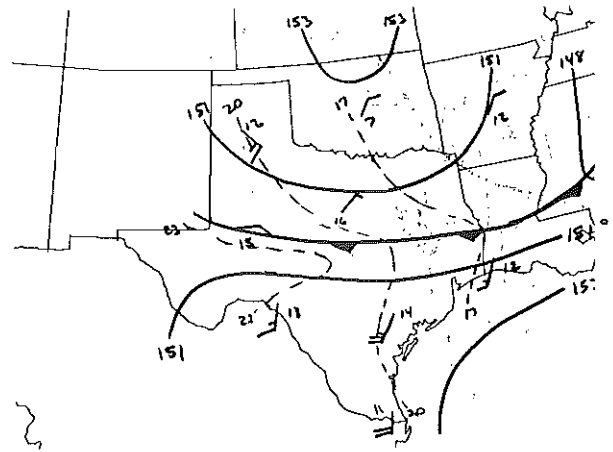
Convection initially began to the southeast of Dallas around 03z, June 30, 1984. Figure 5 shows surface features at 04z June 30, 1984. Note the warm moist flow normal to the old outflow boundary. The strongest winds were normal to the boundary near where the heavy thunderstorms were developing.



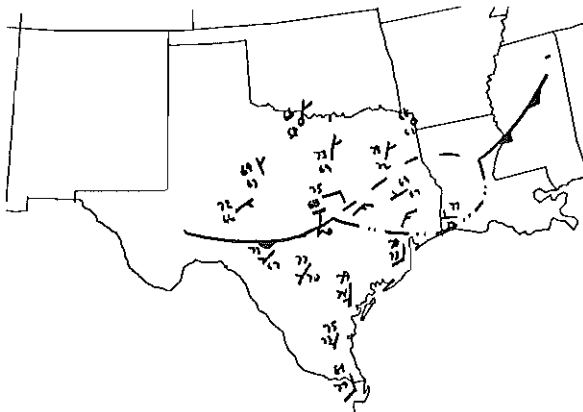
Figure 5. Selected surface observations 04z June 30, 1984.



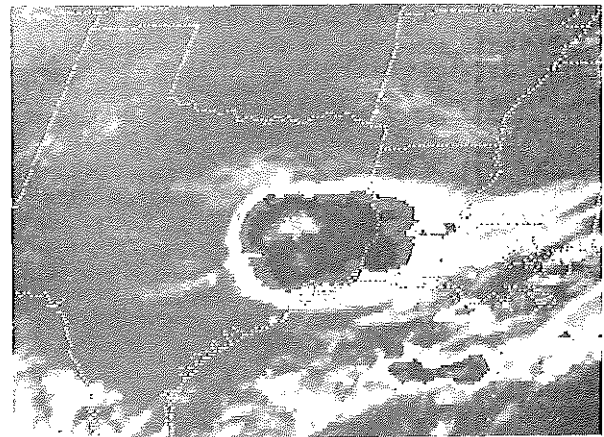
a. 500 mb



b. 850 mb



c. Surface



d. Satellite

Figure 6. Same as Figure 3, except for 12z June 30 1984.

The convection intensified rapidly during the next few hours and became organized in the manner of an MCC. Satellite imagery and radar indicated maximum intensity was reached around 12z, after which convection rapidly decreased. Figure 6 shows surface, 850 and 500 mb analyses and corresponding satellite imagery for 12z June 30, 1984. Again, 500 mb features had changed little from 00z. On the other hand, 850 mb features had become even better defined overnight, possibly in response to the organized convective complex. Note the pooling of dewpoints (15 degrees C or greater) and stronger winds normal to the boundary. Surface features had continued to move steadily southward without changing significantly since the previous day.

## 6. CONCLUSIONS

The main purpose for studying heavy rain events is to attempt to determine if such events can be forecast. Some of the results of this study suggest that NWF heavy rain events are forecastable in the short range (less than 12 hours). The following factors should be considered by North Texas forecasters when a NWF pattern exists during the summer:

1. The presence of a front/strong outflow boundary oriented generally east-west. Just having a front in North Texas during the summer is relatively rare and implies enhanced thunderstorm probability.

2. The presence of high moisture content in the soundings. This condition is a must for excessive rain. This will likely cover an extensive area.

3. Very unstable conditions as indicated by Lifted Indices of -4 or less. This also will likely cover an extensive area.

4. If conditions 1,2 and 3 are present, is either a vigorous short wave going to approach from the northwest or is the synoptic/subsynoptic low level setting favorable for nocturnal onset? This aspect may be the least forecastable as small scale short waves are frequently missed by the models and also, nocturnal events still not completely understood.

The mesoscale nature of the heavy rain event also makes narrowing down the area to be effected rather difficult prior to onset. For this study, only heavy rain days with northwest flow were examined. Northwest flow days without heavy rain need to be examined to determine if the results of this study are exclusive to heavy rain days.

#### REFERENCES

- Forbes, Gregory S., Paul D.G. Heppner, John J. Cahir and Walter D. Lottes, 1984. Prediction of delayed onset nocturnal convection based on air trajectories. Preprints, 10th Conf. on Weather Analysis and Forecasting, Clearwater, Fl, AMS, 474-479.
- Johns, Robert H., 1984. A synoptic climatology of northwest-flow severe weather outbreaks. Mon. Wea. Rev., 112, 449-464.
- Keeter, Kermit K., 1982. Flash flooding in Northcentral Texas. WSFO Fort Worth local study.
- Maddox, R.A., C.F. Chappell and L.R. Hoxit, 1979. Synoptic and mesoscale aspects of flash flood events. Bull. Amer. Meteor. Soc., 60, 115-123.



CLIMATOLOGY OF HEAVY RAIN PRODUCING  
SYNOPTIC PATTERNS IN NORTH FLORIDA

Raymond E. Biedinger  
National Weather Service Forecast Office  
Miami, Florida

1. INTRODUCTION

While investigating the spring floods of 1984 in the Suwannee River Basin of north Florida, it became evident that certain synoptic patterns were responsible for producing the heavy rains that resulted in the flooding. Four 500 mb patterns were identified with heavy rains during the first four months of 1984. Each 500 mb pattern related well with a distinct surface pattern.

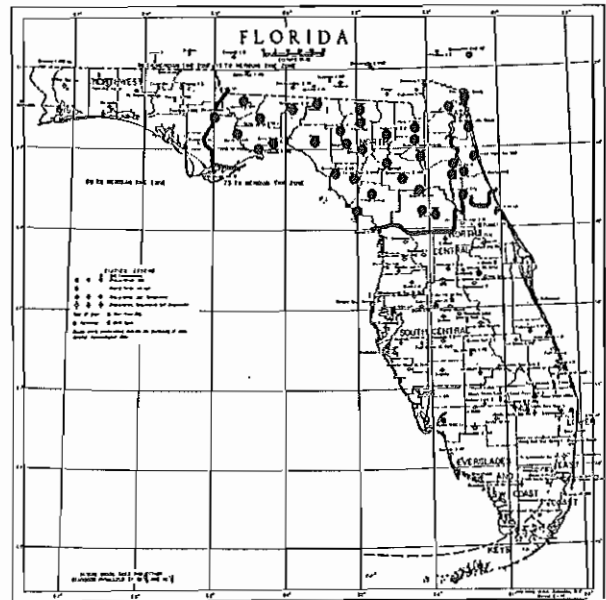
This finding led to further examination of past years to see if these correlations held true. Thirty-five years of data were readily available for this study and were used to develop this climatology of synoptic patterns at 500 mb and at the surface that produced heavy rainfall in north Florida during the winter season, November through April.

2. DATA USED FOR THE STUDY

The period examined was November 1948 through December 1950 and January 1952 through April 1984. Data for the calendar year 1951 were missing from station records. This results in the equivalent of 35 winter seasons. A rain amount of three inches or more in a 24-hour period was considered a heavy rain event for this study.

The area used in this study was north Florida which includes Florida zones 5, 6, 7, 8, and 9. It is in this region where most of the winter flooding of rivers occurs as a result of repeated heavy rains. This area is east of the Apalachicola River and generally north of a line from Daytona Beach to Cedar Key (Attachment 1). The Florida panhandle west of the Apalachicola River was not included in this study because it is not in the area of forecast responsibility of the Miami Forecast Office. However, this climatology probably applies to the panhandle also.

Thirty-five observation sites of precipitation are located in this area and are included in the Daily Precipitation Totals (NOAA, 1948-1983) and the Hourly Precipitation Data (NOAA, 1952-1983) which are monthly climatological publications. Each time at least one of these sites recorded three inches or more, it was considered a heavy rain event, and the synoptic situation causing the heavy rain was investigated. There were 133 such heavy rain events during these 35 winter seasons.



Attachment 1. Area included in the heavy rain study. Dots mark the locations of the 35 precipitation observation sites.

The Daily Series of Synoptic Weather Charts (NOAA, 1968) for the period of November 1948 to April 14, 1968 and the Daily Weather Maps (NOAA, 1983) for the period April 15, 1968 through April 1984 which include both 500 mb and surface analyses were used to examine the patterns that produced the heavy rain.

During these 35 winter seasons when 133 heavy rain events occurred over north Florida, five distinct 500 mb patterns were identified. With each of these 500 mb patterns, a definite surface pattern existed.

3. INDENTITY OF 500 MB PATTERNS

There were two general 500 mb patterns associated with the heavy rains, split flow and full latitude flow. The split flow, as it's name implies, was where 500 mb flow was not uniform over the United States, but the flow was characterized by troughs in the northern and southern branches being out of phase. There were distinct regions of confluence and diffluence in the flow. The full latitude 500 mb flow was where the long wave trough was the dominant feature with no noticeable regions of confluence or diffluence.

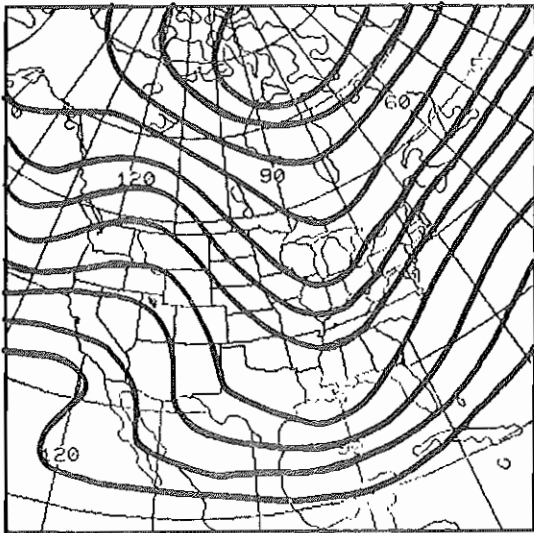


Figure 1a. Example of a Type I 500 MB Pattern. Major Short Wave moving in the southern branch of split flow south of 35N.

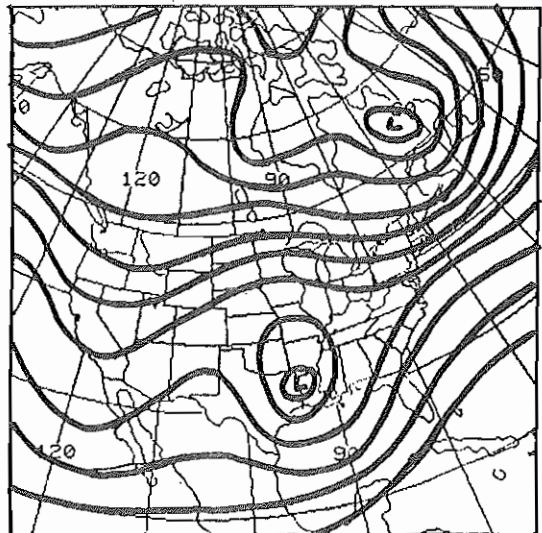


Figure 1c. Example of Type I 500 MB Pattern. Closed low moving in the southern branch of split flow south of 35N.

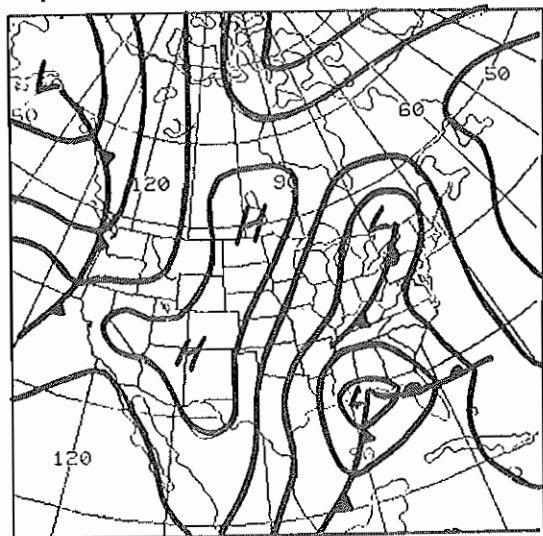


Figure 1b. Example of a Type I Surface Pattern. Surface low pressure system forms in Gulf of Mexico with central pressure 1000 MB to 1010 MB.

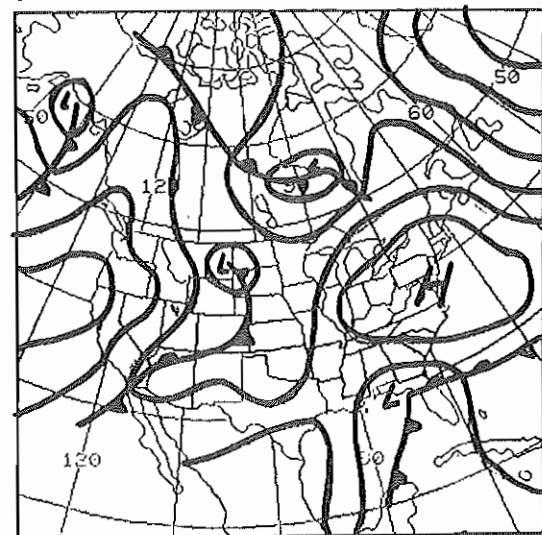


Figure 1d. Example of Type I Surface Pattern. Surface low pressure system forms in Gulf of Mexico with central pressure 1000 MB to 1010 MB.

The split 500 mb pattern which was observed more frequently than the full latitude pattern was subdivided into three types. Type I was a pattern in which a short wave without closed circulation (Fig. 1a) or with a closed circulation (Fig. 1c) in the southern branch of the 500 mb flow moved eastward across the southern United States south of latitude 35N. This is the 500 mb pattern that has been found to produce heavy rainfall in Louisiana. Belville and Stewart (1983) labeled this the "New Orleans Type". Type II was either a stationary cutoff low or a stationary long wave trough over the southwestern United States or the Baja, California/Mexico region (Fig. 2a). This type of 500 mb pattern was identified by Grice and Maddox (1982) to be the pattern that resulted in a typical frontal type heavy rain event over south Texas. Type III was a closed low or occasionally an open short wave which moved eastward across the central United States and passed north of

latitude 35N in relation to the study area (Fig. 3a).

The full latitude 500 mb pattern was subdivided into two types. The first type, designated Type IV, was a pronounced full latitude long wave trough (Fig. 4a) which moved slowly eastward across the entire United States. Maddox (1979a) classified this pattern as the Synoptic Type Flash Flood or Heavy Rain Event in his methodology for forecasting heavy precipitation. The second type, called Type V, was a zonal flow without a significant trough in the area of the study (Fig. 5a).

#### 4. CORRESPONDING SURFACE PATTERNS

Type I 500 mb pattern (Figs. 1a and 1c) was almost always, 38 out of 41 times (93%), accompanied by a surface pattern, called Type I, shown in Figs. 1b and 1d. Type I surface pattern was a low pressure system originating in the

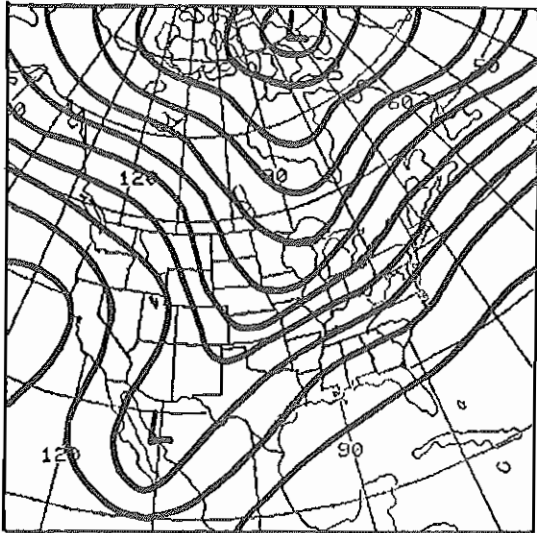


Figure 2a. Example of Type II 500 MB Pattern. Cutoff low or long wave trough stationary over southwest United States.

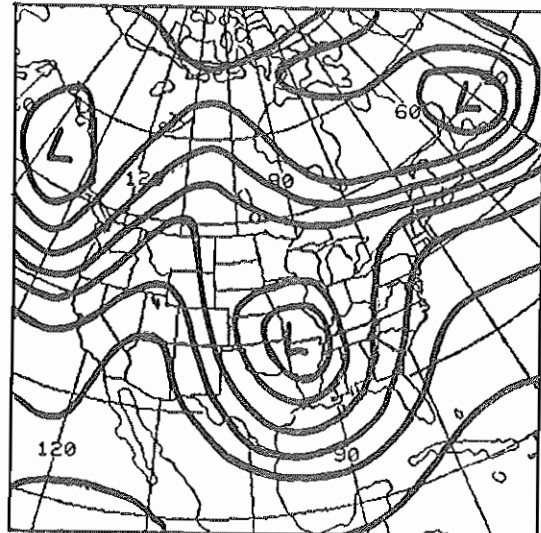


Figure 3a. Example of Type III 500 MB Pattern. Closed low or major short wave trough moving eastward across the United States north of 35N.

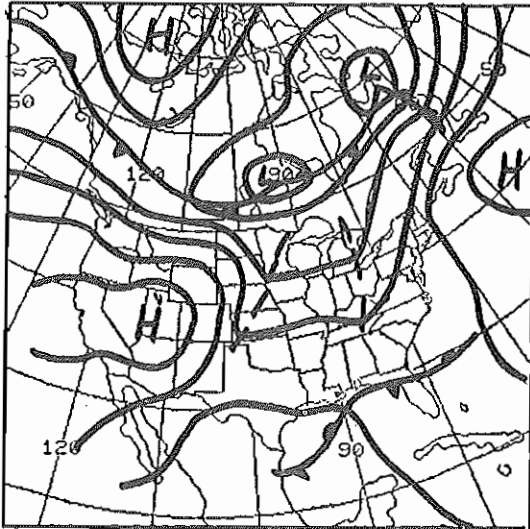


Figure 2b. Example of Type II Surface Pattern. Stationary front across north or central Florida.

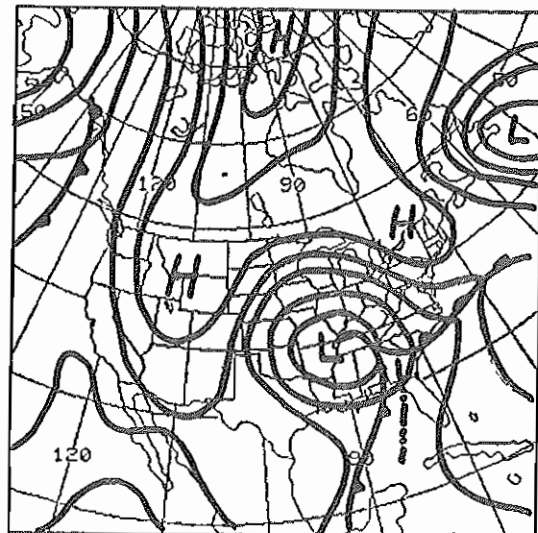


Figure 3b. Example of Type III Surface Pattern. Strong low pressure system with central pressure below 1000 MB moving across the southern Appalachian Mountains.

northern Gulf of Mexico and moving east or northeast across north Florida and south Georgia. The central pressure of the low center was usually between 1000 mb and 1010 mb. The three remaining Type I 500 mb patterns not producing Type I surface patterns were related to two other types of surface patterns. Two of the three had a stationary front across north Florida, and the other had a north-northeast to south-southwest oriented cold front. These two surface patterns were usually associated with different 500 mb patterns which will be discussed later.

Type II 500 mb pattern (Fig. 2a) was always, 21 out of 21 times (100%), accompanied by a surface pattern, called Type II, shown in Fig. 2b. Type II surface pattern was a stationary front lying across north or central Florida. Frequently subsynoptic scale lows (SSL) developed on the front and moved eastward in the frontal zone. This occurrence was also observed by Belville, et al (1983). Lowest pressures with

these lows were usually 1010 mb to 1020 mb. This phenomenon usually occurred when the cutoff low or the trough moved out of the southwest United States and progressed east-northeastward across the southern United States. Maddox (1979a) classified this type pattern as the Frontal Type Flash Flood or Heavy Rain Event.

Type III 500 mb pattern (Fig. 3a) was almost always, 37 out of 39 times (95%), associated with a strong surface low pressure system similar to Fig. 3b. The low pressure systems had central pressures below 1000 mb in most cases and moved across the southern Appalachian Mountains or remained west of the mountains, and a secondary low center formed near the southeast United States' coast. Much of the rainfall with this type system was produced by a cold front/squall line combination. One event with a Type III 500 mb pattern that did not have a Type III surface pattern had a cold front/squall line combination without a surface low pressure system over the

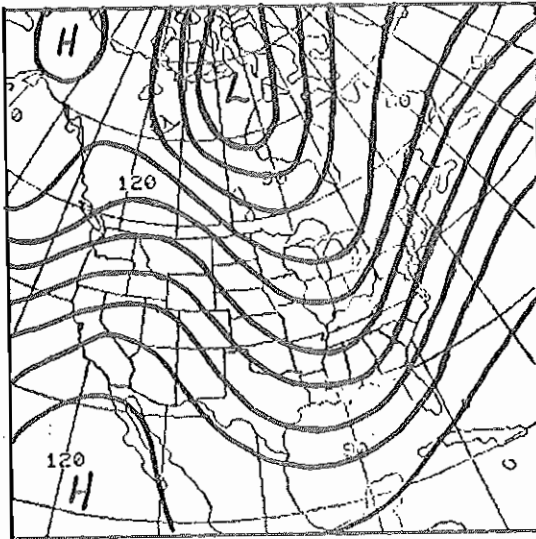


Figure 4a. Example of Type IV 500 MB Pattern. Full latitude trough moving slowly eastward.

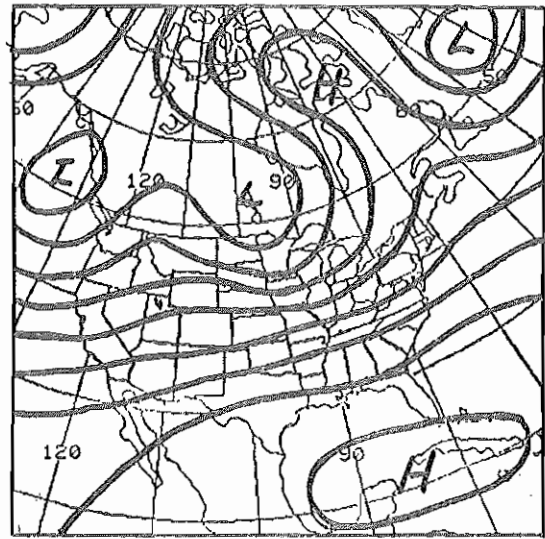


Figure 5a. Example of Type V 500 MB Pattern. Zonal flow at 500 MB.

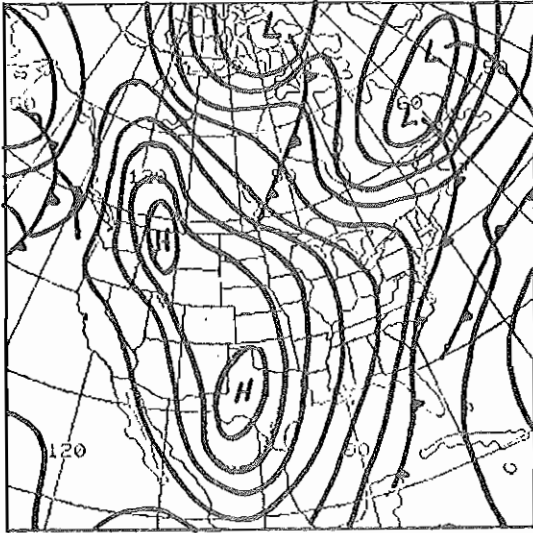


Figure 4b. Example of Type IV Surface Pattern. North-northeast to south-southwest oriented cold front moving slowly eastward usually preceded by a squall line.

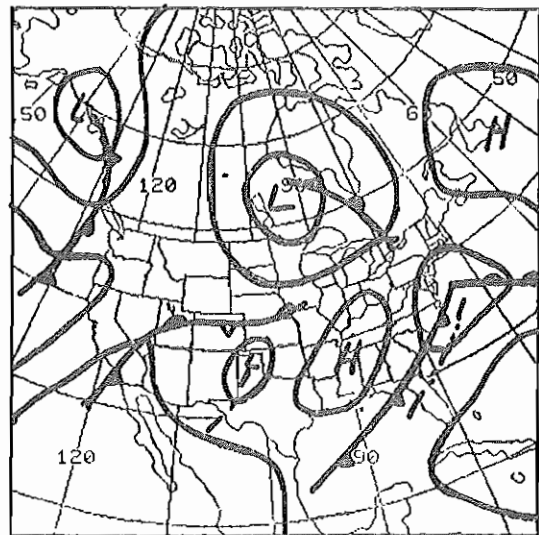


Figure 5b. Example of Type V Surface Pattern. Northeast to southwest oriented cold front usually preceded by a squall line.

United States, similar to the next surface pattern. The other Type III 500 mb pattern was associated with a Type I surface pattern.

Type IV 500 mb pattern (Fig. 4a) was almost always, 23 out of 25 times (92%), accompanied by a rather slow moving cold front/squall line combination oriented north-northeast to south-southwest (Fig. 4b). Occasionally minor SSLs formed on the front near the Gulf of Mexico coastline which enhanced the rainfall with this type system. Of the two non-Type IV surface patterns associated with the Type IV 500 mb pattern, one pattern was a low pressure system coming out of the Gulf of Mexico, a Type I surface pattern, and the other was a stationary front across north Florida, a Type II surface pattern.

Type V 500 mb pattern (Fig. 5a) was always, 7 out of 7 times (100%), associated with a northeast to southwest oriented cold front/squall line combination (Fig. 5b).

Table 1 represents the frequency of occurrence of the 500 mb types and the surface types. Clearly, the majority of heavy rain events, (90%) were caused by Types I, II, III, and IV. Type I produced the greatest percentage of events while Type III accounted for the second highest frequency of occurrences.

Included in the 133 events were 37 events where five inches or more of rain were measured in the study area by at least one observer. Table 2 shows the frequency of occurrence of the five inch or greater events with the various 500 mb and surface patterns. Seventy-six percent of these events were produced by Types I, III, and IV.

#### 5. MONTHLY CLIMATOLOGY OF THREE INCH OR GREATER RAINFALL PATTERNS

During these 35 winter seasons, 12 heavy rain events occurred in November. Five, (42%),

		500 MB PATTERN					
S U R F A C E  P A T T E R N	TYPE	I	II	III	IV	V	# EVENTS
	I	38 (29%)	0	1 (.8%)	1 (.8%)	0	40
	II	2 (2%)	21 (16%)	0	1 (.8%)	0	24
	III	0	0	37 (28%)	0	0	37
	IV	1 (.8%)	0	1 (.8%)	23 (17%)	0	25
	V	0	0	0	0	7 (5%)	7
# EVENTS	41	21	39	25	7	133	

Table 1. Frequency of occurrence of three inch or greater rainfall events with various 500 mb and surface patterns for 35 winter seasons.

		500 MB PATTERN					
S U R F A C E  P A T T E R N	TYPE	I	II	III	IV	V	# EVENTS
	I	7 (19%)	0	0	0	0	7
	II	0	5 (14%)	0	1 (3%)	0	6
	III	0	0	10 (27%)	0	0	10
	IV	0	0	0	11 (30%)	0	11
	V	0	0	0	0	3 (8%)	3
# EVENTS	7	5	10	12	3	37	

Table 2. Frequency of occurrence of five inch or greater rainfall events with various 500 mb and surface patterns for 35 winter seasons.

were Type I 500 mb/surface patterns (Fig. 1), and three, (25%), were Type IV (Fig. 4). Table 3 presents the November frequency of occurrence of three inch or greater rainfall related to the different 500 mb/surface patterns.

There were 18 heavy rain events in December. Again, Type I 500 mb/surface pattern had the greatest number of occurrences with 7 events, (39%). Type IV was the second most frequent with 5 events, (28%). Table 4 shows December's occurrences.

January had 13 heavy rain events. Type I pattern was again the most frequent to occur with 4 events, (31%). Type III pattern was the second most frequent with 3 events, (23%). Table 5 shows the January occurrences.

February had the second highest frequency of heavy rain events. There were 29 events. Type I pattern was clearly the most frequent heavy rain producer with 12 events, (41%). Type IV pattern was second with 7 events, (24%). Table 6 presents February's occurrences.

March was close behind February with 27 heavy rain events. Type II and III patterns produced 10 events each, (37% each). Table 7 shows the March occurrences.

The month of April had the highest frequency heavy rain events during the winter season with 34 events. Type III produced the greatest number of events with 14, (41%). Type I produced 9 events, (26%). Table 8 shows April's occurrences.

These statistics show that Type I 500 mb/surface pattern (Fig. 1) was the type of synoptic pattern that produced most of the heavy rain events over north Florida during the early and middle months of the winter season, November through February. This pattern is the surface low pressure system moving out of the northern Gulf of Mexico across north Florida related to a split 500 mb flow which has either an open short wave or a closed low moving across the southern United States. Then during the latter months of the winter season, March and April, Type III 500 mb/surface pattern produced most of the heavy

NOVEMBER  
500 MB PATTERN

SURFACE	TYPE	I	II	III	IV	V	# EVENTS
F	I	5 (42%)	0	0	0	0	5
C	II	1 (8%)	2 (17%)	0	0	0	3
E	III	0	0	1 (8%)	0	0	1
P	IV	0	0	0	3 (25%)	0	3
T	V	0	0	0	0	0	0
E							TOTAL
R	# EVENTS	6	2	1	3	0	12

Table 3. Frequency of occurrence of three inch or greater rainfall with various 500 mb/surface patterns for 35 winter seasons during the month of November.

FEBRUARY  
500 MB PATTERN

SURFACE	TYPE	I	II	III	IV	V	# EVENTS
F	I	12 (41%)	0	0	0	0	12
C	II	0	4 (14%)	0	0	0	4
E	III	0	0	6 (21%)	0	0	6
P	IV	0	0	0	7 (24%)	0	7
T	V	0	0	0	0	0	0
E							TOTAL
R	# EVENTS	12	4	6	7	0	29

Table 5. Frequency of occurrence of three inch or greater rainfall with various 500 mb/surface patterns for 35 winter seasons during the month of February.

DECEMBER  
500 MB PATTERN

SURFACE	TYPE	I	II	III	IV	V	# EVENTS
F	I	7 (39%)	0	0	0	0	7
C	II	0	2 (11%)	0	0	0	2
E	III	0	0	3 (17%)	0	0	3
P	IV	1 (6%)	0	0	5 (28%)	0	6
T	V	0	0	0	0	0	0
E							TOTAL
R	# EVENTS	8	2	3	5	0	18

Table 4. Frequency of occurrence of three inch or greater rainfall with various 500 mb/surface patterns for 35 winter seasons during the month of December.

MARCH  
500 MB PATTERN

SURFACE	TYPE	I	II	III	IV	V	# EVENTS
F	I	1 (4%)	0	0	0	0	1
C	II	0	10 (37%)	0	1 (4%)	0	11
E	III	0	0	10 (37%)	0	0	10
P	IV	0	0	0	4 (15%)	0	4
T	V	0	0	0	0	1 (4%)	1
E							TOTAL
R	# EVENTS	1	10	10	5	1	27

Table 7. Frequency of occurrence of three inch or greater rainfall with various 500 mb/surface patterns for 35 winter seasons during the month of March.

JANUARY  
500 MB PATTERN

SURFACE	TYPE	I	II	III	IV	V	# EVENTS
F	I	4 (31%)	0	0	1 (8%)	0	5
C	II	0	2 (15%)	0	0	0	2
E	III	0	0	3 (23%)	0	0	3
P	IV	0	0	0	2 (15%)	0	2
T	V	0	0	0	0	1 (8%)	1
E							TOTAL
R	# EVENTS	4	2	3	3	1	13

Table 5. Frequency of occurrence of three inch or greater rainfall with various 500 mb/surface patterns for 35 winter seasons during the month of January.

APRIL  
500 MB PATTERN

SURFACE	TYPE	I	II	III	IV	V	# EVENTS
F	I	9 (26%)	0	1 (3%)	0	0	10
C	II	1 (3%)	1 (3%)	0	0	0	2
E	III	0	0	14 (41%)	0	0	14
P	IV	0	0	1 (3%)	2 (6%)	0	3
T	V	0	0	0	0	5 (15%)	5
E							TOTAL
R	# EVENTS	10	1	16	2	5	34

Table 8. Frequency of occurrence of three inch or greater rainfall with various 500 mb/surface patterns for 35 winter seasons during the month of April.

rain events. Fig. 3 shows this synoptic pattern, which is a well developed storm system at the surface associated with a major short wave, either open or closed, in the southern branch of the 500 mb split flow. The monthly distribution of 3-inch or greater rainfall is given in the bar graph presented in Fig. 6.

#### 6. MONTHLY CLIMATOLOGY OF FIVE INCH OR GREATER RAINFALL PATTERNS

Table 9 displays the monthly occurrences of five inch or greater rainfall in relation to the type of 500 mb and surface patterns that produced the rainfall. March had the highest frequency of 5 inch or greater rainfall events followed by April. Eight of these March/April occurrences, (40%), were produced by the Type III 500 mb/surface pattern (Fig. 3). Goodman, et al (1983) found in their studies of heavy rainfall in Alabama that March and April were the preferred months for 5 inch or more rainfall in that area also. The monthly distribution of 5-inch or greater rainfall is shown in the bar graph in Fig. 6.

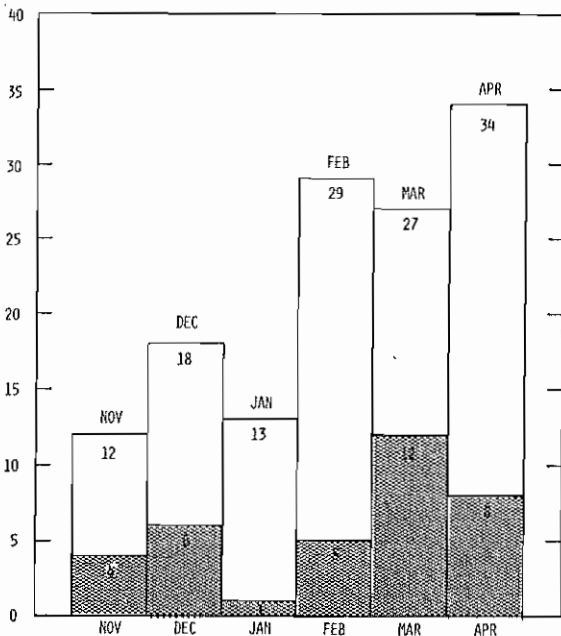


Figure 6. Monthly distribution of heavy rainfall in north Florida during the winter season. Shaded area is rainfall of 5 inches or more during a 24-hour period. Unshaded area is rainfall of 3 inches or more during a 24-hour period.

#### 7. OTHER SIGNIFICANT METEOROLOGICAL PARAMETERS RELATED TO HEAVY RAIN

While the sole intent of this paper was to identify those synoptic patterns at 500 mb and at the surface that were associated with heavy rains in north Florida in the winter, there are many other meteorological parameters that must be considered when forecasting heavy rainfall other than the 500 mb patterns and the surface patterns. Heavy rains were not always observed when these synoptic patterns described in this paper existed.

To accurately forecast heavy rainfall, the forecaster must consider the meteorological conditions not only from the surface and 500 mb levels, but at levels in between and above. In recent years numerous studies have related various meteorological parameters to the occurrence of heavy rainfall. Robert A. Maddox (1979a, 1979b, 1981) has probably been the most prolific in this area. The reader is referred to his papers and others such as James D. Belville, et al (1983), Gary K. Grice, et al (1982, 1983), and Ronald R. Goodman, et al (1983), to name a few, for a much more detailed and thorough study on the subject of the dynamics of heavy rainfall.

These papers stressed the importance of the existence of certain conditions at various levels in the atmosphere. At the surface, a front, convergence zone, or other surface boundary was an important feature as well as the development of a mesoscale or subsynoptic scale low. Other important parameters in the low levels were high dew point temperatures with a moisture ridge or tongue being advected into the area of concern by the low level jet. At mid levels, the position of the long wave trough and the presence of short wave troughs along with high moisture levels were also important. At upper levels, the location of the polar or subtropical jet stream with their associated regions of divergence was another important consideration. A heavy rain checklist was developed by Grice and Ely (1983) to provide forecasters in south Texas a means of evaluating the heavy rain potential. With slight adjustments, this checklist could probably be used in other areas as well.

When the forecaster recognizes the development of a synoptic pattern shown to have a potential for producing heavy rainfall, he/she should then proceed to the mesoscale level to look for these other more detailed features to identify the heavy rain area and ultimately the maximum rain area in his/her forecast area. This was the goal of Goodman, et al (1983) in their study of heavy rains in Alabama.

#### 8. CONCLUSION

The heavy rainfall data for north Florida for these 35 winter seasons clearly indicate that the majority, (95%), of the heavy rains, three inches or more during a 24-hour period, are caused by five distinct synoptic patterns. The five types are summarized below.

Type I: Split flow pattern at 500 mb with a major short wave trough, either open or closed, moving eastward in the southern branch of the 500 mb flow over the southern United States south of 35N. This was accompanied by a surface low pressure center in the northern Gulf of Mexico with a central pressure from 1000 mb to 1010 mb that moved across north Florida and/or south Georgia. Type I is shown Fig. 1.

Type II: Split flow pattern at 500 mb with a stationary cutoff low or trough over the southwestern United States. This was accompanied by a stationary front at the surface over north or central Florida. Type II is shown in Fig. 2.

MONTHLY DISTRIBUTION AND TYPE OF 500 MB/SURFACE PATTERNS  
PRODUCING RAINFALL OF FIVE INCHES OR MORE

500/SURFACE PATTERN	# EVENTS	% OF OCCURRENCES	NOV	DEC	JAN	FEB	MAR	APR
TYPE I	7	19%	2	1	0	2	1	1
TYPE II	5	14%	1	0	0	0	4	0
TYPE III	10	27%	0	2	0	0	3	5
TYPE IV	11	30%	1	3	0	3	4	0
TYPE V	3	8%	0	0	1	0	0	2
TOTAL	36	98%*	4	6	1	5	12	8

\* one additional event in March was caused by a Type IV 500 mb pattern and a Type II surface pattern, 3% of the occurrences.

Table 9. Monthly distribution and type of 500 mb/surface patterns that produced rainfall of five inches or more during the 35 winter seasons.

Type III: Split flow pattern at 500 mb with a major short wave trough, usually with a closed low, moving eastward and passing the study area north of 35N. Normally, a strong surface low pressure system, central pressure below 1000 mb, moved east or northeast across the southern or central Appalachian Mountains. Type III is shown in Fig. 3.

Type IV: A full latitude trough at 500 mb moving slowly eastward across the central and eastern United States. A cold front, and usually a squall line, oriented generally in a north-northeast to south-southwest direction, moved slowly eastward with the upper trough. Type IV is shown in Fig. 4.

Type V: A zonal flow at 500 mb with a northeast to southwest oriented cold front frequently preceded by a squall line and sometimes accompanied by a minor low pressure system. Type V is shown in Fig. 5.

The remaining occurrences of heavy rain, (5%), were produced by various combinations of the above 500 mb and surface patterns.

In this study of 35 winter seasons for the months of November through April, there were 133 heavy rain events which covered a period of 175 days. The reason for this difference is that some heavy rain events included two or three consecutive 24-hour periods when at least one observation site reported rainfall of 3 inches or more. During the study period, there were a total of 6,344 calendar days. Heavy rainfall of three inches or more fell some place in north Florida on 2.8 percent of the days during these 35 winter seasons. Table 10 lists, by month, every heavy rain event included in this study.

#### ACKNOWLEDGMENTS

I wish to thank Mr. Mike Mogil, Southern Region, Scientific Services Division, for his

helpful comments on the content of this study. I also wish to thank Mr. Paul Hebert, MIC/AM of Florida, for his thorough review of the paper and helpful suggestions. My gratitude is also expressed to Mrs. Mary Davis for typing the manuscript in its final form.

#### REFERENCES

- Belville, J.D. and N.O. Stewart, 1983: Extreme rainfall events in Louisiana: The "New Orleans Type". Preprints, 5th Conference on Hydrometeorology. Tulsa, Amer. Meteor. Soc., Boston, MA, 284-290.
- Goodman, R.R., R.C. Charnick, and R.E. McNeil, 1983: Forecasting heavy rain in Alabama. Preprints, 5th Conference on Hydrometeorology, Tulsa, Amer. Meteor. Soc., Boston, MA, 279-283.
- Grice, G.K. and R.A. Maddox, 1982: Synoptic aspects of heavy rain events in south Texas associated with the Westerlies. NOAA Tech. Memo., NWS SR-106, Fort Worth, TX.
- , and G.F. Ely, 1983: Surface subsynoptic and upper air analysis: An integral part of the shift routine. Preprints, 5th Conference on Hydrometeorology. Tulsa, Amer. Meteor. Soc., Boston, MA, 252-258.
- Maddox, R.A., 1979a: A methodology for forecasting heavy convective precipitation and flash flooding. Nat. Wea. Digest, Vol. 4, No. 4, 30-42.
- , C.F. Chappell, and L.R. Hoxit, 1979b: Synoptic and mesoalpha scale aspects of flash flood events. Bull. Amer. Meteor. Soc., 60, No. 2.

-----, and W. Deitrich, 1981: Synoptic conditions associated with the simultaneous occurrence of significant severe thunderstorms and flash floods. Preprints, 4th Conference on Hydrometeorology, Reno, Amer. Meteor. Soc., Boston, MA, 181-187.

NOAA, 1948-1984: Daily Precipitation Totals. Climatological Data, Florida. NOAA, EDIS, Federal Bldg, Asheville, NC.

----, 1952-1983: Hourly Precipitation Data, Florida. NOAA, EDIS, Federal Bldg, Asheville, NC.

----, 1968: Daily Series, Synoptic Weather Maps, Part I, Northern Hemispheric Sea Level and 500 Millibar Charts, Jan. 1948 to Apr. 14, 1968, NCDC, Asheville, NC.

----, 1984: Daily Weather Maps--Weekly Series, Apr. 15, 1968 to Apr. 30, 1984, U.S. Govern. Printing Off., Washington, D.C.

HEAVY RAINFALL EVENTS INCLUDED IN THIS STUDY  
NOVEMBER 1948 THROUGH APRIL 1984\*

November	Pcpn	500	Surface	January	Pcpn	500	Surface
5 1953	3.43	I	I	6-7 1949	3.35	IV	IV
29-30 1957	3.53	IV	IV	9 1953	4.50	III	III
5 1958	3.00	II	II	12 1963	5.61	V	V
21 1959	5.01	II	II	8 1964	4.00	II	II
24 1960	3.94	I	I	12 1964	3.00	III	III
5 1963	3.82	I	I	26 1966	3.00	I	I
1 1964	5.30	I	I	7 1971	3.75	II	II
1 1969	5.00	I	I	26-27 1976	4.00	IV	IV
6 1972	3.00	I	II	19 1978	3.00	I	I
25 1972	4.00	III	III	12-13 1979	3.33	I	I
27-28 1976	5.00	IV	IV	24 1979	3.10	III	III
21-22 1983	3.50	IV	IV	27 1980	3.25	I	I
				14 1982	3.00	IV	I
December	Pcpn	500	Surface	February	Pcpn	500	Surface
8 1948	4.04	I	I	16-17 1952	4.78	I	I
6 1950	3.27	IV	IV	7 1953	6.00	IV	IV
23 1953	3.47	II	II	6 1956	3.17	III	III
13 1963	3.13	II	II	4 1959	3.71	II	II
31 1963	3.00	I	I	27-1959	3.00	II	II
3-5 1964	9.27	IV	IV	13 1960	3.93	I	I
27 1964	6.46	IV	IV	25 1960	3.39	III	III
19-20 1965	3.00	I	I	3 1963	3.16	I	I
10 1966	4.35	I	IV	27-28 1964	5.60	I	I
10-11 1967	5.50	III	III	12 1965	3.13	IV	IV
3-4 1968	5.41	III	III	11-12 1966	3.22	II	II
10 1969	5.05	I	I	23 1966	4.92	I	I
3 1971	4.00	I	I	28 1966	3.00	III	III
21-22 1972	3.50	I	I	7 1967	4.30	I	I
31 1975	3.50	III	III	12-13 1967	3.40	I	I
15 1976	3.25	I	I	9 1969	3.10	III	III
1 1977	3.00	IV	IV				
28-29 1983	6.00	IV	IV				

\* (Calendar year 1951 not included in study)

Table 10. Heavy rainfall events included in the study. Column one includes 24-hour periods when at least one observation site reported 3.00 inches or more. Consecutive days counted as one heavy rain event. Column two gives maximum rainfall total for the event. Column three lists 500 mb type. Column four lists the surface type.

## HEAVY RAINFALL EVENTS (continued)

February	Pcpn	500	Surface	April	Pcpn	500	Surface
15 1969	3.75	I	I	5-6 1949	4.85	I	I
2-3 1970	7.00	IV	IV	4-5 1950	4.19	IV	IV
8 1971	4.75	IV	IV	27 1950	3.75	V	V
2 1973	3.16	III	III	6-7 1953	5.40	I	I
9 1973	3.00	I	I	12-13 1953	4.60	III	III
4 1977	3.60	I	I	19 1953	3.00	V	V
3 1978	3.75	II	II	11 1955	4.31	I	I
8 1978	3.50	I	I	14 1955	3.00	III	III
25 1980	3.25	IV	IV	9-10 1958	6.86	III	III
8 1981	3.00	IV	IV	15 1958	3.67	I	I
11 1981	7.00	IV	IV	21 1959	3.15	I	I
19 1981	5.00	I	I	2 1960	4.20	III	III
27 1984	3.50	III	III	9 1961	3.28	III	III
				1 1962	10.20	III	III
March	Pcpn	500	Surface	27-28 1964	8.36	III	III
16 1950	3.44	V	V	20 1965	3.00	I	II
22 1953	5.51	IV	II	27 1965	5.93	V	V
24 1957	4.77	III	III	4 1966	3.00	V	V
6 1958	3.89	II	II	28 1968	3.44	II	II
5-6 1959	6.81	III	III	6 1971	3.36	I	I
15 1959	5.19	IV	IV	29 1972	4.08	I	I
17 1960	6.35	III	III	1 1973	5.00	III	III
31 1962	8.90	IV	IV	3-4 1973	8.45	III	III
1-2 1965	6.72	IV	IV	10-11 1975	4.80	I	I
5 1966	4.76	III	III	19 1978	3.25	III	III
8 1970	5.00	I	I	5 1979	4.75	IV	IV
28-29 1970	7.00	II	II	13-14 1979	3.00	III	IV
29-31 1972	3.37	II	II	25 1979	3.00	I	I
8-9 1973	4.87	II	II	3 1980	3.50	III	III
29-30 1973	3.50	II	II	8-9 1982	5.00	V	V
25 1973	3.50	III	III	9 1983	4.50	III	III
23 1974	5.75	II	II	23 1983	4.00	III	III
25-26 1974	6.70	II	II	3-4 1984	4.00	III	III
18 1975	4.33	III	III	9 1984	3.30	III	I
9 1976	6.00	III	III				
9-10 1980	4.00	II	II				
30 1980	3.00	III	III				
4-5 1981	4.00	III	III				
6 1982	3.00	II	II				
6-7 1983	4.70	III	III				
6-7 1984	5.65	IV	IV				
27-28 1984	6.46	II	II				

Table 10. (continued) Heavy rainfall events included in the study.

THE DIURNAL DISTRIBUTION OF SUMMERTIME HEAVY PRECIPITATION  
IN THE EASTERN AND CENTRAL UNITED STATES

Julie A. Winkler<sup>1</sup> and Jerome P. Charba

Techniques Development Laboratory  
Office of Systems Development  
National Weather Service, NOAA  
Silver Spring, Maryland 20910

1. INTRODUCTION

Even though several recent studies have dealt with the diurnal distribution of excessive precipitation, considerable confusion still exists on the time of day of greatest threat of extreme rainfall. Wallace (1975) found that south and east of the Ohio and Mississippi valleys heavy precipitation, defined as  $\geq .10$  inch  $h^{-1}$ , is most common in the late afternoon, while in the Central Plains the time of maximum occurrence is shortly after midnight. A more detailed analysis by Wallace of the precipitation data for Iowa alone suggested that in the Central Plains rainfall rates  $\geq .50$  inch  $h^{-1}$  normally occur before midnight, while less intense rainfalls are most common in the early morning. Wallace concluded that severe storms capable of producing flooding are most frequent during the late afternoon and early evening both in the eastern and in the central United States. Huff's (1978) findings for Illinois are similar. Most of the heavy rainstorms included in his sample occurred in the afternoon and early evening hours.

On the other hand, Maddox et al. (1979), after studying more than 150 flood events, found that heavy rainstorms and flash flooding are most frequent during the late evening and early morning. These apparently contradictory findings prompted Crysler et al. (1982) to look at the effect of rainfall intensity and duration on the diurnal distribution of intense rainstorms for eight states (Nebraska, Missouri, Illinois, Kentucky, Tennessee, West Virginia, Pennsylvania, and Virginia). They concluded that short duration storms are most frequent in the afternoon and early evening, while long duration events occur most often during the evening and early morning. However, the frequency distributions presented by Crysler et al. suggest that the diurnal pattern may vary significantly across the United States. For example, in Nebraska, short duration events

occurred later in the evening and early morning than did longer duration storms; while in Kentucky and Tennessee, short duration events were most frequent in the afternoon, and long period storms were primarily nocturnal.

In a more recent study, Giordano and Fritsch (1983) found that long duration heavy rain events in the mid-Atlantic states occurred in the afternoon and evening, approximately 3 to 6 hours earlier than the midnight maximum reported for Pennsylvania and Virginia by Crysler et al. (1982). They attributed the conflicting results to the small number of long period storms in Crysler et al.'s sample.

The objective of this study is simply to study in greater detail the diurnal distribution of heavy precipitation in the eastern and central United States. The spatial variations in the diurnal cycle of extreme rainfall as a function of both rainfall intensity and duration are described.

2. DATA AND METHODOLOGY

Hourly precipitation data from the United States climatological network for June, July, and August during 1973-1981 were used in the study. Each reporting station was assigned to a 40x40 n mi grid cell. From all the observations falling within a given grid cell, only the maximum value during a particular hour or accumulation period was retained. Precipitation totals per cell were used instead of station totals so that a continuous period of record at each station would not be necessary and to reduce the amount of data analysis.

The number of rainfall events per hour was calculated for the same intensity levels defined by Wallace (1975): .25-.49 inch  $h^{-1}$ , .50-.99 inch  $h^{-1}$ , 1.00-1.59 inch  $h^{-1}$ , and  $\geq 1.60$  inch  $h^{-1}$ . Also, the frequency of rainfall totals  $\geq 2$  inches in 6 hours was determined for overlapping 6-h periods. The number of occurrences per grid cell for the heavier rainfall intensities was too small to accurately describe the diurnal cycle, so the frequency data for all categories were summed over overlapping 160x160 n mi areas. The centers of the analysis areas are shown in Fig. 1.

<sup>1</sup>Dr. Winkler is an Assistant Professor, Department of Geography, University of Nebraska. This research was conducted while Dr. Winkler was a National Research Council post-doctoral fellow at the Techniques Development Laboratory.



Figure 1. Centers of the analysis areas. Frequency distributions and harmonic dials for the lettered gridpoints are shown in Figs. 4 and 5.

To describe the form of the diurnal and semi-diurnal cycles, the frequency counts of each 160x160 n mi area were harmonically analyzed for the different rainfall intensities. The time of maximum, reduction in variance, and normalized amplitude of the first and second harmonics were mapped.

### 3. HOURLY PRECIPITATION TOTALS

Significant differences in the time of maximum of the first harmonic for the hourly precipitation amounts exist across the eastern two-thirds of the United States. For all intensity levels, the hour of maximum occurrence increases along the East Coast from approximately 1530 Local Standard Time (LST) in Florida to 1730 LST in New England (Fig. 2). From east to west along the Gulf Coast, the phase of the first harmonic shifts from mid-afternoon to before noon in southeast Texas. The dominant feature in the central United States is the nocturnal precipitation maximum extending from Minnesota and Wisconsin to central Oklahoma, where the hour of maximum varies from 2200 to 0200 LST for rainfall intensities of .25-.49 inch  $h^{-1}$  (Fig. 2a). A strong gradient in the time of peak occurrence extends across eastern Oklahoma, Arkansas, Missouri, Illinois, and Indiana. This gradient marks the transition zone between the afternoon maximum in the eastern United States and the nocturnal maximum in the Central Plains. From the western Dakotas to eastern New Mexico, the time of maximum is approximately 1800 to 2000 LST. For most of the eastern United States, the phase of the first harmonic remains the same or shifts only slightly (one-half hour to 1 hour) later with increasing rainfall intensity (Fig. 2b). However, in the nocturnal precipitation region, the hour of maximum is as much as 4 hours earlier for rainfall intensities of 1.00-1.59 inch  $h^{-1}$  compared to .25-.49 inch  $h^{-1}$ .

The variance accounted for by the first harmonic is largest (over 70%) in the central United States from northern Kansas to southern Minnesota and in the southeast from Georgia to Ohio for all intensity levels, including

1.00-1.59 inch  $h^{-1}$  (Fig. 3a). Little variance is explained by the first harmonic from south central Texas to southern Missouri. This zone corresponds to the area of steepest gradient in the time of maximum of the first harmonic. Also, the first harmonic accounts for less than 50% of the variance along the Great Lakes. The effect of the lakes on precipitation and the small number of heavy rain events contribute to the small reduction in variance values in this area. For all intensity levels, the variance accounted for by the second harmonic is greatest in northeastern Texas. In the central United States, the variance explained by the semi-diurnal curve is close to zero (Fig. 3b).

The normalized amplitude, defined as the amplitude of the first harmonic divided by the mean, has been used by Wallace (1975) and Skaggs (1980) to indicate the suppression of the phenomenon under study during the nonpeak hours. Normalized amplitudes  $> 1.0$  often occur when the phenomenon, such as precipitation events, is strongly suppressed during half of the day (Wallace, 1975). The normalized amplitudes (not shown) are largest in the Southeast and from the western Dakotas to northwestern Texas. The values increase substantially with rainfall intensity in these areas and are greater than one for rainfall rates of .50-.99 inch  $h^{-1}$  and larger. Normalized amplitudes also increase with rainfall intensity in the Central Plains and in New England, although most values remain less than one. The smallest amplitudes are found from central Texas to Illinois and along the Great Lakes.

Inspection of the spatial patterns of the time of maximum, explained variance, and normalized amplitude of the diurnal and semi-diurnal cycles for the hourly rainfall rates suggests that the eastern and central United States can be regionalized into five areas on the basis of the diurnal distribution of extreme precipitation.

The first region includes the central United States where rainfall of all intensities is primarily nocturnal, although the heavier intensities occur considerably earlier in the evening than lighter amounts. These characteristics are illustrated by the smoothed frequency plots and harmonic dial for southwestern Iowa (Figs. 4a and 5a). Note also that the frequency distributions become more peaked with increasing intensity suggesting that during the middle of the day there is a greater suppression of heavy rain events than light or moderate events. The diurnal cycle of precipitation is markedly different than the temporal pattern of severe weather; tornadoes and hail are most frequent in the late afternoon (Skaggs, 1969; 1980).

In the mid-Atlantic states and the Ohio Valley, most heavy rain events occur in the middle to late afternoon regardless of rainfall rate (Figs. 4b and 5b). There is little change in the time of maximum of the first harmonic for the different categories. Normalized amplitudes are small for the lighter rainfall rates but increase with increasing rainfall intensity. Tornadoic storms occur at approximately the same time as extreme rain events

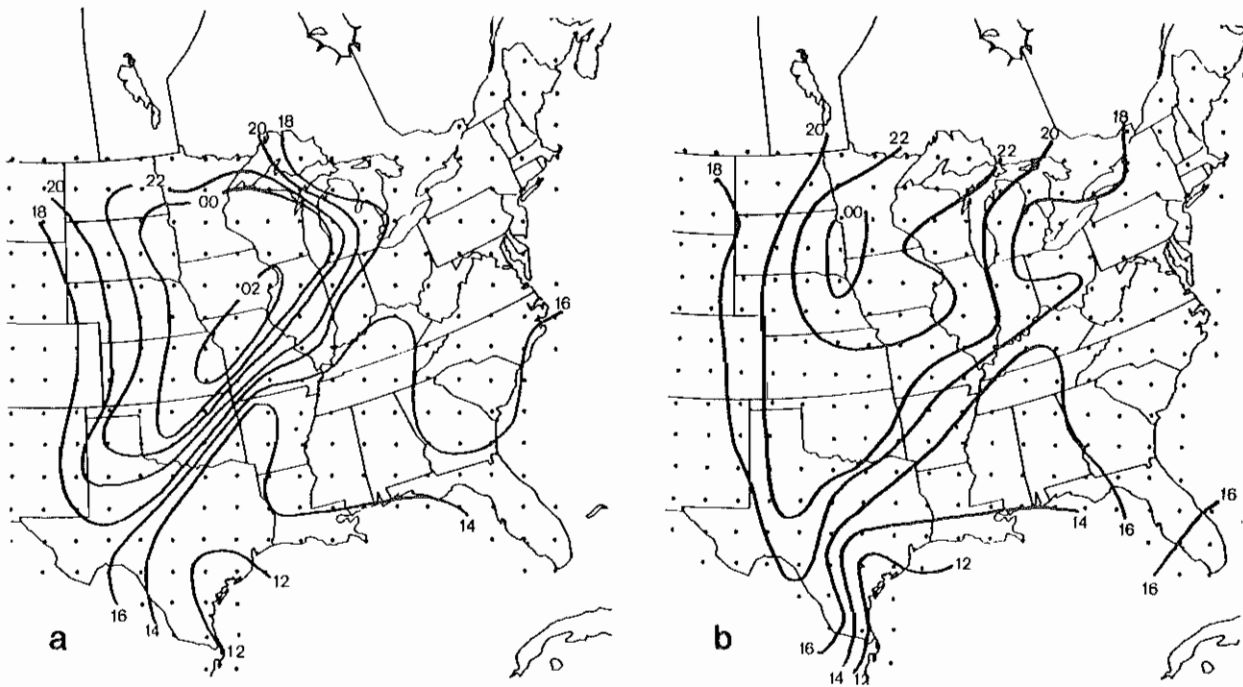


Figure 2. Time of maximum of the first harmonic (LST): (a) .25-.49 inch h<sup>-1</sup>; (b) 1.00-1.59 inch h<sup>-1</sup>.

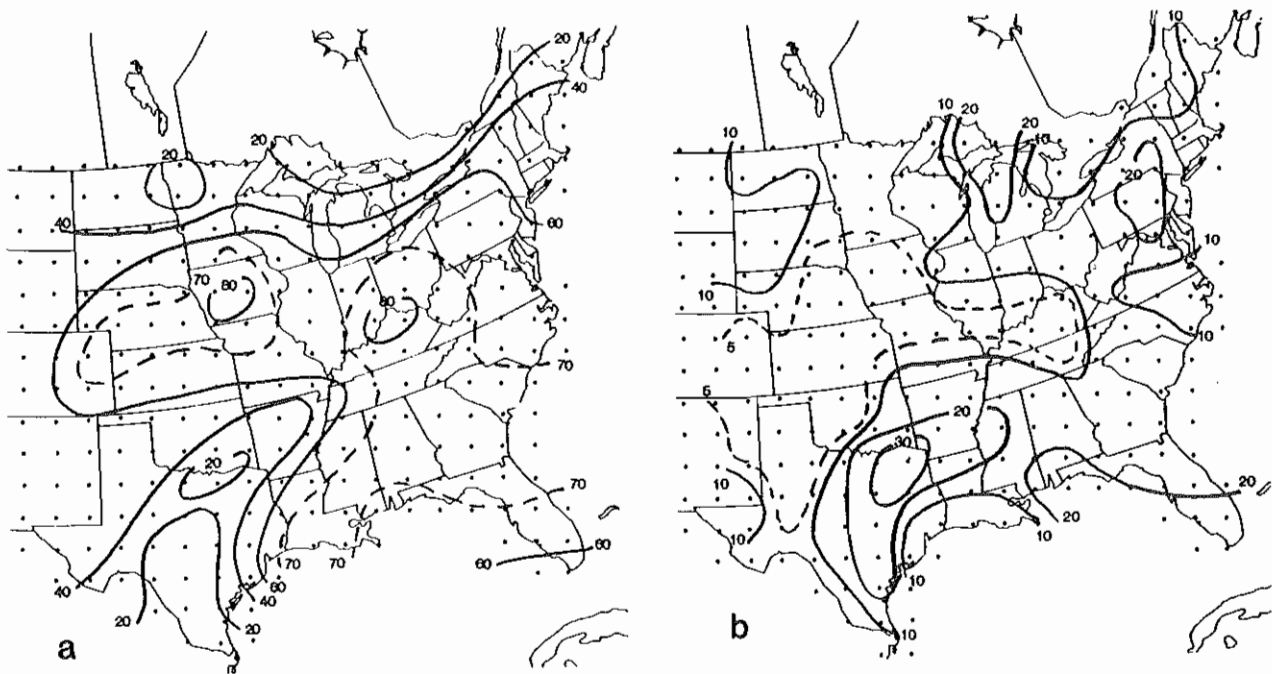


Figure 3. The percent of variance accounted for by the first harmonic (a) and by the second harmonic (b) for rainfall totals of 1.00-1.59 inch h<sup>-1</sup>.

(Skaggs, 1969), although large hail is most frequent several hours earlier (Skaggs, 1980).

The diurnal pattern in the southeastern United States is similar to that of the Ohio Valley and mid-Atlantic states, although the frequency distributions for all categories are more peaked and the time of occurrence is slightly earlier (Figs. 4c and 5c). Tornadoes and large hail also have a mid-afternoon maximum in this area (Skaggs, 1969; 1980).

Along the Texas coast, the time of occurrence of the first harmonic is close to noon for all rainfall categories, although the frequency distributions have a very broad maximum (Figs. 4d and 5d). This is especially evident for the heavier rainfall rates. Severe weather normally occurs later in the day compared to heavy precipitation.

The final region extends from central Texas to Illinois and is the transition zone between the nocturnal rainfall regime of the Central Plains and afternoon precipitation regime in the eastern United States. The frequency distributions for all rainfall categories are very flat, indicating heavy precipitation can occur any time of day (Figs. 4e and 5e). The diurnal

distribution of precipitation differs markedly from the diurnal cycle of severe weather. Hail and tornadic storms have a very distinct afternoon maximum in this region (Skaggs, 1969; 1980).

A sixth region possibly exists along the Great Lakes, but the frequency of heavy rain events in this area is too small to accurately describe the diurnal pattern.

#### 4. LONG DURATION HEAVY RAIN EVENTS

Comparison of the diurnal distributions of short duration (hourly) and longer period rain events suggests that storm duration has little effect on the temporal characteristics of heavy precipitation. Six-hour accumulations of  $\geq 2$  inches were used to represent long period storms, although in some cases the precipitation occurred in only 1 or 2 hours of the 6-h period. The number of occurrences per grid cell was calculated for overlapping 6-h periods (0000-0600, 0100-0700, ..., 2300-0500 LST), and the consequent time series were harmonically analyzed.

The distribution of the time of maximum of the first harmonic (not shown) resembles the pattern for the hourly totals. The hour of peak occurrence increases from early afternoon to

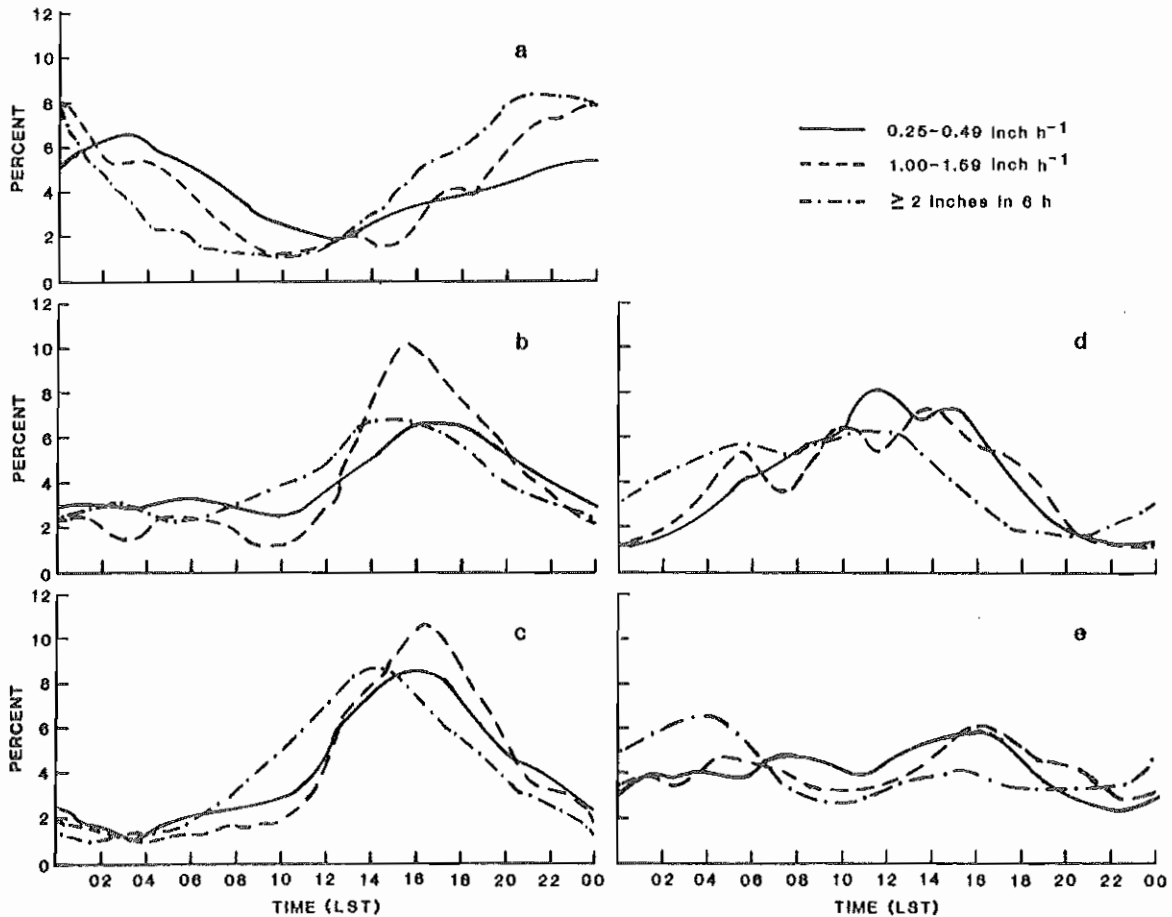


Figure 4. Percent frequency of heavy precipitation events for (a) southwest Iowa, (b) eastern Pennsylvania, (c) northwestern Georgia, (d) coastal Texas, and (e) northeastern Texas. Refer to Fig. 1 for locations of gridpoints.

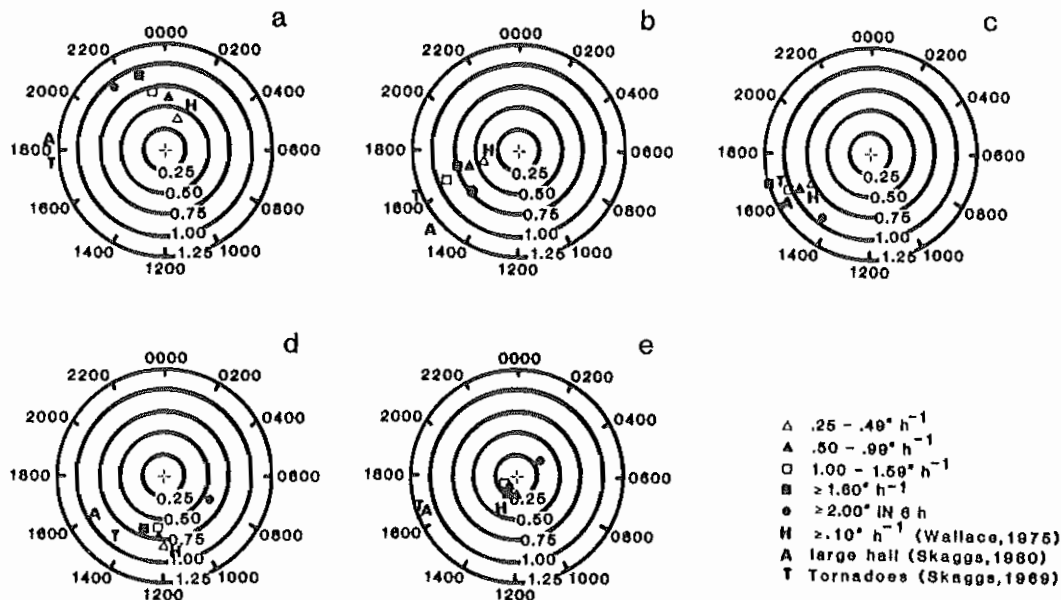


Fig. 5. Harmonic dial showing phase of diurnal cycle (LST) and normalized amplitude of various rainfall categories: (a) southwest Iowa, (b) eastern Pennsylvania, (c) northwestern Georgia, (d) coastal Texas, and (e) northeastern Texas. Refer to Fig. 1 for locations of gridpoints. Only the phase was given in Skaggs (1969), so tornado occurrences are plotted at the same amplitude as large hail events.

late afternoon northward along the East Coast. In the central United States, the time of maximum is in the late evening, while along the western Gulf Coast, the hour of maximum occurs before noon. The variance accounted for by the first harmonic (not shown) is greater than 80% in the central United States and in the Ohio Valley. From central Texas to southern Illinois the explained variance was less than 40%.

The smoothed frequency distributions and harmonic dials show that the time of maximum occurrence of the long duration events precedes that of hourly events by 1 to 2 hours (Figs. 4 and 5). This is the result of plotting the frequency at the initial hour of the 6-h period. The frequency distributions for eastern Pennsylvania and northwestern Georgia show a distinct maximum in the afternoon (Figs. 4b and 4c). Along the southeast Texas coast,  $\geq 2$  inches of precipitation was most frequent in the 6-h period from 11-17 LST, although the frequency distribution has a very broad maximum (Fig. 4d). In northeastern Texas, long duration storms occur any time of day (Fig. 4e). Only in the central United States are longer duration heavy rainstorms most frequent at night (Fig. 4a). Precipitation totals  $\geq 2$  inches in 6 hours occurred most often from 21-03 LST in southwest Iowa. The results of this analysis do not support Crysler et al.'s (1982) contention that long duration events occur later in the evening than short duration intense rainfalls.

## 5. SUMMARY

Significant and interesting spatial variations in the diurnal cycle of extreme precipitation exist across the eastern and central United States. Along the East Coast, the threat of heavy precipitation is greatest

in the afternoon regardless of rainfall intensity or duration. Along the western Gulf Coast, heavy precipitation is most likely around noon, although the frequency distributions display a broad maximum. Only in the central United States is heavy precipitation primarily nocturnal. Storms with heavier rainfall intensities and longer durations in this area begin 1 to 2 hours before midnight, while less intense events normally begin after 0000 LST. A transition zone between the nocturnal precipitation regime to the west and the afternoon regime to the east extends from central Texas to Illinois. In this area, heavy precipitation is uniformly distributed throughout the day.

## 6. ACKNOWLEDGMENTS

This research was supervised by Dr. Wayne E. McGovern. Normalee Foat helped prepare the illustrations.

## 7. REFERENCES

- Crysler, K. A., R. A. Maddox, L. R. Hoxit, and B. M. Muller, 1982: Diurnal distribution of very heavy precipitation over the central and eastern United States. *National Weather Digest*, 7, 33-37.
- Giordano, L. A., and J. M. Fritsch, 1983: The atypical mid-level flow for flash floods in the mid-Atlantic states. *Preprints Fifth Conference on Hydrometeorology*, Tulsa, Amer. Met. Soc., 142-148.
- Huff, F. A., 1978: Characteristic properties of midwestern flash flood storms. *Preprints Conference on Flash Floods, Hydrometeorological Aspects*, Los Angeles, Amer. Met. Soc., 29-33.

Maddox, R. A., C. F. Chappell, and L. R. Hoxit,  
1979: Synoptic and mesoscale aspects of  
flash flood events. Bull. Amer. Meteor.  
Soc., 60, 115-123.

Skaggs, R. H., 1969: Analysis and regionali-  
zation of the diurnal distribution of  
tornadoes in the United States. Mon. Wea.  
Rev., 97, 103-115.

\_\_\_\_\_, 1980: The diurnal distribution of large  
hail over the United States. Professional  
Geographer, 32, 293-299.

Wallace, J. M., 1975: Diurnal variation in  
precipitation and thunderstorm frequency  
over the conterminous United States. Mon.  
Wea. Rev., 103, 406-419.

THE TULSA FLOOD OF 27 MAY 1984. PART I: SYNOPTIC AND MESOSCALE OVERVIEW

Michael L. Branick

National Weather Service Forecast Office  
Oklahoma City, Oklahoma 73159

1. INTRODUCTION

Flash flooding in Tulsa, Oklahoma on the early morning of 27 May 1984 claimed 14 lives and resulted in property damage estimated at well over \$100 million. The flooding followed excessive rainfall of over 30 cm in less than 6 h, with maximum rainfall concentrated directly over the Tulsa metropolitan area (Fig. 1).

The purpose of this study is to document the evolution of synoptic and mesoscale features prior to and during the period of heavy rainfall in Tulsa. Surface and upper-air analyses from 1200 GMT 26 May to 1200 GMT 27 May, inclusive, are presented in section 2. In section 3, the analyses are used to infer some of the physical mechanisms responsible for triggering and focusing the heavy rainfall over the Tulsa area.

2. SYNOPTIC AND MESOSCALE OVERVIEW

Conditions at 1200 GMT 26 May, some 18 to 24 h prior to the Tulsa flood, are shown in Fig. 2. Analyses at 200 mb (Fig. 2a) and 500 mb (Fig. 2b) reveal a shortwave trough moving eastward across the upper Midwest. The strongest westerlies were well north of Oklahoma at both levels. Two speed maxima (jet streaks) were evident at 200 mb, one over northern Illinois and the other over western Wyoming.

At 850 mb (Fig. 2c), a well-defined trough was located from western Texas to northern Arkansas. A pronounced east-west thermal ridge was located south of the trough, resulting in a narrow zone of (geostrophic) warm advection along the Texas-Oklahoma border. Moisture was abundant in the southwesterly flow over Texas, with dewpoints in excess of 12°C.

A quasi-stationary surface front extended from western Texas eastward into Tennessee (Fig. 2d). A significant thermal gradient was evident north of the front. Dewpoints exceeded 20°C from eastern Texas and southeastern Oklahoma eastward. Scattered showers and thunderstorms (not shown) were occurring north of the front from northern Oklahoma eastward into Arkansas, and northward into Kansas and southern Missouri.

Significant changes occurred in the sub-synoptic environment by 0000 GMT 27 May, many of which provided evidence to suggest that an excessive rainfall event would unfold in or near eastern Oklahoma within the following 12 h. Heavy rain was in fact already occurring at 0000 GMT, a result of intense convection that developed over a concentrated area in east central Oklahoma (Fig. 3). Thunderstorms with tops exceeding 15 km (50 thousand feet) produced rainfall totals of

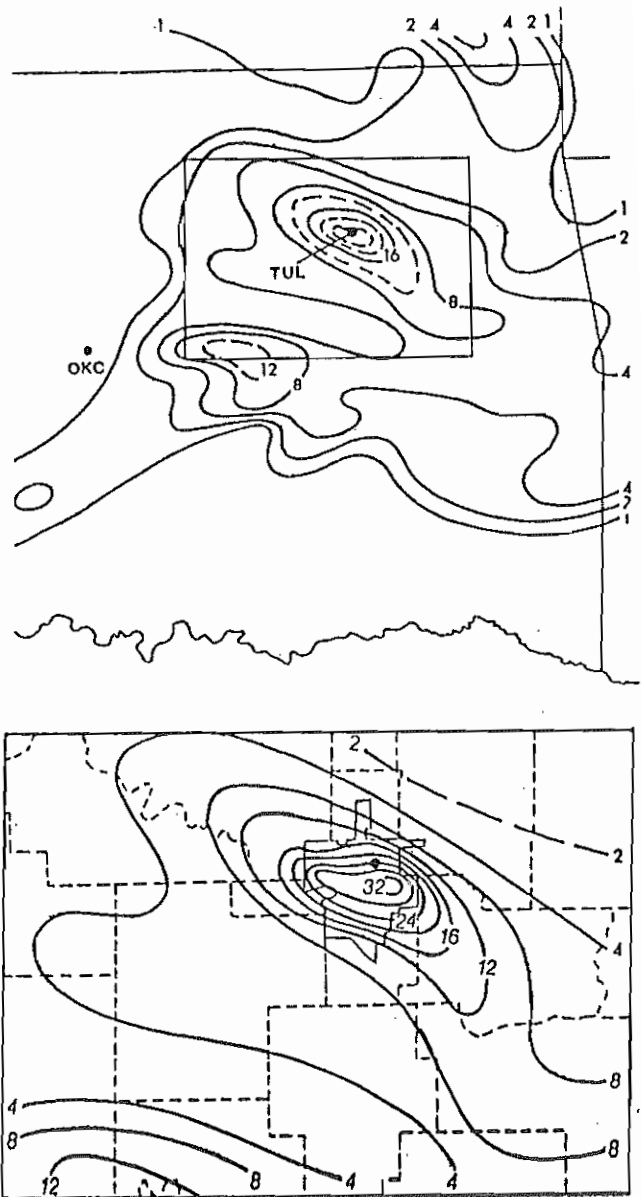


Fig. 1. Observed 24-h rainfall (cm) ending at 1200 GMT 27 May 1984. Locations of Oklahoma City (OKC) and Tulsa (TUL) are shown for reference. In the inset, Tulsa city limits are shown as thin solid lines; dashed lines are county boundaries.

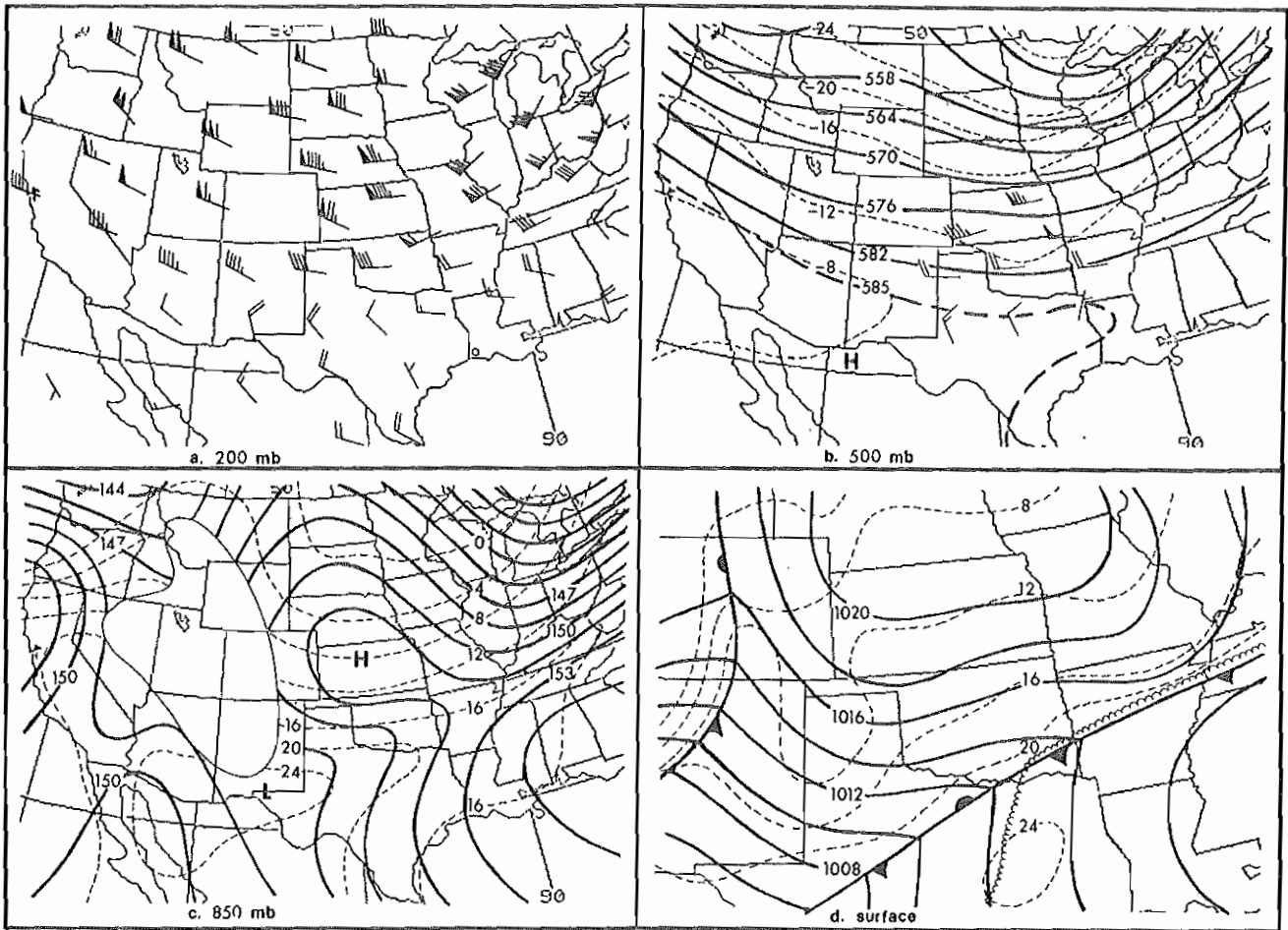


Fig. 2. Surface and upper-air charts valid at 1200 GMT 26 May 1984. Winds in a and b are plotted conventionally; full barb =  $5 \text{ m s}^{-1}$ , flag =  $25 \text{ m s}^{-1}$ . Heavy solid: height contours (Dm) in b and c, and msl pressure (mb) in d. Dashed: isotherms ( $^{\circ}\text{C}$ ) in b, c, and d. In d, scalloped line is  $20^{\circ}\text{C}$  isodrosotherm.

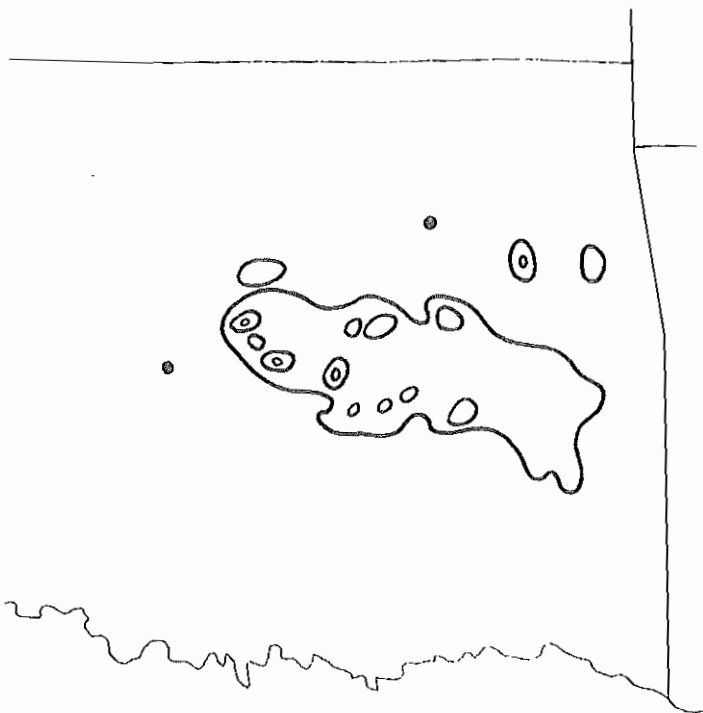


Fig. 3. Overlay from Oklahoma city WSR-57 radar display at 2330 GMT 26 May 1984. VIP contour levels 1, 3, and 5 are shown.

over 10 cm between 0000 and 0300 GMT, resulting in flooding over a small area roughly 100 km southwest of Tulsa (see Fig. 1).

Conditions at 0000 GMT 27 May are shown in Fig. 4. Very pronounced speed divergence was indicated over northeastern Oklahoma at 200 mb (Fig. 4a). Speed divergence was also evident in the same area 12 h earlier (Fig. 2a), but the magnitude of the divergence had increased considerably. The strongest westerlies remained well north of Oklahoma. The speed maximum formerly over Illinois moved to lower Michigan, while the jet streak over Wyoming 12 h earlier moved only slightly eastward.

At 500 mb (Fig. 4b) a pronounced shortwave trough appeared in the height field over central Oklahoma. "Appeared" seems appropriate in this case, since the 500 mb analysis at 1200 GMT 26 May (Fig. 2b) revealed no evidence of a trough approaching from the west. Furthermore, the trough was ageostrophic in nature, as evidenced by pronounced cross-contour flow toward higher heights from southern Missouri to northeastern Texas.

The 850 mb trough moved northward into northern Oklahoma and southwestern Missouri (Fig. 4c). However the thermal ridge remained stationary across northern Texas, resulting in a meso-scale region of strong warm advection centered over eastern Oklahoma. Winds north of the trough

veered to southwesterly and southerly, drawing moisture northward into the Dakotas.

The surface front sagged slowly southward into extreme southern Arkansas (Fig. 4d) but remained stationary across northern Texas. The thermal gradient north of the front strengthened considerably in response to outflow from the convection occurring over eastern Oklahoma and western Arkansas. Surface dewpoints remained high in the warm air over eastern Texas and Louisiana.

The sounding from Oklahoma City (OKC) at 0000 GMT 27 May (Fig. 5) reveals a deep moist layer extending to near 500 mb, and a strong frontal inversion below 850 mb. Precipitable water (surface to 500 mb) was 3.76 cm, or 151 percent of normal. The boundary layer was relatively stable, as indicated by a lifted index of 5. However, a showalter index of -3 and a K index of 38 indicate that the atmosphere was quite unstable above the frontal inversion. Branick (1982) found a similar distribution of stability preceding the disastrous flooding in New Orleans on 3 May 1978.

The vertical wind profile reveals strong veering in the lowest 200 mb, confirming the presence of strong low-level warm advection. Wind speeds were light, measuring less than 20 m s<sup>-1</sup> at all levels below 100 mb.

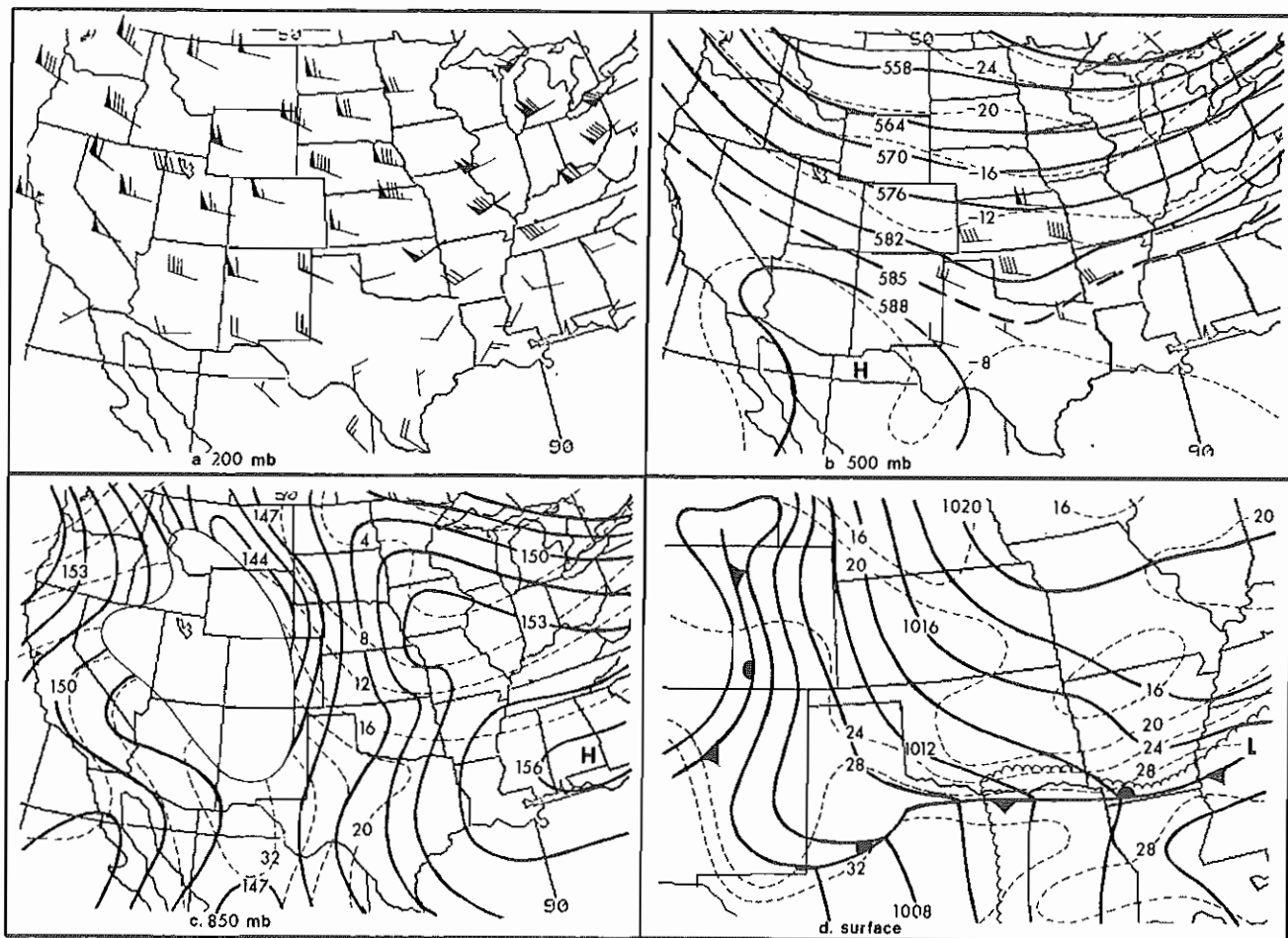


Fig. 4. As in Fig. 2, except valid at 0000 GMT 27 May 1984.

Most of the flood-producing rainfall in Tulsa fell between 0500 GMT and 1000 GMT. Mesoscale surface analyses during this time regrettably suffered from a loss of data resolution owing to the nighttime closing of several surface observation sites. Nonetheless, hourly surface analyses based on available data yield some insight into the mesoscale processes at work just prior to and during the deluge in Tulsa.

Surface analyses at 2-h intervals from 0300 GMT to 0900 GMT inclusive are shown in Fig. 6. The loss of data resolution precluded the accurate location of individual thunderstorm outflow boundaries during this period. However the analyses reveal several significant features, not the least of which is a distinct mesoscale pressure perturbation (trough?) that developed over southeastern Oklahoma by 0300 GMT and moved northward across Tulsa during the period of heaviest rainfall. The trough is evident in the wind field as well as the pressure field, suggesting that surface convergence was focused along the trough axis. A persistent moisture axis over southeastern Oklahoma advanced slowly northward with the surface trough. (Note the northward advance of the 16°C isodrosotherm into northeastern Oklahoma.) The surface front also drifted slowly northward into extreme southern Oklahoma, but remained well south of Tulsa.

Analyses valid at 1200 GMT 27 May (Fig. 7) depict the "post-storm" environment. Although extensive flooding was still occurring in Tulsa at 1200 GMT, heavy rainfall ended several hours earlier.

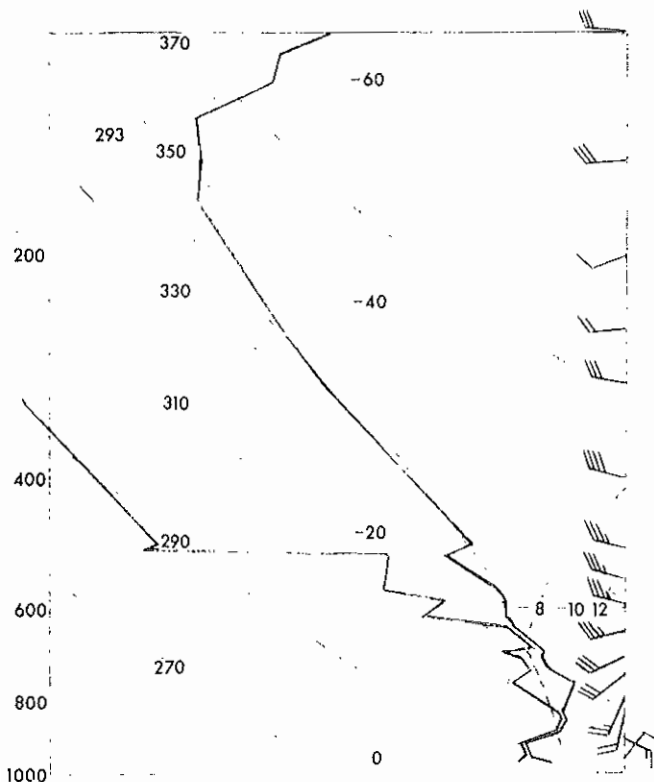


Fig. 5. Oklahoma City sounding, valid at 0000 GMT 27 May 1984. Winds are plotted conventionally; full barb = 5 m s<sup>-1</sup>.

Wind speeds increased slightly over the central Plains (Fig. 7a), with strong speed divergence still occurring over eastern Oklahoma and extending into central Kansas. Note that this area of divergence was located in the right rear quadrant of a speed maximum located over southern Iowa. At 500 mb (Fig. 7b), a shortwave trough was weakly evident over Missouri, moving eastward in advance of another (stronger) trough heading for the central Plains. Cooling of some 2°C had taken place over central Oklahoma, resulting in a thermal trough lagging behind the shortwave trough in Missouri.

At 850 mb, southerly winds increased over much of the central United States. Winds veered to southwesterly over Oklahoma as the 850 mb trough advanced northward into Kansas and Missouri (Fig. 7c). Strong warm advection preceded the trough into the central Plains and the upper Mississippi Valley. The strongest warm advection had thus moved north of Oklahoma, coinciding with the ending of heavy rain in the Tulsa area. A warm pocket developed from the 850 mb thermal ridge over southern Oklahoma and northern Texas. This warm pocket may have helped to focus low-level forcing (i.e. warm advection) and destabilization over northeastern Oklahoma during the night.

Surface data resolution improved by 1200 GMT with the reopening of several observation sites, revealing a rather strong mesohigh centered over the Oklahoma-Arkansas border (Fig. 7d). An associated wind shift line marked the leading edge of thunderstorm outflow from western Arkansas through southeastern Oklahoma into southern Kansas. The surface front appeared to be redeveloping further north across Kansas. Interaction between the thunderstorm boundary and this new front may have aided the development of new convection over south central Kansas (not shown).

### 3. DISCUSSION

The analyses presented in the previous section reveal key parameters at all levels that favored the development of deep convection and heavy rainfall. An examination of the interrelations between these parameters suggests that several known physical principles were at work during the Tulsa flood. These principles are discussed in the following subsections.

#### a) Transverse circulations accompanying jet streaks

Upper tropospheric jet streaks are subject to mass and momentum adjustments that result in transverse circulations within the entrance and exit regions of the jet streak. Uccellini and Johnson (1979) examined these circulations and investigated their role in the interaction (coupling) of upper and lower tropospheric jet streaks. The circulations, which are thermally direct (indirect) in the entrance (exit) regions of the jet streak, imply upward motion in the left front and right rear quadrants of the jet streak. As was shown in Figs 2a, 4a, and 7a, a jet streak was present at 200 mb to the northeast of Oklahoma. Thus the area in which flooding occurred was located in the right rear quadrant of an upper-tropospheric jet streak prior to and during the period of heavy rainfall. Although the jet

streak was centered some 1000 km northeast of the heavy rain area, it is plausible that a transverse circulation in the entrance region contributed to upward motion (and upper-tropospheric divergence) over northeastern Oklahoma.

b) Low-level warm advection

The role of low-level warm advection in forcing upward motion is often underestimated relative to the similar role of differential vorticity advection. Maddox and Doswell (1982) examined several cases of severe convection that occurred in areas of relatively weak mid-level vorticity advection, and found that each event developed within a strong and persistent region of lower-tropospheric warm advection. They concluded that thermal advection fields likely dominate differential vorticity advection in forcing vertical motion in these cases.

The diagnostic omega equation, from quasi-geostrophic theory (see, e.g., Holton, 1972, pp. 136-140), confirms the importance of both terms in forcing vertical motion. Physically, warm advection at a given level contributes hydro-

statically to a thickness increase that results in height falls (rises) below (above) that level. The resulting convergence/divergence leads to upward forcing by mass continuity. Adiabatic cooling of the ascending air offsets the warming due to advection, thus maintaining hydrostatic and geostrophic balance in the absence of pronounced differential vorticity advection. As such, the two terms often tend to cancel each other (Trenberth, 1978), so it is not unreasonable to expect warm advection to dominate in regions of weak (or even negative) differential vorticity advection.

Mid-tropospheric vorticity advection was indeed weak over Oklahoma prior to the Tulsa flood. (Recall that the shortwave trough over central Oklahoma at 0000 GMT 27 May was ageostrophic; vorticity advection by the observed winds was not well defined.) Hence we have another case of severe convection occurring in a region of strong low-level warm advection under relatively weak mid-level forcing. This finding supports the conclusions of Maddox and Doswell, i.e. that emphasis should be shifted from the 500 mb level to low-level thermal advection in order to better

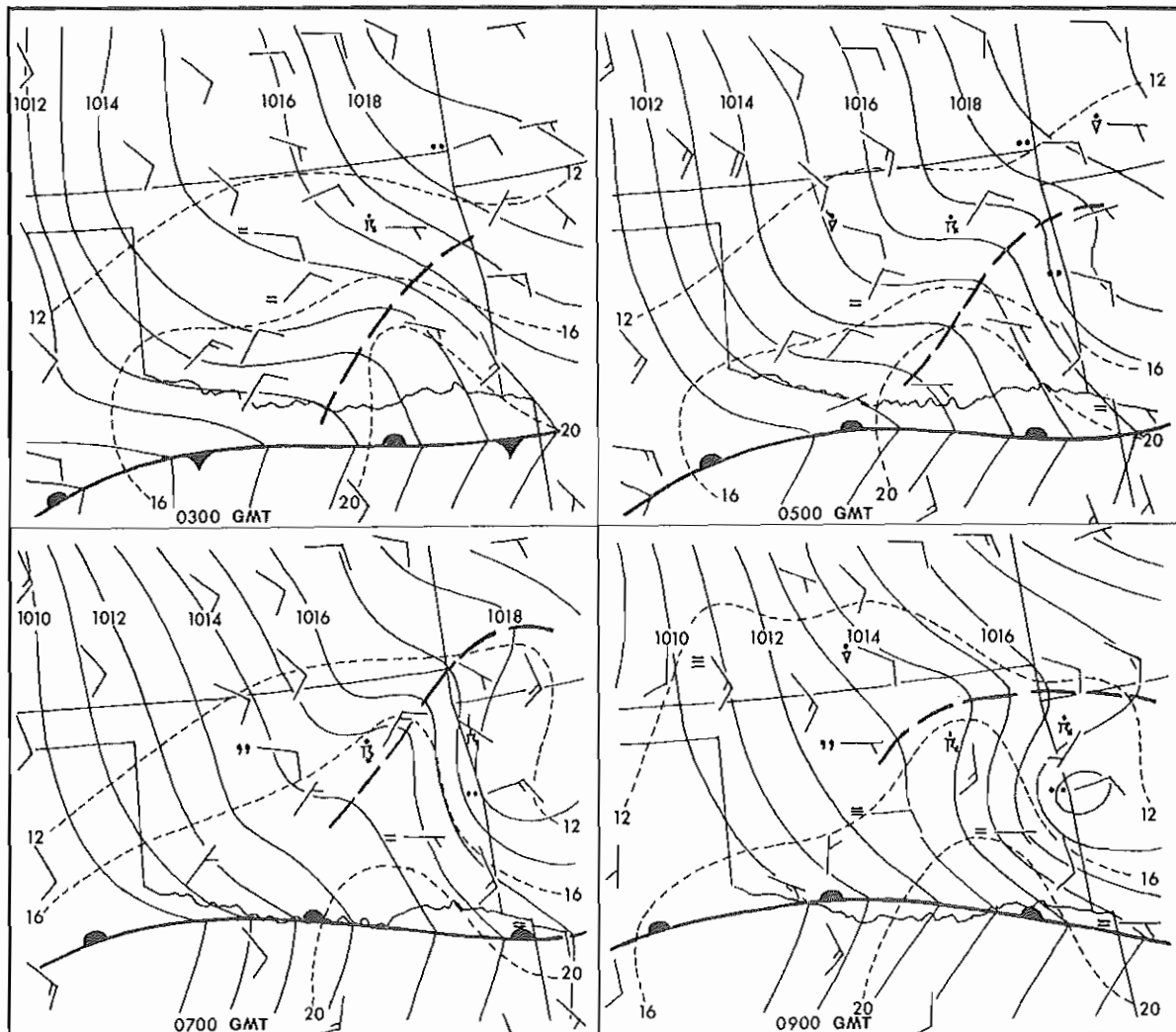


Fig. 6. Surface analyses at 2-h intervals from 0300 GMT to 0900 GMT, inclusive, 27 May 1984, Mean sea level pressure (solid) at 1-mb intervals. Surface dewpoint (dashed) at 4°C intervals. Surface winds and present weather are plotted conventionally.

anticipate organized convective outbreaks that occur within relatively benign synoptic settings.

c) Modification by convection

The increase in upper tropospheric divergence, and the appearance of subsynoptic-scale height falls and ageostrophic flow at 500 mb, suggests that the environmental setting was modified by intense convection prior to the occurrence of heavy rainfall in Tulsa. At 850 mb, the presence of strong warm advection south of the height trough suggests that the trough itself might have arisen (in part, at least) from convective modification. The fact that the 850 mb trough advanced northward while the surface front remained stationary further suggests that the 850 mb trough was not frontal in nature.

Convection may also have played a role in the development of the mesoscale surface pressure perturbation that enhanced surface convergence over Tulsa (Fig. 6). This perturbation, perhaps best described as a weak mesolow embedded in the larger-scale gradient flow, may have originated in the same manner as the 850 mb trough. Both features might have been the result of hydrostatic adjustments arising from the strong warm advection at low levels, enhanced by upper-tropospheric divergence. Although convection was not the main source of warm advection, additional warming above 850 mb may have been supplied by the convection via either latent heat release or convective-scale subsidence in the immediate

periphery of the convection. Hoxit et al. (1976) attributed the formation of mesolows or pressure troughs downwind of convective systems to upper-tropospheric subsidence warming. Similar regions of compensating subsidence might also focus pressure falls in other areas relative to the convection.

4. CONCLUSIONS

The interrelationships between the various changes and developments observed at virtually all levels suggest that complex interactions were taking place between the intense convection and the subsynoptic environment. As is often the case with convective events of this type, the precise nature of the interaction is elusive, owing to the "chicken-egg" question as to whether the changes resulted in or from the convection.

One possible sequence of events is as follows: Intense convection developed in an area of conditional instability and abundant moisture over eastern Oklahoma, aided by forcing at both upper levels (divergence) and at lower levels (warm advection). The convection enhanced upper-level divergence, which in turn generated height falls from 500 mb down to the surface. Height falls in lower levels (850 mb and below) were further enhanced hydrostatically by the strong low-level warm advection, and were focused into smaller-scale features by the pre-existing convection.

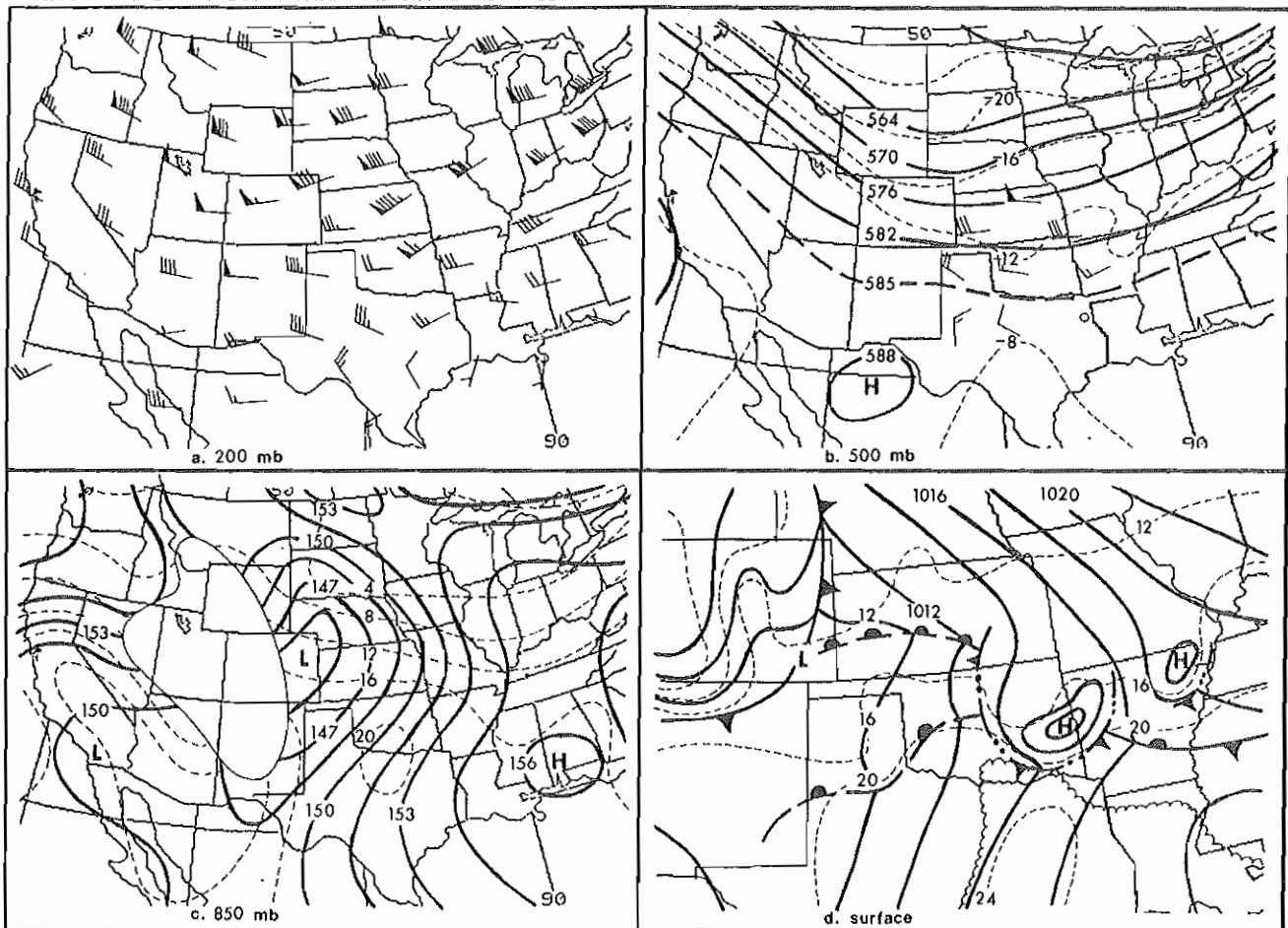


Fig. 7. As in Fig. 2, except valid at 1200 GMT 27 May 1984.

This scenario suggests a complex "convective feedback" mechanism, whereby intense convection developed within a favorable environment and modified the environment, which in turn aided the development of new convection and focused it over a small geographic area (in this case, Tulsa) in northeastern Oklahoma.

By relating these conclusions to the operational problem of forecasting an event such as the Tulsa flood, it becomes apparent that the task remains a difficult one. Although the subsynoptic environment may have provided sufficient cause for concern up to 12 h in advance, the scale of the event itself suggests that its ultimate character was governed by atmospheric interactions on scales that are too small to be resolved by current forecasting and observing techniques. It is beyond the scope of this study to say why the Tulsa metropolitan area was "selected" in this case, rather than some other area 50 or 100 km away. If that question cannot be answered through a post-analysis of operational data, then it certainly cannot be answered by the forecaster in real time.

Substantial improvements in forecasting such events will only come after we attain a more solid understanding of mesoscale phenomena and their interactions with other (larger and smaller) scales of motion. Until then, it will be up to the forecaster to assimilate all available subsynoptic data and delineate a larger area within which the potential exists for such an event.

#### ACKNOWLEDGEMENTS

The author wishes to thank Drs. Robert Maddox and Kenneth Crawford, Prof. Lance Bosart, Jim Belville, Mike Mogil, and Dave Olson for their helpful comments and reviews of the original manuscript. The author also acknowledges Eldon Beard for his assistance in obtaining rainfall data, and the staffs of the National Severe Storms Forecast Center and the Heavy Precipitation Branch, NMC, for assistance in obtaining selected radar and upper-air data.

#### REFERENCES

- Branick, M. L., 1982: Mesoscale Analysis of the 3-4 May 1978 Mesoscale Convective Complex over the Southern United States. M. S. Thesis, State University of New York at Albany, 107pp.
- Holton, J. R., 1979: An Introduction to Dynamic Meteorology, second edition. Academic Press, Inc. (New York), 391pp.
- Hoxit, L. R., C. F. Chappell and J. M. Fritsch, 1976: Formation of mesolows or pressure troughs in advance of cumulonimbus clouds. Mon. Wea. Rev., 104, 1419-1428.
- Maddox, R. A. and C. A. Doswell III, 1982: An examination of jet stream configurations, 500 mb vorticity advection and low level thermal advection patterns during periods of intense convection. Mon. Wea. Rev., 110, 184-197.
- Trenberth, K. E., 1978: On the interpretation of the diagnostic quasi-geostrophic omega equation. Mon. Wea. Rev., 106, 131-137.
- Uccellini, L. W. and D. R. Johnson, 1979: The coupling of upper and lower tropospheric jet streaks and implications for the development of severe convective storms. Mon. Wea. Rev., 107, 682-703.



SYNOPTIC PATTERN TYPES ASSOCIATED WITH HEAVY SNOWFALL EVENTS IN OKLAHOMA

Michael L. Branick

National Weather Service Forecast Office  
Oklahoma City, Oklahoma 73159

1. INTRODUCTION

The establishment of a climatology for any type of hazardous weather event is vital to the effective forecasting of such an event. Identification of synoptic pattern types associated with these events has been shown to be an important part of such a climatology. Maddox *et al.* (1979) and Belville (1982) have identified pattern types associated with heavy rain and flash flood events. In this study, synoptic pattern types accompanying heavy snowfall events in Oklahoma have been identified.

Heavy snow is quite rare in Oklahoma compared to other parts of the United States. Yet snowfalls of four inches or more in 24 h occur within the state on the average of more than four times a year. Hence heavy snow occurs with sufficient frequency to pose a significant challenge to the forecaster, yet is rare enough that the public response to the related hazards can easily become one of apathy.

Using monthly climatological data, 137 heavy snow events were identified in Oklahoma during the period 1951-1984. An event was defined as a 24-h snowfall of four inches or more at one or more reporting stations. (Since snowfall measurement techniques are somewhat less objective than those for rainfall, at least two reports of heavy snow were required if the maximum amount was between four and six inches.) Heavy amounts occurring during two consecutive periods, whether in the same area or in different parts of the state, were generally treated as a single event. The 137 events thus identified were used to generate monthly frequency statistics that are presented in the next section.

Surface and 500 mb charts from the Daily Weather Map series were used to identify synoptic pattern types for 79 of the events occurring between October 1968 and May 1984. The charts in the Daily Weather Map series are rather crude, but provided enough detail to determine the synoptic pattern type that accompanied each of the 79 events.

2. SEASONAL AND GEOGRAPHIC DISTRIBUTIONS

The monthly distribution of heavy snowfall events in Oklahoma, 1951-1984, is shown in Fig. 1. Heavy snow has fallen in Oklahoma as early as October 7 and as late as May 2, but reaches a peak in frequency sometime in February. The frequency increases gradually during late fall, but drops off sharply in April. This difference can be attributed to the southerly low-level jet (LLJ), which climatologically appears more frequently over the Plains in early spring than

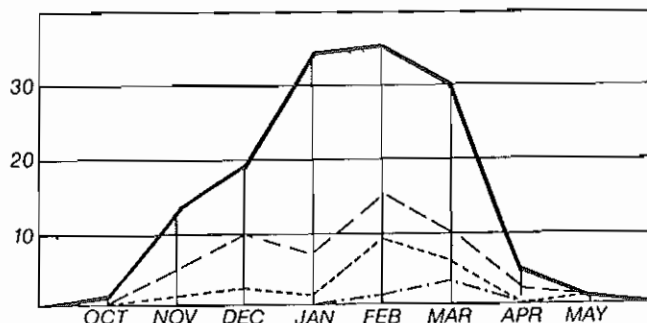


Fig. 1. Total number of heavy snow events in Oklahoma by month, 1951-1984. Heavy solid: all events of four inches or more in 24 h. Long dashed: events of eight inches or more. Short dashed: events of 12 inches or more. Dash-dot: events of 16 inches or more.

in late fall (see, e.g., Bonner, 1968). During April, warm air moves northward with increasing frequency, and the associated LLJ often transforms many "would-be" April snowstorms into rain events.

The LLJ is also believed to contribute to another interesting pattern in Oklahoma, namely the preponderance of "major" snowstorms (with amounts in excess of 12 inches) in March. As shown in Table 1, three of the four heaviest snowstorms that have occurred in Oklahoma since 1951, and five of the top 11, have occurred in March. The increase in LLJ frequency as spring approaches results in an increasing influx of moisture from the Gulf of Mexico - a moisture source not normally as "open" during late fall and winter. Low-level moisture convergence associated with both the LLJ and nearby surface cyclogenesis (which peaks in March over the Colorado area; see Whittaker and Horn, 1981)

Table 1. Ten heaviest snowstorms in Oklahoma, 1951-1984. Geographic location of each site, e.g. PH (panhandle), NC (north central), etc. are given in parentheses.

Date	Max. storm total (in.)
1. February 21-22, 1971	36.0 at Buffalo (NW)
2. March 16, 1970	20.0 at Bartlesville (NE)
3. March 6-7, 1958	18.0 at Boise City (PH)
4. March 30-31, 1973	17.0 at Kenton (PH)
5. February 4, 1954	15.0 at Reydon (WC)
6. November 1, 1951	14.0 at Alva (NW)
7. December 10-11, 1960	14.0 at Buffalo (NW)
8. March 11-12, 1968	14.0 at Jay & Miami (NE)
9. March 14-15, 1969	14.0 at Beaver (PH)
10. January 22, 1973	14.0 at Woodward (NW)
February 2-3, 1982	14.0 at Helena (NC)

also contributes to greater precipitation amounts in early spring.

The monthly distribution of eight- and 12-inch events (Fig. 1) reveals a distinct relative minimum in January, although the January total for all events is quite high. In other words, a high percentage of January heavy snow events are only in the four- to eight-inch range. This result reflects the dominance of cold arctic air masses in January; although cold air is plentiful, moisture is suppressed further south during the heart of the cold season.

The geographic distribution of heavy snow events from 1969 to 1984 is shown in Fig. 2. While frequencies generally decrease from north to south (as might be expected), the smaller-scale variations strongly suggest that orography plays a major role. Maximum values tend to occur in either high-elevation areas, where surface air is generally colder, or in areas that are subjected to upslope conditions when the surface flow is easterly or northeasterly.

The analysis of surface synoptic patterns reveals that surface winds are almost always easterly or northeasterly during the period of heavy snowfall. In this flow regime, the frequency maxima in the western panhandle, in the interior northwest, and in a band through interior southern Oklahoma coincide with regions of upslope surface flow (see Fig. 2). Frequencies are also related directly to elevation itself, as evidenced by higher frequencies in the higher

elevations of the northwest, the Ozark Plateau in the northeast, and along the Arbuckle and Ouachita Mountains in south central and southeastern Oklahoma. Minima appear in the Arkansas and Red River basins of northeastern and extreme southern Oklahoma respectively. Note that these areas of minimum frequency also appear to be correlated with downslope flow under northeasterly wind conditions.

The variations found in heavy snow frequency over northwestern Oklahoma can not be correlated entirely to orographic effects. Pronounced maxima found near Boise City and Woodward, and the minimum near Kingfisher, may reflect either sampling deficiencies or deficiencies in snowfall measurement as discussed in section 1.

### 3. SYNOPTIC PATTERN TYPES

Several factors combine to make the classification of synoptic pattern types difficult for heavy snow events. For one, each event is actually unique; although two events may exhibit the same synoptic-scale flow pattern, the subsynoptic and mesoscale features are often entirely different. Secondly, synoptic flow patterns often undergo significant changes over a relatively short time during the cold season. Sudden amplification or rearrangement of the 500 mb longwave pattern can create difficulty in identifying a single pattern type should heavy snow fall during the period of change. As such, many events are "hybrids" that exhibit qualities of two pattern types. Finally, most of the events are actually mesoscale, not synoptic-scale, phenomena. Hence the classification of

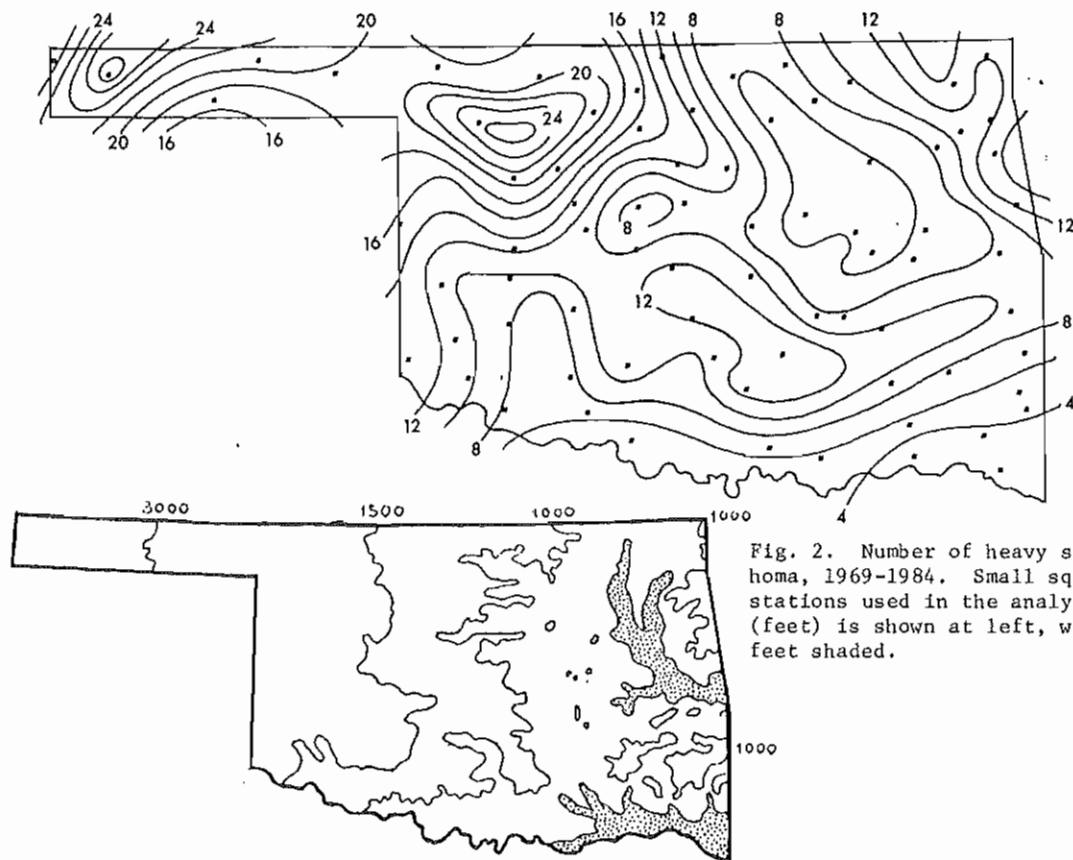


Fig. 2. Number of heavy snow events in Oklahoma, 1969-1984. Small squares represent stations used in the analysis. Elevation (feet) is shown at left, with areas below 600 feet shaded.

synoptic pattern types will typically provide little information on the precise timing and location of the heaviest snow. In this sense, the recognition of pattern types will only alert the forecaster that heavy snow is possible somewhere. Subsequent subsynoptic analyses are needed to determine the exact focusing mechanism and thus "zoom in" on the main threat area. This approach is similar to that developed by Belville (1982) in his analysis of heavy rainfall patterns on Louisiana.

Despite these shortcomings, six synoptic pattern types have been identified that are associated with heavy snow in Oklahoma. Although upper-level support is present in each type, it must be remembered that two other ingredients - moisture and cold air - must also be present. A shortage of either will seriously reduce the chance of heavy snow, even if the synoptic pattern is identical to one of the six identified herein.

The six pattern types are based on the following 500 mb longwave patterns:

- A) Ridge to the west with an embedded shortwave trough;
- B) Broad trough over central North America;
- C) Trough to the west with southwesterly flow aloft;
- D) Migratory eastward-moving closed low;
- E) Migratory eastward-moving open trough;
- F) Deepening low (with surface cyclogenesis).

Before discussing the pattern types individually, it is worthwhile to discuss several general characteristics of Oklahoma snowstorms that frequently appear regardless of pattern type. To begin with, heavy snowfall is usually highly localized, with the heavy snowfall area often no larger than two or three counties. This finding implies that heavy snow events are predominantly mesoscale phenomena in Oklahoma, rather than synoptic or even subsynoptic. Another common feature (observed in 80 percent of the events) is the presence of a closed low at 500 mb. When a closed low is present, heavy snow typically falls north of the track of the low. But even if no low is present at 500 mb, heavy snow almost always falls to the north of the track of the cyclonic vorticity maximum. (This maximum sometimes tracks further south than the low center. In these cases, heavy snow occurs in a band south of the track of the low, and north of the track of the vorticity maximum.) This finding is consistent with the results of Fawcett and Saylor (1965) and Goree and Younkin (1966); both studies found a pronounced maximum occurrence of heavy snow along and to the north of the track of the 500 mb vorticity maximum.

At the surface, winds inevitably begin with an easterly component (usually northeasterly), but back to northwesterly or northerly by the time snow ends. Backing sometimes occurs with the passage of a cold front, or of a surface low to the south of the heavy snow area. However a significant number of events occur without a surface low or front present in or near Oklahoma. A vast majority of events occurred with a surface low, initially west of Oklahoma, that weakened or dissipated as it moved eastward, only to redevelop well to the east or southeast

of Oklahoma. In these cases, winds backed in response to either a redeveloping low, the passage of an inverted surface trough, or surface pressure rises to the west as the surface ridge redeveloped further westward.

In the following discussion of pattern types, four composite charts are presented for each type. The two charts on the left are 500 mb and surface composites representing the (first) 24-h period in which heavy snow fell. The remaining two charts are composites valid 24 h later. The charts thus do not necessarily correspond to the actual beginning and end times of heavy snow, but rather bracket the (first) 24-h period in which heavy snow fell.

#### 1. Pattern A

Pattern A is identified by a longwave ridge west of Oklahoma, and a trough near the East Coast (Fig. 3). Although this pattern implies northwesterly flow over Oklahoma, such is not the case; a shortwave trough breaking through the ridge provides the upper-level support for precipitation, and usually maintains a 500-mb flow over Oklahoma that is south of west. The shortwave trough often extends from Mexico well north into northern Canada. In roughly half of the cases, a closed low developed in the southern end of the trough before it moved into Oklahoma.

This type exhibits a distinct surface pattern characterized by a massive arctic high over the western Great Lakes, with a ridge southward through the Mississippi Valley. The surface flow is thus easterly over Oklahoma. The ridge persists throughout the event despite the approach of the upper-level trough. A weak low sometimes develops in the Gulf of Mexico; otherwise no

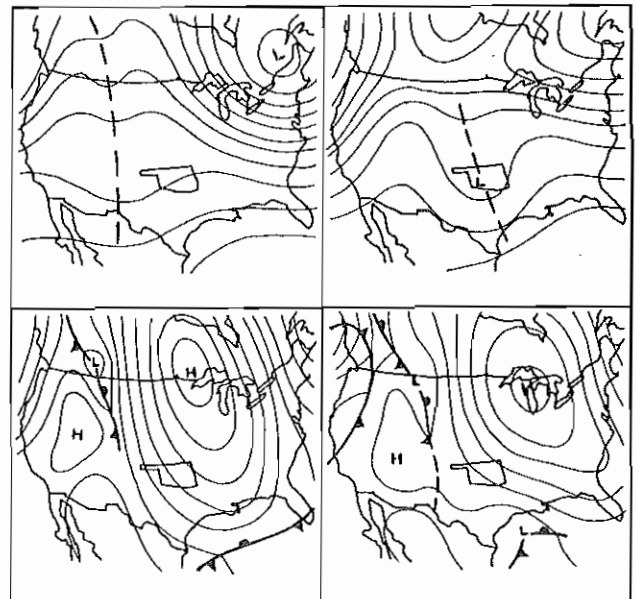


Fig. 3. Composite 500 mb (top) and surface (bottom) charts for pattern A heavy snow event. Left and right charts are separated by 24 h (see text).

surface low or front is present. In fact, surface streamlines typically remain anticyclonic over Oklahoma. Upslope flow thus appears to be the main low-level forcing mechanism. (Note: the longwave trough near the East Coast often results in surface cyclogenesis near the coast. Pattern A events in Oklahoma are often preceded within 48 h by a "Nor'easter" over New England or the mid-Atlantic states.)

This pattern was identified in 12 events, or 15 percent of the total. Snowfall is typically localized, with amounts usually in the four- to six-inch range.

#### ii. Pattern B

A broad cyclonic flow at 500 mb dominates most of the United States in this type, with a major trough axis over or just west of Oklahoma (Fig. 4). A strong ridge is typically present over the eastern Pacific, resulting in pronounced meridional flow over western North America. Winds aloft are very strong relative to most of the other pattern types.

Pattern B is unique in that the longwave pattern is almost totally dominant. A shortwave trough is often present upstream from the major trough axis, and occasionally carries enough energy to shift the longwave trough slightly further east. However, many pattern B events occur without the presence of a discernible shortwave trough.

This is a cold pattern for much of the central and western United States, as the strong northerly flow aloft drives repeated surges of arctic air southeastward from western Canada. Heavy snow typically falls within 12 h after the passage of a cold front as a new surge of arctic air arrives. However, events of this type that strike the panhandle area are often associated with upslope flow, with snow falling well north of the front.

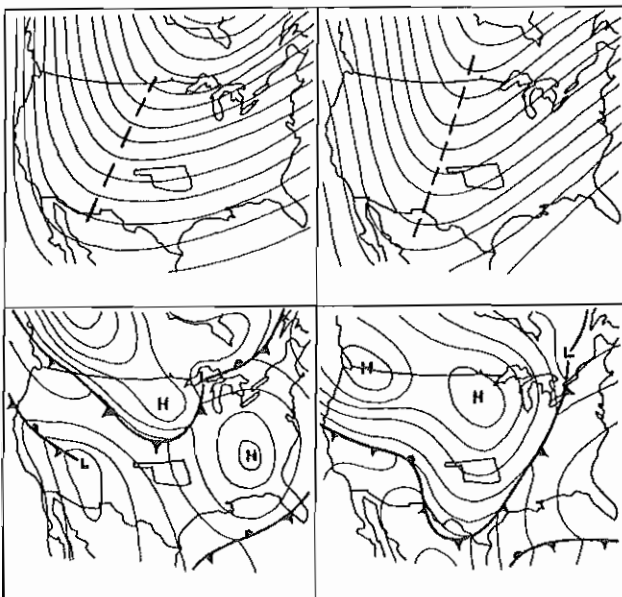


Fig. 4. Pattern B 500 mb and surface composite charts. Format as in Fig. 3

Of all the pattern types, this is perhaps the most difficult to forecast because of the lack of a strong shortwave trough. Accurate forecasts of a pattern B event may depend almost entirely on detailed examination of low-level features such as convergence and warm advection. Nine events of this type were found (12 percent of the total), most of which occurred in northwestern or southern Oklahoma. Four of the nine events produced storm totals of more than eight inches.

#### iii. Pattern C

Pattern C is identified by a stationary or slow-moving 500 mb trough that remains west of Oklahoma. The occurrence of heavy snowfall with this pattern is rather surprising, since the prevailing southwesterly flow aloft would seemingly inhibit the intrusion of sufficient cold air. However this pattern type evolves from an almost total reversal of the longwave pattern that takes place one or two days before the event. The flow aloft initially resembles pattern A, with a ridge to the west and a shortwave trough breaking through it. But the shortwave trough intensifies rapidly; a closed low develops and moves almost due south into the southwestern United States (Fig. 5). Heights rise to the east as the East Coast trough lifts out, and the flow aloft over Oklahoma becomes southwesterly. A weak shortwave trough is usually present in the southwesterly flow.

Surface features are also initially similar to pattern A, with an arctic ridge to the east and easterly flow over Oklahoma. However pressures are much lower over the southwestern states, and a closed low is usually present over New Mexico. The low moves southeastward and dissipates, and its associated front becomes stationary well south of Oklahoma. Pressures rise over the northern Rockies, and the arctic ridge becomes reoriented east-west to the north of Oklahoma. Surface winds back to northerly,

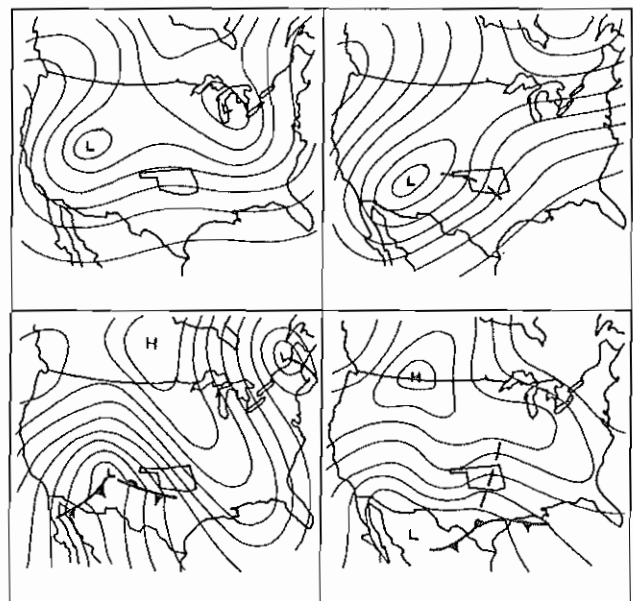


Fig. 5. Pattern C 500 mb and surface composite charts. Format as in Fig. 3.

often due to the passage of an inverted surface trough.

Only six cases of this type were identified, or eight percent of the total. Most occurred in February or March, and all were confined to the northern third of the state. Three of the six events produced storm totals of over eight inches; maximum amounts were directly related to the strength of the initial easterly surface flow.

#### iv. Pattern D

A closed low tracking eastward across (or near) Oklahoma at 500 mb identifies pattern D. This pattern type may often resemble pattern A; in fact, most of the hybrid events were combinations of A and D. But in pattern D the entire longwave trough progresses eastward with the low. The actual configuration of the trough varies. In many cases the flow is meridional and the trough and low are of considerable magnitude (Fig. 6a). In other cases the longwave pattern may be closer to zonal; the low, although well-developed, is detached from the main westerlies (Fig. 6b). But in all cases the low is associated with a split-flow regime, and the southern branch of the westerlies is well defined to the south of the low. (In meridional flow cases, the southern branch is typically dominant.) The upper low typically passes very close to the four-corners area, then tracks east or east-southeast during the following 24 h.

The surface pattern is typically dominated by a northeasterly flow of arctic air, which backs to northwesterly as surface cyclone development takes place to the east or southeast of Oklahoma. Only about a third of the pattern D cases were accompanied by a surface low tracking eastward across Oklahoma or Texas. In most of these cases the low weakened or dissipated as it moved eastward, but redeveloped further east. (Cyclogenesis in the northern Gulf of Mexico is common with this pattern type.) Only a very few events of this type were accompanied by a frontal passage. In most cases, the front had already moved well south and east of Oklahoma prior to the beginning of heavy snow.

Pattern D is by far the most prolific of the heavy snow patterns in Oklahoma, accounting for 32 events or 42 percent of the total. Storm snowfall totals of up to 20 inches have occurred, with amounts of over eight inches common. In fact, amounts of 12 inches have occurred as far south as Durant in southeastern Oklahoma. Events of this type tend to occur most often during the early winter and again in March. Snowfall is frequently accompanied by thunder in these events, especially if the surface front remains relatively close to Oklahoma (e.g. northeastern Texas or southern Arkansas).

#### v. Pattern D1

This is a subtype of pattern D, and is identified by a very large and intense cutoff low at 500 mb initially over northern Baja California. The low is totally detached from the main westerlies, which lie across southern Canada or the northern United States. The

westerlies are quite active, with shortwave troughs initially located well to the northeast and northwest of the low. A shortwave ridge is thus located directly north of the low. Action begins when the upstream trough dives south-eastward and becomes a "kicker" for the upper low (Fig. 7). The low is thus ejected north-eastward across Oklahoma.

A large surface high dominates much of the western and central United States, but shifts eastward as 500 mb heights build over the eastern United States and surface pressures fall ahead of the upper low. A surface low develops over western Texas, with a secondary low often forming near the Gulf coast. Both lows remain quite weak. The upper trough diving into the western United States is accompanied at the

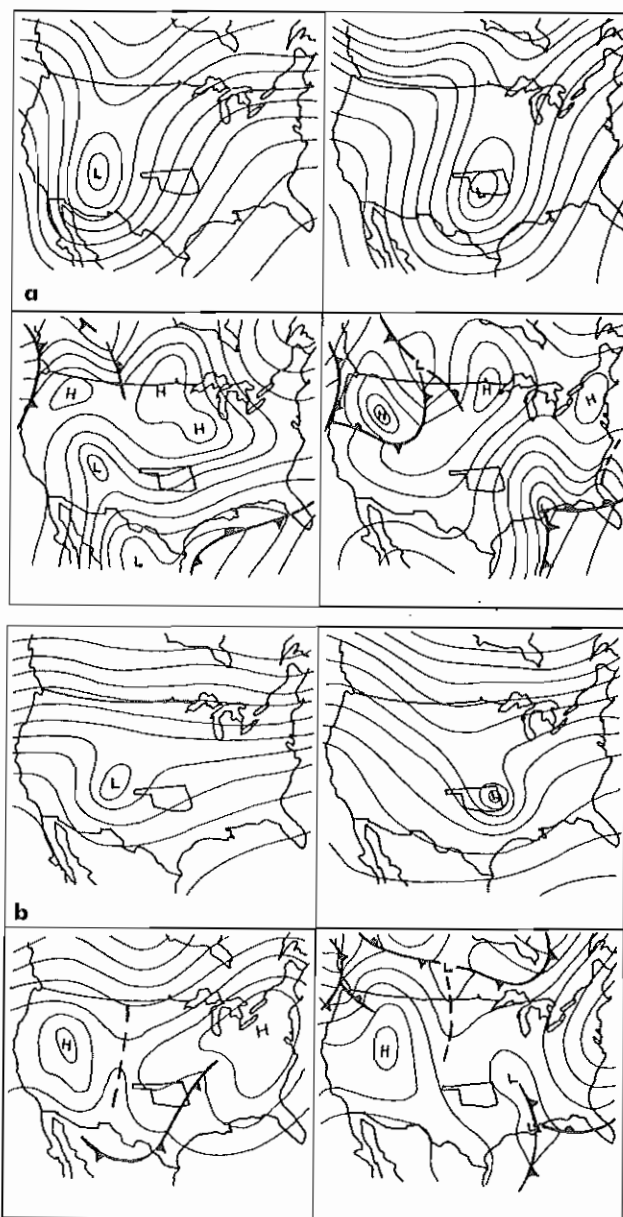


Fig. 6. Pattern D 500 mb and surface composite charts; meridional flow (a) and zonal flow (b). Format as in Fig. 3.

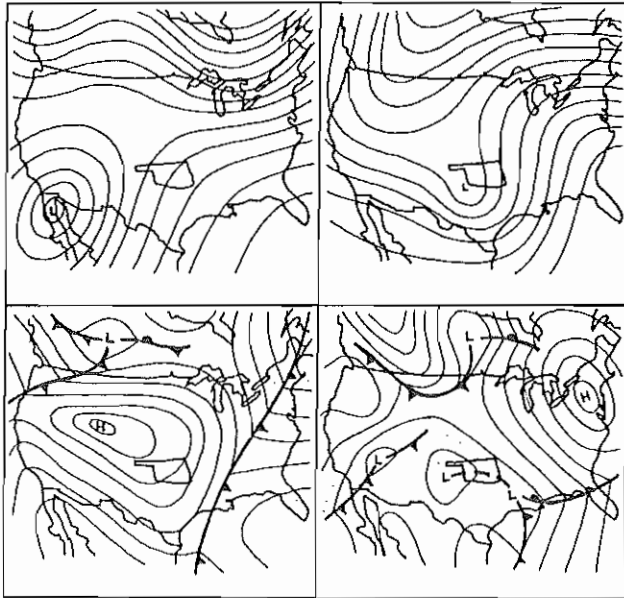


Fig. 7. Pattern D1 500 mb and surface composite charts. Format as in Fig. 3.

surface by a strong surge of arctic air into the northern Rockies and Plains. This air typically arrives in Oklahoma one or two days after the heavy snow.

Pattern D1 is rare, accounting for only three events. All three occurred in late December or early January. Snowfall was relatively light (seven inches or less), and all events were confined to the northwestern third of Oklahoma.

#### vi. Pattern E

Pattern E is in many ways similar to pattern D, the main difference being the lack of a closed low at 500 mb. A split-flow trough is initially present to the west of Oklahoma, but the split disappears as the trough moves eastward (Fig. 8). A closed low may initially be present in the southern part of the trough, but the low opens up before reaching Oklahoma.

The surface pattern is also similar to that of pattern D, a quasi-stationary front is usually present from the mid-Atlantic coast into the western Gulf of Mexico. A large, cold high is centered north and east of Oklahoma, but this high gives way as a wave of low pressure develops along the front near the Gulf coast. Surface winds back to northwesterly over Oklahoma as this low intensifies and a surface high over the Rocky Mountains builds southeastward.

Fourteen events of this type were found, or 18 percent of the total. This pattern is typically not conducive to major snowfalls in Oklahoma, as none of the events produced a storm total of over eight inches. However the area of heavy snowfall can be extensive (as much as half the state).

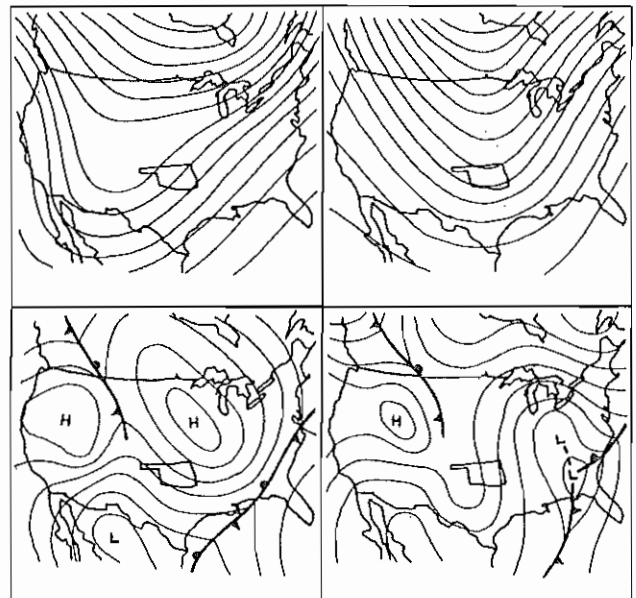


Fig. 8. Pattern E 500 mb and surface composite charts. Format as in Fig. 3.

#### vii. Pattern F

The 500 mb flow in this type is dominated by a rapidly-intensifying low over the central United States. This pattern type can actually evolve from any of the others (usually pattern D), but the key to pattern F is intensification. Meridional flow is initially present, with a trough over the western United States. The strongest winds are on the back (west) side of the trough; a shortwave trough dives southeastward in this flow and phases with the low or trough in the southern branch, forming a deep closed low. The low then moves eastward and continues to intensify, often becoming elongated with a negative tilt before it turns northeastward (Fig. 9).

Cyclogenesis is the key to the surface pattern in this type. A surface low forms initially over the four-corners area or the Front Range of eastern Colorado, then deepens and moves southeastward toward Texas. Deepening continues as the low turns northeastward across Oklahoma or Arkansas. The central pressure typically falls 6 to 12 mb during the ensuing 24 h and reaches its lowest value over the upper Mississippi Valley.

Pattern F events are notorious for more than just heavy snow in Oklahoma. A deepening surface cyclone tracking through the state can generate just about any type of hazardous weather imaginable. Tornadoes, hailstorms, flooding, and ice storms have occasionally accompanied this type of event in addition to heavy snow. Roughly half of the pattern F events were accompanied by severe thunderstorms in Oklahoma, but in all cases the severe weather reports were isolated and confined to the southeastern half of the state. (More widespread outbreaks typically occur over

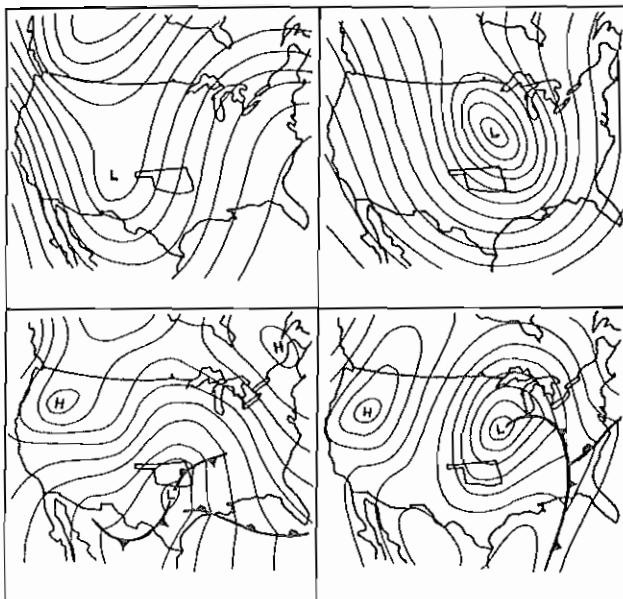


Fig. 9. Pattern F 500 mb and surface composite charts. Format as in Fig. 3.

Texas or the Gulf states, if they occur at all.) Temperature spreads of 20°C or more are common between the panhandle and southeastern Oklahoma, adding to the enormous forecasting challenge posed by a pattern F event.

Eleven events of this type were found, or 14 percent of the total. Five of these events produced storm totals of eight inches or more, one of which was the blizzard of 21-22 February 1971 that dropped a state-record 36 inches on Buffalo, in northwestern Oklahoma. All but the south central parts of the state have been hit. The heavy snow typically falls in the "backlash" area to the northwest of the deepening surface low; thus the track of the low is critical when determining the best threat area. Pattern F is mainly a mid-winter event, with all but two of the events occurring in January or February. Only one event occurred in March; the other occurred in early October, and was the only October event found in the entire study.

#### viii. Pattern F1

This subtype of pattern F is also characterized by cyclogenesis at both the surface and 500 mb. The only difference is in the track of the low - the pattern F1 low develops and moves further east (Fig. 10).

This subtype was primarily included because of the origin and track of the surface low. In pattern F1, the low develops over extreme southern Texas or along the Texas coast, rather than over the southern Rockies. The northeastward track of the pattern F1 low is significantly further south and east of the pattern F low. (This track, across northern Mississippi to near Lake Erie, was remarkably consistent in the few events identified.) Maximum strength is usually attained when the low reaches the eastern Great Lakes. A secondary low may form near the mid-Atlantic coast and take over thereafter.

Deepening rates are greater than those of pattern F lows; a 24-h fall in central pressure of 40 mb was observed on one occasion.

Pattern F1 is rare, accounting for only four events. However snowfall can be excessive, as two of the four events produced storm totals of over 12 inches in parts of eastern Oklahoma. Pattern F1 is the only pattern type identified that does not affect northwestern Oklahoma; all four events were confined to the southeastern half of the state. (As in pattern F, heavy snow falls to the northwest of the deepening surface low. Northwestern Oklahoma is therefore too far from the low in this pattern.) All four events occurred during the heart of the cold season, January and February.

#### 4. LIMITATIONS TO SYNOPTIC PATTERN RECOGNITION - TWO CASE STUDIES

As mentioned in the previous section, identification of synoptic pattern types is subject to a number of limitations. In this section, two case studies are examined that demonstrate these limitations.

##### i. Case 1: The blizzard of 21-22 February 1971

This case was chosen because of its extreme severity. Numerous stations in northwestern and north central Oklahoma recorded storm totals of over 18 inches, and the maximum storm total of 36 inches at Buffalo was nearly twice that of any other event in this study.

This case was classified as a pattern F event. The 500 mb flow was dominated by the development of a large and intense low over southern Kansas (Fig. 11). Surface features reflected this development, as a surface low initially over eastern Texas deepened and moved northeastward into Missouri (see Fig. 11).

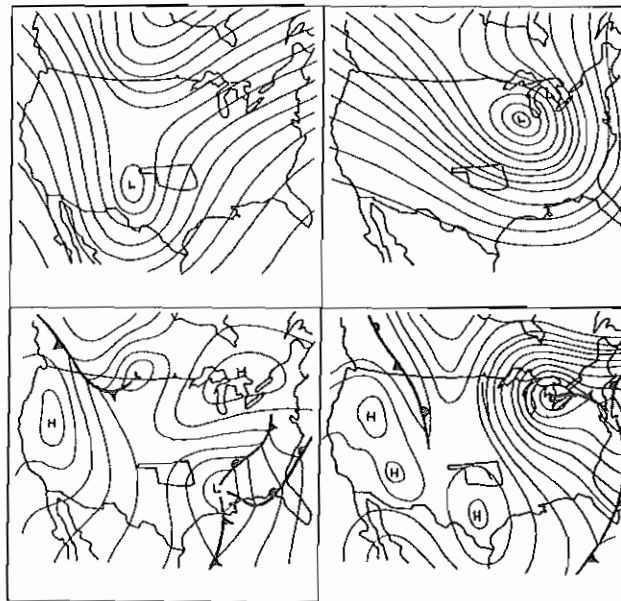


Fig 10. Pattern F1 500 mb and surface composite charts. Format as in Fig. 3.

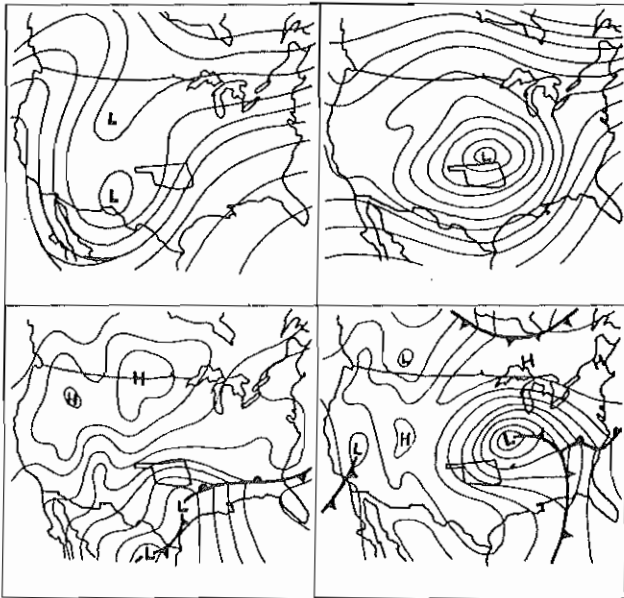


Fig. 11. 500 mb (top) and surface (bottom) charts valid at 1200 GMT 21-22 February 1971.

Comparison of the pattern F composite charts with those of 21-22 February 1971 reveals that the general evolution of the February 1971 storm is similar to pattern F, but that the details are quite different. The small-scale differences are due to generalizations that, by necessity, were incorporated into the composites. These differences, such as in the exact locations and intensities of the various troughs, ridges, pressure centers, and fronts, will occur with virtually every event regardless of the pattern type. As such, the composites should not be interpreted as exact replicas of a "typical" pattern type event, since a "typical" event will probably never occur.

ii. Case 2: 19-20 January 1983

Of the 79 events used to identify pattern types, there was only one event that could not be classified. That event, which occurred on 19-20 January 1983, produced a band of four- to six-inch snowfall from south central to north-eastern Oklahoma.

The winter of 1982-83, which coincided with an unusually strong "El Nino" phenomenon over the equatorial Pacific, was a meteorological oddity in many ways (Quiroz, 1983). The 500 mb flow over the United States (Fig. 12) was relatively weak but unusually chaotic, with closed lows appearing at a variety of latitudes and no well-organized jet stream. Although characteristics of nearly every pattern type can be found in the January 1983 charts, the overall flow pattern does not correlate with any of the flow patterns identified in the other 78 events. Hence it becomes apparent that the pattern types identified in this study do not represent all heavy snow events that may occur in Oklahoma. "Freak" snowstorms may rarely occur under flow patterns that do not match any of the six pattern types.

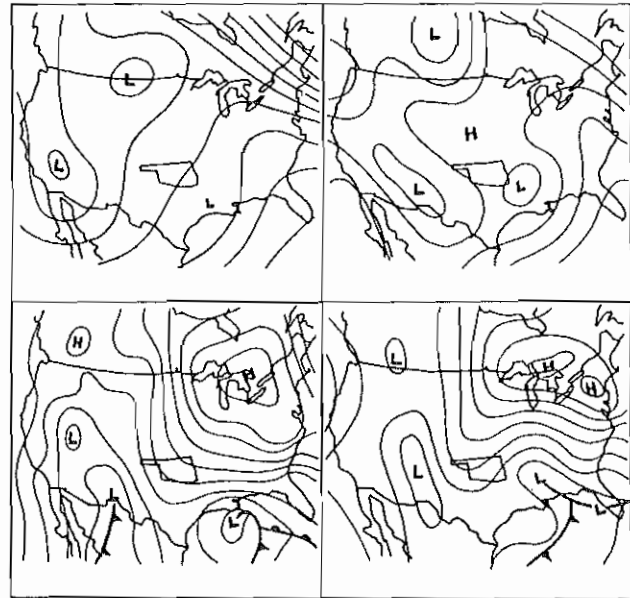


Fig. 12. 500 mb (top) and surface (bottom) charts valid at 1200 GMT 19-20 January 1983.

5. CONCLUDING REMARKS

Recognition of synoptic pattern types can play an important role in the medium-range forecasting (one to two days in advance) of heavy snowfall. Numerical forecast output may reveal a developing flow pattern resembling one (or more) of the heavy snow patterns, thus alerting the forecaster with the first clue that heavy snow may be on the way. Subsequent monitoring of the developing situation will then narrow down the most likely time and location of heavy snowfall.

Pattern recognition will only help with the initial recognition of heavy snow potential. Further studies of subsynoptic and mesoscale flow patterns are needed to help with the assessment of heavy snow potential on smaller time and/or space scales. A closer examination of mean threshold values of some of the key rain/snow parameters (such as 850 mb temperature or 1000-500 mb thickness) would also improve the forecaster's ability to narrow down the heavy snow threat area. Future studies on these topics would be a logical step toward formulating a more complete climatology of heavy snow events.

Finally, it must be remembered that the significant effects of a synoptic pattern type can vary considerably over relatively short geographic distances. In other words, a pattern type conducive to heavy snow in Oklahoma will not necessarily produce heavy snow in adjacent states. If it does, the subsynoptic characteristics of the pattern are likely to be different. Hence, local studies for other states or regions must be undertaken in order for the pattern recognition principle to work in those areas. It is hoped that this study will serve as a foundation from which these other studies can be developed.

#### REFERENCES

- Belville, J. D., 1982: 500 mb flow patterns and related surface features associated with heavy rainfall events in Louisiana. WSFO New Orleans Area Technical Note 12.
- Bonner, W. D., 1968: Climatology of the low-level jet. Mon. Wea. Rev., 96, 833-850.
- Fawcett, E. B. and H. K. Saylor, 1965: A study of the distribution of weather accompanying Colorado cyclogenesis. Mon. Wea. Rev., 93, 359-367.
- Goree, P. A. and R. J. Younkin, 1966: Synoptic climatology of heavy snowfall over the central and eastern United States. Mon. Wea. Rev., 94, 663-668.
- Maddox, R. A., et al., 1979: Synoptic and meso-alpha scale aspects of flash flood events. Bull. Amer. Meteor. Soc., 60, 115-123.
- Quiroz, R. A., 1983: The climate of the "El Nino" winter of 1982-83 - a season of extraordinary climatic anomalies. Mon. Wea. Rev., 111, 1685-1706.
- Whittaker, L. M. and L. H. Horn, 1981: Geographical and seasonal distribution of North American cyclogenesis. Mon. Wea. Rev., 109, 2312-2322.



# AN INVESTIGATION OF LFM DERIVED FIELDS

Gifford F. Ely, Jr.

National Weather Service Forecast Office  
Fort Worth, TX 76102

## 1. INTRODUCTION

The advent of AFOS (Automation of Field Operations and Services) in the National Weather Service has given forecasters the opportunity to examine meteorological analysis and forecast fields in a different "mix" than was previously possible with facsimile. Snellman (1982) anticipated that the capability to overlay different meteorological fields would allow the forecaster to have greater scientific input into the "man-machine" mix, and result in improved forecasts. While the former is certainly true, there seems to be less evidence of the latter. Part of the reason may be that the fields available to the forecaster can only be overlaid (usefully) in so many ways.

Rogers, et.al. (1984) suggested that it might be useful for forecasters to examine different meteorological fields, regularly computed from the LFM run. On the other hand, Chisolm (1984) suggested that the density of observational input (both time and space) into the model is a limiting factor to the usefulness of derived model fields. Since there is strong competition on AFOS communication lines for data, strong justification is usually necessary to see new keys.

An opportunity arose for forecasters at WSFO Fort Worth to receive some "derived fields" in the form of grid point data (example, Fig 1.) through the neighboring RFC's RJE computer. The fields examined included 850 mb moisture divergence, 850 mb and 700 mb temperature advection, and 700 mb omega (vertical velocity). We received the initial, twelve, and twenty-four hour forecast for each field (excepting

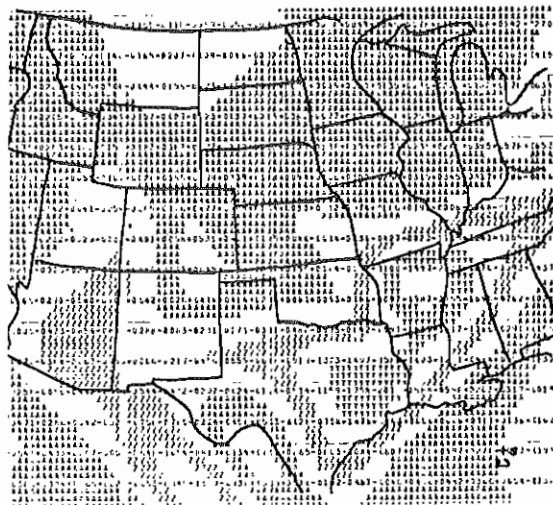


Fig. 1. Sample LFM grid point data (with overlay) as received at WSFO Fort Worth.

the analysis for the omega field). In most instances the printouts were available by midnight and noon local time, so they were able to be considered in making the morning and afternoon forecast.

## 2. MAP FACTORS AND UNITS

Schwartz (1983) summarized the map factors and units for several of the LFM derived fields; the ones we used are listed in table one. Also included are some arbitrary assignments of weak, moderate, and strong values, based on our experience with the June through October printouts.

## 3. CASE STUDIES

In the following sections, three cases will be reviewed, including the forecasts prior to the Tulsa flood May 27, 1984.

DERIVED FIELD	UNITS	WK	MDT	STG
Moisture Divergence	g/kg sec $-1 \times 10^{-8}$	5	10	20
Temperature Advection	deg sec $-1 \times 10^{-5}$	5	10	20
Omega (vert. vel.)	mb sec $-1 \times 10^{-4}$	1	2	4

TABLE ONE. Units and representative values of LFM derived fields used at WSFO Fort Worth, summer and fall, 1984.

### 3.1 CASE ONE: SUMMERTIME THUNDERSTORMS IN NORTHWEST FLOW

During the early morning hours of August 30, 1984, thunderstorms moved into north central Texas under northwest flow aloft. The thunderstorms formed late in the afternoon along a weak cold front located in western Oklahoma and southern Kansas. The locally analyzed surface map for 21Z August 29, 1984 is shown in Figure 2.

Figure 3 shows the standard 24 hour LFM progs valid for 12Z, August 30. Note that while weak convergence is implied along the surface boundary in Texas and Oklahoma, moisture values are marginal and mid level dynamics are negligible. Mankin (1984) cited mid tropospheric warming from the upper ridge over Arizona as the primary reason for expecting the thunderstorms to weaken as they moved south in the northwest flow.

The twenty-four hour 850 mb moisture divergence field valid for 12Z August 30 is shown in Figure 4. Note that moderate values of moisture convergence (negative divergence) is indicated for a large portion of west central Texas. Note also that this aspect of the forecast is not indicated elsewhere.

Figure 5 shows the infrared satellite imagery for 11Z August 30. The convection associated with the decaying MCC over north central Texas is not aligned perfectly with the moisture convergence forecast for that time period, but is close enough to be of interest given that all other forecast fields were weak or negligible.

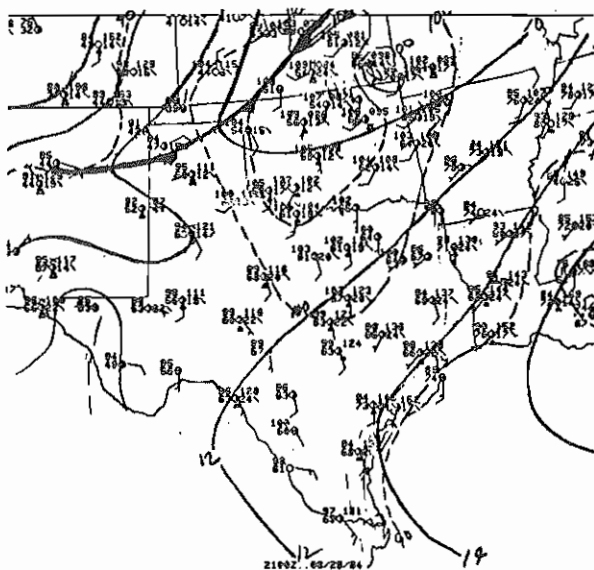


Fig. 2. Local Surface Map for 21Z Aug 29 1984. Solid lines: isobars; dashed lines: isotherms.

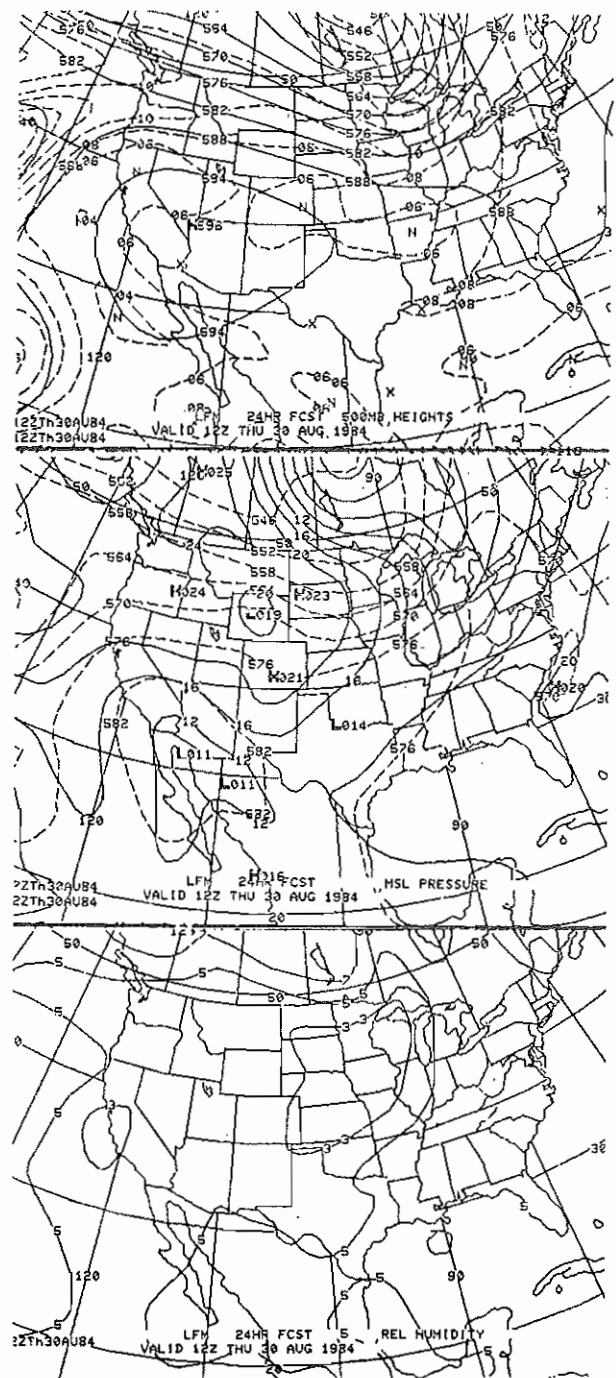


Fig 3. 24 hour LFM progs valid for 12Z Aug 30, 1984. Top: 500 mb and vorticity; middle: MSL pres and 1000-500 mb thickness; bottom: surface-500 mb mean RH.

### 3.2 CASE TWO: HEAVY RAINS OVER EAST CENTRAL TEXAS

Heavy rains fell overnight on October 28, 1984, just north of Bryan-College Station, in east central Texas. Nearly six (5.75) inches of rain fell at Hearne, Texas, in Madison

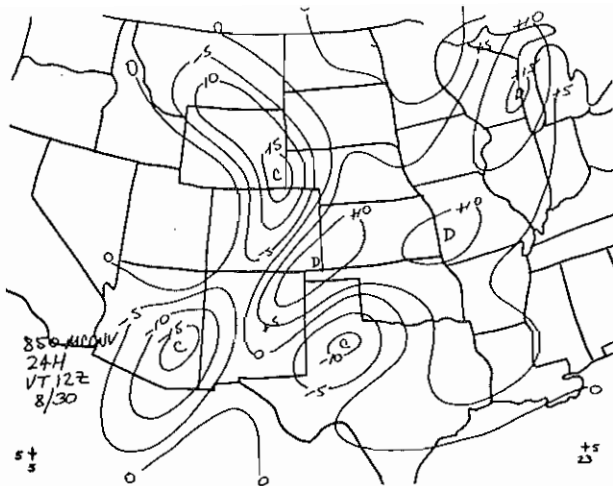


Fig 4. 24 hour LFM derived 850 mb moisture divergence valid 12Z Aug 30 1984. Negative values represent moisture convergence. See table 1 for units.

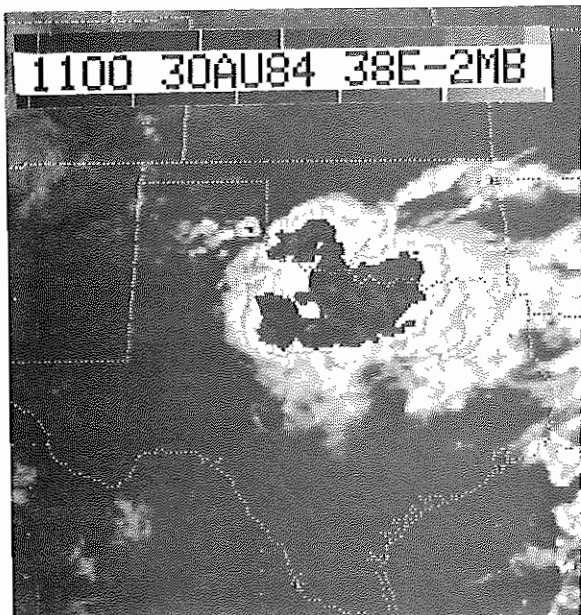


Fig 5. Satellite imagery (MB curve) for 11Z Aug 30 1984.

county. In a WSFO case study, Alexander (1984) cited the role of warm air advection and horizontal moisture transport near an outflow boundary from previous convection as the primary meteorological factors contributing to the heavy rain event.

Figure 6 shows the locally analyzed surface map for 18z October 27, 1984. Outflow boundaries from morning convection were well defined but weakening as the vigorous short wave that set them off move northeast in the broad southwest flow aloft. There was no clouds or weather associated with the moderate cold front moving through Kansas and the Texas Panhandle.

Figure 7 again shows the standard LFM forecast fields valid for 12Z October 28. Note again that moisture values are marginal and dynamics weak for north Texas.

Figure 8 shows the 24 hour forecast derived fields for 850 mb moisture divergence and omega (vertical motion). The omega field is available in AFOS but the resolution is not as great as was available to us in the grid point data. In this case both the omega and moisture divergence fields are weak, but note the coincidence of the centers over east Texas. The temperature advection fields at 850 and 700 mb showed weak to negligible warm air advection over North Texas and are not shown. The satellite imagery at 12Z October 28 (Figure 9) shows what happened.

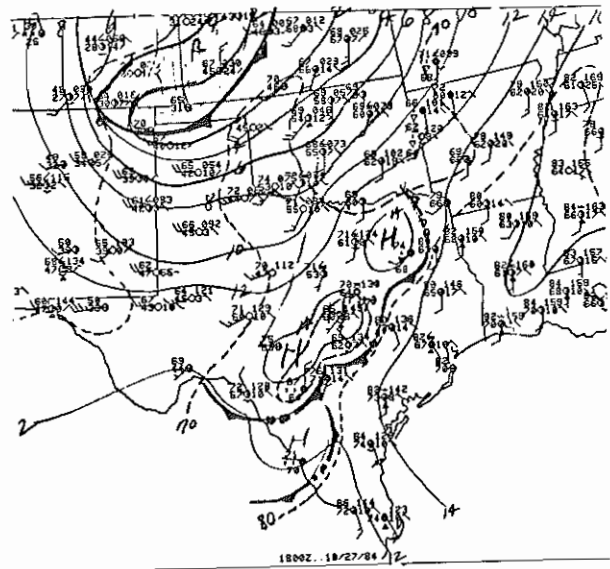


Fig 6. Local surface map for 18Z Oct 27, 1984. Same convention as Fig 2.

### 3.4 CASE THREE: THE TULSA FLOOD 27 MAY 1984

Now let's examine the 12 hour LFM derived fields valid for 00Z May 27, 1984 (Fig 10.). Branick (1984) described the primary factors contributing to the cause of the event as strong low level convergence and warm air advection north a quasistationary front enhanced by convection. Synoptically, Branick point out that the event occurred under relatively weak forcing conditions aloft. But even though this was primarily a meso-scale event, Branick noted that the LFM progs were, in general, quite good.

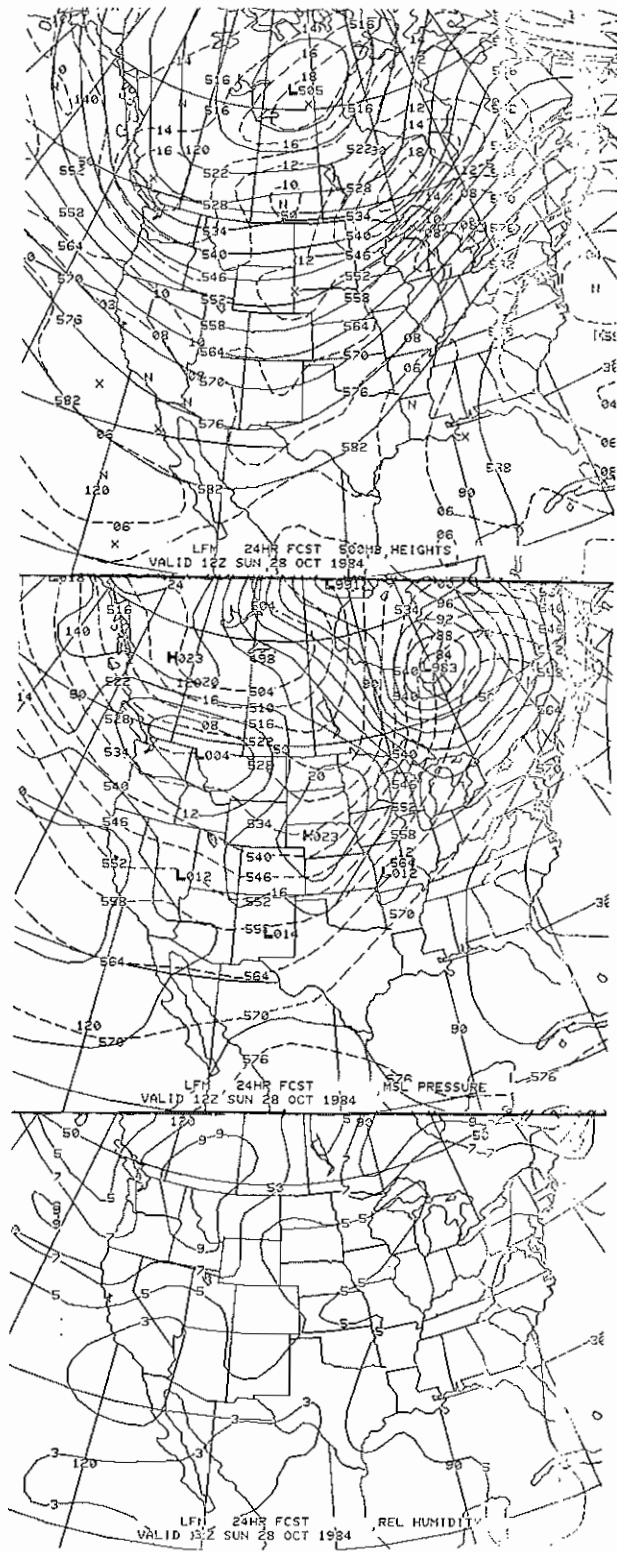


Fig 7. 24 hour LFM progs valid for 12Z Oct 28 1984. Same conventions as Fig 3.

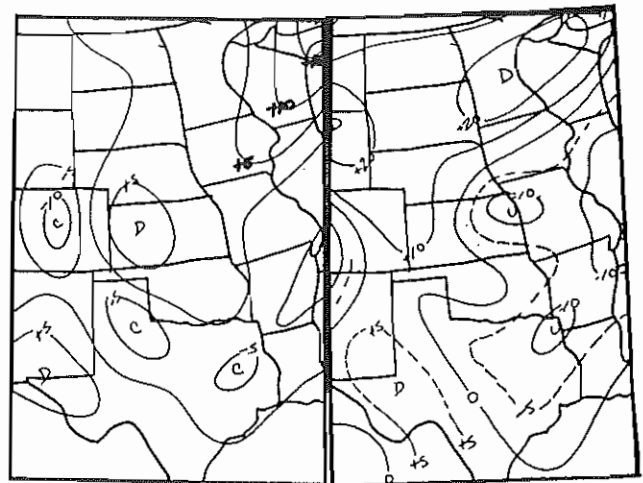


Fig 8. 24 hour LFM derived field of 850 mb moisture divergence (left) and 700 mb omega (right) valid for 12Z Oct 28 1984. See table 1 for map units.

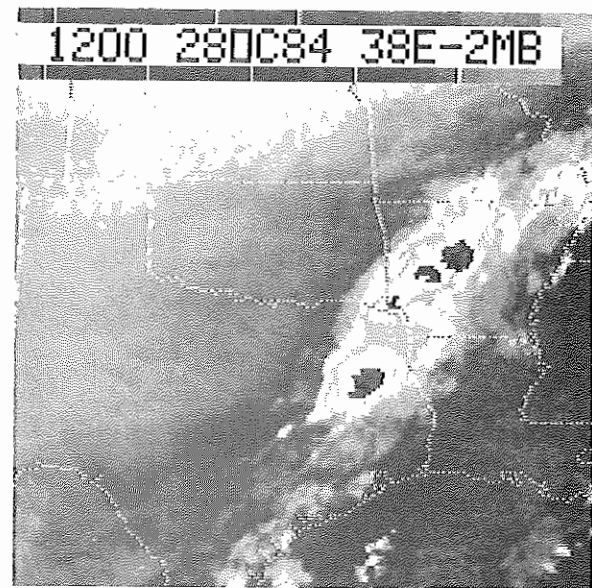


Fig 9. Satellite imagery (MB curve) for 12Z Oct 28 1984.

Figure 11 shows the 12 hour forecast derived fields from the LFM valid for 00Z May 27. Note that the temperature advection fields at 850 and 700 mb are relatively weak; no doubt the mesoscale nature of the event enhanced the thermal contrast and is therefore not well depicted by the model. Note, however, the strong omega field associated with the weak short wave. Again, even though this field is available in AFOS, the resolution is greater with the grid point data. Finally, note the maximum of moisture convergence centered over eastern Oklahoma. This forecast field shows extremely good correlation to the precipitation that subsequently occurs (Figure 12).

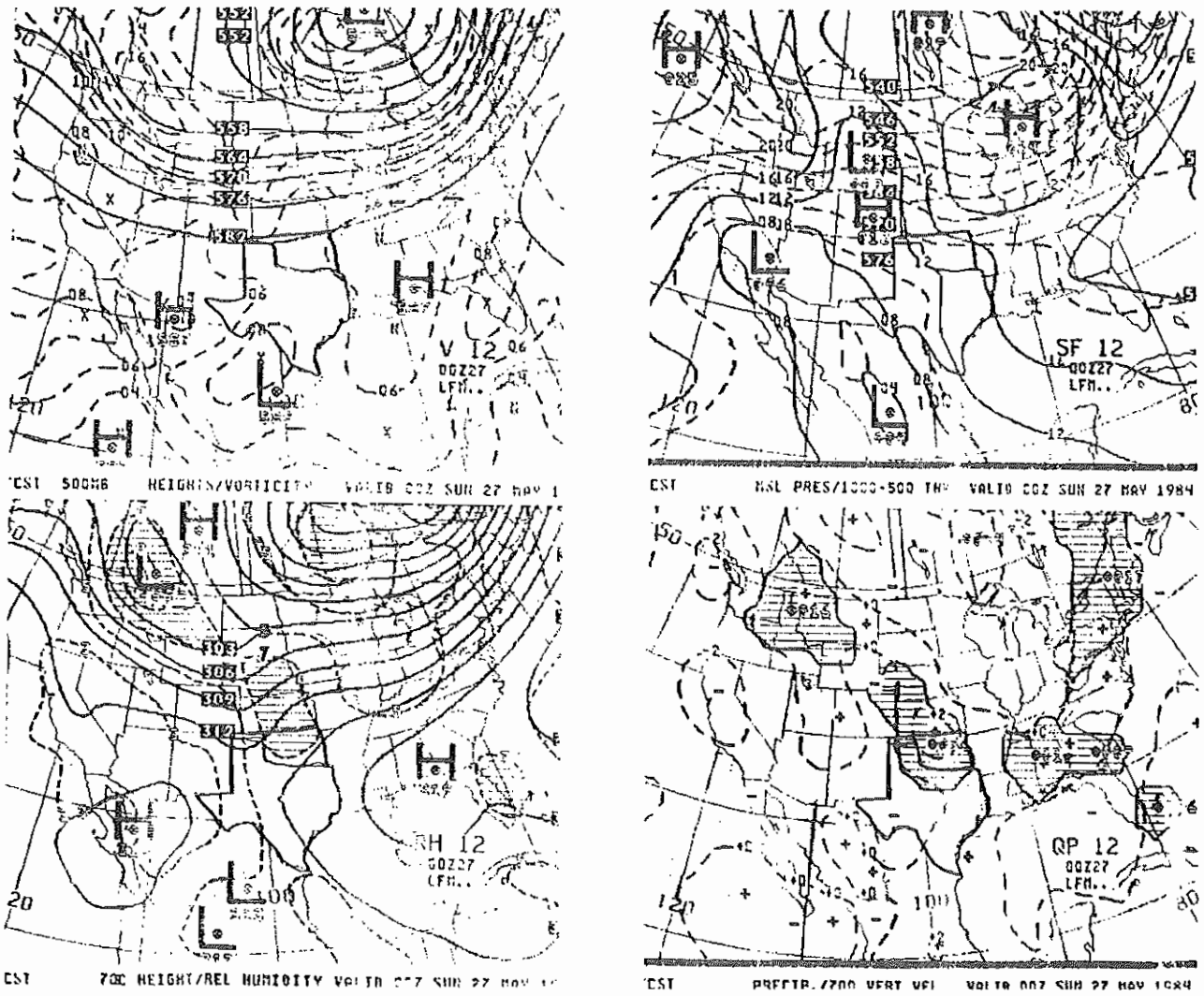


Fig 10. 12 hour LFM progs valid for 00Z 27 May 1984. Top left: 500 mb height and vorticity; top right: MSL pres and 1000-500 mb thickness; bottom left: 700 mb height and sfc-500 mb mean RH; bottom right: omega and qpf.



Fig 11. From left to right, 12 hour derived fields for 700 mb temperature advection, 700 mb omega, 850 mb temperature advection, and 850 mb moisture divergence. See table 1 for units.

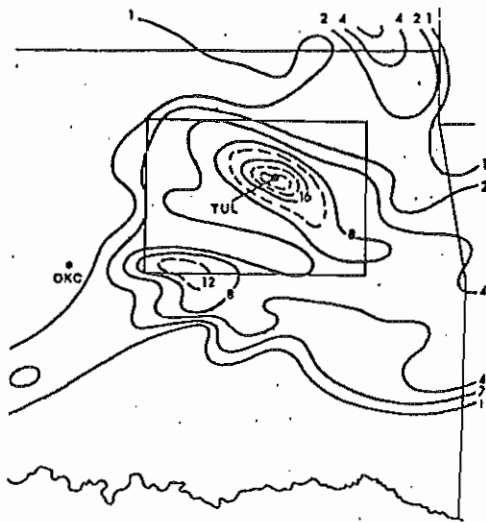


Fig 12. Observed 24 hour rainfall (cm) ending 12Z 27 May 1984 in Oklahoma (after Branick, 1984)

#### 4. OPERATIONAL CONSIDERATIONS

Operationally, we have encountered these difficulties in fully utilizing the LFM derived fields:

A. The gridded output we used needed to be contoured manually and a background overlaid with either a plastic transparency or a light table. This was time consuming and cumbersome. In addition, the output could not be utilized effectively with other AFOS fields.

B. The period of initial study (June through September) turned out to be drier than normal in an already climatologically dry period. Consequently, not as many precipitation cases were available to study.

C. We initially had trouble relating map factors and representative values. Eventually we figured out what values represented weak, moderate and strong factors.

D. The derived fields were no better than the rest of the LFM model, and were subject to the same limitation in time and space. If the model incorrectly forecast a certain weather system (ie, too fast, slow, etc), the derived fields were consistent and showed similar trends.

#### 5. SUMMARY AND CONCLUSIONS

Are the derived fields useful? That's hard to say based on our limited experiences. Certainly the fields forced us to look further than just the standard parameters (vorticity, thickness, etc) we frequently get locked into. But it is hard to quantify the relative contribution of each bit of new information into the total forecast product.

Never the less, it may be that we should re-think the mix of fields from the models that we make available to the operational forecaster. Numerous case studies have shown that forecasters tend to place too much emphasis on dynamics in forecasting (especially heavy rain events); perhaps if other innovative fields were available to the forecaster, other aspects of meteorological processes would be encouraged.

#### 6. ACKNOWLEDGEMENTS

Thanks go to Barry Schwartz of the NWS TDL for his help in obtaining the grid point data and interpreting the output. Thanks also to Mike Mogil (Southern Region SSD) for his enthusiasm and encouragement to do the study. Finally, appreciation is expressed to the Fort Worth RFC for the use of their computer in securing the data.

#### REFERENCES

- Alexander, W.O., 1984: Nocturnal Heavy Rains in East Central Texas: A Case Study. WSFO Fort Worth, 21 pgs. (Unpublished).
- Branick, M. 1984: The Tulsa Flood of 27 May, 1984. Part I: Overview of Subsynoptic Conditions and Operational Procedures. WSFO Oklahoma City, 27 pgs. (Unpublished)
- Chisolm, D.A., and Jackson, A.J., 1984: Short Range Terminal Forecasting Using Interactive Computer Display Systems. Preprints, 10th Conference on Weather Forecasting and Analysis, AMS, Boston, Ma. pg 226-233.
- Mankin, D., 1984: Early Morning August Thunderstorms: A Case Study. WSFO Fort Worth, 23 pgs. (Unpublished).
- Rogers, D.M., Bartels, D.L., Menard, R.D., and Arns, J.H., 1984: Experiments in Forecasting Mesoscale Convective Weather Systems. Preprints, 10th Conference on Weather Forecasting and Analysis, AMS, Boston, Ma. pp 486-491.
- Schwartz, B.E., 1983: MOS System Identification, Units, Map Factors, and Representative Values for Typical Diagnostic Parameters in Association with Synoptic Scale Weather Systems. Branch Note No. 1: NWS Mesoscale Techniques Branch, 9 pp.
- Snellman, L.W., 1982: Impact of AFOS on Operational Forecasting. Preprints, 9th Conference on Weather Forecasting and Analysis, Boston, Ma. pp 13-16.

OMEGA DIAGNOSTICS AS A SUPPLEMENT TO LFM/MOS GUIDANCE  
IN A WEAKLY-FORCED CONVECTIVE SITUATION

Stanley L. Barnes

NOAA, Environmental Research Laboratories  
Boulder, Colorado

## 1. INTRODUCTION

The synoptic conditions associated with many mesoscale convective complexes (MCCs) that occur in middle latitudes have been documented by Maddox (1983). Typically, MCCs develop in a region of the lower troposphere which is characterized by warm air advection, veering of wind with height (but with small speed shear), deep moisture content ( $> 10 \text{ g kg}^{-1}$  in the lowest 200 mb), and significant convective instability. Initiation of MCCs often takes place in advance of a weak middle tropospheric wave of meso-alpha scale (250 - 2500 km). An observed characteristic of MCCs is the development of a mesoscale circulation whose duration is considerably longer than the individual convective components (Fritsch and Maddox, 1981). The following questions arise: What role does the upper air wave play in the initiation of convection and in the development of the subsequent mesoscale circulation?

The answer to those questions very likely involves complicated inter-scale processes that I am not prepared to address. Rather, I am addressing a simpler question, which is "Might quasi-geostrophic adjustment theory explain some part of the apparent larger-scale forcing in such situations as described above?"

The tools brought to bear on the question were a firm background in objective interpolation techniques and their implementation on computers, a microcomputer system of modest capacity, a quite rusty and somewhat dated understanding of quasi-geostrophic theory, and a group of interested colleagues urging, guiding and educating me along the way. The outcome, though limited to a single case study, has been so encouraging and the means required to attain it so nearly trivial that I could not pass up this opportunity to share with you the operational forecasting possibilities of the scheme with the hope that future tests will justify our initial enthusiasm.

In the following sections, I will describe the weather situation facing a duty forecaster, say, in Denver or Amarillo, on the morning of 25 June 1982. Together, we will then take a look at some of the typical guidance for considering convective storms in his forecast, consider the results of the omega diagnostics, and finally look at what actually happened that day in eastern Colorado and the adjacent areas. Technical details are relegated to the Appendix.

## 2. THE SYNOPTIC SITUATION

One of the first available information sources indicating what the atmosphere is doing prior to the morning data cycle are the satellite IR images. A depiction (Fig. 1) near the time of the morning rawinsonde releases confirms what inhabitants of northern Texas have known all night, that widespread thunderstorms have been occurring, Amarillo being in one activity zone. Over the central and northern Rockies, middle and high cloudiness occurs in advance of an apparently weakening short wave at 500 mb (Fig. 2) that is about to penetrate through a larger scale ridge. The desert states of the southwest and most of California are experiencing only patchy middle and high clouds. At first glance, it looks like another typical summertime day over the mountainous west; more or less scattered

thundershowers over the mountains, more in the north, less in the south. The Amarillo forecaster's experience with nighttime thunderstorms probably tells him that those in his area will be gone by noon.

If, however, our two forecasters have picked up on pattern recognition of surface features associated with high-plains severe thunderstorms (Doswell, 1980), they may well experience their first doubts about how typical the day will be when they look at the 1200Z surface map. Principal features (abstracted from the NMC version in Fig. 3) indicate the warning flags: continental polar air of high moisture content streaming upslope over the high plains from Texas to Wyoming behind a front that has penetrated across the mountains into Utah. A further complication to the forecast picture is a 70-knot "jetlet" (as used here, a small wind maximum not connected to the main polar-front jet) at 200 mb over southern California (Fig. 3, inset). Very likely our forecasters already have strong suspicions that something more than a typical summertime thunderstorm forecast is called for today.

## 3. LFM/MOS GUIDANCE

Although probably leery of the appropriateness of LFM/MOS guidance in the synoptic situation described, nonetheless, our forecasters are obliged to consider it. As the products come up on AFOS, sure enough the 12Z initial LFM panels show a sizeable cyclonic vorticity center over Nevada (Fig. 4a) that is predicted to weaken slightly in 12 hours while moving into southwestern Wyoming (Fig. 4b). Certainly some "PVA" is going on in western Colorado and Wyoming. If our forecasters have read Trenberth's article (1978) and are advecting the vorticity with the thermal wind (1000-500 mb thickness contours are also shown in Fig. 4), they could deduce some potential for large scale forcing in that region. The 12-hour LFM forecast 700-mb vertical motion and precipitation panel (Fig. 5) is a little confusing, showing only vertical motion centers in southwestern Colorado and eastern Utah by 00Z, the strongest activity being predicted over northern Idaho. Precipitation in amounts near 5 mm is predicted in eastern Wyoming and extreme northeastern Idaho. Subsidence and no precipitation are predicted for the Texas panhandle.

Not too surprised that the LFM does not confirm our two forecasters' suspicions for their respective regions, they next look to MOS, the QPF guidance and what NSSFC is saying about the situation. Fig. 6 is a composite of two guidance products, MOS precipitation probabilities (light lines), Lifted Indexes (heavy lines showing only unstable regions), and the station values of precipitable water and Lifted Index from the morning soundings. I will explain the stippled area later.

It is clear that MOS guidance favors the area from Washington state to the Black Hills of South Dakota. The only areas of negative LI are near Salt Lake City and from the Texas panhandle southeastward. A look at the morning soundings, however, suggests some possibilities. At Denver (Fig. 7), the depth of the polar air indicates why  $LI = 3$  there. The temperatures above 680 mb suggest there is a large amount of potential buoyancy for any storms that might develop. Similarly, at Grand Junction (Fig. 8) the air above the frontal surface has a very steep lapse rate.

Considering the soundings, the over three-quarters inch precipitable water, a LI = 3 and the knowledge of some possible help from the approaching short wave, the Denver forecaster might decide to slant his forecast toward the eventuality that some of the predicted Wyoming action might indeed tail into northeastern

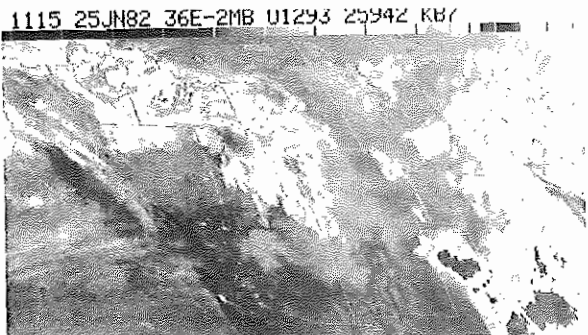


Fig. 1. Satellite IR image near time of morning rawinsonde release, 1115Z 25 June 1982.

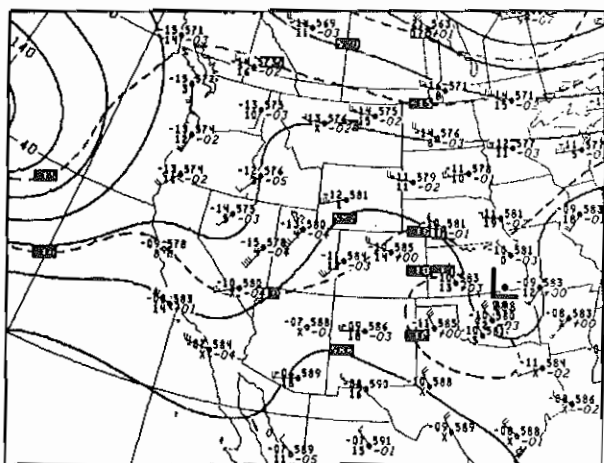


Fig. 2. NMC 500-mb facsimile chart for 12Z 25 June 1982. Solid lines are height contours in decameters; dashed lines are isotherms in degrees Celsius.

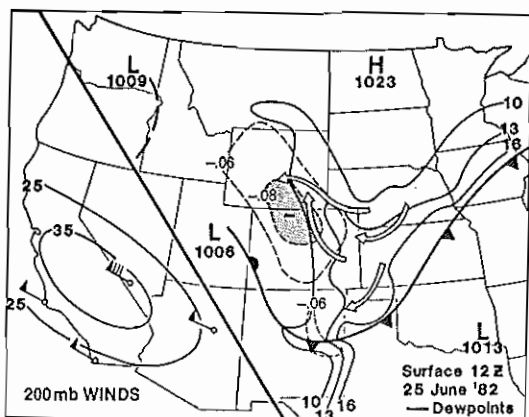


Fig. 3. Selected details from NMC surface facsimile chart for 12Z 25 June 1982. Broad arrows indicate easterly upslope streamlines advecting moist air (light solid lines are dew point isopleths). Dashed lines depict region where local (dry) stability is decreasing most rapidly in 850-300 mb layer (see Sec. 4). A 70-90 knot jetlet is over California at 200 mb (inset).

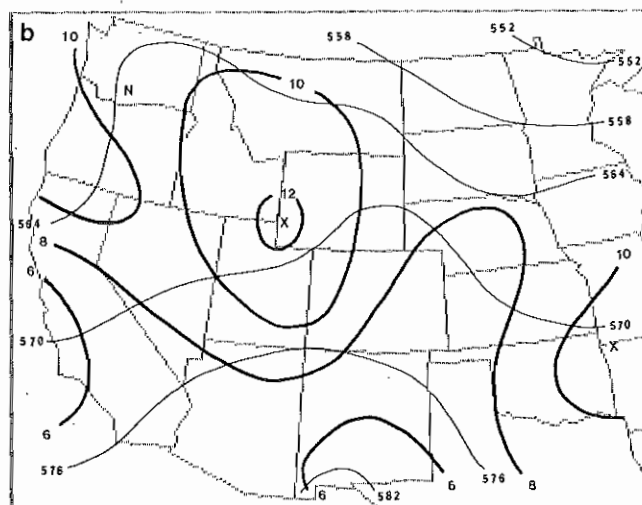
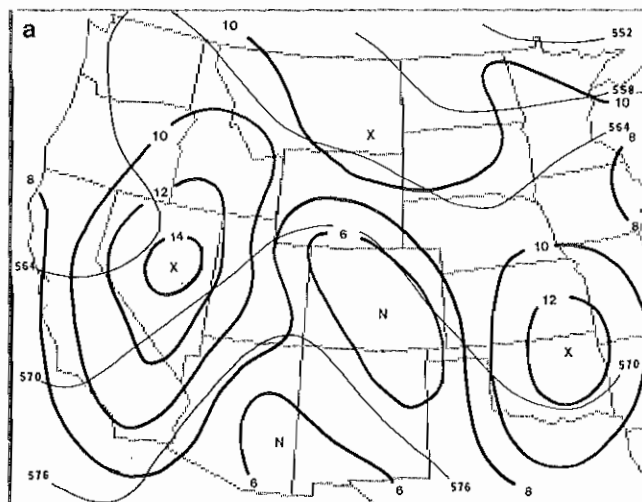


Fig. 4. LFM vorticity and 1000-500 mb thickness for a) initial time (12Z 25 June 1982) and b) 12-hour forecast valid at 00Z 26 June 1982.

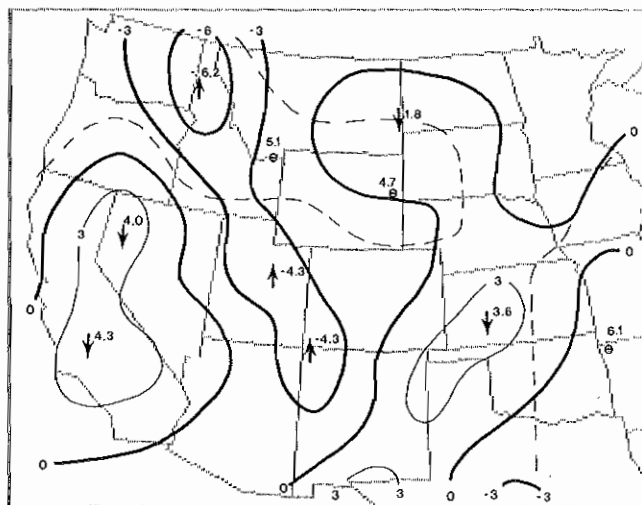


Fig. 5. LFM 12-hour forecast of 700-mb vertical motion (solid lines) and precipitation (dashed lines) valid at 00Z 26 June 1982. Vertical motion centers are indicated in  $\text{mb hr}^{-1}$  and precipitation centers are in millimeters.

Colorado and (Fig. 9) have a slight chance that some thunderstorms could become severe.

In Amarillo, meanwhile, the forecaster might decide to go against the MOS probability of only 10 per cent in view of the 1.04 inches of precipitable water in the air, the nearby front and the NSSFC outlook (Fig. 9).

#### 4. OMEGA DIAGNOSTICS

Suppose now that our forecasters could bring up on their AFOS screens various diagnostic patterns based upon quasi-geostrophic theory. Would it add anything to their forecasts of anticipated convection? (Of course, already you suspect that it will in this case!)

In the examples that I am presenting, the meteorological data input for the calculations were geopotential heights of four standard pressure surfaces, 850, 700, 500 and 300 mb, at 38 stations in the western United States. Data were interpolated using a Gaussian weight function (Barnes, 1964, and Appendix Sec. 8.2) to a 190.5 km grid on a polar stereographic projection, standard latitude 60° North. This is the same projection and grid from which the contoured LFM gridpoint values were traced as represented in Fig. 4 and 5.

Fig. 10 depicts a typical microcomputer-generated graphic that could be an AFOS product, this for the 500-mb height field at 12Z. The mesh size is identifiable by the distance from the cross near the upper left corner and the corner which is itself a gridpoint. This height pattern compares quite well with the NMC analysis of the same data (Fig. 2). Only the contour interval suggests somewhat more detail in Fig. 10 than Fig. 2, but in fact the short wave has about the same amplitude in both. I do not know what grid point height values might have gone into the LFM initial conditions, but judging from the vorticity panel (Fig. 4a), it is likely they were smoother than either of these depictions (Fig. 2 and 10).

The 500-mb vorticity pattern (Fig. 11) computed from the height analysis (Fig. 10) does depict different details than the LFM version (Fig. 4a.) While the main centers are in nearly the same positions and are of the same magnitudes, there are differences. Particularly note in Fig. 11 the smaller minimum center in Arizona, the shift in the Utah "ridge" northeastward, and the centers in California and New Mexico.

Also shown in Fig. 11 are the 700-300 mb thickness contours revealing the pattern of thermal winds. If one were using the advection of cyclonic vorticity by the thermal wind as an indicator of large-scale forcing of upward motion, the Wyoming and northern Colorado area would again appear to have the highest probability of experiencing significant afternoon convection.

The same information at 700-mb (Fig. 12) suggests a slight modification should perhaps be made to the forecast. In the layer 850-500 mb, the vorticity and thickness patterns indicate that forcing in western Colorado might extend southward into northern New Mexico along the relatively strong thickness gradient extending from north-central Colorado through the Texas panhandle.

The presence of a strong (for the time of year) front in the 850-500 mb layer suggests that an analysis of quasi-geostrophic forcing based only on thermal advection of cyclonic vorticity may not tell the whole story. The deformation components, which the vorticity advection analysis ignores, could be significant.

Using a version of the Hoskins *et al.* (1978) Q-vector formulation of the diagnostic omega equation which includes ageostrophic adjustments to the quasi-geostrophic forcing, a scaled parameter which is proportional to omega (vertical motion in a pressure coordinate system) was computed at two levels, 500 and 700 mb. In this version (which is described in the Appendix), the troposphere was divided into two overlapping layers, 850-500 mb and 700-300 mb.

The resulting vertical motions at 500 mb are indicated in Fig. 13, and they don't bear much resemblance to the vertical motions predicted by the LFM model 12 hours later (Fig. 5). There are, of course, important reasons why the two vertical motion patterns are not similar, other than the fact that one is diagnostic and the other predicted. The diagnostic omegas do not include boundary layer forcing, terrain influences, or any of a number of parameterized effects included in the LFM field. On the other hand, the LFM field includes a considerable amount of rather arbitrary numerical and dynamical smoothing which the diagnostic omega does not. There is a crude convective parameterization in the LFM and the diagnostic omega does not include the effect of convective latent heat release, although Hoskins and Pedder (1980) note that the Q-vector diagnostics do reflect adjustments to previous diabatic processes.

The most notable feature in the 500-mb omega field is the adjustment taking place in response to the 200-mb jetlet over southern California and western Arizona (Fig. 3 inset). The Q-vectors themselves are shown in Fig. 14. Hoskins and Pedder (1980) instruct us to expect rising motion where Q-vectors indicate convergence, sinking where they indicate divergence. Furthermore, they demonstrate that the low-level ageostrophic wind is proportional to and in the direction of the Q-vector. From the pattern of Q-vectors, it is obvious that the ageostrophic circulation associated with the jetlet is producing rising motion in its right forward quadrant.

The most significant upward motion occurring elsewhere is with the short wave in Utah. At this point in our experience with these diagnostics, one is hard pressed to say what magnitude of computed omegas is really significant, but judging by the small values elsewhere (except for the southwest desert) the Utah values could be interpreted as important.

The distribution of omegas at 700-mb (Fig. 15) indicates a somewhat more definite protrusion of the Utah upward motion center into northwestern Colorado, and we also note a small feature along the front in northeastern New Mexico. Montana is the locale of another upward motion center, and although there is adequate moisture both at the surface (Fig. 3) and aloft (Fig. 6), the atmosphere there is presently very stable.

We also learn from Hoskins and Pedder (1980) that the Q-vector pattern viewed against the pattern of temperature distribution indicates the tendency for frontogenesis and frontolysis. Those patterns at 700-mb (Fig. 16) indicate weak frontogenesis in the eastern New Mexico - eastern Colorado region and on into Wyoming. This might tell our forecasters that the front is not likely to weaken during the day as the LFM seems to predict (Fig. 4b thickness lines).

The eastern border region of Wyoming and adjacent portions of adjoining states appear to be experiencing descent of cold air near the surface which might be construed to mean that any convective activity moving into that area would be diminished or suppressed.

In the Texas panhandle, little dynamic forcing can be expected, at least during the next few hours, and the sinking apparent in the omega field would herald the demise of the ongoing thunderstorms, in accord with that forecasters' previously-hypothesized experience.

Finally, there is some additional information in the thickness fields of the two layers that is not represented by the Q-vector analysis. First, the thickness of each layer represented by a mean potential temperature ( $\bar{\theta}$ ), and the vertical difference in the two  $\bar{\theta}$  which represents a type of mean (dry) stability pattern. Second, as a by-product of the Q-vector computation, advection of thickness temperature by the geostrophic wind was computed for the two layers. It can be shown (but not in this space-limited paper) that differential thickness advection is proportional to the local stability tendency.

The pattern of these two parameters at 12Z indicate 1) there is a large area of minimum stability extending from Salt Lake City to El Paso (Fig. 6; stippled

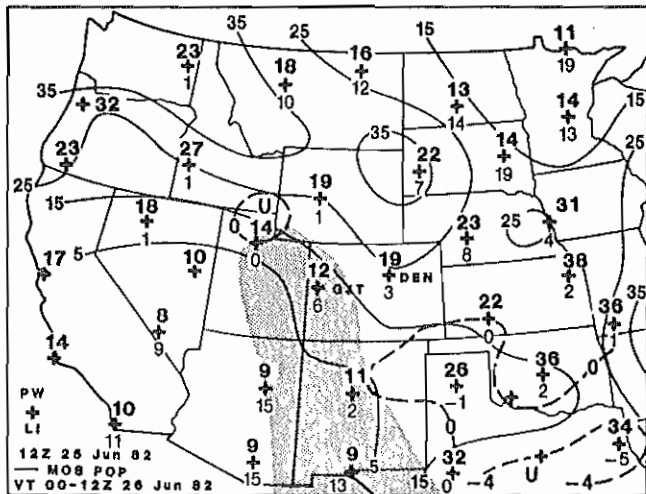


Fig. 6. Composite of MOS precipitation probabilities (solid lines valid for period 00Z - 12Z 26 June 1982), Lifted Index analysis (heavy dashed lines) showing only unstable regions, and region of minimum potential temperature stability (explained in Sec. 4) in layer 850-300 mb (stippled area) which has centers in western Colorado and southern New Mexico. Station values of precipitable water (upper value) and Lifted Index (lower) are plotted for 12Z 25 June 1982 soundings.

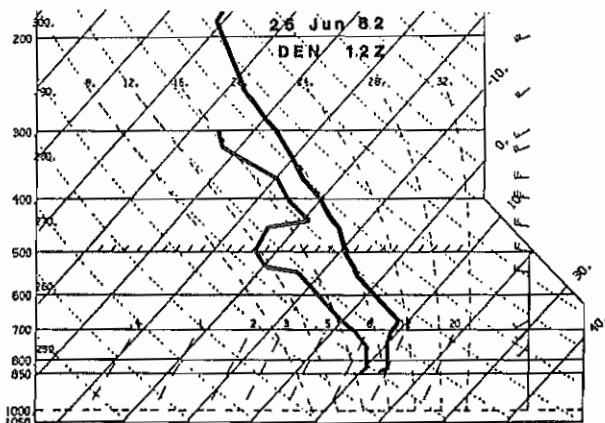


Fig. 7. Denver sounding for 12Z 25 June 1982.

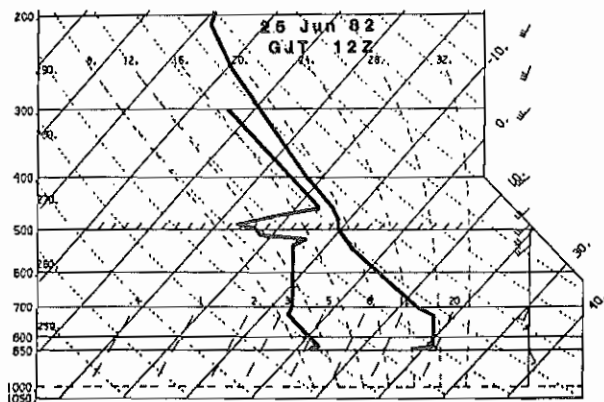


Fig. 8. Grand Junction sounding for 12Z 25 June 1982.

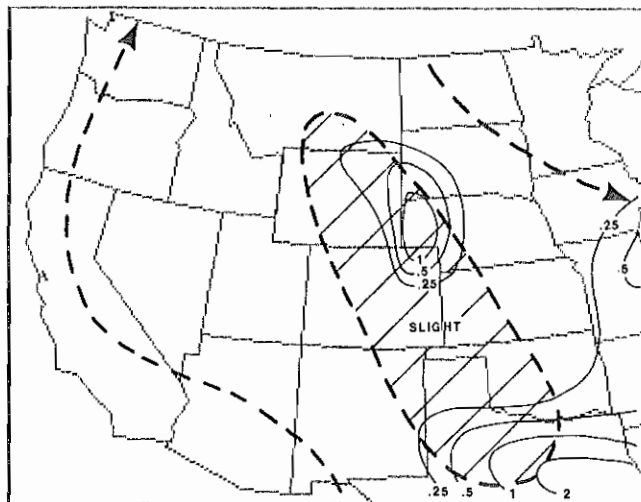


Fig. 9. Severe weather outlook valid for 00Z to 12Z, 26 June 1982 and 24-hr quantitative precipitation forecast (inches) ending 12Z 26 June 1982. Area to right of dashed area is region of expected thunderstorm activity. The hatched area indicates the thunderstorms are expected to have a "slight" chance of becoming severe.

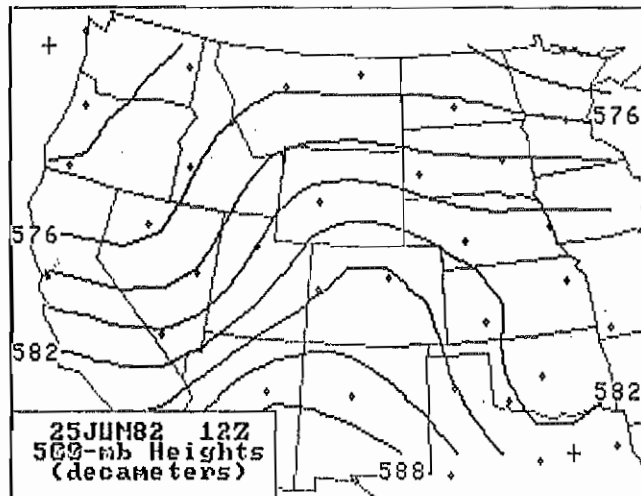


Fig. 10. Microcomputer graphic of analyzed 500-mb heights for 12Z 25 June 1982. Compare with Fig. 2.

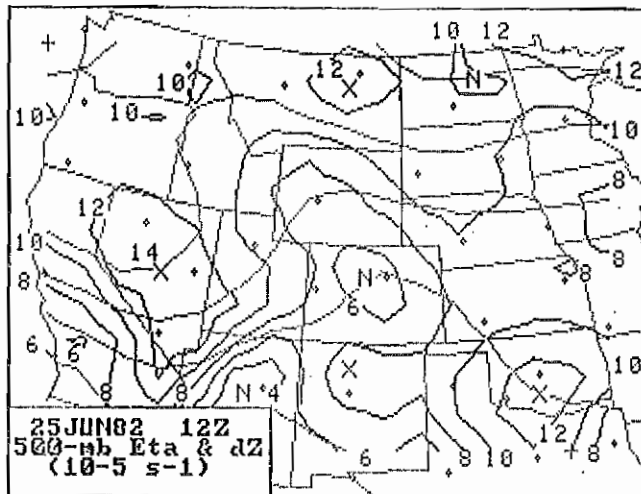


Fig. 11. 500-mb absolute vorticity (heavy lines) and 700-300 mb thickness contours (light lines). Vorticity units are  $10^{-5} s^{-1}$  and thickness contour interval is 40 m. Compare with Fig. 4a.

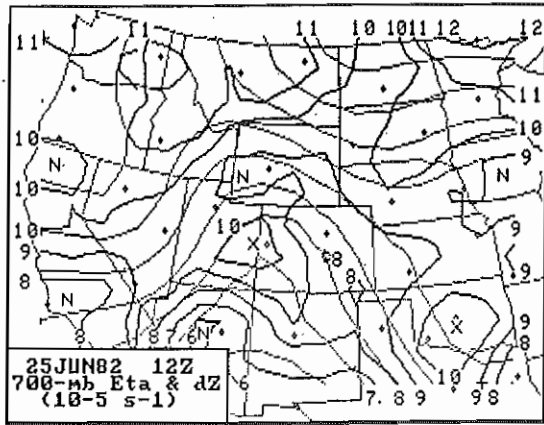


Fig. 12. 700-mb absolute vorticity (heavy lines) and 850-500 mb thickness contours (light lines). Units are same as in Fig. 11.

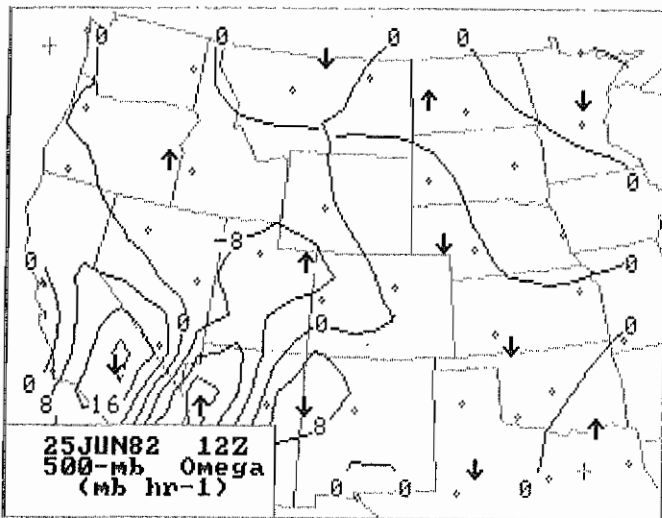


Fig. 13. 500-mb "omega" (actually divergence of the Q-vector representation of quasi-geostrophic forcing scaled in  $\text{mb hr}^{-1}$ ) for 12Z 25 June 1982.

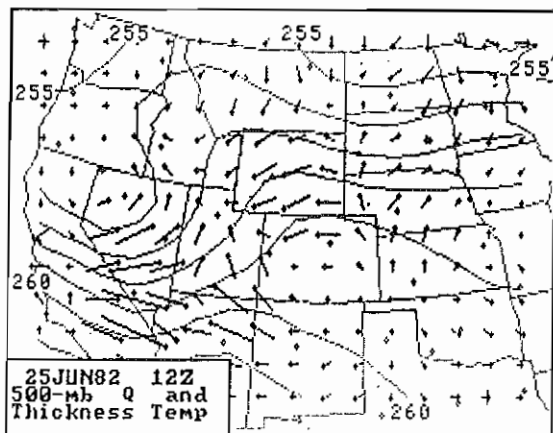


Fig. 14. 500-mb Q-vectors that generated the omega pattern shown in Fig. 13 and 700-300 mb thickness temperature.

area), and 2) differential thickness advection (Fig. 3; dashed lines) is decreasing the stability most rapidly over a large area on the Wyoming-Colorado border. A secondary destabilization center exists over east central New Mexico. As was the case with the omega distributions, it is more the pattern of information we are using rather than the magnitudes themselves, since we don't have the necessary experience to interpret the latter.

With all this information available to them, our Denver forecaster might conclude that northeastern Colorado and extreme southeastern Wyoming were the areas most threatened by intense thunderstorms on this day, and the Amarillo forecaster might well be keeping his eye on what develops over the northeastern quarter of New Mexico during the day.

## 5. AND WHAT HAPPENED WAS ...

Thunderstorms developed by 1945Z in northwestern Colorado, northeastern Utah and southwestern Wyoming, as well as along the higher mountains from northern New Mexico through Wyoming and into western Montana, and by 2315Z (Fig. 17) they were influencing a broad area of the high plains from New Mexico to Montana.

From Storm Data we learned that on the afternoon of the 25th of June 1982,

Severe thunderstorms, torrential rain and hail battered portions of Boulder, Larimer, and Weld counties. Golfball size hail was observed in Loveland, and near Greeley, Fort Collins, and Lucerne. Three-quarters inch hail fell in Longmont, and three inches of small hail piled up near Estes Park. Rainfall was extremely intense. Four and one-half inches of rain fell in two hours four miles east of Fort Collins. Three inches fell in just 45 minutes west of Loveland ...

Around 1845 MST, at least one tornado touched down in the Fort Collins - Greeley area. All of these locations are in the northeastern quadrant of Colorado.

In Wyoming, sometime during the day high winds broke windows, downed telephone poles, fences and antennas in Rock Springs and Green River (Sweetwater County), a tornado was sighted about 1330 MST in the Laramie Range (Albany County), and lightning caused several fires in Cheyenne where three-quarters of an inch rain fell in 20 minutes.

Satellite and radar information (Fig. 18) gave the impression that a convective complex was developing in the early evening. As an independent test of the value of these diagnostics, they were computed again for the 00Z 26 June 1982 rawinsonde data at the same levels as before.

The surface map for 00Z (Fig. 19) indicates the front which was trailing through New Mexico to a low pressure center in Utah had progressed eastward. Easterly upslope winds behind the front continued to supply considerable surface layer moisture to the storms. The issue now to be addressed is where will the thunderstorms diminish and where might they continue or intensify as night progresses.

LFM guidance (Fig. 20) suggests east central Colorado and northwestern Kansas can expect to bear the brunt of the most intense convective activity during the night. Omega diagnostics, which now reflect whatever height adjustments have occurred in response to the afternoon convection, suggest that the center of quasi-geostrophic forcing is shifting to southeastern Colorado and northeastern New Mexico (Fig. 21 and 22). Furthermore, through differential thickness advection, the same area is destabilizing more rapidly than elsewhere (Fig. 19).

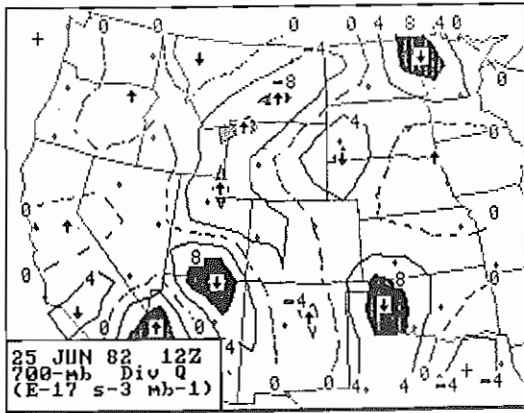


Fig. 15. 700-mb omega for 12Z 25 June 1982.

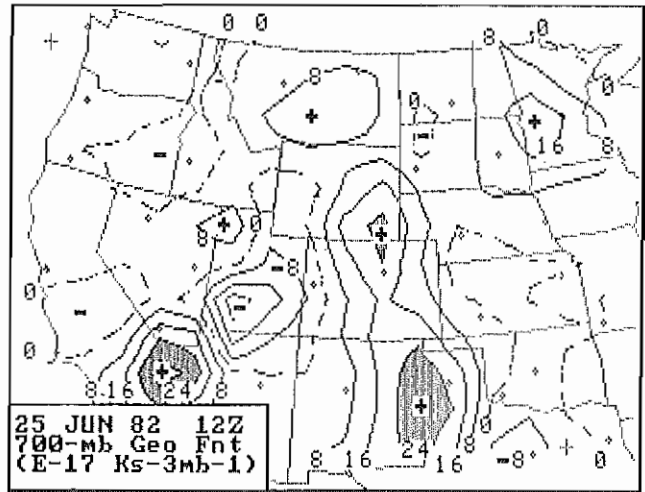


Fig. 16. 700-mb geostrophic frontogenetic function computed as  $Q \cdot \nabla T$  for 12Z 25 June 1982.

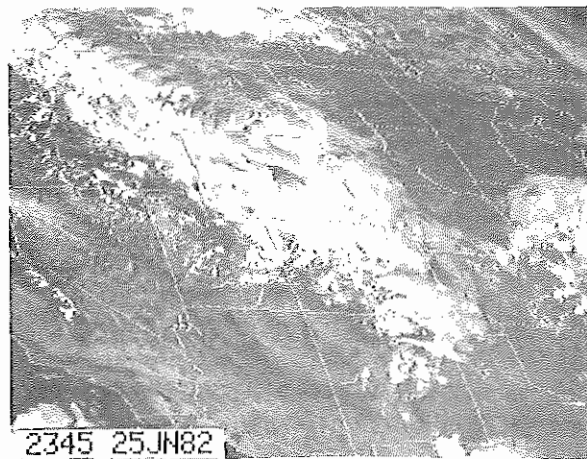
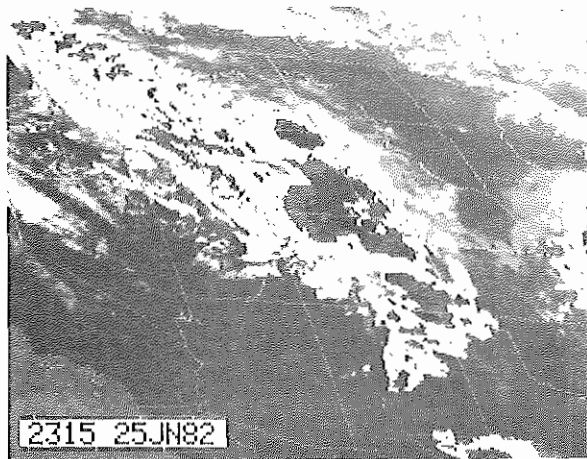


Fig. 17. Satellite IR and visible images of convective activity near the time of evening sounding releases.

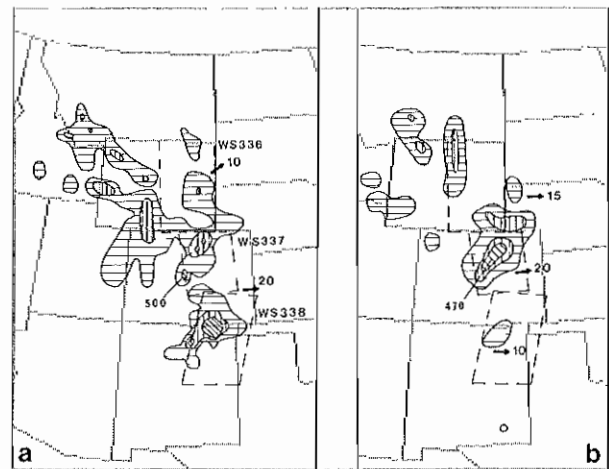


Fig. 18. Radar summary charts for a) 2335Z and b) 0235Z, 25-26 June 1982. Severe weather watch areas issued by NWSFC are shown by labelled dashed boxes.

## 6. DISCUSSION

What has been demonstrated here is the apparent utility, and somewhat surprising power, of some simple diagnostic products that are based on nothing more than geopotential height fields and quantities derived from them. Also made evident by these results is the value in looking at multiple layers of the troposphere rather than just 1000-500 mb thickness and 500 mb vorticity. Had results been computed only for the 700-300 mb layer, the important ageostrophic circulations associated with the front might well have missed.

That these products seem to add valuable information to a fictitious forecasting process\* is decidedly encouraging. However, a considerable amount of testing and evaluation remains before their general value can be assessed. In view of the simplicity of the

Through the nighttime, satellite images (Fig. 23) indicate that the Colorado complex reached its maximum intensity about 0500Z and thence diminished as it moved into western Kansas. The New Mexico system, on the other hand, became the dominant convective area as it moved into the Texas panhandle.

\* A comparison could have been made with the actual forecasts issued from the Denver and Amarillo NWS offices, but I chose not to, reasoning that the purpose here is to introduce diagnostic products which are not presently available to NWS forecasters, not to test the skill of a hindcast against an operational forecast.

procedures and tools required to implement the diagnostics, perhaps some of this testing can be done in an operational arena, thereby speeding up any technology transfer that may become warranted.

The fact that information concerning quasi-geostrophic adjustments and the distribution and tendency of tropospheric (dry) stability is obtainable from only pressure height data over at least two layers should catch the eye of researchers who are seeking uses for VAS sounding information, as well as those in the community who are trying to decide what proportion of radar wind profilers to radiometric profilers should be incorporated in future sounding networks.

## 7. ACKNOWLEDGEMENTS

Several people made substantive contributions to this work. Space does not permit elaboration, but I wish to thank Prof. Lance Bosart, State University of New York at Albany, his colleague, Dr. Song Chin Lin, also, Mr. Barry Schwartz, Techniques Development Laboratory, National Weather Service, and my colleagues Drs. Fernando Caracena, Charles Doswell, and Robert Maddox.

## 8. APPENDIX

### 8.1 Omega diagnostics formulation

Lin\*\* derived a form of the quasi-geostrophic omega equation in a pressure coordinate system:

$$\nabla^2(\sigma\omega) + f^2 \frac{\partial^2 \omega}{\partial p^2} = -2 \mathbf{v} \cdot \mathbf{Q} \quad (\text{A.1})$$

where  $\sigma = -\alpha/\theta(\partial\theta/\partial p)$ ,  $f$  is Coriolis parameter, and the components of  $\mathbf{Q}$  are expressed by

$$\mathbf{Q} = \left[ -\frac{\partial \mathbf{v}_g}{\partial x} \cdot \nabla \left( -\frac{\partial \Phi}{\partial p} \right), -\frac{\partial \mathbf{v}_g}{\partial y} \cdot \nabla \left( -\frac{\partial \Phi}{\partial p} \right) \right], \quad (\text{A.2})$$

$\mathbf{v}_g$  being the geostrophic wind vector and  $\Phi$  is geopotential. Lin's formulation also includes forcing terms for diabatic heating and the longitudinal variation of Coriolis, both of which I have chosen to omit, although the effect of the diurnal heating cycle is likely an important contributor to omega at 700 mb over the mountainous west.

On the basis of (A.2), I computed the  $\mathbf{Q}$ -components using the horizontal variation of geostrophic wind at 700 mb for the 850-500 mb layer, and at 500-mb for the 700-300 mb layer. This was done as a convenience, since the actual mean pressure levels for these layers are 652 and 458 mb, respectively. Thickness of the appropriate layer was determined from the differences in reported heights.

At the interior of the grid, centered differences were used for the gradient computations; at the edges, the gradient at the two adjacent interior points was extrapolated outward.  $\mathbf{Q}$ -components were then calculated at each point of the mesh, but only values at the interior points are displayed.

Rather than solving (A.1) explicitly for omega, I chose the expedient of scaling the r.h.s. results, since it is really the pattern and sign of omega that is important for diagnostic purposes rather than omega's magnitude.

### 8.2 The Interpolation Function

Interpolation of height and thickness data from reporting stations to gridpoints was accomplished through a two-pass Barnes (1964) analysis for which the weight function has the form

$$WT = \exp(-R^2/4C), \quad (\text{A.3})$$

where  $R$  is distance from data point to gridpoint and  $C$  is a selectable parameter which governs the response of the interpolated pattern to the initial data. That is,  $C$  determines the amount of smoothing and the wavelength at which it occurs.

For the first pass,  $C = 63000 \text{ km}^2$  and for the second pass,  $C = 31500 \text{ km}^2$ . The response

( $D = \exp(4\pi^2 C/\lambda^2)$ ) of the two passes versus wavelength is shown in Fig. A1, as is the amplitude gained by making the second pass. The points to note in the figure are that the maximum amplitude gain occurs at 1500 km wavelength which has been smoothed by 30 per cent of its "true" amplitude, and the Nyquist interval variations (about 800 km for NWS rawinsonde data) are retained with only 15 per cent of their possible amplitude. The analyses were purposely kept on the "smooth" side in order to compare more realistically with the LFM output.

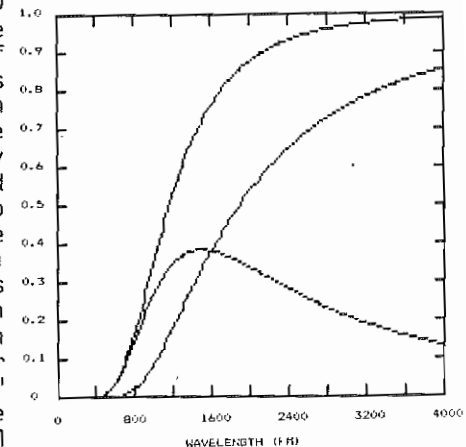


Fig. A1. First and second pass response curves and their difference for weight function expressed by (A.3) as a function of wavelength ( $\lambda = 0$  to 4000 km). Maximum amplitude is gained by second pass at  $\lambda = 1500$  km.

### 8.3 Bits and Pieces

The initial calculations of omega were coded in BASIC for an APPLE II computer with 48K memory. Results were graphed on an approximately two-degree latitude grid and crudely positioned geographically relative to Colorado. Later, when the gridded LFM printouts were received from the National Weather Service's Techniques Development Laboratory, there was reason to recompute the results on a grid of the same scale and map projection as the NWS output. For this, an IBM PC (128K memory) was used along with a slightly higher resolution graphic screen to produce better quality figures. Data entry was manually from the keyboard, and the screen graphics were dumped to scale on a dot-addressable matrix printer.

Individually, the programs run in an interpretive mode in from three to 15 minutes, the interpolation procedure taking the longest and the contouring next (10 minutes). When run in a compiled mode on the APPLE II, these same programs ran in six minutes and one minute, respectively.

The point of all this is that it doesn't take much computer power to execute the procedures and obtain hardcopy results. With automated data entry and machine language code, I estimate that procedures could easily be executed in ten minutes per layer. The potential for operational implementation on mini- or mid-sized computers in a weather forecast office is obvious.

\*\* Personal communication.



## OPERATIONAL SATELLITE PRECIPITATION ESTIMATES

Charles Kadin and Dane Clark  
National Oceanic and Atmospheric Administration  
National Environmental Satellite, Data and Information Service  
Satellite Services Division  
Camp Springs, Maryland

### 1. INTRODUCTION

Satellite meteorologists in the Synoptic Analysis Branch (SAB) of the National Environmental Satellite, Data, and Information Service (NESDIS) have been analyzing satellite imagery to produce precipitation estimates for flash flood threatening storms since 1978. In the early years, these estimates were generally limited to storms with cold top signatures in the Infrared (IR) satellite imagery as described in the original Scofield/ Oliver convective estimate technique. Estimates of maximum precipitation were computed by county and relayed by telephone to National Weather Service Forecast Offices with flash flood warning responsibilities.

Over the past six years, several important changes have occurred in the precipitation estimate program of SAB. First, through a joint effort between SAB and the Satellite Applications Laboratory (SAL), the precipitation estimate technique has evolved to improve the meteorologists ability to diagnose and estimate precipitation associated with many different types of rain and snow events. The present technique can handle various types of satellite signatures, IR temperature enhancements and meteorological conditions. Recent improvements which have significantly reduced the time required to produce and disseminate estimates include the operational use of the Interactive Flash Flood Analyzer (IFFA) computer system and the Automation of Field Operations and Service (AFOS) communications system.

This paper describes the current satellite precipitation estimate program of SAB including: the IFFA interactive computer system, the basic estimate technique, routine procedures, dissemination methods and recent advances. Several operational cases from the 1983-84 season are presented as examples including a brief discussion of verification. Finally, future plans for the SAB precipitation program are discussed.

### 2. THE ESTIMATE PROGRAM

The satellite precipitation estimate program of SAB has two major responsibilities. The first responsibility is to provide real-time precipitation estimates for the continental U.S. to NWS Field Forecast Offices as guidance information for flash flood watches and warnings (when requested, estimates can also be provided for Puerto Rico). The SAB also provides real-time precipitation estimates and guidance information to the Heavy Precipitation Branch (HPB) of the National Meteorological Center (NMC). HPB utilizes this guidance in preparing Quantitative Precipitation Forecasts (QPF's) and excessive precipitation outlooks. Both these responsibilities are part of the overall NOAA Flash Flood Plan.

### 3. THE IFFA SYSTEM AND OPERATIONAL PROCEDURES

The Interactive Flash Flood Analyzer (IFFA), a refinement of the University of Wisconsin's Man-Computer Interactive Data Access System (McIDAS) became operational in 1983. IFFA is operated by a meteorologist entering commands through a keyboard onto the accompanying alpha-numeric CRT screen. Once the GOES visible and infrared data are automatically stored on disk, the meteorologist can begin the estimation process.

Real-time GOES visible and infrared data are displayed every half-hour on the IFFA color monitor. The satellite meteorologist selects an event area with excessive precipitation potential to perform estimates. The GOES data in the event area are enlarged and animation sequences of both visible and infrared data are created. Current National Weather Service surface and upper air observations are also displayed on the color monitor. At this point, the meteorologist identifies and analyzes important cloud signatures producing heavy precipitation.

Three precipitation estimate techniques have been developed for interactive use on the IFFA. These are the Convective Technique for thunderstorms, the Winter Storm Technique for rain and snow, and the Tropical Cyclone Technique used for precipitation associated with tropical storms and hurricanes. Using the appropriate technique, the satellite meteorologist analyzes consecutive (infrared and visible) images by interactively drawing the estimated precipitation on the graphics screen of the color monitor using a data tablet system. Each half hour estimate can be summed with other half hour estimates in the event area to produce precipitation totals. These products are annotated with state and county boundaries (fig. 1) and hard copy prints are made.

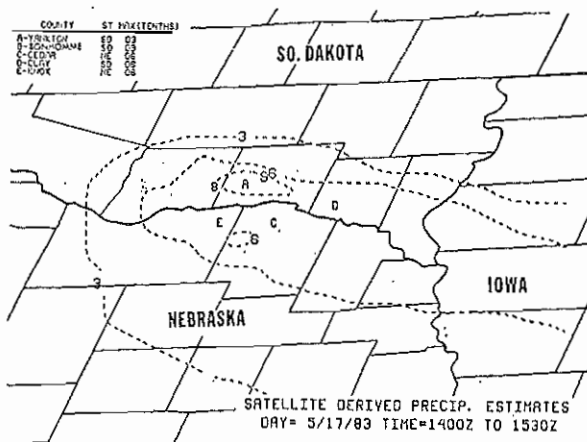


Figure 1. Example of a hard copy product from the IFFA

The satellite meteorologist uses this hard copy print to compose a brief message describing the location and time period of the precipitation estimates. Remarks about the precipitation event and short range outlooks based on the anticipated movement and changes in intensity can also be included. These messages are disseminated in real time using the AFOS communication system and are generally available to NWS offices within 30 minutes after the latest satellite image used (fig. 2).

As an operational experiment, estimates are also disseminated to the West Gulf River Forecast Center (WGRFC) when heavy rain is occurring over Texas. The estimate fields are hand digitized and grid point values are entered into the NOAA Central Computer. The WGRFC accesses these estimates from the NOAA computer and inputs estimate values into their River Forecast Model. Preliminary evaluations indicate that satellite estimates have proven to be critical inputs for severe rainstorms affecting the state at night when the gage reporting network is largely inactive.

Location	Hrly Rate	Totals	Time	Remarks
S Maine	.1"-.2"	.3"-.6"	15-18Z	Slow N Movmnt
S NH				
Cent NH	.1"-.2"	.2"-.4"	15-18Z	Rain and Snow
E Ma				

GENERAL REMARKS: WRMG CLD TOPS N NY WILL BE REPLACED BY NEW SURGE OF COLD TOPS AND PCPN S ME TO N VT. THEREFORE, PCPN WILL GENERALLY REMAIN UNCHANGED. HVST PCPN NR S EDGE OF COLDEST CLD TOPS.

EXPERIMENTAL SHORT-RANGE OUTLOOK - 3 HRS OR LESS

Location	Amount	Time
N NY	.2"-.4" R/S	18-21Z
Cent NH, N & Cent VT.	.3"-.6" Rain	18-21Z

Figure 2. AFOS SPE message at 1830Z Nov. 4, 1983

#### 4. ESTIMATING TECHNIQUES

The precipitation estimates for convective storms are computed on a half hourly or hourly basis using the Scofield/Oliver convective technique. The technique was empirically derived and relates half hourly cloud top temperatures and cloud top growth to maximum half hourly rainfall amounts. Rainfall estimates are also adjusted for the presence of overshooting tops, convective cluster and line mergers, quasi-stationary storms, and the prevailing atmospheric circulation and moisture fields. The technique is based on the Mb infrared enhancement curve. The technique can be used with 8 km resolution infrared data alone, but using 1 km visible data yields a more detailed analysis of the active precipitating areas and overshooting cloud tops.

During the winter of 1983-84, SAB produced realtime estimates of winter time heavy rain and heavy snow for the entire U.S. A winter storm precipitation technique was used to estimate precipitation from extra tropical cyclones (Scofield, 1983). This system relies heavily on satellite signature characteristics that correlate strongly with heavy precipitation. In many cases these satellite signatures evolve through a predictable life-cycle of growth and decay. Using this information and the translation speed of the system, SAB meteorologists have included experimental short - range outlooks for 0-3 hours in the estimate message. These outlooks are limited to cases where definite satellite system signatures are observed with recognizable growth rates.

## 5. OPERATIONAL CASES

### 5.1 Cold Top Convection - Mississippi Valley

In this example, an east west area of convection over northern Indiana (fig. 3) developed and spread westward to Iowa during the night of July 2, 1983 (fig. 4). This convection developed along a surface trough where dew points were high and low level moisture was abundant (fig. 5).

Maximum rainfall amounts estimated by SAB ranged from 5.1 inches in Iowa to 8.4 inches in northern Indiana. Maximum reports ranged from 3.8 to 7.4 inches. Satellite rainfall estimates were used directly in the flash flood warnings issued for northern Indiana.

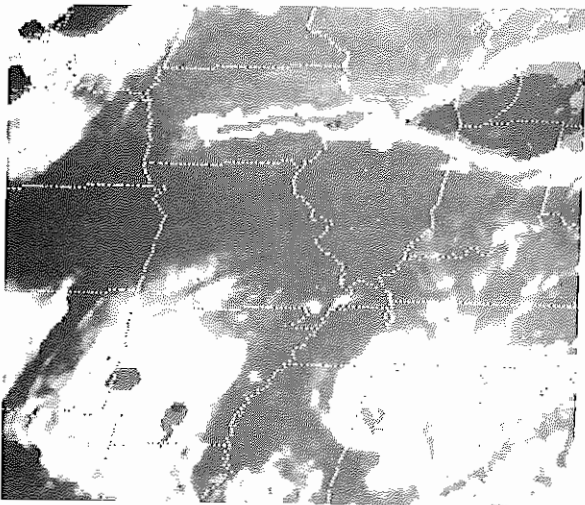


Figure 3. IR imagery (Mb curve) at 0430Z July 2, 1983

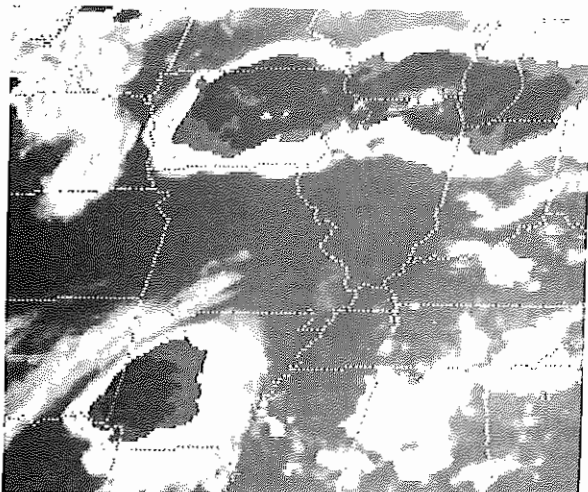


Figure 4. IR imagery (Mb curve) at 0830Z July 2, 1983

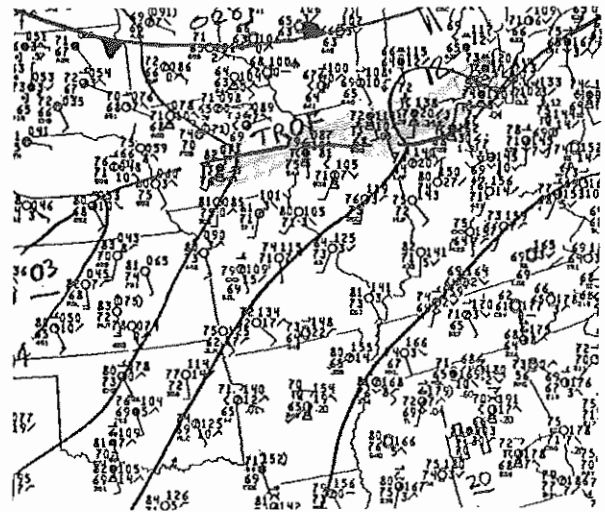


Figure 5. Surface analysis at 0600Z July 2, 1983

Also notice the convective complex in southwest Arkansas in figure 4. Although the cloud tops were not as cold as cloud tops over northern Illinois, this system moved very slowly and produced up to 8.7 inches of rain in southwest Arkansas. SAB operational estimates reached a maximum of 9.3 inches for the storm total in this area.

### 5.2 Warm Top Convection - Texas - Louisiana

This heavy rain event occurred between the early morning of December 10, 1983, and the morning of December 11, 1983 from east Texas to Louisiana. On the morning of December 10, satellite imagery (fig. 6) showed coldest tops were only dark gray (no colder than  $-58^{\circ}\text{C}$ ) and also revealed two separate relative cold spots corresponding to two separate rain maximums.

The largest estimate calculated using the IFFA and transmitted via AFOS to the NWS at 12Z was 2.7 inches (fig. 7). Although this turned out to be an underestimate (later reports indicated maximums were 3 to 4 inches), it did exceed the flash flood guidance values and probably was an early indication to the NWS that rainfall was heavy enough to produce flooding. Warnings were later issued for that area.

### 5.3 Winter Storm - Baroclinic Leaf

On December 16, 1983, an unusual and somewhat unexpected area of heavy snow spread across northern Texas into southern Arkansas and northern Louisiana. This snowstorm occurred well north of the surface front in a surface ridge of high pressure, where pressures were rising. However, a strong 500 mb trough and moisture advection pattern at 850 mb triggered the activity and prevailed over the unfavorable surface conditions to produce up to 9 inches of snow in southwest Arkansas (fig.8).

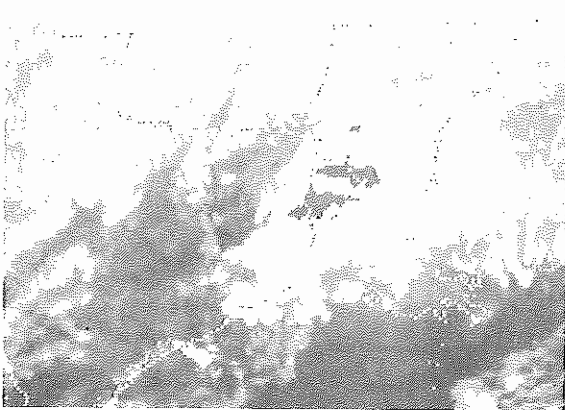


Figure 6. IR imagery (Mb curve) at 1300Z Dec. 10, 1983

Location	Hrly Rate	Totals	Time
S CADDO CO, LA & E HARRISON CO, TX	1.1"	2.4"	09-12Z
N SAN AUGUSTINE CO, TX & E SHELBY CO, TX	.8"	2.7"	09-12Z
		2.1"	09-12Z

Figure 7. AFOS SPE message at 1200Z Dec. 10, 1983

The cloud pattern observed in figure 9 is the baroclinic leaf category from the winter storm estimate technique. IR cloud tops gradually cooled during most of the period of heavy snow and reached a maximum shade of light gray ( $-52^{\circ}\text{C}$ ). Estimates were done using IFFA and reached a maximum of 0.8 inches liquid from 13-18Z (fig. 10). The overall pattern of the estimate is very similar to the analysis of the reported values, particularly in the area of maximum precipitation (fig. 11). A snow to rain ratio of 10:1 is assumed with temperatures near or slightly below freezing.

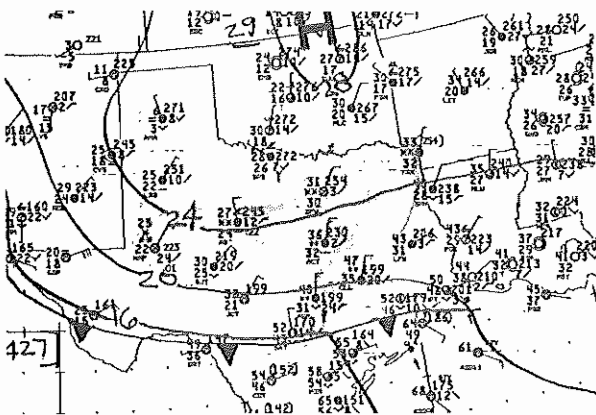


Figure 8. Surface analysis at 0900Z Dec. 16, 1983



Figure 9. IR imagery (Mb curve) at 1330Z Dec. 16, 1983

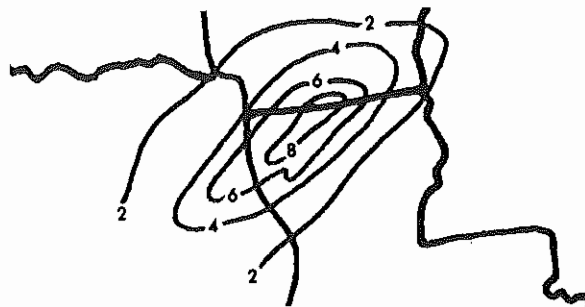


Figure 10. Snowfall estimates 1300-1800Z Dec. 16, 1983

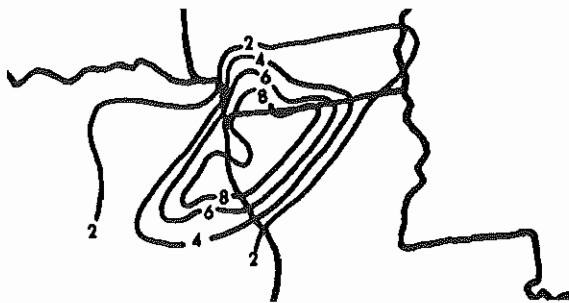


Figure 11. Snowfall observations 1200-1800Z Dec. 16, 1983

## 6. LIMITATIONS

There are many factors involved in the decision making process to estimate precipitation and disseminate guidance products to the National Weather Service. First, there is a physical limit to the volume of estimates that can be produced on the IFFA system in a recurring 30 minute image cycle. Satellite meteorologists use their analytical skills to determine which convective systems are producing excessive rainfall. To assist them in these decisions, SAB meteorologists consult with the Heavy Precipitation Branch of NMC, coordinate with WSFO's and SFSS's and use many sources of conventional data including radar, surface observations, and flash flood potentials. Although this limitation is an important one, it is only one of several reasons why some events go unestimated.

In a recent study, a NOAA summer employee from the University of Wisconsin found that for the summer season of 1984, a significant excessive rainfall event (3 inches) was missed only about 19% of the time. Some reasons for these non-estimated storms include:

- 1) The rainfall rate may not exceed the flash flood guidance values for the area.
- 2) The precipitation may be an unrecognized warm top event on the satellite imagery and is either undetected or underestimated.
- 3) The event could have a subtle heavy rainfall signature and is undetected.
- 4) Problems with the IFFA system and/or the manual back-up procedure.

The so called "warm top" problem is probably the single most limiting factor in estimating all types of flash flood producing precipitation. Scofield has developed modifications for some types of warm top events which have improved the estimates. More research is needed to maximize the use of the satellite data with different types of enhancement as well as the possibility of incorporating radar data directly into the IFFA system.

## 7. 1984 OPERATIONS

In 1984, the IFFA system was used for over 4,000 hours to produce real-time precipitation estimates. These estimates were disseminated to NWS forecast offices in more than 2500 satellite precipitation estimate messages on the NWS AFOS communications system. The first full year of service of the IFFA in operations has been a major success.

Using IFFA, and the AFOS communications system, SAB meteorologists delivered accurate and timely rainfall estimates to NWS forecasters 30 minutes faster than with the older manual method. In 1984, many flash flood watches, warnings and special statements contained references to the SAB estimates. It is evident that many NWS forecasters are using the estimates as a reliable data source to initiate flash flood statements, watches, and even warnings -- especially when no conventional observations are available.

One of the major rainfall events of 1984 in the United States occurred with the landfall of Hurricane Diana. SAB meteorologists monitored and estimated rainfall associated with the hurricane for 3 days. The heaviest rain occurred as the hurricane crossed the North Carolina coast on September 11 (fig. 12). Three day totals of the operational estimates performed during Diana are shown in figure 13. Observed data from this same period verified extremely well. Wilmington, North Carolina reported 17-18 inches for this period, which compared favorably with the 20" maximum estimate in the same area.

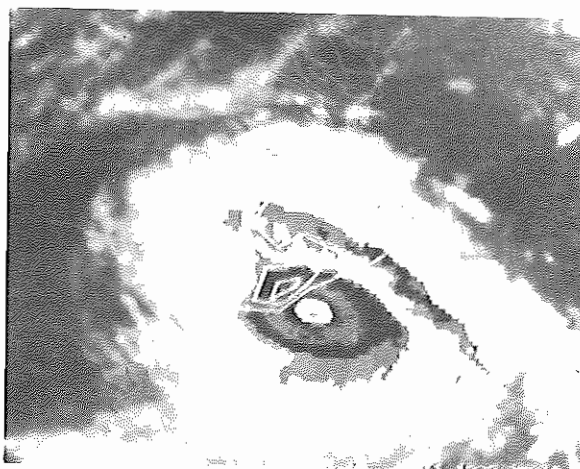


Figure 12. Hurricane Diana prior to landfall. GOES Mb IR image at 1900z Sept. 11, 1984

DIANA STORM TOTAL  
SAB PRECIPITATION ESTIMATES  
1200z 11 SEP - 2200z 14 SEP 84

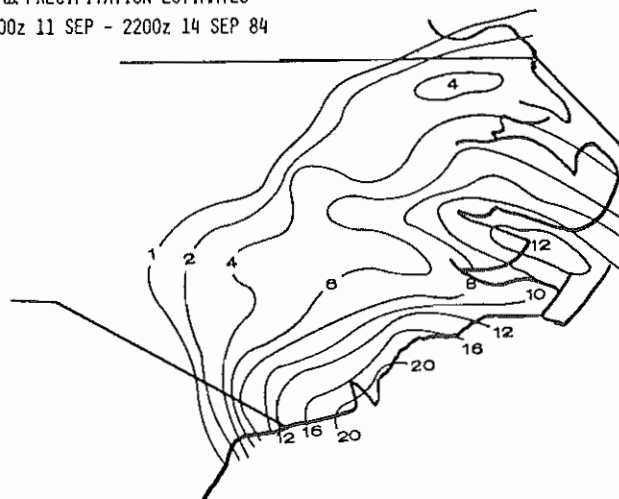


Figure 13. Operational precipitation estimates for Hurricane Diana

## 8. VERIFICATION

During the summer of 1984, a verification procedure was used to compare precipitation estimates with observed precipitation for the period May 1 to July 31, 1984. Comparisons were made for estimated rainfall maximums exceeding two inches when adequate observations were available to describe the rain event. Table 1 shows the results of this study.

Observed Data	Cases	Avg. of [Est.-Obs.]	Avg. % error	% of cases underestimated	% of cases overestimated
2-3"	130	0.7"	28.0	35.7	60.0
3-4"	72	1.0"	28.6	52.8	43.1
4-5"	40	1.5"	33.3	65.0	32.5
5-6"	8	1.8"	32.7	87.5	12.5
6-7"	5	2.9"	44.6	80.0	20.0
7-8"	6	2.0"	26.7	83.3	16.7
8-9"	5	2.8"	32.9	100	0
9-10"					
10-11"					
11-12"	1	4.1"	35.7	100	0
12-13"					
13-14"	1	7.0"	51.9	100	0

Table 1. Results from 3-month verification study 268 cases

The main finding of this study was that the average percent error ranged from 28% to 33% for rain events between 2 and 6 inches and was very consistent for nearly every rainfall category. The average absolute error ranged from 0.70" for 2-3 inch rains, to 1.8" for 5-6 inch rains. The location error of the estimates was difficult to specify since estimates are produced for a county (or part of a county) and not for a specific point. Most of the maximum observations occurred within the estimated county with the average estimate no more than 10-20 miles from the maximum observation reported.

It was further observed that when a precipitation event was widespread, with similar heavy amounts over a large area, the estimates were extremely good. Magnitude errors with estimates for localized convective events were more variable.

## 9. FUTURE DIRECTION

Current plans in NESDIS call for the upgrading of the IFFA system in the late 1980's. With a larger and faster system, several new applications currently under development can become a reality. These new potential capabilities include: more sophisticated nowcasting software, automated precipitation estimation technique, VAS data utility, storm tracking algorithms, and satellite radar composites.

Future products may include graphic rainfall estimates available 10-15 minutes after image time and 30 minutes to one hour forecasts of heavy precipitation. The results should be improved guidance products for forecasters and more timely and accurate flash flood watches and warnings.

## 10. REFERENCES

- Clark, J.D. and R. Borneman 1984: Satellite Precipitation Estimates Program of the Synoptic Analysis Branch. Proceedings from the Tenth Conference on Weather Forecasting and Analysis, June 25-29, 1984, Clearwater, FL, AMS, Boston, MA, 392-399.
- \_\_\_\_\_, J.D. and M.O. Perkins 1985: The NOAA Interactive Flash Flood Analyzer. Proceedings from the International Conference on Interactive Information and Processing Systems for Meteorology, Oceanography, and Hydrology, January 7-11, 1985, Los Angeles, CA, AMS, Boston, MA 255-259.
- Morris, David G. 1985: West Gulf River Forecast Center Operations Using Satellite Estimations of Rainfall. Proceedings from the NWS Fourth Southern Region Quantitative Precipitation Forecasting Workshop, January 28-30, 1985, San Antonio, TX.
- Moses, J.F., L.E. Spayd, Jr., R.S. Gird, and A.L. Siebers 1981: Interactive techniques for estimating precipitation from GOES imagery. Proceedings of Joint Automatic Control Conference, June 1981, Charlottesville, VA, 9 pages.
- Scofield, R.A. 1984: The NESDIS Operational Convective Precipitation Estimation Technique. Proceedings from the Tenth Conference on Weather Forecasting and Analysis, June 25-29, 1984, Clearwater Beach, Fla., Boston; MA, 171-180.
- \_\_\_\_\_, R.A. and V.J. Oliver, 1980: Some improvements to the Scofield/Oliver technique. Proceedings on Second Conference on Flash Floods, March 18-20, 1980, Atlanta, GA, AMS, Boston, MA 115-122.
- \_\_\_\_\_, R.A. and V.J. Oliver, 1977: A scheme for estimating convective rainfall from satellite imagery, NOAA Technical Memorandum NES-86, Washington, D.C., April 1977, 47 pages.
- \_\_\_\_\_, R.A., V.J. Oliver and L.E. Spayd, 1980: Estimating rainfall from thunderstorms with warm tops in the infrared imagery. Proceedings from the Eighth Conference on Weather Forecasting and Analysis, June 10-13, 1980, Denver, CO., AMS, Boston, MA 85-92.
- \_\_\_\_\_, R.A. and L.E. Spayd 1983: A technique that uses satellite, radar and conventional data for analyzing precipitation from extratropical cyclones. Proceedings from the Fifth Conference on Hydrometeorology, October 17-19, 1983, Tulsa, OK, AMS, Boston, MA 259-268.
- Spayd, L.E., Jr., 1981: Interactive precipitation estimates for hurricane Allen using geostationary satellite data. Proceedings of the Fourth Conference on Hydrometeorology, October 7-9, 1981, Reno, NE, AMS, Boston, MA 159-165.

Satellite Convective Cloud Categories Associated With  
Heavy Rainfall

by

Roderick A. Scofield  
NOAA/NESDIS  
Washington D.C. 20233

1. Introduction

The purpose of this paper is to present satellite convective cloud categories associated with heavy rainfall. These categories are then applied to significant flash flood events which occurred over Texas between 1981-1983.

2. The Categories

Satellite meteorologists do their best work in estimating rainfall from Mesoscale Convective Complexes (MCC) observed in Figure 1a. This MCC is embedded in a moderate vertical wind shear environment; heaviest rainfall is occurring along the upwind edge of the anvil (between A and A' in Figure 1a). The accompanying radar data (Figure 1b) shows heavy rainfall intensities (VIP levels 3 and 5) near the upwind edge between A and A'.

Very frequently, flash floods are produced by subtle satellite observed cloud signatures. These thunderstorms with subtle signatures are quite different from MCC's; they usually have warm-tops (warmer than -62°C), are smaller, do not last as long and are often quite differently shaped as compared to MCC's. Most importantly, these thunderstorms share the same importance as MCC's with respect to producing heavy rainfall and flash floods. As a result, flash-flood producing thunderstorm systems were separated into various categories based on their distinctly different cloud top characteristics, life cycles, and mechanisms which initiate, focus, and maintain the convection. The categories include: MCC's (Maddox, 1980), synoptic-scale tropical systems (Ward, 1981), large-scale wedges and linear multi-clustered systems (Clark, et al., 1980), single-clustered, regenerative, and circular multi-clustered convective systems and convection embedded in large/small-scale overrunning systems (Spayd, et al., 1983), synoptic-scale cyclonic circulations (Spayd, 1982) and squall lines (Fleming, et al., 1984). The categories along with characteristics in the satellite, conventional and radar data are presented in Figures 2a, 2b and 2c.

3. Satellite Characteristics of Flash Flood Events Over Texas

One hundred and twenty significant flash flood events were examined from 1981 through 1983 for Texas. Each event was categorized into the type of satellite-observed convective system, minimum cloud top temperature during time of heaviest precipitation, time of day and time of year

The categories are shown in the following table:

<u>Type of Convective System</u>	<u>No. of Events</u>
Synoptic Scale Tropical -----	7
MCC -----	13
Large Scale Wedge -----	2
Squall Line -----	26
Single Clustered -----	7
Multi-Clustered Circular -----	11
Multi-Clustered Linear -----	40
Synoptic Scale Cyclonic Circulation -	1
Large Scale Overrunning -----	1
Regenerative: Single Clustered-3 ----	9
Multi-Clustered-6 -----	
Bookkeeping -----	3
Total =	120

Bookkeeping refers to those events where a combination of two or more convective systems transversed the same location. Multiclustered and squall line systems comprised 64% of the flash flood events.

A histogram of minimum cloud top temperature versus the number of events is shown in Figure 3. Sixty-five percent of the flash flood events were cold tops ( $\leq -62^\circ\text{C}$ ); 35% were warm tops.

A histogram of the time of day of maximum rainfall versus the number of events is displayed in Figure 4. Sixty-nine percent of the events occurred between 2PM - 2AM CST.

A histogram of the time of year (semi-monthly) versus the number of events is depicted in Figure 5. Most of the events occurred between mid-April through October; a minimum is observed during July and August. Also indicated in Figure 5 are the number of flash flood events associated with comma tails--frontal systems associated with low pressure systems (comma heads). Comma tail cases comprise 53% of the flash flood events. As seen in Figure 6, there are three types of comma tail cases: I-the comma head moving eastward in Canada; II-the comma head in the central and northern plains and III-the comma head in the Atlantic Ocean with the comma tail extending southwestward through the southern states and into Texas. Type III can be quite difficult to analyze unless continuity is maintained on the comma head-comma tail system as it moves from the continent into the Atlantic Ocean. Difficulty arises because of: (1) an extremely large distance between the comma head and the southern portion of the comma tail and (2) the comma tail over the southern U.S. being masked by diurnal convection (e.g., the sea breeze fronts). The number of comma tail cases comprising a particular type of convective system is shown as follows:

Type of Convective System	No. of Comma-Tail Cases	Total No. of Events
MCC	5	13
Squall Line	22	26
Multi-Clustered Linear	23	40
Multi-Clustered Circular	6	11
Single Clustered	2	7
Regenerative	4	9
Large-Scale Wedge	2	2
Total	64	120

#### 4. Outlook

Additional research is necessary to identify the most frequent and important types of heavy rainfall producing convective systems in other portions of the southern region. Each type of heavy rainfall producing convective system should be researched in detail to provide operational forecasters with the unique atmospheric conditions necessary for their development and evolution.

#### 5. Acknowledgements

The author would like to thank Betty Wilson for typing the manuscript and John Shadid for drafting the figures and layout of the manuscript.

#### 6. References

- Clark, J. D., A. J. Lindner, R. Borneman, and R. E. Bell, 1980: Satellite Observed Cloud Patterns Associated with Excessive Precipitation Outbreaks. Proceedings of the Eighth Conference on Weather Forecasting and Analysis, June 10-13, 1980, Denver, CO, AMS, Boston, MA, 463-473.
- Fleming, E., L. E. Spayd, Jr., R. A. Scofield, 1984: Characteristics of East Coast Convective Flash Flood Events in GOES Imagery. Proceedings of the Tenth Conference on Weather Forecasting and Analysis, June 25-29, 1984, Clearwater Beach, FL, AMS, Boston, MA, 8 pages.
- Maddox, R. A., 1980: Mesoscale Convective Complexes. Bull. Am. Met. Soc., 61, 1374-1387.
- Spayd, L. E., Jr., 1982: Estimating Rainfall Using Satellite Imagery From Warm-top Thunderstorms Embedded in a Synoptic Scale Cyclonic Circulation. Proceedings of the International Symposium on Hydrometeorology, June 13-17, 1982, Denver, CO, AWRA, Minneapolis, MN, 139-146.
- Spayd, L. E., Jr., and R. A. Scofield, 1983: Operationally Detecting Flash Flood Producing Thunderstorms which Have Subtle Heavy Rainfall Signatures in GOES Imagery. Proceedings of the Fifth Conference on Hydrometeorology, October 17-19, 1983, Tulsa, OK, AMS, Boston, MA, 190-197.
- Ward, J. D., 1981: Spatial and Temporal Heavy Rainfall Patterns Overland Associated With Weakening Tropical Cyclones. Proceedings of the Fourth Conference on Hydrometeorology, October 7-9, 1981, Reno, Nevada, AMS, Boston, MA, 174-180.



CHARACTERISTICS OF SATELLITE-OBSERVED HEAVY CONVECTIVE RAINFALL SYSTEMS

TYPES	DIURNAL VARIATIONS	SATELLITE DATA	CONVENTIONAL DATA	RADAR DATA
<p>Ia. TROPICAL SYNOPTIC SCALE TROPICAL</p>	<p>"Peripheral thunderstorms" develop in the afternoon in response to surface heating away from the circulation center. At night, boundary layer stabilizes and "core thunderstorms" develop at circulation center due to maximum moisture convergence. "Core thunderstorms" may form a MCC type system.</p>	<p>Cold tops, readily identifiable, persistent anticyclonic outflow aloft which causes cloud top growth to become quasi-constant. Weak jets in westerlies can cause elliptical elongation in outflow and convection. When system becomes extra-tropical the pattern may resemble that of an occluded frontal cloud structure and the maximum rainfall shifts north and east away from the center of the system. Outer rainbands and in dissipating stages the entire system may become warm-topped.</p>	<p>Remnant of Hurricane, Tropical Storm, or Tropical Depression; initially-persistent forward motion and cyclone symmetry; occurs in extremely moist air mass (<math>PW &gt; 2''</math>), low to mid-level cyclonic vorticity focuses rainfall.</p>	<p>Outer curved rainbands may have a combination of convective and stratiform Z-R rain rates. Large persistent area of VIP 1-3, embedded but non-persistent VIP 4-6. New echoes may reappear hours after previous echoes dissipate. Echoes may appear on periphery of circulation center during afternoon and reappear near circulation center at night. Echo movement is a combination of movement along the spiral band, propagation of spiral band around circulation center, propagation of circulation center.</p>
<p>Ib. TROPICAL MESOSCALE QUASI-TROPICAL (MESOSCALE CONVECTIVE COMPLEX -MCC)</p>	<p>Strong maximum in early evening to early morning; strong minimum in mid-morning.</p>	<p>Cold tops, overshooting tops, and numerous cell mergers observed. Large circular or oval anticyclonic outflow. Speed of movement of coldest tops most important for heaviest rainfall. Intensifying if coldest tops moves to central location in cloud pattern and cirrus outflow becomes increasingly anticyclonic in one or more quadrants. Most efficient precipitation producer 4 to 10 hours after initial convection develops, due to large area of light precipitation saturating the surrounding air mass. Usually produces mid-level cyclonic circulations and upper level mesoscale jet streaks which will alter surrounding and future convection.</p>	<p>Triggered by shortwave trough moving through upper level ridge and focused by low level axis of maximum winds overriding low level boundaries. Vertical circulation similar to Synoptic Scale Tropical system. Cyclonic vorticity in low to mid troposphere couples with anticyclonic outflow aloft. Winds veer strongly with height.</p>	<p>Large, persistent, trackable area of VIP 1-3 with embedded non-persistent VIP 4-6. Numerous echo mergers are detected. Highest VIP levels usually occur in first 5 hours of development when the precipitation efficiency is lowest.</p>
<p>Iia. LINEAR LARGE SCALE WEDGE</p>	<p>No distinct diurnal variation.</p>	<p>Large 50-90 degree angle pointing into the wind. Southern most cluster may be embedded in a N-S oriented squall line. Shortwaves rotating around longwave trough concentrate the convective outbreaks. Due to persistent low-level southerly inflow convection redevelops after weak shortwave passes and thunderstorms become increasingly efficient rainfall producers. As longwave trough approaches cloud tops may become warmer with time.</p>	<p>Forms where polar front jet and subtropical jet separate. Occurs east of deep 500 mb longwave trough with weak or neutral synoptic scale vorticity advection. Outbreaks concentrated by shortwave troughs. Wedges retard movement of 500 mb pattern. Fueled by strong low level axis of maximum winds over a low level boundary. Winds veer strongly with height,</p>	<p>Large areas of VIP 1 and 2 with embedded VIP 3-6. Echoes may redevelop over same area or upwind in surges.</p>

FIGURE 2A

CHARACTERISTICS OF SATELLITE-OBSERVED HEAVY CONVECTIVE RAINFALL SYSTEMS

TYPES	DIURNAL VARIATIONS	SATELLITE DATA	CONVENTIONAL DATA	RADAR DATA
IIB. LINEAR SQUALL LINE	Strong maximum (80%) in late afternoon through evening; minimum in morning.	Cold cloud tops in 75% of cases. Downstream convection may be masked by upstream anvil blowoff. Weakening usually occurs when squall line accelerates away from its initial triggering mechanism (i.e. frontal zone). When convection develops upwind, clusters may pass over the same area if the squall line is slow moving.	Occurs along or ahead of a slow moving cold frontal boundary. Winds veer only 40° with height; winds < 35 knots, PW ~ 1.6", mean RH ~ 80%, triggered by a weak shortwave at 500 mb.	Line Echo Wave Pattern (LEWP) may be observed, an intense line of high VIP 3-6 echos. Echos may suddenly redevelop upwind in surges.
III SINGLE-CLUSTERED	Tied strongly to solar insolation; a strong maximum (80%) in late morning through early evening, and a strong minimum in nighttime and morning.	Very small, round, oval, or carrot shaped. Very rapid growth, stationary, overshooting tops. Usually warm tops. Since tops are so small the actual temperature of the tops may be colder than the resolution of the GOES-IR sensor indicates.	Fueled by solar insolation, anchored by topography, or mesoscale boundaries.	Small, stationary, echo, VIP 3-5.
IVa. MULTI-CLUSTERED CIRCULAR	Eighty percent occur from late afternoon through midnight; minimum in morning.	Warm tops in 70% of cases, round or oval shaped cloud tops, cluster mergers usually evident; usually quasi-stationary. Mergers of separate multi-clustered circular systems may evolve into a MCC-Mesoscale Convective Complex.	Weak upper level flow, develops due to low level forcing.	Quasi-stationary, VIP 3-6, echo mergers may occur.
IVb. MULTI-CLUSTERED LINEAR	Seventy percent occur from late afternoon through evening; weak minimum in morning.	Warm or cold tops, small wedge, carrot or diamond shaped, coldest tops in vertex (enhanced V pattern sometimes observed). Rapid growth and stationary, may build upwind. Much smaller than large scale wedge. The higher the speed shear from mid to high levels the narrower the wedge. Heaviest rain in extreme upwind portion of wedge although thunderstorm cells may stretch linearly from the vertex to the middle of the wedge (in the warmer IR temperatures behind the enhanced V pattern). Existence dependent on jet streak. If jet streak drifts away from wedge in a direction normal to flow, wedge dissipates and new wedges develop where jet subsequently intersects areas with favorable low level conditions. When second wedge develops upstream from the first, the initial wedge is shielded from jet and dissipates unless second wedge induces a mesoscale jet streak that interacts with the first system and intensification results. If another convective system develops upstream and blocks the environmental wind flow (reducing the mid to high level wind shear) the linear multi-clustered system could develop into a MCC.	Upper flow is zonal or weakly diffluent. Strong speed shear from mid to high levels present. May distort upper flow like Mesoscale Convective Complexes - MCC's and produce wind max on northern side. Development due to low level forcing and jet streak aloft.	Individual echo motion may be fast (15-30 knots) but repeated echo development in upwind of cluster may result in slow cluster speed. Persistent VIP 3's are common with embedded non-persistent VIP 4-6. In enhanced V patterns the highest VIP levels are usually at the vertex of the V extending into the warmer temperatures downwind of the vertex.

FIGURE 2B

CHARACTERISTICS OF SATELLITE-OBSERVED HEAVY CONVECTIVE RAINFALL SYSTEMS

TYPES	DIURNAL VARIATIONS	SATELLITE DATA	CONVENTIONAL DATA	RADAR DATA
V. SYNOPTIC SCALE CYCLONIC CIRCULATION	Moderate maximum in the evening into early morning; moderate minimum in mid-morning and afternoon.	Warm tops located in comma head of cyclonic circulation, cyclonic circulation moving E to NE at 2° latitude per 12 hours, rapid cloud growth, overshooting tops, mergers observed, either quasi-stationary or regenerative.	Occurs to north or east of slow moving circular 500 mb vorticity center. Occurs to north of 850 mb low with maximum isotherms rapping around to north of low. Occurs to north and west of 850 mb axis of maximum winds. Occurs north of surface low in cool NE flow. When 500 mb center weak, no surface fronts; when stronger, surface fronts are evident. Winds veer 180° with height; winds < 40 knots. PW ~ 1.3", mean RH ~ 80%. Extremely "wet" when convection is focused along mesoscale surface convergence line.	If quasi-stationary, VIP levels are high, VIP 4-6. If regenerative, echos VIP 3-4.
VI. LARGE/ SMALL SCALE OVERRUNNING	Strong maximum in early evening to midnight; strong minimum in early to mid-morning.	Warm tops located in large anti-cyclonic flow of cirrus. Animation (IR) best for detecting convective bands from cirrus bands. Transverse banding in cirrus appears as textured areas on visible imagery. System doesn't weaken until strong shortwave passes through area.	Cool boundary layer, winds veer over 180° with height, air lifted isentropically until unstable and deep convection is released. Convective bands form perpendicular to 850 mb flow (low level axis of maximum winds), and nearly parallel to 500 mb flow. K index much better than Lifted Index for detection. Extremely moist environments RH > 90%, PW > 1.5" large area of weak maximum surface moisture convergence values, no defined surface low apparent.	Widespread persistent VIP 1 and 2, occasional VIP 3.
VII. REGENERATIVE	Moderate maximum in late afternoon through mid-evening; weak minimum in mid-morning.	Warm or cold tops. Single-clustered and multi-clustered convective systems develop along the upwind portion of a low-level boundary and transverse the same path downwind along the boundary. Animation is the best tool for detection. No cell mergers usually seen. Outflow from new cells may continually reinforce existing quasi-stationary outflow boundary. If regeneration of cells is very rapid (> 1/2 hour) system may resemble a small wedge (linear multi-clustered). Initial thunderstorm cells may saturate the local environment so new thunderstorm cells may be more efficient precipitation producers. The initial thunderstorm cells may also warm the local upper atmosphere causing a lowering (warming) of the equilibrium level; so new thunderstorm cells may have warmer tops. System weakens when triggering shortwave overtakes the quasi-stationary outflow boundary or low level convergence zone. Outflow from new cells may also accelerate existing quasi-stationary outflow boundary away from favored areas of development, so new cells stop regenerating.	Outflow boundary or convergence boundary apparent in surface mesoanalysis. Inflow perpendicular to boundary may be focused by meso-low. Extremely high mesoscale moisture convergence values.	Train echo effect. Individual echos may move at speeds of 15 to 40 knots. New echos may have higher VIP levels than previous echos.

FIGURE 2C

### CLOUD TOP TEMPERATURE

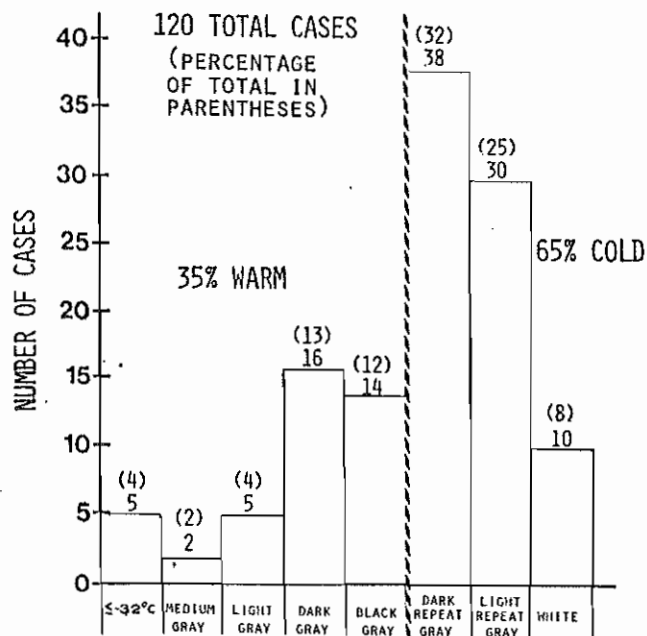


Fig. 3. A histogram showing the minimum cloud top temperature during the period of heaviest rainfall as observed in the infrared Mb enhancement curve.

### TIME OF DAY (OF MAX RAINFALL)

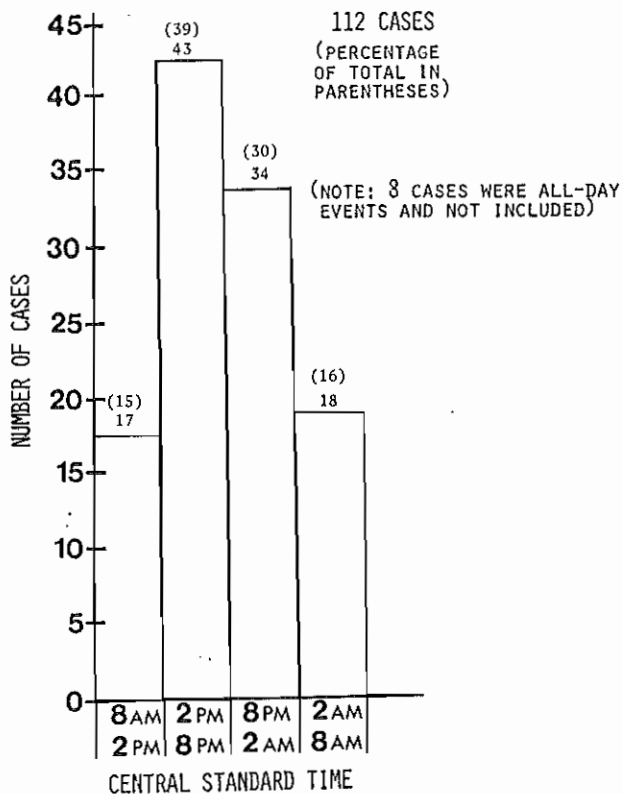


Fig. 4. A histogram showing the variations in the local time of day (CST) of the heaviest precipitation in Texas.

TIME OF YEAR (SEMI-MONTHLY) FOR COMMA-TAIL CASES  
AND TOTAL CASES (IN PARENTHESES)

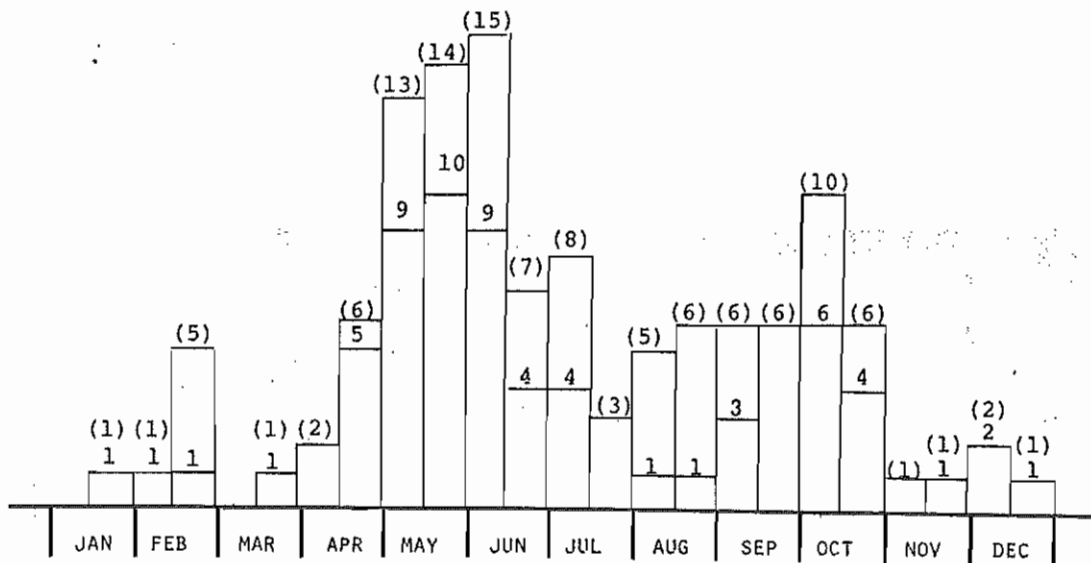


Fig. 5. A histogram of semi-monthly distribution of occurrence.

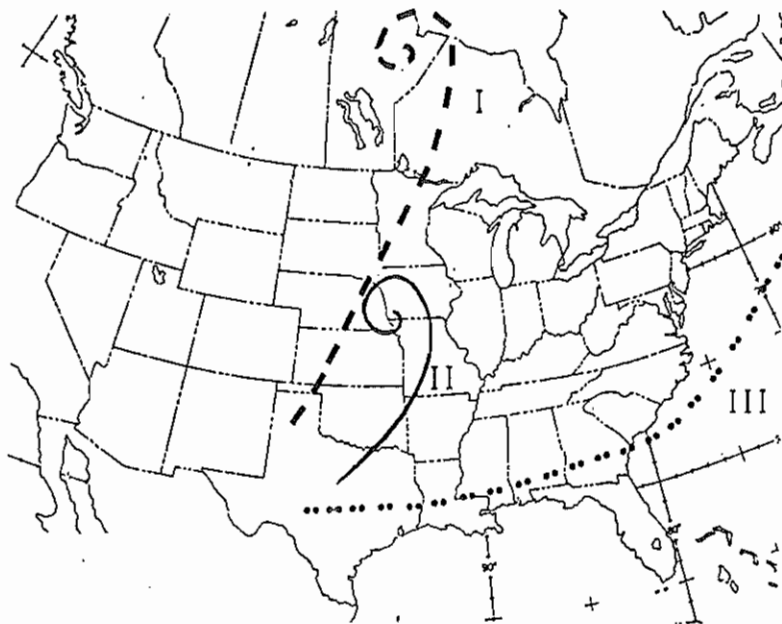


Fig. 6. Three types of comma head-comma tails which produce flash floods over Texas.

WEST GULF RIVER FORECAST CENTER OPERATIONS  
USING SATELLITE ESTIMATIONS OF RAINFALL

David G. Morris, Ph.D., P.E.

National Weather Service River Forecast Center  
Fort Worth, Texas 76102-6171

1. INTRODUCTION

The West Gulf River Forecast Center (WGRFC) has developed the capability to use for river predictions remote sensed rainfall point estimates from the radar (MDR data only), and from the GOES satellite system. The purpose of this report is to highlight the techniques and computer programs employed to process these near real-time data into operationally usable precipitation data sets, with discussion confined almost entirely to the satellite derived information.

2. THE DATABASE STRUCTURE

A grid point system of addressing rainfall observations was developed by Smith (1975) at WGRFC in the mid 1970s as a way of providing needed flexibility to cope with frequent rain gage network changes and observations from unplanned (unofficial) stations that so often report during storm periods. The resulting grid system is independent of gage location, and is therefore also ideally suited to geographically positioned estimates of rainfall from any source. The grid is latitude-longitude based, with six-minute intersections representing "points" that are discrete and computer addressable. All rainfall reports or estimates are "moved" to the nearest grid intersection so that the report may be addressed and computer stored. The grid is sufficiently dense so that any report would be moved no more than approximately three miles, a data positioning accuracy well within that required to develop river forecasts for any basin other than a very small watershed.

Briefly, the grid point addressing system consists of a degree box address (NN), a two digit address 1 through 98, and a point within the box address (IJ), a two digit address 0 through 9. The degree box is bounded by lines of whole degrees of latitude and longitude; six minute intersections of lat/long within each box yields a total of 100 grid points per box area. The computer

address of NN IJ then uniquely positions a data point. For an area the size of Texas, the resulting precipitation data file is nearly 10,000 points, with each point representing zero rain, a report of rain, or an estimate of rain. The database at WGRFC was developed to facilitate the grid point concept, with precipitation totals stored for 24-hour periods, but broken down into lesser time intervals to provide 3 to 6 hour inputs to the river prediction programs. National Weather Service first order reporting stations, MDR reports, and satellite reports may all be used as guidance to "break down" a 24-hour rainfall report into some shorter time interval.

3. DATA PROCESSING/COMPUTER PROGRAMS

The Synoptic Analysis Branch (SAB) of NOAA/NESDIS develops precipitation estimates based on the Scofield/Oliver technique. Using an interactive graphics system, SAB can compute and transmit the estimations generally within thirty minutes after the latest image time used. The procedure for generating such data is well documented (Scofield, 1977, 1980, 1983) and will not be discussed as part of this report. Suffice it to say that visible and infrared images are used by the SAB meteorologist to arrive at half-hour precipitation estimates for the target area and summed into 3-hourly totals for a variety of field applications. What is perhaps unique in hydrologic application at the RFC level is the software developed to facilitate use of the data.

In 1982 NOAA/NESS (now NESDIS) and WGRFC teamed up to develop IBM 360/195 computer programs to move vast amounts of satellite estimated rainfall into the RFC hydrologic precipitation file. NESS programmed the WGRFC grid point system and wrote the associated software to load into a disk file 3-hourly estimation sums for each grid point within the storm area. Standard synoptic times were chosen: 00Z, 03Z, 06Z, 12Z, etc., for a total of eight files. With each data set load a

message is sent to the WGRFC line printer. The RFC then executes its own 360 program to sum the data into 6-hour totals (06Z, 12Z, 18Z, 00Z), for whatever periods are available, and store the 6-hourly grid point amounts. At this point the data are available for input to river forecast support programs, depending on how the hydrologist wishes to combine the data with other precipitation information.

The RFC program that accesses the NESDIS 3-hourly data file and stores for WGRFC 6-hourly totals also generates a line printer listing (see Table 1) of the grid point estimated data. The list is always total rainfall accumulated for the current "hydrologic day." The hydrologic day ends at 12Z and the precipitation totals displayed are totals since 12Z the previous hydrologic day. So, for example, if the program is executed at, say, 01Z, the listing would indicate grid point totals for all SAB 3-hourly loads since 12Z. Should the grid point fall on a station that has a name, the station name is also printed out. A second computer program may be run that accesses the SAB 3-hourly grid point file and line printer plot the data set for the time specified by the RFC hydrologist (00Z, 03Z, etc.). Fig. 1 and Fig. 2 illustrate this output, and will be discussed later in this report. This same computer program may be used to plot observed precipitation, thus facilitating a visual comparison of observed versus estimated.

Precipitation data may, of course, also be available from other sources, so this fact raises the question as to how one should combine data temporally and spatially. A large WGRFC precip processing program called ONECL allows the hydrologist to specify certain options at run time that will dictate how the data are handled. WGRFC maintains grid pointed data in 6/24-hourly form for observed amounts, MDR estimations, and satellite estimations. The following rule applies: In all cases where observations occupy the same address as satellite or MDR estimates, the observation is used. In the event of no observation, satellite estimates override MDR sums. Program options for MDR: 0 - no MDR usage (default); 1 - limited MDR usage - distribute and assign MDR precipitation to 24-hour MDR reflectivity sums of 4 or less only; 2 - full MDR usage - distribute and assign precipitation to all MDR reflectivity sums. Program options for satellite: 0 - do not use satellite estimates (default); 1 - use satellite estimates to distribute precipitation at each grid point where a satellite estimate exists, but do not use the estimates as precip observations; 2 - use satellite

estimates to distribute precipitation at each grid point where a satellite estimate exists, and process each satellite estimate as a precip report. Depending upon how one selects the options, it is possible for ONECL to generate a final rainfall file that includes all three sources of data to spatially define a storm and temporally distribute the rain over the affected basins. The last step in ONECL data processing is to establish a file of basin runoff values for use by the river prediction program.

#### 4. OPERATIONAL USE

By agreement, it has been policy for SAB to initiate estimations over Texas for WGRFC operations only when the RFC has so requested, or when, in the judgment of the SAB meteorologist, a serious storm was developing across the State. WGRFC does not view satellite estimates as a necessary input for routine river predictions. To the extent that the rain gage network will support flood forecasting activities, with radar serving as guidance for storm centers and storm patterns, the office prefers to conduct business using only these data. The RFC does, however, view satellite estimates as potentially critical inputs for severe rainstorms affecting the State at night when the gage reporting network is largely inactive, and also for the western half of the State at any time, since the reporting network for this drainage is very poor. And, undoubtedly, the satellite will prove invaluable to WGRFC forecast operations when tropical storms make landfall along the Texas coast and migrate inland. The fundamental problem in using satellite data to develop flood forecasts for short time periods and for relatively small watersheds (less than 3000 square miles) is twofold: the accuracy in both amount and surface positioning is still largely a matter of speculation, and secondly, dense satellite data are not easily combined with other data to produce an optimum rainfall data set. For any given grid box, it is possible to generate 100 satellite rainfall estimates, and these data will "overwhelm" in a computational procedure what few other reports are available within the same area. Combining "ground truth" reports with remote senses estimates in some intelligent fashion can undoubtedly be done (and has been done), but the algorithm to accomplish this is no small task, given the computer and operational constraints that prevail in the RFC environment. Finally, in the past two years, Texas has not experienced very much the kinds of storms that would allow WGRFC to gain valuable insight as to the utility of SAB estimates for flood forecasting. However, preliminary

SATELLITE RAINFALL ESTIMATES --- SORTED IN DESCENDING ORDER

GRID	RAIN	NAME	GRID	RAIN	NAME	GRID	RAIN	NAME
4314	400		4305	400		4306	400	EASTHAM
4316	400		4408	400				
2920	390		3029	390				
3039	360							
3169	350		4300	350	WOODLAKE	4301	350	
4302	350		4310	350		4311	350	GROVETON
4409	350		4436	350	HUNTINGTON			
2930	310	OVERTON						
2510	300		3030	300	LOGANSPOBT	3022	300	
3507	300		4200	300		4305	300	
4307	300	MIDWAY 4 NE	4305	300		4309	300	
4312	300		4310	300		4314	300	LOVELADY
4327	300		4317	300		4318	300	
4355	300		4360	300		4340	300	
4415	300		4407	300		4414	300	
4421	300	P. WELLS PARK	4411	300		4417	300	
4424	300	ZAVILLA	4425	300		4423	300	
4430	300	FINLAND	4432	300		4422	300	
4433	300	BRADDOUS	4434	300		4432	300	
2911	280		2915	280		2916	280	
2924	280		2925	280		2926	280	
2927	280		2931	280		2932	280	
2934	280		2935	280		2944	280	
3023	280	CARTHAGE	3024	280				
2900	270		2911	270	NEW SUMMERFIELD	2909	270	
2912	270		2921	270		3016	270	
3017	270		4391	270				
2923	260		2933	260				
2810	250		2821	250		2831	250	
2908	250		2918	250		2919	250	
2929	250		2939	250		3001	250	
3034	250		3005	250		3006	250	
3049	250		3010	250		3013	250	
3064	250		3013	250		3021	250	
3082	250		3033	250		3038	250	MANSFIELD JWSW
3095	250		3037	250		3107	250	
3105	250		3116	250		3118	250	
3108	250		3118	250		3118	250	
3109	250		3203	250	PILLTOP LAKES	4204	250	
3111	250		4212	250		4213	250	
3114	250		4305	250		4222	250	
3116	250		4308	250		4366	250	
3118	250		4402	250	HORGER	4403	250	ROUTON LAKE
3120	250		4405	250		4406	250	
3121	250	ROCKLAND	4411	250	SAM RAYBURN DAM	4412	250	
3122	250		4418	250		4415	250	
3123	250		4427	250	FAA LFK	4428	250	DITROLL
3124	250		4435	250				
3125	250							
3126	250							
3127	250							
3128	250							
3129	250							
3130	250							
3131	250							
3132	250							
3133	250							
3134	250							
3135	250							
3136	250							
3137	250							
3138	250							
3139	250							
3140	250							
3141	250							
3142	250							
3143	250							
3144	250							
3145	250							
3146	250							
3147	250							
3148	250							
3149	250							
3150	250							
3151	250							
3152	250							
3153	250							
3154	250							
3155	250							
3156	250							
3157	250							
3158	250							
3159	250							
3160	250							
3161	250							
3162	250							
3163	250							
3164	250							
3165	250							
3166	250							
3167	250							
3168	250							
3169	250							
3170	250							
3171	250							
3172	250							
3173	250							
3174	250							
3175	250							
3176	250							
3177	250							
3178	250							
3179	250							
3180	250							
3181	250							
3182	250							
3183	250							
3184	250							
3185	250							
3186	250							
3187	250							
3188	250							
3189	250							
3190	250							
3191	250							
3192	250							
3193	250							
3194	250							
3195	250							
3196	250							
3197	250							
3198	250							
3199	250							
3200	250							

Table 1. Tabular Computer Listing of Point Rainfall Estimates

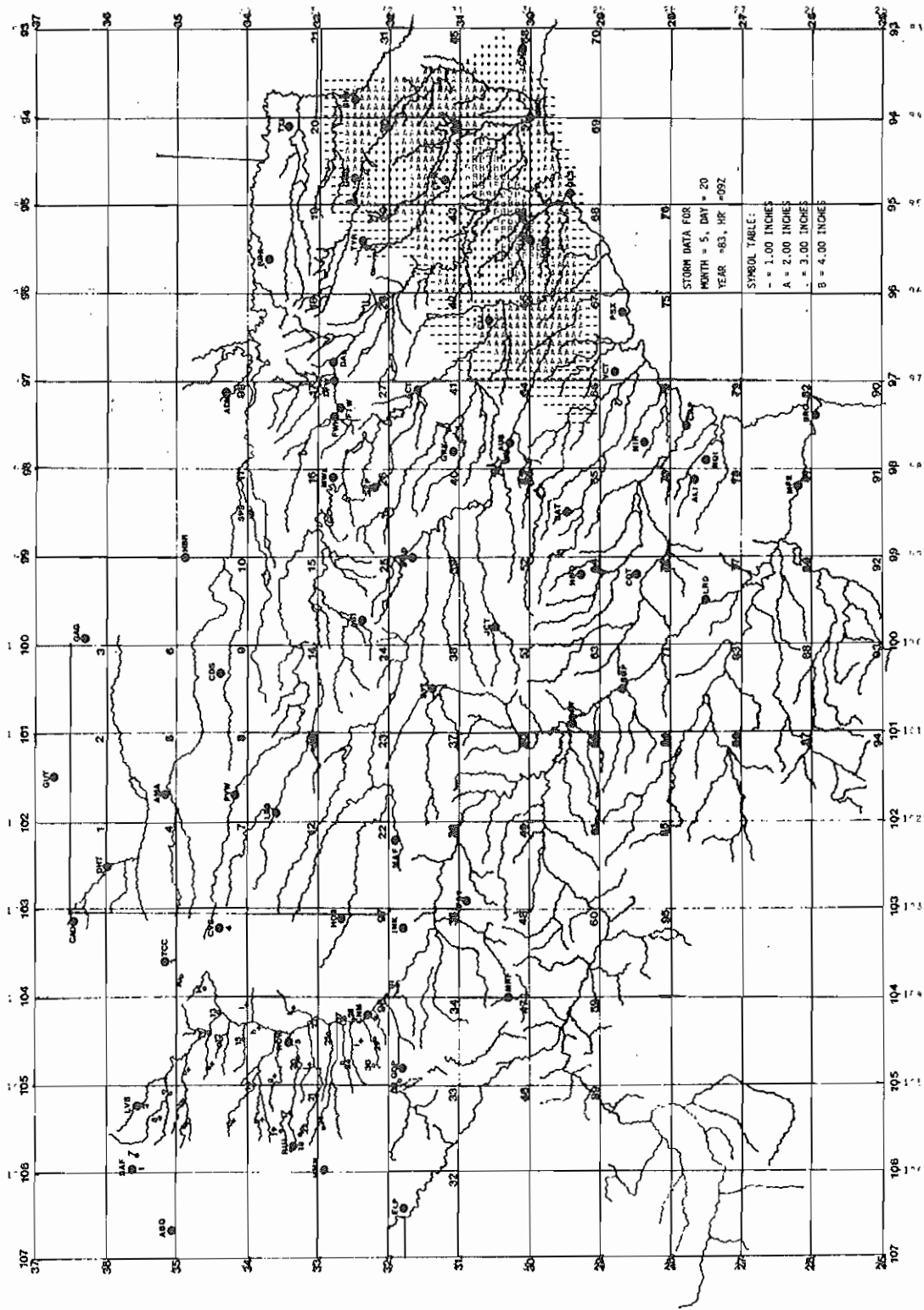


Fig. 1. Computer Plot of 3-Hourly Summed Satellite Rainfall Estimates.

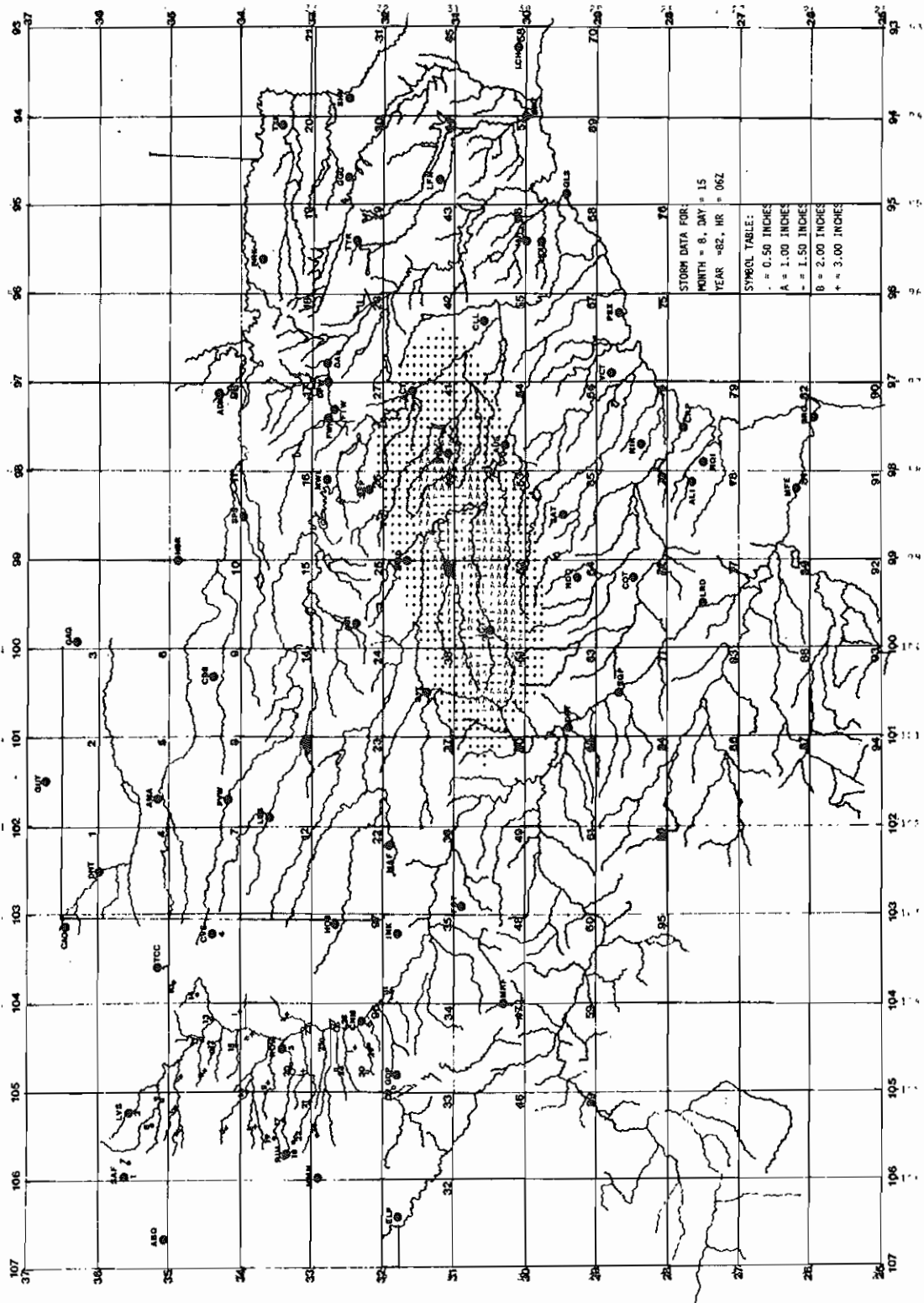


Fig. 2. Computer Plot of 3-Hourly Summed Satellite Rainfall Estimates

evidence indicates that the SAB estimates will likely prove to be very helpful in formulating river predictions under certain circumstances.

Two storms are illustrated in this report. Fig. 1 displays a southeast Texas storm in May, 1983. The computer line printer output has been overlaid by an acetate cover on which is drawn the Texas drainage pattern. The same overlay indicates latitude/longitude and grid boxes. The two digit figure in the lower right hand corner of each box is the "NN" box number. Satellite estimates for each grid point are noted by a symbol (see Fig. 1 symbol table). The plotted data lends itself to a grease pencil isohyetal analysis, which results in a highly informative visual display of storm rainfall. Fig. 2 is a similar presentation for an August, 1982, central Texas storm. Both figures indicate the grid box area of coverage - all of Texas plus extreme southeast New Mexico and most of the Rio Grande drainage in Mexico. SAB can generate real-time estimates for the WGRFC precipitation file for all grid points anywhere within said grid box area. Needless to say, such capability adds real power to the RFC ability to develop river forecasts under certain circumstances. It is a capability that the office fully intends to utilize when called for. It does not take much imagination to think of a situation like a landfalling major hurricane along the Texas Gulf Coast, with attending communications outage, to foresee WGRFC formulating all its southern and western drainage flood forecasts from satellite estimates of rain.

## 5. CONCLUSIONS

WGRFC could increase the usefulness of the satellite data set by reprogramming the ONECL options to include input to only a user specifier portion of the grid point area. In other words, it could be advantageous to, say, over only the drainage west and south of a given lat/long use satellite estimated rainfall, while utilizing gage data and MDR data elsewhere. This kind of flexibility would encourage the hydrologist to use satellite data where likely to offer the best description of the rain field, without "drowning out" other kinds of reports over those basins sufficiently covered by rain gage and radar data. As currently programmed, ONECL requires one to use the satellite data set over the entire storm area, or not at all.

Without a doubt there is a serious need to accomplish long-term and thorough study of the "precision" involved in using satellite imagery to derive point rainfall estimates for

short-time (less than six hours) accumulations. Large rainfall estimates displaced 15 plus miles from actual occurrence could put the predicted flood in the wrong basin. Research by Amorocho (1975), Davis (1973), numerous studies by Barrett (1976), and many other investigations do not provide conclusive evidence that the satellite can consistently provide short-term, reasonably accurate, point estimates of rain accumulations suitable for use in formulating real-time river predictions. However, these studies do offer encouragement, and there is ample evidence that the use of satellite imagery to deduce rainfall amounts for a given area often meets with great success.

Preliminary discussions between WGRFC and NESDIS Synoptic Analysis Branch and Applications Laboratory (AL) meteorologists lead to the conclusion that the following approach to verification could be productive: (1) Verification should be broken down into two categories, maximum point amounts and areal amounts. (2) Verification should compare estimates for the entire storm area, with a breakdown into six hour time intervals to the extent possible. WGRFC hopes to develop a verification program for the SAB provided satellite data that meets these objectives. As a strategy, the RFC would likely use a limited "expanding square search pattern" technique to compare observed data with the estimates, seeking to determine positioning (lat/long) bias in the location of the estimates on the earth, as well as determining errors in the point estimated amounts. The RFC further proposes to do this for several levels of precipitation intensity so as to ascertain bias and errors that may be attributed to certain levels of image reflectivity. This detailed approach to verification would surely require much computer time, but that is what the things are for. Any verification would need to be accomplished shortly after the storm occurrence, with output designed so that SAB and AL personnel could draw conclusions that might lead to improvement in the Scofield/Oliver technique. All data should be stored on magnetic tape for future study. The observed data base upon which comparisons could be made would consist of all rain gage data, official and unofficial, potentially over 2000 gages in Texas alone. An interesting approach, to be considered for the purpose of greatly expanding the number of "ground truth" data points, would be to compute estimations for some grid points near reporting gages, based on all surrounding gaged amounts, and then also use these to compare against the satellite data. However, this obviously

would have to be done with great care, not allowing ground-truth estimates to be made more than, say, one or two grid points away from the actual observations. If it were possible to reliably extrapolate rainfall amounts between distant rain gages, there would be no need for radar and satellite estimated numbers.

#### ACKNOWLEDGEMENTS.

Full credit is due Jerry Nunn, Hydrologist at WGRFC, for developing the software that made it possible for the office to incorporate satellite estimates of rainfall in the river prediction support programs. Jerry's eagerness to accept any task, and his marvelous abilities with large computers is most appreciated by both myself and his fellow workers.

#### REFERENCES:

- Amarocho, J., 1975: "An Application of Satellite Imagery to Hydrologic Modeling the Upper Sinu River Basin, Columbia." Symposium on the Application of Mathematical Models in Hydrology, Bratislava, September 8-13, 1975, 9 pp.
- Barrett, E.C., 1976: "Rainfall in Northern Sumatra: Verification of Rainfall Estimates." Final Report, Supplement 1, Binnie and Partners (Consulting Engineers), London, 7 pp.
- Davis, F.A. and Weigeman, E. J., 1973: "Application of Satellite Imagery to Estimates of Precipitation over Northwestern Montana." Technical and Semiannual Report No. 1 on Contract 14-08-0001-13271, Stanford Research Institute, Menlo Park, CA.
- Scofield, R. A. and Oliver, V.J., 1977: "A Scheme for Estimating Convective Rainfall from Satellite Imagery." NOAA Technical Memorandum NESS-86, Washington, D.C., April 1977, 47 pp.
- Scofield, R.A., Oliver, V. J., and Spoyd, L.E., 1980: "Estimating Rainfall from Thunderstorms with Warm Tops in the Infrared Imagery." Proceedings from the Eighth Conference on Weather Forecasting and Analysis, June 10-13, 1980, Denver, CO, AMS, Boston, MA, 85-92.
- Scofield, R. A. and Spoyd, L. E., 1983: "A Technique that Uses Satellite, Radar, and Conventional Data for Analyzing Precipitation from Extratropical Cyclones." Proceedings from the Fifth Conference on Hydrometeorology, October 17-19, 1983, Tulsa, OK, AMS, Boston, MA, 259-268.
- Smith, D. T., 1975: "River Forecast Application of Grid-Point Addressing." WGRFC internal documentation, non-published, 22 pp.



## METEOROLOGY ASSOCIATED WITH WATER RESOURCES

Jimmy D. Ward

National Weather Service Forecast Office  
San Antonio, Texas 78209

### 1. INTRODUCTION

The management of water resources includes the use of hydrometeorological information ranging from climatological considerations to short-fused reaction during a heavy rain episode. Although fresh water is abundant world wide, unfortunately that fresh water is not distributed in an orderly fashion. In many parts of the world, very rapid population growth is occurring in the arid and semiarid regions. And in the United States, the fastest growing areas are those with present or future water shortages.

Because many groups of people, institutions, and individuals often look to the National Weather Service for assistance during activities related to water management, the NWS should develop plans and policies to address most aspects of water management support. Water management nearly always involves controversial considerations. From population growth controls, to dam construction, development over recharge zones, and weather modification, the NWS is often brought into the discussions, whether planned or not.

### 2. THE TEXAS DROUGHT OF 1983-84

Over the western half of the United States, and in particular in fast-growing areas such as Texas, integrated discussions and policies related to water management are evolving quite rapidly (Grubb and Bomar). Much of Texas experienced a drought during portions of 1983 and 1984. Texas' rapid population growth during the past decade made problems associated with dry spells more acute. The National Weather Service Forecast Office in San Antonio (WSFO) often seemed center stage during activities dealing with the south Texas water shortage.

Either from the effects of the record El Nino or from some other effect, much of Texas had experienced several months of below normal rainfall preceding the spring of 1984. Reservoir levels had

dropped considerably, water tables had lowered, and soil moisture was quite scant. And, most of Texas did not receive the usual heavy spring rains. After a record dry April, it became apparent to local and state officials that an acute water shortage might be imminent. Figure 1 illustrates the rapid drop of water in the Edwards underground aquifer, the sole water source for much of southcentral Texas.

As the probable water shortage became an everyday news item, the WSFO at San Antonio received many inquiries from news and local government officials concerning seasonal precipitation outlooks, climate data, aquifer and reservoir levels, and soil moisture content. Several WSFO staff members began collecting and organizing climate data and water supply data.

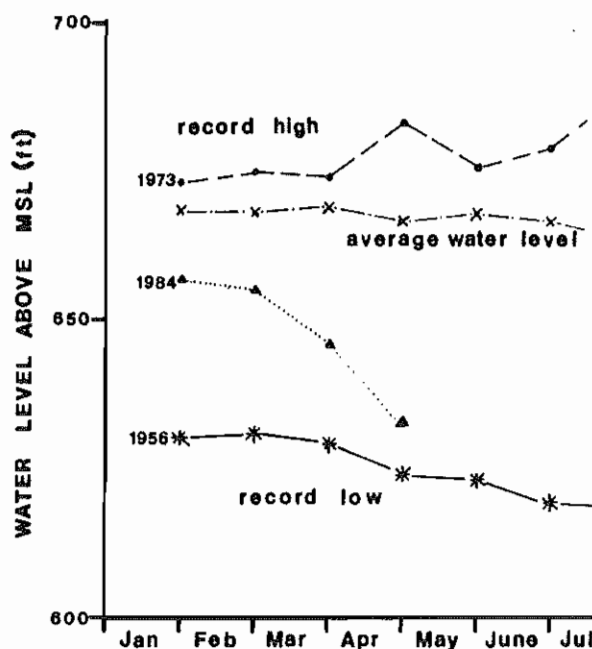


Figure 1. San Antonio Index Well for the Edwards Underground Aquifer. Period of record is January 1932 - May 1984.

Of course the first data examined were the records of precipitation over the south Texas area. Surprisingly, the data showed that the current dryspell was not so unusual. Similar dryspells appeared in the data about 20 percent of the time, or about twice per decade. Some quick correlation studies also pointed to the fact that a below normal April rainfall nearly always was associated with a below normal annual rainfall.

### 3. THE WATER CONSERVATION PROGRAM

With the water levels dropping rapidly and with April, 1984 being the driest April on record, the mayor of San Antonio organized a regional water conservation group. A coordinated water conservation program was quickly designed. The WSFO joined as an advisory member. It quickly became evident that information from the NWS was greatly desired and appreciated by the water conservation group.

The NWS advised the group that the current dryspell was not rare or even unusual. Using climat data, the WSFO advised the group that rain would likely fall during May (a dry May was climatologically rare), but that the rainfall would likely not make up for the shortage already incurred. The group was further advised that summers are typically dry with very high evaporation rates -- water demand would continue very high and soils would be quite dry. Any relief from rain would be short-lived and spotty due to the typical summer rainfall patterns. If rainfall relief came from a significant tropical storm, that relief would likely not occur until the end of summer.

The regional conservation group decided on a three-phase approach to the water shortage problem. The first phase would include a water conservation awareness program which would help develop a water conservation ethic. Phase two, voluntary water conservation, would be initiated when certain water supply levels were reached. It was obvious to the WSFO that such a level would be reached during the summer. Phase three, mandatory water conservation, would be implemented when water supply approached record low levels. Phase three was not required during the summer of 1984, partially due to the voluntary water conservation phase.

### 4. PROBLEMS ASSOCIATED WITH DROUGHT

During the drought of 1984 in south Texas, a variety of drought-related problems became evident. The most obvious and widespread result of the

drought was the decreased agricultural output, including feed for livestock. Reservoir and aquifer levels fell dramatically and springs ceased flowing. Water recreation, such as canoeing and rafting, was either curtailed or halted altogether.

Over the coastal areas, salt deposits on insulators began shorting circuits and damaging transformers. Low fresh-water levels aided pollution of important estuaries.

As water levels lowered, there was an increased rate of pollution of water supply. Some recreational areas were closed after several incidences of human infection. Some town water supplies became polluted, requiring water to be boiled or imported from nearby sources.

Since the water shortage touched nearly all of the society and since attention was often directed toward precipitation forecasts, the NWS offices in south Texas were continuously involved in quantitative precipitation outlooks and forecasts. More specifically, the forecasts were often for certain important reservoir basins or aquifer recharge zones. Figure 2 illustrates the narrow recharge zone of the Edwards underground aquifer, an aquifer which provides water needs for nearly two million people, including agricultural needs and considerable water recreation.

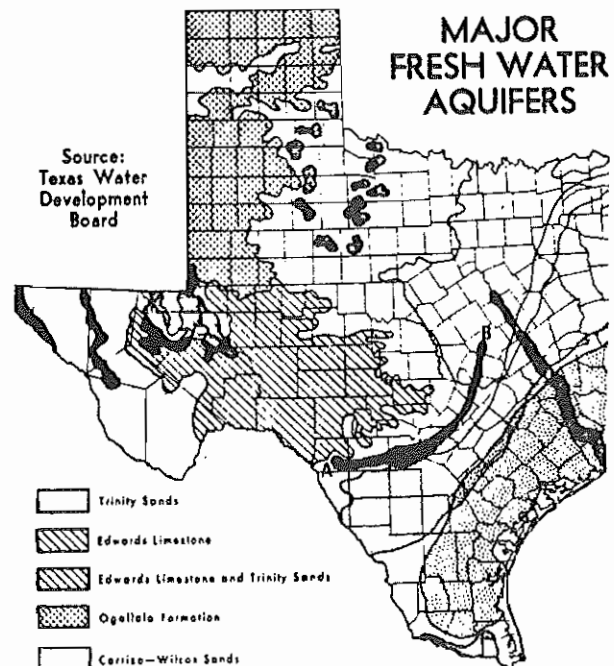


Figure 2. Edwards Underground Aquifer Recharge Zone, narrow strip from point A to point B in southcentral Texas. from 1982-1983 Texas Almanac.

## 5. REQUIRED INFORMATION DURING A DROUGHT

Hydrometeorologists need to know several interrelated types of information in order to provide expert advice during a drought. This information is generally related to supply of and demand for water.

### Supply --

- a. climatology of rainfall
- b. aquifer and reservoir levels
- c. long-range rain outlooks (up to 3 months)
- d. short-term synoptic type rain forecasts

### Demand --

- a. population trends
- b. seasonal water requirements for
  1. agricultural use
  2. urban use (lawn watering, etc.)
  3. recreation

## 1. WATER SUPPLY DURING A DROUGHT

### A. CLIMATOLOGY OF RAINFALL

A comprehensive precipitation database over the area is absolutely necessary. This database should be in a form which allows data manipulation for standard statistical and regression analyses. Spreadsheet software for data manipulation is available with most microcomputers.

During May, 1984, the WSFO was able to use such a database to quickly demonstrate that the dryspell which south central Texas was experiencing was not a rare event. At the same time, the WSFO could also explain that given the dry spring, the chances of 1984 having above normal rainfall were very low (less than 10%). Such information can be very beneficial during water conservation programs.

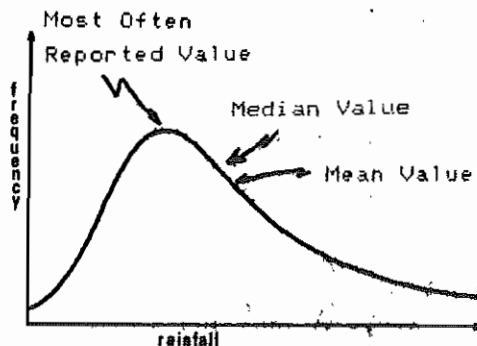


Figure 3. Rainfall Distribution. A typical distribution of seasonal rainfall

When using climatological data, one must decide what form or type of data will be most useful in describing expected precipitation. A case in point is demonstrated in Figure 3. Should the expected precipitation be the value which most often occurs (the peak on the graph), the median value, or the the mean? To forecast the mean or average would more often overforecast precipitation.

### B. AQUIFER AND RESERVOIR LEVELS

The hydrometeorologist needs to have an appreciation for water levels in aquifers and reservoirs which supply water to the society. A climatology of such levels, including long-term trends, is essential.

The hydrometeorologist needs to know how an aquifer or reservoir will respond to a given amount of rainfall over the recharge zone or basin respectively. During a drought, one of the first questions asked will be, "How much will this rain raise the aquifer (or reservoir) level?"

### C. LONG-RANGE RAIN OUTLOOKS

During a drought, long-range precipitation outlooks become very important. Unfortunately, skills for 3-month precipitation forecasts are quite low. Often, climatological data can provide better decision-making information.

### D. SHORT-TERM RAIN FORECASTS

During a drought, the quantitative precipitation forecast becomes extremely important. It can provide valuable information to urban and agricultural interests for water use decision-making.

Previous QPF workshops dealt mainly with forecasting synoptic scale precipitation. The greatest skill today is with the synoptic scale precipitation forecast.

## 2. WATER DEMAND DURING A DROUGHT

### A. POPULATION TRENDS

As stated in the introduction, water demand is obviously rapidly increasing in the areas of fast population growth. As of 1980 in southcentral Texas, the population increased 85% from the time of the severe drought of the 1950s. And, by 1990 the population will be double the 1950s level.

When the aquifer levels began dropping rapidly during the spring of 1984, the WSFO personnel at first guessed that it was mainly due to the lack of

rain. Upon discovering that the dryspell was not so unusual, it became apparent that the increased demand for water was primarily due to the number of people using the water systems.

The above statement may seem too obvious to stress. However, much of the recent population growth in Texas occurred during a period of ample rainfall. In southcentral Texas, aquifer levels were at record highs and apathy about water planning persisted. Using the typical dryspell of 1984 as a gage, a drought on the order of the 1950s would be disastrous to south Texas.

## B. SEASONAL WATER REQUIREMENTS

### 1. Agricultural Use

Hydrometeorologists and agricultural meteorologists must totally appreciate the seasonal agricultural demands for water. Irrigation has increased dramatically in many parts of the nation; and, during dryspells water pumping for planting and plant growth may be tremendous. The rapid drop of aquifer levels in southcentral Texas during 1984 was highly correlated with the planting and growing season. Aquifer levels were able to remain fairly steady by midsummer, when agricultural irrigation decreased during the maturing phase of the crops.

### 2. Urban Water Use

Urban water use can increase dramatically during periods of rapid population growth. The San Antonio Water Board pumping statistics correlated most highly with population growth and secondarily with rainfall and seasonal variations.

Most urban water demand derives from lawn watering. During 1984, lawn watering was prohibited in the Corpus Christi area. Urban water rationing occurred in several south Texas locations.

In a few spot locations, some urban water supplies were contaminated by foreign material and low water levels. There were also some people who were infected by polluted water. Some of the pollution incidences occurred after rains began and pollutants were washed into the water supply. It now appears that if a drought were to occur in south Texas on the order of the 1950s drought that severe water shortages would be a certainty. Strict water rationing would be required.

### 3. Recreational Water Use

Water recreation is very important in certain parts of south Texas. Activities

in water parks, canoeing, rafting, tubing, sailing, fishing and skiing are a main recreational pastime during the summer months in south Texas. Drought is usually most severe during the summer months, and drought severely curtails the recreational activities.

During the 1984 dryspell, most of the sickness from polluted water occurred in the parks which greatly depended on water. Springs and streams which usually provided for canoeing and rafting dried up. Reservoir levels dropped dramatically. In order to decrease evaporation losses, one reservoir was drained completely and the water routed to the next reservoir.

Since drought affected so many people in so many ways, the quantitative precipitation forecast became very critical. The forecaster needed to be quite sensitive to the many ramifications of a rain forecast. A cavalier approach to rainfall forecasts during a drought can adversely affect many sectors of the society.

### 6. WEATHER MODIFICATION

One of the possible offsprings of a drought event is the desire to modify the weather and "make rain." Such was the case in south Texas.

During the convective season of 1985, the Edwards Underground Water District will contract with a company to enhance rainfall over the aquifer recharge zone (see Figure 2). This zone is also very flash flood prone. Weather modification over the flash flood prone area will make the forecasters' task even more complicated.

The weather modification effort should be highly coordinated among the state officials (those responsible for issuing the permit), the WSFO, and the company attempting to enhance rainfall. The WSFO personnel must fully understand the restrictions under which the company operates. The company must appreciate the responsibilities of the WSFO. The company personnel must have a sound knowledge of the hydrometeorological aspects of heavy rain over the area of concern.

### 7. CONCLUSIONS AND RECOMMENDATIONS

With rapid population growth in areas of the United States which have very limited water resources, water shortages should become more frequent. Even fairly frequent "dryspells" may produce water rationing requirements.

Since many people and institutions depend on the National Weather Service to provide climatological data, forecasts

and guidance during periods of water shortages, the NWS personnel should have a good rainfall climatological data base to analyze.

Water availability can be quite complicated. It depends on both supply and demand; and, it is seasonal. The NWS personnel should have knowledge of water supply reservoirs, basins, and aquifers. Quantitative precipitation forecasts can be very critical during water shortages. Timing and location of rainfall can be extremely important in determining expected water availability.

Water use, particularly during a drought, can be a highly political issue. NWS personnel should be sensitive to the issues and consider those issues pertinent to the advice given. The forecaster should be aware of the many different uses of water (agriculture, urban, recreation, etc). The forecaster should also be aware of the pollution potential during water shortages.

Sometimes rain enhancement weather modification activities result from drought. The NWS personnel should be intimately familiar with the weather modification activities. Weather modification can be a highly emotional subject and the NWS is often brought into the related discussion. As a minimum, the NWS forecaster should be aware of place and time of the weather modification efforts. The forecaster should also be aware of the restrictions under which the company may operate.

## 8. ACKNOWLEDGEMENTS

Gary Grice and Tom Hicks contributed to this discussion on drought and NWS activities during the water shortage of 1984. They are forecasters at the WSFO in San Antonio, Texas. Gary assembled much of the data and articles which helped focus some of the issues related to drought in Texas. Tom built a rainfall data base and performed valuable statistical analyses which revealed some of the aspects of rainfall mentioned in this discussion.

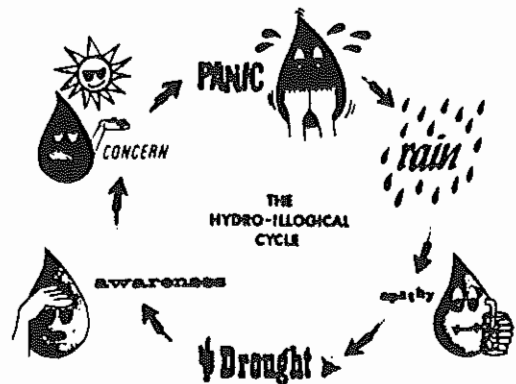
## REFERENCES

Grubb, H.W. and Bomar, G.W., 1983 (Texas Dept of Water Resources, Austin, TX): Water Management Issues in Texas, presented at the Fifth AMS Conference on Hydrometeorology (not in preprints).

1982-1983 Texas Almanac, Fred Pass, ed., Water Supplies and Needs, pp. 88-96. Dallas Morning News Press.

## APPENDIX

**THE HYDRO-ILLOGICAL CYCLE.** In the hydro-illogical cycle, the NWS personnel are often deluged with requests for climatological information, forecasts and advice during the PANIC stage. With a good data base, a sound understanding of the seasonal water needs, and an appreciation of the complicated issues during a water shortage, the NWS should be able to provide valuable service during the CONCERN and PANIC stages. Planning during the APATHY stage can be very beneficial when rains stop falling.





# COMPUTER ANALYSES OF HOURLY RECORDING RAIN GAGE DATA FOR THE U.S. GULF COAST

Jerry R. Rogers, Ph.D., P.E.

Department of Civil Engineering, University of Houston  
Houston, Texas 77004

## 1. INTRODUCTION

Examples of derivations of rainfall intensity and intensity-duration-frequency curves were published in early textbooks (Fair and Geyer, 1961). These examples have not been cited in many recent books, and the method of developing an intensity-duration-frequency curve is not well known. Tables 1, 2, and 3 are examples of rainfall data with intensity computations and i-d-f analysis.

## 2. COMPUTER APPLICATIONS OF HOURLY RECORDING RAIN GAGE DATA

(Murray and Rao, 1978) outlined a computer method for hourly rainfall data to develop intensity-duration-frequency curves in Pennsylvania. They suggested getting short duration 15-minute data for time intervals less than one hour. The hourly rainfall data method was applied to City of Houston hourly recording rain gages for frequencies of ten years or less by (Rogers, 1983). This method is being extended to seven regional rain gages for the Harris County Flood Control District for 15-100 year frequencies.

The hourly rainfall computer method steps are:

- a. Obtain a list of available hourly rainfall stations from Asheville, N.C. National Climatic Data Center (such as a 1979 listing where stations are coded with c = continuous hourly data and 2 = Total rainfall).
- b. Select the primary stations, draw an area location map, and record the years of record and elevation of gage.
- c. Order hourly computer tape for stations:
  - (1) get large area (state) data tape for all stations, or
  - (2) get local gage data only.
- d. Write a computer program to count rainfall intensities (for 0.05

inch/hour to 6 inches/hour for various durations from one hour to 24 hours).

- e. Trace the frequency curve through the rainfall counts (Fair and Geyer, 1961 example: 45 years & 5 years = 9 times as a count).

The correlation between data from near-by gages should be checked. When correlation is low, the gage data is somewhat independent and counts can include all gage data lumped together for the total years of record. Literature concerning this method has been cited by (Rogers, 1983).

The rain gages selected for the HCFCD analysis were Alief, Addicks, Satsuma, Inter-continental, Conroe, Richmond, and Thompsons. The HCFCD study will be completed in November, 1985.

## 3. ACKNOWLEDGEMENTS

Financial assistance for these studies was provided by the City of Houston Public Works Department and by the Harris County Flood Control District. Technical advice was provided by John Lott and David Brown (formerly with the City of Houston Storm Sewer Department), and Michael Talbott and Steve Fitzgerald (Harris County Flood Control District).

## REFERENCES

- Fair, G.M. and J.C. Geyer, 1961. Water Supply and Wastewater Disposal, Wiley & Sons Publishing, New York, NY.
- Murray, G.A. and G.N.S. Rao, 1978. Computer Methods for Rainfall Intensity-Duration-Frequency Relationships. International Symposium on Urban Storm Water Management, Lexington, KY.
- Rogers, J.R., 1983. Rainfall Analysis for Storm Sewer Criteria in Metropolitan Areas. Presented at the 19th Annual American Water Resources Association Conference, San Antonio, TX.

TABLE 1

RAINFALL INTENSITY EXAMPLE

from Fair and Geyer, Water Supply and Waste-Water Disposal, Wiley Publ. Co.

Given a rain-gage record for successive periods of a storm, find the arithmetic mean rate, or intensity of precipitation for various durations. The gage record is shown in Columns 1 and 2. The necessary calculations are added in Columns 3 to 7. It should be noted that Columns 5 to 7 are independent of the preceding Columns.

Time and Intensity of a Storm Rainfall (Oct. 27-28, 1908 at Jupiter, Fla.)

Rain-gage record				Time-intensity relationship		
Time from beginning of storm min (1)	Cumulative rainfall in. (2)	Time interval, min (3)	Rainfall during interval, in. (4)	Duration of rainfall min (5)	Maximum total rainfall, in. (6)	Arithmetic mean intensity, in. per hr (7)
5	0.31	5	0.31	5	0.54	6.48**
10	0.62	5	0.31	10	1.07*	6.42
15	0.88	5	0.26	15	1.54	6.16
20	1.35	5	(5) 0.47	20	1.82	5.46
25	1.63	5	(4) 0.28	30	2.55	5.10
30	2.10	5	(3) 0.47	45	3.40	4.53
35	2.64	5	(1) 0.54	60	3.83	3.83
40	3.17	5	(2) 0.53	80	4.15	3.11
45	3.40	5	0.23	100	4.41	2.65
50	3.66	5	0.26	120	4.59	2.30
60	3.83	10	0.17			
80	4.15	20	0.32			
100	4.41	20	0.26			
120	4.59	20	0.18			

Column 6 records maximum rainfall in stated consecutive periods. The magnitudes are obtained from Column 4 by finding the value, or combination of consecutive values, that produces the largest rainfall for the indicated period. Column 7 = Column 6 X 60/Column 5.

$$*0.54 + 0.53 = 1.07 \quad **0.54 \times 60/5 = 6.48$$

In this example the maximum rate of rainfall was experienced during the 5-min interval between the 30th and 35th minute.

TABLE 2

INTENSITY-DURATION-FREQUENCY CURVE EXAMPLE

from Fair, Geyer, Water Supply and Waste-Water Disposal, Wiley Publ. Co.

The number of storms of varying intensity and duration recorded by a rain gage in 45 years are listed below from New York City from 1869 to 1913. Determine the time-intensity values for the 5-year storm.

Record of Intense Rainfalls

Duration Min.	Number of Storms of Stated Intensity (inches per hour) or More												
	1.0	1.25	1.5	1.75	2.0	2.5	3.0	4.0	5.0	6.0	7.0	8.0	9.0
5							123	47	22	14	4	2	1
10					122	78	48	15	7	4	2	1	
15				100	83	46	21	10	3	2	1	1	
20			98	64	44	18	13	5	2	2			
30	99	72	51	30	21	8	6	3	2				
40	69	50	27	14	11	5	3	1					
50	52	28	17	10	8	4	3						
60	41	19	14	6	4	4	2						
80	18	13	4	2	2	1							
100	13	4	1	1									
120	8	2											

If it is assumed that the 5-year storm is equaled or exceeded in intensity  $45/5 = 9$  times in 45 years, the generalized time-intensity values may be interpolated from the summary by finding (a) for each specified intensity the duration that is equaled or exceeded by 9 storms and (b) for each specified duration the intensity that is equaled or exceeded by 9 storms. Interpolation proceeds along the broken diagonal line.

TABLE 3

A smooth curve drawn through data from Table 2 traces the course of the 5-year storm rainfall.

## Calculation of Storm Frequencies

a. Duration, min	5	10	15	20	30	40	50	60	80	100
a. Intensity, in. per hr	6.50	4.75	4.14	3.50	2.46	2.17	1.88	1.66	1.36	1.11
b. Intensity, in. per hr	1.0	1.25	1.5	1.75	2.0	2.5	3.0	4.0	5.0	6.0
b. Duration, min	116.0	89.9	70.0	52.5	46.7	29.0	25.7	16.0	9.3	7.5



INTEGRATED HYDROMETEOROLOGICAL FORECAST SYSTEM - DESIGN AND TESTS

Konstantine P. Georgakakos and Michael D. Hudlow

Hydrologic Research Laboratory  
National Weather Service, NOAA  
Silver Spring, Maryland 20910

1. INTRODUCTION

Improvements in hydrologic forecast lead time (the difference in time between the time of the occurrence of the forecasted hydrologic phenomenon and the time when the forecast is issued) and accuracy could be achieved if reliable quantitative precipitation forecasts (QPFs) were available for specific watersheds as input to the hydrologic forecast models. Unfortunately, current QPF models and procedures generally do not provide sufficiently accurate values (at least for forecast periods exceeding 30-60 min) for direct input to hydrologic models. Although current QPF products provided by the National Meteorological Center (NMC) provide generalized guidance information which is very useful in roughly indicating rainfall amounts and locations of rainfall areas, they do not provide the detail and accuracy required for assigning QPF values to individual watersheds. There is a need for more direct incorporation of QPF information into the hydrologic modeling and prediction procedures. This is especially important to the improvement of forecasts for small watersheds where the lag time between rainfall occurrence and outflow from the basin is short. According to a recent Program Development Plan for Improving Hydrologic Services (NWS-Office of Hydrology, 1982), 50 percent of the forecast points for communities across the U.S. have potential forecast lead times less than 10 hr and 25 percent have less than 4 hr. Clearly, accurate QPF information for even a few hours into the future would result in valuable increases in effective lead time.

In a review paper, Georgakakos and Hudlow (1984) examine various approaches to rainfall prediction that potentially can provide useful input information for hydrologic forecasting. One of these is the coupled approach to quantitative precipitation - river flow forecasting based on the work of Georgakakos and Bras (1982a). This procedure couples precipitation and drainage basin models both through the mass continuity physical law and through the update component of a state estimator that uses the residual errors in the prediction of rainfall and riverflow to correct the states of the coupled precipitation and drainage basin models.

Figure 1 gives a schematic representation of the coupled system with the links among the various system components indicated explicitly.

The integrated hydrometeorological system of Figure 1 offers high efficiency in the meshing of precipitation and streamflow forecasts, and provides real time estimates of the uncertainty associated with each forecast.

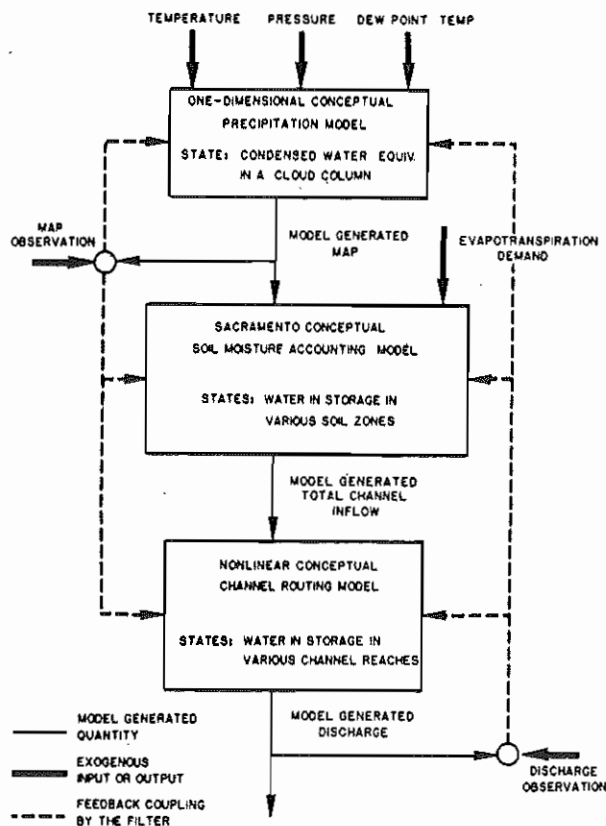


Figure 1. Schematic representation of the integrated hydrometeorological model. Explicitly shown are the model components, inputs and outputs.

It is the purpose of this paper to give a short description of the components of the integrated system and to summarize results of a real world application with six-hourly data from the Bird Creek basin in Oklahoma. At the end, the design of a flash-flood prediction system based on the integrated hydrometeorological system concept is presented. Preliminary results of its "operational" use in the prediction of flash floods in Virginia catchments are also reviewed.

## 2. THE PRECIPITATION MODEL

Georgakakos and Bras (1984a,b) formulated a station precipitation model in state space form. Based on the surface pressure, temperature and dew-point temperature, their model gives as an output the precipitation rate. The model state is the mass of the condensed liquid water equivalent in the area characterized by the input temperature and pressure indices. The model formulation is based on pseudo-adiabatic ascent of the air-masses and on simplified cloud microphysics with exponential particle-size distribution and linear dependence of the particle terminal fall-velocity on the particle diameter. Evaporation of the falling particles, for unsaturated sub-cloud layer, is explicitly taken into account by the model. Predictions of snowfall vs rainfall are based on the surface air-temperature.

Figure 2 presents a sketch of the physical mechanisms that are modeled. The upper part of

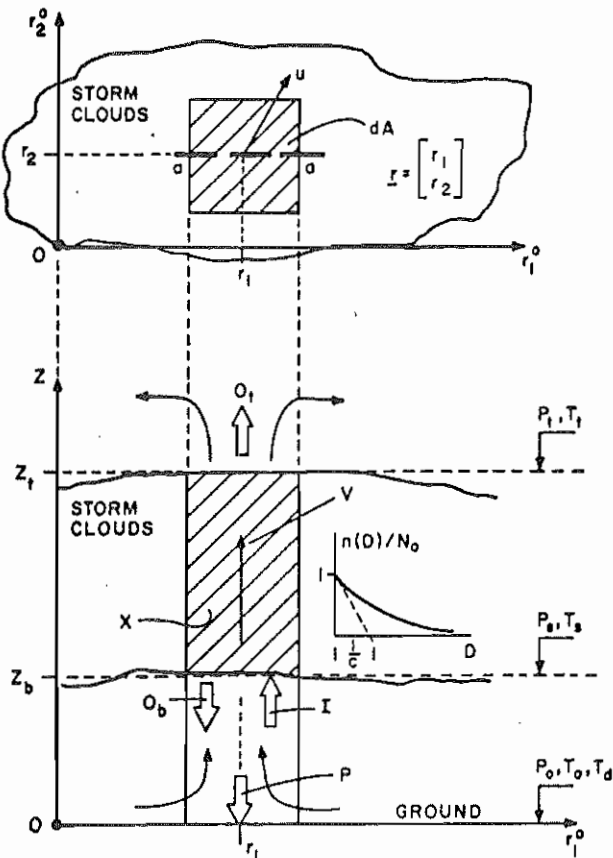


Figure 2. Schematic representation of the precipitation model physical components.

the figure is a plan-view of the moving (velocity denoted by  $u$ ) storm clouds, while the lower part is a cross-section through them. The shaded regions correspond to a cloud-column characterized by the input variables: air-temperature,  $T_0$ ; air-pressure,  $p_0$ ; and dew-point temperature,  $T_d$ , at the ground level. The model developed simulates the dynamics in this column. Air rises pseudo-adiabatically in the clouds with updraft velocity  $v$  (possibly height-varying), producing an input rate of condensed water equivalent  $I$ . The input mass of condensed water is distributed to different droplet diameters according to an exponential particle size distribution,  $n(D)$ , whose parameters  $N_0$  and  $c$  (see Figure 2) are possibly height-varying. Due to the action of the updraft at the cloud top, a portion of the water mass leaves the column with a rate  $O_t$ . The larger droplets fall through the cloud bottom with a rate  $O_b$ . The precipitation rate  $P$  at the ground level is computed from  $O_b$  by subtraction of the mass evaporation due to possible unsaturated conditions below the cloud base. The model dynamics equation consists of a statement of the conservation of the condensed water equivalent mass  $X$  within the cloud column. Heat-adiabatic ascent is used to determine the cloud-base (level  $Z_b$ ) pressure,  $p_b$ , and temperature,  $T_b$ . Pseudo-adiabatic ascent and the terminal pressure  $p_t$  at the cloud-top (level  $Z_t$ ) are used to determine the temperature  $T_t$  and, subsequently, the water vapor condensed per unit mass of moist air. The physical quantities  $v$ ,  $c$  and  $p_t$  are parameterized using the input variables  $p_0$ ,  $T_0$ , and  $T_d$  in an effort to obtain a storm and location invariant structure.

As a first step toward model verification, Georgakakos and Bras (1984a,b) considered uniform profiles of updraft velocity and cloud-particle layer-average diameter. In addition, the cloud-particle layer-average diameter was held constant independent of the input variables. The free model parameters in this case are:

- 1) The ratio EPS1 of the updraft velocity to the square root of the potential thermal energy per unit mass of the ascending air at the height of average updraft velocity, and
- 2) the time- and storm-constant cloud-particle layer-average diameter denoted by EPS4 (equal to  $1/c$ ).

Georgakakos and Bras give the details of the model formulation as well as encouraging results of model application to several storms of various meteorological characteristics.

Georgakakos (1982, 1984) examined the parameter identification issue in detail. Contour maps of various performance criteria indicated that the model is robust to parameter changes and that it may not require recalibration for different storms and topographic locations. The latter is especially convenient for real-time forecasting uses.

The most important aspect of the precipitation model under consideration is its state space mathematical form. It is this aspect that makes the model compatible with operational hydrologic models and allows the use of a

state-estimator (i.e. Kalman Filter) for real-time updating.

### 3. THE SOIL-MOISTURE ACCOUNTING MODEL

The precipitation forecast averaged over the basin area, obtained from the precipitation model, feeds the Sacramento Soil-Moisture Accounting model (Figure 1).

The Sacramento model is a conceptual, spatially lumped model. Its equations describe the movement of water through the various storage elements of the drainage basin (Figure 3). The model distinguishes two zones in the soil: an upper zone that represents the upper soil layer and interception storage and a lower zone that represents the bulk of the soil moisture and groundwater. Each zone stores water in tension elements and in free elements. The tension water is closely bound to the soil particles and can be depleted only by evapotranspiration. The free water moves through the various elements under the force of gravity and contributes to the channel inflow. The model accepts as input the mean areal precipitation over the basin and the potential evapotranspiration rate and produces as output the total channel inflow.

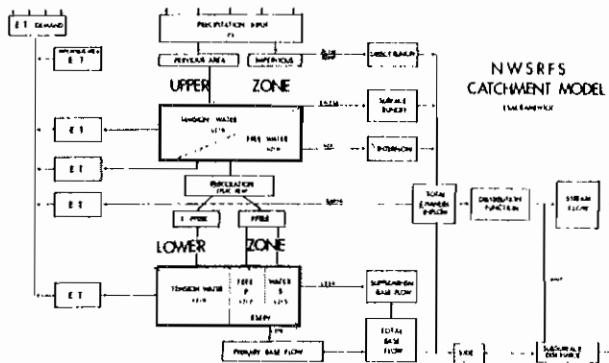


Figure 3. Schematic representation of the Sacramento Soil-Moisture Accounting scheme. See Peck, 1976, for a more precise definition of the parameters appearing in this figure.

Georgakakos and Bras (1982a) give the complete set of the differential equations that describe the state of the soil moisture of the various model storages. The equations are in state space form.

The Sacramento model in state space form has been successfully used with modern estimation theory techniques for the real time forecasting of river flows (Kitanidis and Bras, 1980a,b; Georgakakos and Bras, 1979, 1982a). Armstrong (1978) gives the physical interpretation of the model components in terms of observable soil characteristics. Restrepo-Posada and Bras (1982) study the parameter estimation issue for the model using maximum likelihood techniques.

### 4. THE CHANNEL ROUTING MODEL

Georgakakos and Bras (1980, 1982b) presented a conceptual, nonlinear reservoir-type channel

routing model in state space form, which, when tested with the Sacramento accounting scheme, showed improved performance over linear black-box type routing models.

The drainage basin river system is subdivided into hydromorphologically homogeneous channel segments in series. Each segment is modeled as a reservoir that temporarily stores the water on its way to the drainage basin outlet. The model differential equations are the expressions of the mass continuity law for each reach. The discharge at the outlet of each reach is related by a power law to the water in storage in the same reach. The model uses as input the total channel inflow and produces as output the discharge at the drainage basin outlet.

Real world applications of the routing model with 6-hour data from the Bird Creek basin (2344 mi<sup>2</sup>), Oklahoma, gave very good results in the real-time forecasting of flood flows. In particular, delays at the peak of the hydrograph that were observed when linear black-box type models were used in real-time forecasting, were eliminated.

Georgakakos and Bras (1980, 1982b) give the details of model formulation as well as ways of estimating model parameters from 1) the basin observable hydromorphological characteristics, and 2) input-output time-series data.

### 5. THE INTEGRATED HYDROMETEOROLOGICAL MODEL STATE SPACE FORM

The differential equations that describe the time-evolution of the states of the various components of the hydrometeorological model can be written as follows.

#### Precipitation component:

$$\frac{d}{dt} \underline{x}_p = \underline{F}_p(\underline{x}_p, \underline{u}_p; \underline{a}_p) \quad (1)$$

#### Soil-moisture accounting component:

$$\frac{d}{dt} \underline{x}_s = \underline{F}_s(\underline{x}_p, \underline{x}_s, \underline{u}_p, \underline{u}_e; \underline{a}_p, \underline{a}_s) \quad (2)$$

#### Channel routing component:

$$\frac{d}{dt} \underline{x}_c = \underline{F}_c(\underline{x}_p, \underline{x}_s, \underline{x}_c, \underline{u}_p, \underline{u}_e; \underline{a}_p, \underline{a}_s, \underline{a}_c) \quad (3)$$

The observation equations that relate the observed quantities (precipitation and runoff) to the model states follow.

#### Precipitation:

$$z_p = H_p(\underline{x}_p, \underline{u}_p; \underline{a}_p) \quad (4)$$

#### Runoff:

$$z_c = H_c(\underline{x}_c; \underline{a}_c) \quad (5)$$

The state of the precipitation model is denoted by  $\underline{x}_p$ , the vector state of the Sacramento Soil-Moisture Accounting model is denoted by  $\underline{x}_s$ , and the vector state of the channel router is denoted by  $\underline{x}_c$ . The vector  $\underline{u}_p$  represents the meteorological input to the precipitation model and the scalar  $u_e$  represents potential evapotranspiration. The vectors  $\underline{a}_p$ ,  $\underline{a}_s$ , and  $\underline{a}_c$  are

the parameter vectors for the precipitation, the soil, and the channel components respectively.  $F_p$ ,  $F_s$ ,  $F_c$  are nonlinear (in general) functions describing the system dynamics for the precipitation, soil, and channel components respectively.

The mean areal precipitation observation over the basin is denoted by  $z_p$  and the discharge at the basin outlet by  $z_c$ .  $H_p$  and  $H_c$  are nonlinear (in general) functions relating the observations to the states for the precipitation and the channel components respectively.

The system of equations (1) through (5) constitutes the state space form of the integrated hydrometeorological model equations. In a more compact form the system is written as:

Dynamics Equation:

$$\frac{d}{dt} \underline{x} = \underline{F}(\underline{x}, \underline{u}; \underline{a}) \quad (6)$$

Observation Equation:

$$\underline{z} = \underline{H}(\underline{x}, \underline{u}; \underline{a}) \quad (7)$$

where,

$$\underline{x} = \begin{bmatrix} x_p \\ x_s \\ x_c \end{bmatrix} \quad \underline{u} = \begin{bmatrix} u_p \\ u_e \end{bmatrix} \quad \underline{a} = \begin{bmatrix} a_p \\ a_s \\ a_c \end{bmatrix}$$

$$\underline{z} = \begin{bmatrix} z_p \\ z_c \end{bmatrix} \quad \underline{F} = \begin{bmatrix} F_p \\ F_s \\ F_c \end{bmatrix} \quad \underline{H} = \begin{bmatrix} H_p \\ H_c \end{bmatrix}$$

## 6. STATE ESTIMATOR

The previous formulation presents the coupling of the equations corresponding to three different models of the storm-basin system. Thus, consideration of the set of Eqs. (1) through (3) shows that the state of the precipitation model,  $x_p$ , directly affects the equations of time-evolution of the soil states,  $x_s$ . Both  $x_p$  and  $x_s$  affect the channel-states differential equation [Eq. (3)]. Coupling is due to the enforcement of the conservation of water-mass (or volume) law at the boundaries of each model. Note, however, that it is a one-way coupling. That is, the states of the channel or the soil models do not affect the precipitation state. Therefore, information on those states cannot be passed, with the present deterministic formulation, to the precipitation model.

It is this open link in the overall rainfall-runoff model that modern estimation theory techniques close, using observations on all the model outputs (Eqs. (4) and (5)). State estimators will effectively couple the state variables of the soil and channel models with those of the precipitation model. This is a different coupling from the one due to the conservation of water-mass law. The effect that each state variable has on the overall storm-basin models outputs, is monitored through the filter equations. Each state variable is updated from the system observations (see Figure 1), based on the degree of its correlation to the

model outputs and to the rest of the model variables. In this way, the errors in predicting the discharge at the catchment outlet have a bearing on the specification of the initial conditions of the precipitation model variables. Similarly, observations of the precipitation state variables and parameters have an effect on the determination of the drainage basin related state variables. This assures coordination in the operation of the coupled storm and basin models in real time. Georgakakos and Bras, 1982a, develop the formulation of the stochastic hydrometeorological model in a linear state-estimator framework.

Their formulation allows for uncertain inputs with given mean and variance. Since the system equations [i.e., Eqs. (1) through (5)] are non-linear both in the system states and the inputs, the Extended Kalman Filter is used as the state estimator (e.g., Gelb, 1974). The procedure is straightforward to implement, and the interested reader is referred to Georgakakos and Bras, 1982a, for the details.

## 7. METEOROLOGICAL INPUT SPATIAL INTERPOLATION

The Georgakakos and Bras (1984a,b) precipitation model uses surface meteorological data as input, in order to forecast the precipitation rate in the area characterized by the input. It is often the case, with the present state of the surface meteorological data network (average distance between stations of the order of 100 km), that the precipitation rate is sought in areas where no observations (or accurate forecasts) of the input exist. Interpolation of the surface meteorological observations is then necessary. This section examines the issue of the spatial interpolation of air temperature,  $T_o$ ; pressure,  $p_o$ ; and dew-point temperature,  $T_d$ , near the ground surface under altitude varying terrain.

It is assumed that the surface meteorological input is the result of both the topography and the atmospheric disturbances. The input is decomposed into two corresponding parts  $u_t(z)$  and  $u_a$ , according to

$$u = u_t(z) + u_a \quad (8)$$

where  $u$  denotes input (any of  $T_o$ ,  $p_o$ ,  $T_d$ );  $u_t(z)$  denotes the topography component dependent on the altitude,  $z$ ; and  $u_a$  is the atmospheric component.

The topography component is determined based on the thermal and water vapor properties of an air-parcel as it is forced by the topographic relief to ascend from the lowest point in the area under consideration. Thus, starting from the meteorological station with the lowest elevation in a radius of up to 200 km from the basin, one determines the topographic component of  $u$  at the altitudes of all the stations and at the altitude of the point of interest (area-weighted elevation of the drainage basin). Then, one subtracts  $u_t(z)$  from the actual observations at the meteorological stations and interpolates linearly the residuals to the point of interest. The value of  $u$  at the point of interest is the sum of its topographic component at that point and the interpolated residual at the same point.

Note that dry-adiabatic ascent is used, up to the level where the parcel becomes saturated with respect to water vapor, and pseudo-adiabatic ascent is used above that level.

An important good characteristic of the procedure used is that it provides self-consistent interpolated values for  $T_o$ ,  $p_o$ ,  $T_d$ . Tests of the procedure for a relatively flat terrain (Tulsa, Oklahoma) and for a mountainous terrain (Lewistown, Montana) show standard errors ranging from 1 to 2 °K for  $T_o$ , from 80 to 90 kg/(m sec<sup>2</sup>) for  $p_o$  and from 1.5 to 1.9 °K for  $T_d$ .

#### 8. TESTING OF THE INTEGRATED HYDRO-METEOROLOGICAL MODEL

The Bird Creek basin near Sperry, Oklahoma, served as the test basin. The basin area is 2344 km<sup>2</sup>. The elevation ranges from 200 to 350 meters. The wettest seasons are spring and summer with rainfall mainly in the form of showers and thunderstorms. Snowfall is very light. There are significant evapotranspiration losses in the period July to September due to the high air temperature (100°F common), the low relative humidity, and the good southerly breeze.

Six-hourly data were used. Periods of high flows were selected. Six-hourly discharge data are available at the basin outlet, mostly for the months in spring and summer when the flow is high. Mean areal potential evapotranspiration estimates are available at six-hour intervals computed by standard National Weather Service (NWS) procedures (NOAA-NWS, 1972; Day and Farnsworth, 1982). Six-hourly mean areal precipitation estimates are also available based on data from stations both within and outside of the basin, and on NWS procedures (Larson, 1975; Larson and VanDemark, 1979).

The meteorological input spatial interpolation procedure presented in the previous section was utilized to obtain six-hourly temperature,  $T_o$ ; pressure,  $p_o$ ; and dew-point temperature,  $T_d$ , data corresponding to the basin center, assuming the characteristic basin-elevation of 220 meters. Data from the meteorological stations 1) at Springfield, Missouri, at a distance of 165 km, 2) at Wichita, Kansas, at a distance of 95 km, 3) at Oklahoma City, Oklahoma, at a distance of 105 km, and 4) at Tulsa, Oklahoma, at a distance of 30 km, were used in the interpolation scheme.

The model and the state estimator parameters were obtained from previous studies (Georgakakos and Bras, 1982b; Georgakakos and Bras, 1979; Kitanidis and Bras, 1980; Georgakakos, 1984) independent of the present one. The parameters were held constant for all the integrated hydro-meteorological model tests.

Figure 4 presents the frequency plot of the peak magnitude of the observed hydrographs that were included in the model tests. Hydrographs with peaks greater than 0.5 mm/6 hours (or 54 m<sup>3</sup>/sec) in magnitude were studied. The bulk of the events were in the range 0.5 to 3 mm/6 hours (or 54 to 324 m<sup>3</sup>/sec) and include several flood events. The test period also included some rare events that caused very high flows (at the right end of the magnitude axis).

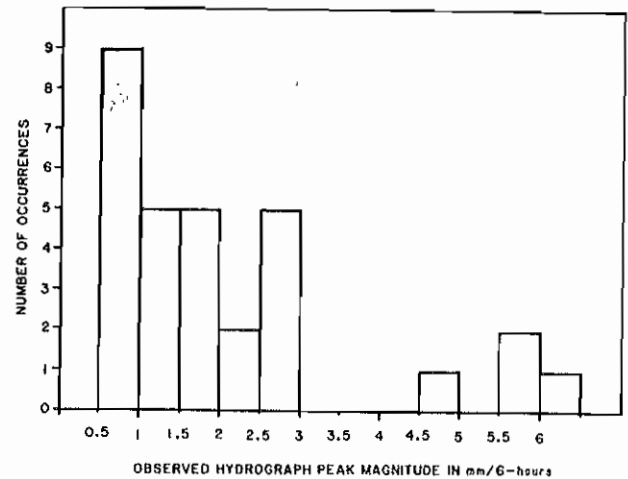


Figure 4. Frequency plot of the peak magnitude of the observed hydrographs for the Bird Creek test basin.

The frequency plot of the difference, expressed in time-steps, between predicted and observed peak flows for a six-hour forecast lead time is shown in Figure 5. Positive numbers indicate a late lag of the predicted flows after the observed ones. The model predicted the hydrograph peak on time or six hours early in more than 70 percent of the cases. Figure 5 shows that, for the majority of the events, the hydrograph peak time was accurately forecast.

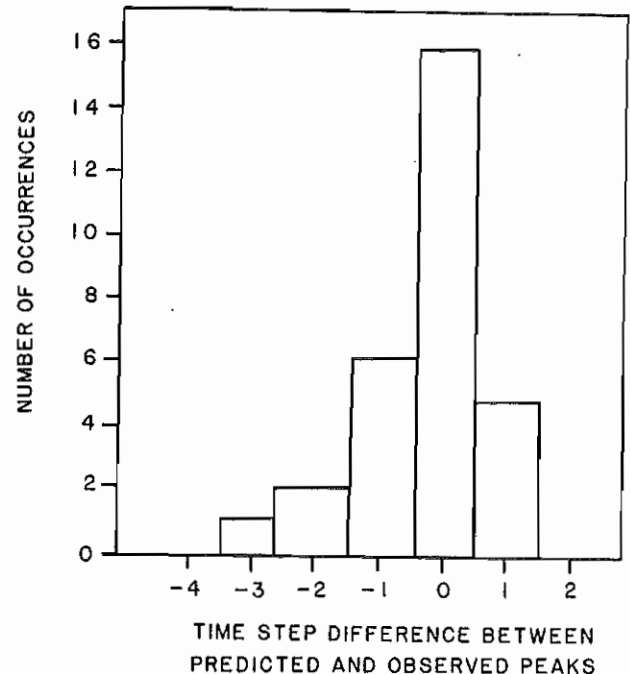


Figure 5. Frequency plot of the time-step difference between predicted and observed peaks for the Bird Creek test basin.

The frequency plot of the percent error in forecasting hydrograph peak magnitude for a six-hour forecast lead time is shown in Figure 6. Positive values on the magnitude axis signify overprediction by the hydrometeorological model. The hydrograph peak magnitude was predicted with less than 20 percent error in more than 70 percent of the cases.

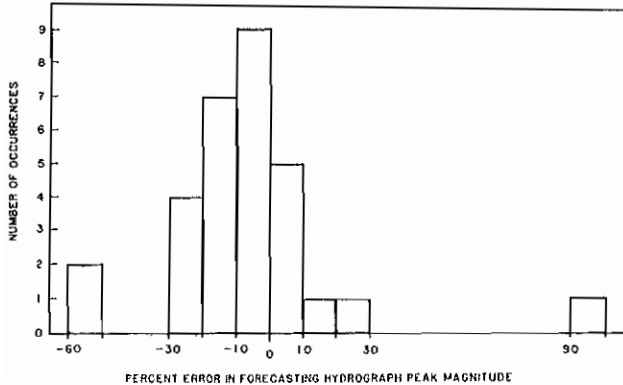


Figure 6. Frequency plot of the percent error in forecasting hydrograph peak magnitude for the Bird Creek test basin.

The results shown in Figures 5 and 6 point to the usefulness of the model as an operational tool in the real-time forecasting of flood flows.

Examination of the detailed results for a six-hour forecast lead time revealed the performance deterioration of the precipitation component in cases when the surface meteorological data are not indicative of the thermal and vapor structure of the atmosphere aloft (e.g., in cases of thermal inversions). Work is underway to incorporate upper air data into the precipitation model of Georgakakos and Bras (1984a) to alleviate the problem.

Tests for longer forecast lead times were also conducted for the hydrometeorological model. Forecast lead times up to 30 hours (approximately equal to the basin response time) were studied. Both actual meteorological data and forecasts of meteorological data were used as input to the precipitation component for the longer forecast lead times. The input forecasts were based on a persistence scheme that forecasts the current observation of the meteorological variables. A typical example of the model performance in extended forecasts is presented in Figure 7. The model discharge forecasts both with observed input and with forecast input are compared to the forecasts of a persistence scheme and an extrapolation scheme. (The forecast is the value linearly extrapolated from current and previous observations.)

The longer-range hydrometeorological model forecasts were better in a least squares sense than both the persistence and the extrapolation forecasts. Also apparent is the deterioration of the hydrometeorological model performance when forecast input is used. It is expected that a more accurate forecast procedure for the meteorological input will improve model performance for

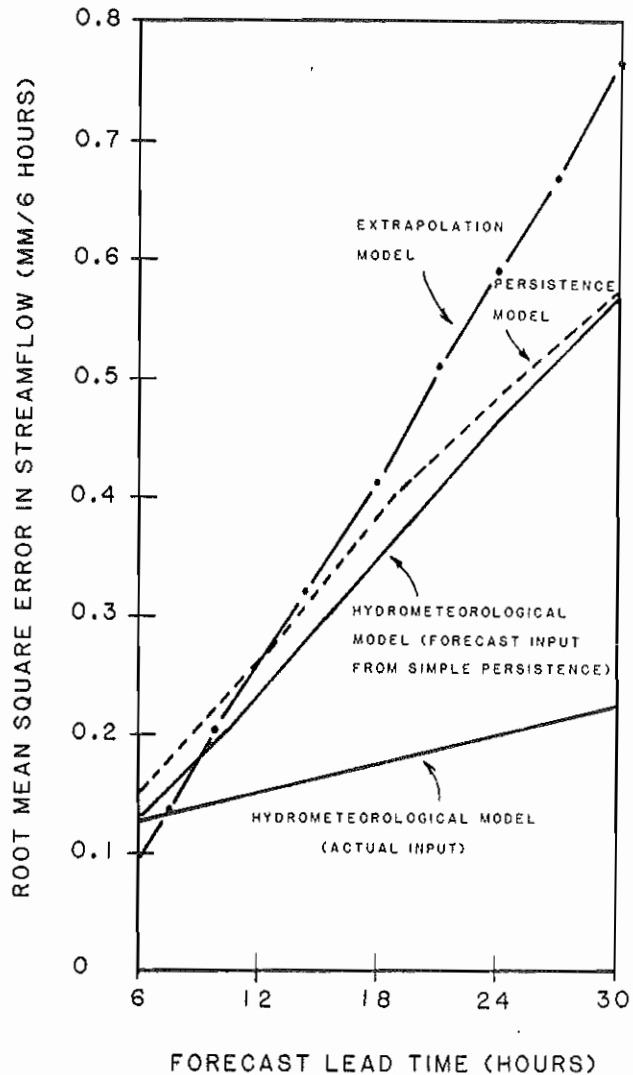


Figure 7. Extended forecasts of the hydro-meteorological model (solid lines), the persistence model (dashed line), and the extrapolation model (chain-dotted line).

the longer forecast lead times. Work is underway to incorporate the operationally issued meteorological forecasts from the large scale numerical weather prediction models into the structure of the precipitation component.

The extrapolation scheme showed a better performance for the six-hour forecast lead time. Note, however, that predictions based on extrapolation and persistence will always have a late lag with respect to the observed hydrograph peak.

#### 9. DESIGN OF A FLASH-FLOOD PREDICTION SYSTEM - IHFS

Based on the concept of coupled precipitation and catchment models, a prototype system for the real-time prediction of flash floods was designed.

The flash-flood phenomenon is characterized by very short catchment response times and by intense local precipitation. The time constants of the precipitation formation process are of the same order of magnitude as the time constants of the catchment response process. Because of the intense rainfall, only the upper layers of the soil respond dynamically to the input rainfall rates and generate the bulk of the channel inflow.

In view of the short forecast lead times in flash-flood prediction and of the characteristics of the flash-flood phenomenon (indicated above), the Sacramento Soil-Moisture Accounting model used in the integrated hydrometeorological model in the previous sections was replaced by a simple Antecedent Precipitation Index (API) procedure.

Given parameters  $m$  and  $D$ , and denoting by  $P$  the precipitation volume over time  $\Delta t$ , the API procedure gives the channel inflow  $R$  over time  $\Delta t$  as:

$$R = (P^m + D^m)^{1/m} - D$$

Use of an API procedure drastically reduces the number of states in the integrated hydro-meteorological model, since it eliminates the six soil states of the Sacramento Soil-Moisture Accounting scheme. This translates into significant computational savings both in execution time and in computer storage locations. The flash-flood system under study is, therefore, suitable for implementation in mini- and micro-computers at the local level (e.g., the Weather Service Forecast Offices). We will refer to the flash-flood system as the Integrated Hydrometeorological Forecast System (IHFS) in the following.

The IHFS system is an event-oriented system designed to operate at the local level. It contains both meteorological and hydrological models together with updating procedures, and its purpose is to forecast flash-flood flows. The system uses surface temperature, surface pressure, and surface dew-point temperature as input variables and it forecasts local precipitation and discharge for a few hours (up to 6 hrs) into the future. After the collection of the observations of precipitation and discharge, an updating mechanism compares in real time these observations with the forecasts issued and makes corrections to the model states. Thus, the next forecasts are made based on improved initial conditions.

The preliminary configuration for the IHFS is depicted in Figure 8. The primary links of IHFS with existing sources of information are displayed in the figure. The meteorological input that feeds the precipitation component is obtained from the Automation of Field Operations and Services (AFOS) system.

The necessary API parameters will also be obtained from AFOS. The relevant message is sent by the River Forecast Center (RFC) in charge of the flash-flood area under consideration. The RFC will help identify the flash-flood prone areas for the system operation. After each update-predict cycle, the IHFS state variables are stored in carry-over storage on-line, so that

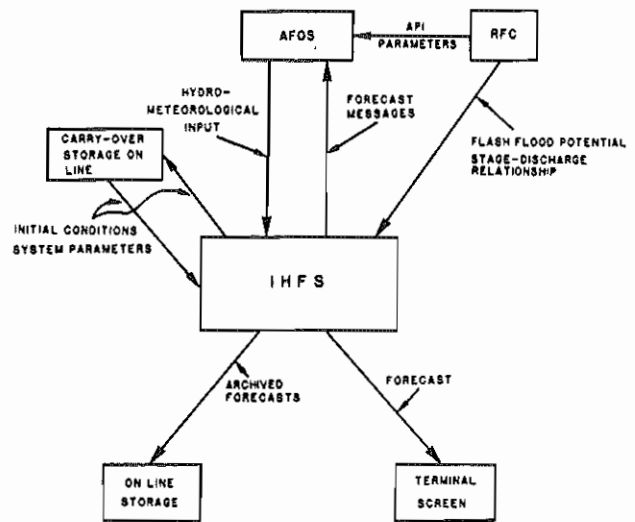


Figure 8. Preliminary configuration for IHFS.

when new data become available, a new update-predict cycle can commence.

The IHFS will produce both precipitation and flow stage forecasts and it will give the one standard deviation upper and lower bound for each forecast. Given flood-stage threshold values, the system will produce the probability that flooding will occur.

#### 10. PRELIMINARY TESTS OF THE IHFS

In cooperation with the Weather Service Forecast Office staff in Washington, D.C., a 625 mi<sup>2</sup> headwater basin was selected in Virginia for the preliminary testing of IHFS in an experiment that simulated real-time operations. The watershed is located in Rappahannock County and has its outlet at Remington. Six-hourly precipitation and stage data for the period 7:00 p.m. February 13, 1984, to 7:00 a.m. February 16, 1984, were used. Daily values of the parameters of the API procedure were obtained from the Middle Atlantic RFC located at Harrisburg. The surface meteorological data that drive the precipitation model were obtained from the Washington Dulles Airport meteorological station in the D.C. metropolitan area. The station lies approximately 30 miles to the northeast of the watershed. The flood stage at Remington is 15 ft.

During the tests, real-time conditions were simulated. Forecasts were made based on currently available information only. A simple persistence scheme was used to forecast the surface temperature, pressure and dew-point temperature to serve as input to the precipitation model. The model parameters were not fine tuned for the basin under study.

Figure 9 shows the stage observations (black circles) and the six-hourly (solid line) and twelve-hourly (dashed line) IHFS forecasts for Remington, Virginia. Even for a twelve-hour lead

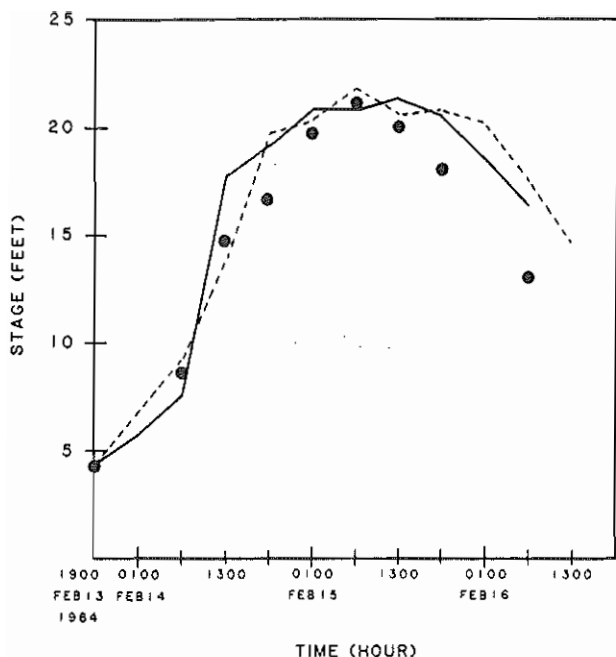


Figure 9. Six-hour (solid line) and twelve-hour (dashed line) stage forecasts of IHFS using forecast input based on persistence. The observations are in black circles. Forecasts at Remington, Va.

time the IHFS forecasts are satisfactory. In particular, the timing and magnitude of the peak are correctly forecasted.

The IHFS produces estimates for the mean and the standard deviation. Based on those estimates, and given the flood stage at the outlet of the basin, IHFS produces forecasts of the probability of flood occurrence. The ability of IHFS to predict the occurrence of flooding at Remington can be assessed from Figure 10. There, probabilistic forecasts of the occurrence of flooding are shown by black circles for a six-hour forecast lead time, and by open squares for a twelve-hour forecast lead time. Values in the (0.7 - 0.85) range were forecasted for both forecast lead times for the period when excessive flooding occurs. This indicates that IHFS produces reliable probabilistic forecasts of flooding occurrence.

#### 11. SUMMARY AND CONCLUSIONS

A novel approach to the real-time forecasting of floods has been presented. Direct coupling of physically based precipitation, soil, and routing models through mass continuity and through a state estimator resulted in an efficient system for flood prediction.

Testing of the system in Bird Creek, Oklahoma, produced very encouraging results for a six-hour lead time, with hydrograph peaks predicted on time and with the correct magnitude, for most of the flood cases examined. The ability of the model to forecast accurately for longer forecast lead times compared favorably with the skill of purely statistical models based on persistence and extrapolation.

Figure 10. Six-hour (black circles) and twelve-hour (open squares) forecast probabilities that the stage will exceed the 15 ft. flood stage at Remington. The shaded region signifies times when flooding actually occurred.

Simplification of the soil component of the integrated model led to the design of a computationally efficient system, IHFS, suitable for use in flash-flood situations. Preliminary results in tests simulating real-time operations pointed to the ability of the system to predict excessive flooding periods with a good degree of reliability.

Extensive tests of IHFS in real time are planned for the future at various locations in the U.S. to establish the utility of the system in flash-flood prediction.

#### 12. ACKNOWLEDGEMENTS

Parts of this paper were presented at the 1985 Fall Meeting of the American Geophysical Union (San Francisco, December 1985) under the title "Dynamically Coupled Precipitation and Drainage Basin Models."

#### 13. REFERENCES

Armstrong, B.L. (1978), "Derivation of Initial Soil Moisture Accounting Parameters from Soil Properties for the National Weather Service River Forecast System," NOAA Technical Memorandum NWS HYDRO-37, U.S. Department of Commerce, Silver Spring, Maryland.

- Day, G.N. and R.K. Farnsworth (1982), "Mean Areal Potential Evaporation," National Weather Service River Forecast System (NWSRFS) User's Manual, Part III, Chapter 9. Available from the Hydrologic Research Laboratory, NWS, NOAA, Silver Spring, Maryland.
- Gelb, A., ed., (1974), Applied Optimal Estimation, The M.I.T. Press, Cambridge, Massachusetts.
- Georgakakos, K.P. (1984), "Model-Error Adaptive Parameter Determination of a Conceptual Rainfall Prediction Model," Proceedings of the 16th Southeastern Symposium on System Theory, March 25-17, 1984, Mississippi State, Mississippi, pp. 111-115.
- Georgakakos, K.P. (1982), "Structure and Parameter Determination of a Hydrologically Useful Rainfall Prediction Model," presented at the 1982 Fall Meeting of the American Geophysical Union, San Francisco, California. Available from the Hydrologic Research Laboratory, NWS, NOAA, Silver Spring, Maryland.
- Georgakakos, K.P. and R.L. Bras (1984a), "A Hydrologically Useful Station Precipitation Model, 1, Formulation," Water Resources Research, 20(11), pp. 1585-1596.
- Georgakakos, K.P. and R.L. Bras (1984b), "A Hydrologically Useful Station Precipitation Model, 2, Case Studies," Water Resources Research, 20(11), pp. 1597-1610.
- Georgakakos, K.P. and R.L. Bras (1982a), "A Precipitation Model and Its Use in Real-Time River Flow Forecasting," Ralph M. Parsons Laboratory Hydrology and Water Resource Systems Report No. 286, MIT Dept. of Civil Engineering, Cambridge, Massachusetts.
- Georgakakos, K.P. and R.L. Bras (1982b), "Real-Time Statistically Linearized Adaptive Flood Routing," Water Resources Research, 18(3), pp. 513-524.
- Georgakakos, K.P. and R.L. Bras (1980), "A Statistical Linearization Approach to Real-Time Nonlinear Flood Routing," Ralph M. Parsons Laboratory for Water Resources and Hydrodynamics Report No. 235, MIT Dept. of Civil Engineering, Cambridge, Massachusetts.
- Georgakakos, K.P. and R.L. Bras (1979), "On-Line River Discharge Forecasting Using Filtering and Estimation Theory," Ralph M. Parsons Laboratory for Water Resources and Hydrodynamics Progress Report, Sept. 13, 1978 - Feb. 13, 1979, Contract No. 7-35112, MIT Department of Civil Engineering, Cambridge, Massachusetts.
- Georgakakos, K.P. and M.D. Hudlow (1984), "Quantitative Precipitation Forecast Techniques for Use in Hydrologic Forecasting," Bulletin American Meteorological Society, Vol. 65, No. 11, November 1984, pp. 1186-1200.
- Kitanidis, P.K. and R.L. Bras (1980a), "Real-Time Forecasting with a Conceptual Hydrologic Model, 1, Analysis of Uncertainty," Water Resources Research, 16(6), pp. 1025-1033.
- Kitanidis, P.K. and R.L. Bras (1980b), "Real-Time Forecasting with a Conceptual Hydrologic Model, 2, Applications and Results," Water Resources Research, 16(6), pp. 1034-1044.
- Larson, L.W. (1975), "Precipitation Model," National Weather Service River Forecast System (NWSRFS) User's Manual, Part II, Chapter 6. Available from Hydrologic Research Laboratory, NWS, NOAA, Silver Spring, Maryland.
- Larson, L.W. and S. VanDemark (1979), "Mean Areal Precipitation Program (MAP), 1979," National Weather Service River Forecast System (NWSRFS) User's Manual, Part III, Chapter 7. Available from Hydrologic Research Laboratory, NWS, NOAA, Silver Spring, Maryland.
- NOAA-NWS (1972), "National Weather Service River Forecast System Forecast Procedures," NOAA Technical Memorandum NWS HYDRO-14, U.S. Department of Commerce, Silver Spring, Maryland.
- NWS Office of Hydrology (1982), "Program Development Plan for Improving Hydrologic Services," Office of Hydrology, NWS, NOAA, Silver Spring, Maryland.
- Peck, E.L. (1976), "Catchment Modeling and Initial Parameter Estimation for the National Weather Service River Forecast System," NOAA Technical Memorandum NWS HYDRO-31, U. S. Department of Commerce, Silver Spring, Maryland.
- Restrepo-Posada, P.J. and R.L. Bras (1982), "Automatic Parameter Estimation of a Large Conceptual Rainfall-Runoff Model: A Maximum Likelihood Approach," Ralph M. Parsons Laboratory Hydrology and Water Resource Systems Report No. 267, MIT Dept. of Civil Engineering, Cambridge, Massachusetts.



## A PROBABILISTIC APPROACH TO FLASH FLOOD FORECASTING

Susan F. Zevin

National Weather Service  
Office of Hydrology  
Silver Spring, Maryland 20910

Donald R. Davis

Department of Hydrology and Water Resources  
University of Arizona  
Tucson, Arizona 85721

### 1. INTRODUCTION

A major area targeted for hydrometeorological forecast service improvements has been that of flash flood forecasting (NOAA, 1984; NWS, 1982; NACOA, 1983; Barrett, 1983). The need for such improvements arose from several occurrences of disastrous flash floods that resulted in major loss of life and extensive property damage (ESSA, 1969; NOAA, 1972; NOAA, 1976). The greater awareness of the operational and theoretical problems of providing flash flood forecast services has also helped focus attention on the less spectacular, but more prevalent situations in which one or two persons are swept away by rapidly formed torrents of water. Current statistics show that 80-90 percent of the 200 annual flood related deaths are caused by flash floods.

As part of its hydrologic services program, the NWS provides site-specific flood forecasts for 3000 of the approximately 20,000 flood prone communities in the U.S. These places are located mostly on large rivers which take 24 hours or more to crest from the time of onset of rainfall.

However, floods which form in less than 24 hours and flash floods, i.e. those floods occurring within 6 hours of the causative event, defy forecasting by the traditional data collection, analysis, forecast, dissemination, and response system. This is because the full operational procedure in the NWS forecast framework takes too long to complete for effective response and because of a

lack of sufficient rainfall data in space and time to forecast the smaller basins. Therefore, approximately 1000 communities are aided by so-called community self-help schemes. It is projected that about 2000 more of these procedures will be implemented by the 1990's.

The rest of the 16,000 flood-prone communities are provided forecast services through flash flood Watches and Warnings. The NWS record on providing watches and warnings show a major problem in providing these services with sufficient lead time for meaningful response, particularly the warnings. Thus, it remains for the NWS to improve its generalized services to the thousands of communities for which explicit forecast schemes are not available. The nature of these improvements should be concentrated in providing more lead time for both watches and warnings, possibly at the expense of forecast accuracy.

#### 1.1 Advances in Flash Flood Forecasting

Advances are being made in the observation systems, both remote and on-site, and in data processing techniques. Some of the improvements are being implemented now in NWS field offices, and some are part of long term development projects which will become operational in stages. A few of these are: ALERT systems (NWS, 1982), the Next Generation Radar Precipitation Processing Algorithm (NWS, 1984), Analysis of Satellite Imagery (Scofield, 1978) and a system of coupled hydrometeorological models to produce short-term (1-3 hr)

forecasts of streamflow (Georgakakis and Bras, 1982; NWS, 1984). In addition, improvements in 6 hr and beyond QPF's are being sought by the Heavy Precipitation Branch of the National Meteorological Center.

A forecaster must rely on knowledge of the forecast area, incorporating past experiences during flash flood producing rainfall situations with local physical, geographical and demographic characteristics. Post-storm analyses of the meteorological characteristics of numerous flash flood producing rainfalls have been documented (Maddox, et al., 1980). The information is used subjectively and is not linked objectively to other real-time forecast procedures.

Additional advances will be made in data analysis and forecasting as the NWS field operations are restructured for the 1990s to take advantage of NEXRAD Doppler radar technology (that will provide 15-30 minute estimates of rainfall), and local, on-site processing capability for mesoscale weather forecasting.

#### 1.2 Community Needs for Information

Decisions for storm responses must be made preceding the occurrence of flash floods or severe storms. Information is crucial for determining how and when personnel and equipment will be deployed. One to 6 hour probabilities of flash floods could satisfy the needs of community emergency response officials to act on criteria based on local requirements (Zevin, et al, 1983). These criteria would depend on the time and resources necessary to respond given a specific probability of occurrence. Therefore, response could be carried out as cost effectively as possible (Krzysztofowicz, 1983) and with enough lead time for evacuation from isolated areas.

With NWS's advances in technology, and considering the high costs of repair of damages versus those of community response, it is possible for the NWS to serve sophisticated users through probability forecasts of flash

floodings for a specific forecast period could form the basis for public issuance of flash flood watches or warnings depending on preset criteria for the local forecast area. Or, where more sophisticated users are involved, the output could be used for mobilizing manpower and equipment. The ability of local agencies to prepare for flooding using a probability forecast would be more cost effective than awaiting issuance of a flash flood watch or warning.

## 2. BACKGROUND

There has been extensive investigation and operational use of probabilistic forecasts of meteorological conditions. A thorough history and bibliography is traced by Hughes (1980). From its beginning in the early 1900's, probability forecasts gradually gained acceptance within the Weather Bureau, until widespread use began with the Model Output Statistics in 1968. Since then, use of probability forecasts has been expanded to cover some severe weather and even hurricane situations.

### 2.1 The Value of Probabilistic Forecasts

The value of probabilistic forecasts has been investigated frequently since the early 1950's. Thompson (1952) pointed out the suitability of probability forecasts over categorical forecasts to economic evaluation. Thompson and Brier (1955), Gringorten (1958, 1959), Gleeson (1960), and Nelson and Winter (1960, 1964) analyzed the economic value of forecasts through the cost/loss ratio, a matrix of economic payoffs. These economic evaluations are usually performed using an ex post approach in which the value of the forecasts is measured after the forecasts and events have occurred (Winkler and Murphy 1979).

Krzysztofowicz and Davis (1984) determined the value of categorical flood forecasts by calculating the expected annual reduction of losses (costs of response plus flood damage sustained).

More recently, Alexandridis and Krzysztofowicz (1982) applied a decision model in the framework of Bayesian decision theory to the evaluation and use of categorical and probabilistic forecasts to the short term scheduling of power generation based on a single-period power load forecast. The Alexandridis and Krzysztofowicz study is the first to apply decision models to the use and evaluation of continuous variables, in this case a 12-24 hr. categorical forecast of temperature.

Winkler and Murphy (1971) described the forecaster's aggregation, assimilation and use of information as a subjective forecasting process in the framework of Bayes' Theorem. They speculated that the Bayesian process is used intuitively by forecasters to make subjective evaluations of event probabilities.

## 2.2 Use of Probability Approaches in Hydrological Forecasting

The operational need and possible solution for an objective approach to the assessment of flash floods to aid forecasters grew out of the NWS Southern Region's Manually Digitized Radar program (Smith 1975; Moore and Smith, 1979; Tetzloff, 1980; NWS 1984). Tetzloff (1980) developed a computer program which related the three-hour accumulations of rainfall, based on MDR, to 3 hour flash flood guidance values issued by the Tulsa River Forecast Center (RFC). This was the first automated link between the rainfall observation system and the runoff prediction system for evaluation of flash flood potential.

The MDR program and its subsequent relation to RFC guidance was a major first step in implementing objectivity into flash flood forecasting. Based on the popularity of the MDR approach and acceptance of the in-house operational use of probabilities for objective decisions, a similar scheme is proposed for inclusion in the NEXRAD applications software (NWS, 1984). The NEXRAD proposal acknowledges the need for a system to integrate hydrometeorological information to produce probabilistic information of

flash flood potential. The scheme will be used with estimates of observed rainfall, a qpf procedure, and a link to rainfall-runoff criteria provided by NWS hydrologists. The program will produce probability curves and maps of flash flood potential.

Other studies have addressed individual components, either rainfall-runoff models, improved measurement systems and forecast rainfall models. Johnson and Bras (1978) recognized the non-stationarity of rainfall, an element lacking in previous statistical prediction systems of rainfall, and they accounted for it in a multivariate statistical model for predicting future rainfall rates at specified locations. Kitanidis and Bras (1980) applied the concepts of state in mathematical systems theory to the problem of forecasting river flows.

For short duration rainfall, Bras (1976), and Johnson and Bras (1978), and Georgakakis and Bras (1982) have demonstrated that the state-space formulation of the QPF problem is valid and applicable. Their work is being pursued toward implementation into NWS real-time forecasting operations.

## 3.0 Hydrologic Concepts

For purposes of this discussion the following definitions apply:

Data refer to any observation of forecast rainfall amount identified by its source and its duration;

Event refers to the true state of nature, the true precipitation amount, or the true potential of the atmosphere to produce a certain amount of rainfall.

### 3.1 Concept of Flash Flood Guidance

Usually in river forecasting, values of observed rainfall are input to a rainfall/runoff model with the result a discharge value which is converted to stage. The stage or discharge is compared with a predefined flood criteria in order to determine the seriousness or importance of the streamflow

conditions. The concept of a threshold rainfall amount representative of the maximum storage capacity of a hydrologic system, and its inverse, the storage capacity representative of a maximum rainfall amount which can be absorbed by the system, are basic tenets of river forecasting. By keeping track of the rainfall coming into the system, and the states of the hydrologic system, the forecaster may continue to reevaluate the amount of water in the system relative to the storage capacity of the system. Put another way, the forecaster may track the minimum amount of water which must be introduced to the system in a given time to produce flooding. The minimum rainfall amount added to the system which will produce flooding is flash flood guidance (Zevin, et al 1983).

For purposes of this study, the rainfall/runoff processor is viewed as a black box; its total water holding capacity is assumed to be known at any time and the moisture content of the system can be computed. The concept is, then, amenable to the introduction of potential rainfall amounts as estimators of the future states of moisture and runoff in the system.

It is on these principles that NWS River Forecast Centers prepare their flash flood guidance. There are, in each basin, specific river forecast points for which a rainfall/runoff relationship has been derived and calibrated. Using the previous 24 hour rainfall data for a given catchment after soil moisture parameters have been updated, and based on unit-hydrograph analysis, the RFC's introduce varying 3-hour rainfall amounts into the calculations to determine the value above which flooding will occur. The rainfall totals are introduced as a lump sum, with no time variation on the amount assumed to have fallen within the 3 hour time frame. Also, flash flood guidance is derived from a unit hydrograph, again implying an assumption of uniform distribution of rainfall in time and space over the basin.

These concepts are adequate for evaluation of flash flood potential for a large area, and also are

applicable for rainfall/runoff models of a finer spatial and time resolution than the large lumped parameter models and procedures employed by the NWS. A model based on these concepts allows varying time steps for data input, subject to the availability of data for the given time step and computational or data base size restrictions.

Development of a probability procedure can be based on the principles discussed above. As is now the case, at the beginning of each day the previous 24 hour rainfall would be used to compute soil moisture and runoff conditions. And based on these computations a sequence of potential flood producing rainfall values (flash flood guidance) would be derived. Rather than computing only the 3 hour guidance, the RFC could compute a number of guidance values (for example 1,3,6 and possibly 12 hour periods) to account for changing soil moisture states. (In lieu of this the RFC's may wish to update guidance values more frequently in response to changing soil moisture conditions.)

Guidance values have an implicit assumption that amounts of rain falling within a given time period are uniformly distributed over time and space. Thus, a threshold value of 3 inches of rain in 3 hours (for a given area) assumes a uniform intensity of 1 inch/hour for 3 hours.

A direct comparison can be made between a precipitation amount forecast to occur in a given forecast period and a flash flood guidance value valid for the same time period (Zevin, et al 1983). Thus, both forecast and precomputed threshold precipitation amounts represent uniform rainfall intensities which can be compared.

For example, in a basin where no rainfall has occurred for two weeks or more, the flood threshold rainfall amounts might be computed to be 2 inches/hr for a 1 hour forecast period, 1 inch/hour for a forecast period of 3 hours, and .80 inches/hr for 6 hours. Given a precipitation forecast of 2 inches to fall in 3 hours, with no information on the time distribution of the forecast rainfall,

a forecaster might assume the rainfall will fall uniformly over the 3 hours. At .75 inches/hr for 3 hours, no flooding will be expected to occur.

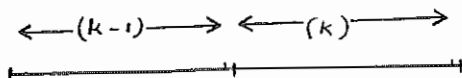
The guidance amount is the sum of the current water holding capacity of the system and the runoff required to produce flooding. This sum is the forecaster's measure of how close the system is to flood conditions at any given precipitation observation time. If the remaining capacity is less than or equal to zero, flooding is imminent. Otherwise, the rainfall amount corresponding to the remaining capacity must enter the system before flooding will occur.

### 3.2 A Deterministic Discrete Linear System

Based on the previous discussions, a system composed of two discrete linear models is used to estimate the present and future hydrologic and meteorologic states of nature from which flash flood potential is computed. The system described is deterministic; its parameters are evaluated probabilistically.

The system is based on the premise that rainfall, both on the ground and in the atmosphere observed and predicted may be used to express the capability of nature to produce flash flooding. Thus, the two systems described below use rainfall, either potential or already produced, as the states of the system. Rainfall potential is defined from the present state to some future time. This is the potential for nature to produce rainfall over a given period of time and area. Rainfall on the ground is that amount which has occurred since some past given state (the beginning of the computational period--the period of time the guidance is to cover) up to the present state. The present state of the system is defined up to a time just before the updating is made.

#### Time Intervals of States



Rainfall on the ground may be represented by the following equation:

$$x_g(k) = x_g(k-1) + u_{g_1}(k-1) \quad (1)$$

where  $x_g(k)$  is the true state of rainfall on the ground, an accumulated amount since the beginning of the computational time period;  $x_g(k-1)$  is the previous state of accumulated rainfall;  $u_{g_1}(k-1)$  is an input to the system, the true amount of rainfall during the last state.

The true potential for rainfall may be stated similarly:

$$x_f(k) = x_f(k-1) - u_{g_1}(k-1) + u_{f_1}(k-1) \quad (2)$$

where  $x_f(k)$  represents the potential for a certain amount of rainfall to occur over a specified time period in the future beginning at (k);  $x_f(k-1)$

is the potential rainfall during the previous time period;

$u_{g_1}(k-1)$  is as defined before, and  $u_{f_1}(k-1)$

represents other atmospheric and meteorological conditions in which are manifested the dynamics of changing rainfall potential.  $u_{g_1}(k-1)$  appears in each equation since it represents both the changing future potential for rainfall and the changing soil moisture conditions.

The total time represented by the two equations is equal to the time period covered by flash flood guidance. The two equations represent the states and state transitions needed to evaluate current and future rainfall conditions against a flash flood guidance.

### 3.3 A Probabilistic System

The previous section describes the deterministic framework on which a probabilistic approach can be built. That is, if  $x_g(k) + x_f(k) \geq \text{Guidance}$ ,

then flash flooding will occur. However, the quantities  $x_g(k)$  and

$x_f(k)$  and the flash flood guidance are never known with certainty. Thus, if probability distributions are available for  $x_g(k)$  and  $x_f(k)$ , then the probability of flash flooding can be expressed as the sum of two random variables (Zevin, et al, 1983):

$$p(\text{flash flood/flash flood guidance}) = p(x_f(k)) * p(x_g(k)) \quad (3)$$

for all  $(x_f(k) + x_g(k)) \geq$  flash flood guidance.

Key to this integrated approach is an assumption that it is possible to know or estimate the probability distributions of the random variables which comprise equations (1) and (2). Investigations are underway to determine the validity of this assumption.

Equation (3) may be solved through the use of Bayes' Theorem (Winkler, 1974) and transformation of variables (Taha, 1976).

#### 4.0 Summary

A system is proposed that will integrate the rainfall and runoff forecasting schemes to provide probability information on the potential for flash flooding. The approach obtains the probability density functions for forecast and observed areal rainfall directly using Bayes' Theorem and transformation of variables. The results are coupled with a runoff component in order to evaluate flood potential. The system accounts for the uncertainty in the models and measurements feeding into the system. The system proposed is a framework for coupling the models and information necessary for flash flood prediction, and requires no physical parameters to be estimated or calibrated. Since the Bayesian framework is used, the system can account for any probability density functions of observed or predicted rainfall so that the extremes of flash flood situations are preserved. The system transformations are described deterministically in linear state-space for convenience.

The framework provides probability assessments of flash flood

potential suitable for input to an economic utility function. However, the development of these utility functions is not described here. These functions will have to be calibrated for each location or area where the flash flood potential model is used.

#### References

- Alexandridis, Mark G., and Roman Krzysztofowicz, 1981, "Value of categorical and probabilistic temperature forecasts for scheduling of power generation," Report Number 282, Ralph M. Parsons Laboratory, Hydrology and Water Resource Systems, MIT, Cambridge, Mass.
- Bras, Raphael L., 1976, "Short-term forecasting of rainfall and runoff," IASA Workshop on Recent Developments in Real-time Forecasting of Water Resource Systems, Luxemburg, Austria, October 1976, pp. 125-137.
- Environmental Science Services Administration, 1969, The Virginia Floods, August 19-22, 1969: A Report to the Administrator, U. S. Department of Commerce.
- Georgakakis, Konstantine P., and Raphael Bras, 1982, "A precipitation model and its use in real-time river forecasting," Report Number 286, Ralph M. Parsons Laboratory, Hydrology and Water Resource Systems, MIT, Cambridge, Mass.
- Gleeson, Thomas A., 1960, "A prediction and decision method for applied meteorology and climatology, based partly on the theory of games," Journal of Meteorology, Vol. 17, no. 2, pp. 116-121.
- Gringorten, I. I., 1958, "On the comparison of one or more sets of probability forecasts," Journal of Meteorology, vol. 15, no. 3, pp. 283-287.
- Gringorten, I. I., 1959, "Probability estimates of weather in relation to operational Meteorology," vol. 16, no. 6, pp. 663-671.

- Hughes, Laurence A., 1980, Probability forecasting--reasons, procedures, problems, NOAA Technical Memorandum, NWS FCST 24, NOAA, National Weather Service, Meteorological Services Division.
- Johnson, Edward R., and Raphael Bras, 1978, "Short term rainfall prediction: A non-stationary multivariate stochastic model," Report Number 233, Ralph M. Parsons Laboratory for Water Resources and Hydrodynamics, MIT, Cambridge, Mass.
- Kitanidis, Peter K., and Raphael Bras, (1980), Real-time forecasting with a conceptual hydrologic model, 2, applications and results, Water Resources Research, Vol. 16, no. 6, pp. 1034-1044.
- Krzysztofowicz, Roman, 1983, "Why should a forecaster and a decision maker use Bayes theorem?" Water Resources Research, Vol. 19, no. 2, pp. 327-336.
- Krzysztofowicz, Roman, and Donald R. Davis, 1983, "A methodology for evaluation of flood forecast-response systems, 1, Analysis and concepts," Water Resources Research, Vol. 19, no. 6, pp. 1423-1430.
- Maddox, Robert A., L. Ray Hoxit, and Faye Canova, 1980, "Meteorological characteristics of heavy precipitation and flash flood events over the western United States," NOAA, Environmental Research Laboratory, Atmospheric Physics and Chemistry Laboratory, Boulder, Colorado.
- Moore, Paul L., and Daniel L. Smith, 1979, Manually digitized radar data--interpretation and application, NOAA Technical Memorandum NWS SR-99, Scientific Services Division, Southern Region, National Oceanic and Atmospheric Administration.
- Nelson, R.R. and Winter, S.G., 1960, Weather Information and Economic Decisions: A Preliminary Report, The RAND Corp., RM-2620-NASA.
- Nelson, R.R. and Winter, S.G., 1964, "A case study in the economics of information and coordination: The weather forecasting system," Quarterly Journal of Economics, Vol. 78, no. 3, pp. 420-441.
- NACOA, 1983, The Nation's River and Flood Forecasting and Warning Service, National Advisory Committee on Oceans and Atmosphere.
- NOAA, 1972, "Black Hills Flood of June 7, 1972," Natural Disaster Survey Report 76-1, National Oceanic and Atmospheric Administration.
- NOAA, 1977, "Kansas City, flash flood of September 12-13, 1977," Natural Disaster Survey Report 77-2, National Oceanic and Atmospheric Administration.
- NOAA, 1978, National Flash Flood Program Development Plan, FY 1979-84, U.S. Department of Commerce, National Oceanic and Atmospheric Administration, Washington, D. C.
- NWS, 1982, Automated Local Evaluation in Real-Time, A Cooperative Flood Warning System for your Community, Western Region, National Weather Service, National Oceanic and Atmospheric Administration.
- NWS, Office of Hydrology, 1984, Proposal to Develop and Validate "A flash flood potential algorithm" for the Next Generation Weather Radar (NEXRAD), (unpublished).

- Scotfield, Roderick A., 1978, "Using satellite imagery to detect and estimate rainfall from flash flood producing thunderstorms," Preprints, Conference on Weather Forecasting and Analysis and Aviation Meteorology, October 16-19, 1978, Silver Spring, Maryland, American Meteorological Society, Boston, Mass.
- Smith, Paul L., and Douglas E. Cain, 1979, "Use of radar data to determine gaging requirements for measuring rainfall from convective complexes," Preprints, Seventh Conference on Inadvertent and Planned Weather Modification, October 8-12, 1979, Banff, Alberta, Canada.
- Taha, Hamdy A., 1976, Operations Research, An Introduction, second edition, Macmillan Publishing Co., Inc., New York.
- Tetzloff, Randy, 1980, private conversation on software developed at Tulsa River Forecast Center, Tulsa, Okla.
- Thompson, J.C., 1952, On the Operational Deficiencies in Categorical Weather Forecasts, Bulletin of the American Meteorological Society, Vol. 33, no. 6, pp. 223-226.
- Thompson, J.C. and Brier, G.W., 1955, The Economic Utility of Weather Forecasts, Monthly Weather Review, Vol. 83, no. 11, pp. 249-254.
- Winkler, Robert L., 1972, An Introduction to Bayesian Inference and Decision, Holt Rinehart and Winston, Inc., New York.
- Winkler, Robert L., and Allan H. Murphy, 1971, "Probability forecasting: The aggregation of information," Proceedings, International Symposium on Probability and Statistics in the Atmospheric Sciences, American Meteorological Society, pp. 83-89.
- Winkler, Robert L., and Allan H. Murphy, 1979, "The value of weather forecasts in the cost-loss ratio situation: An ex ante approach," Proceedings, Sixth Conference on Probability and Statistics, American Meteorological Society, pp. 83-89.
- Zevin, Susan F., Donald R. Davis and Suzanne Shields, 1983, "A decision theoretic approach to flash flood forecasting," Technical Conference on Mitigation of Natural Hazards Through Real-Time Data Collection Systems and Hydrological Forecasting, unpublished.

## QPF WORKSHOP PANEL DISCUSSION

The following is a summary of a Panel Discussion held at the close of the QPF Workshop. Panelists were: Dr. Ray Jensen, Ray Biedinger, Jim Belville, Bob Bell, Dr. Rod Scofield, Dr. Jack Sheridan, Dr. Jerry Rogers, Dan Berkowitz, and Dr. Bob Maddox. Unless otherwise noted, the comments below reflect input from each panelist.

Mike Mogil (meteorologist - SSD, SRH) moderated the discussion and charged the panel with "examining the present and future states of heavy PRECIPITATION forecasting". Panel members were encouraged to present solutions as well as problems.

Reflecting on the nature of the conference (which was conceived and carried out primarily by field people), Mogil applauded SR Director Ray Jensen's support for the present and similar earlier workshops. He also noted four MEGATREND aspects of the workshop (MEGATRENDS is a book written by John Naisbitt). Specifically:

- the most reliable way to anticipate the future is to UNDERSTAND the present
- despite conceits of New York City and Washington, almost NOTHING starts there
- TRENDS are bottom up; FADS are top down
- trends, like horses, are easier to ride in the direction they are already going

Belville (meteorologist - WSFO New Orleans) argued for eliminating "the middle ages" from NWS operations. The 1950's brought new radars (WSR-57's) and numerical models, and forecasters are still tied to the earlier vestiges of these. Included are over-reliance on MOS and numerical guidance, and non-scientific use of radar (e.g. relation of depth of convection to tropopause height rather than equilibrium level). As a result, we too frequently react to, rather than anticipate, a significant event.

Another problem centers on funding for heavy rainfall R & D. Heavy rain/snow doesn't have the same charisma as tornadoes (although recent statistics indicate precipitation events are more deadly and costly). Rainfall R & D is shortchanged. Increased local "R & D", within a flexible operational environment is an

alternative. Belville (and others) noted that during "good weather" shifts, one forecaster might cover two desks, freeing a forecaster to work on local studies. Another possibility could allow for a rotation into a dedicated R & D position for short periods (e.g., a month or two). Forecasters should also be encouraged to follow-up on "busted" (and exceptionally well-made) forecasts. Station management needs to encourage and support these opportunities.

The NWSTC Flash Flood Course does not use enough field-generated case studies. They need to get these from regional SSD's and field offices and incorporate them into the course. One attendee voiced concern that a lot of good, useful information from NWSH and research facilities isn't reaching the field, either. NWSTC should also provide guidance on how to develop local studies. Local training seminars are needed to ensure forecasters keep abreast of latest scientific developments.

Biedinger (DMIC - WSFO Miami) agreed that local studies were needed. Biedinger felt creation of a dedicated "research and computer specialist" (not to be used in the operational staffing rotation) might increase local computer use and could contribute to having local/national computers perform more of the "busy" work. Locally developed applications programs should be developed to solve local forecast problems. Several attendees favored such a dedicated position; but others pointed out that staffing reductions prohibited the approach except, perhaps, in special situations.

Walter Anderson (MIC, WSFO Lubbock) suggested the RWCC (Regional Warning and Coordination Center) concept offered a middle-ground approach. RWCC's existed for several years in each NWS region and were staffed with carefully selected meteorologists who routinely focused on critical weather events, but who had the time and ability to undertake techniques development activities in good weather. Such a group could provide more tailored service than a national center, and also provide the focus for increased applications work without the manpower demands of the Biedinger proposal. Automated systems now in place and planned for NWS field sites

only increase the likelihood of success with such a concept.

Biedinger felt that by placing meteorologists at WSO's, more responsibility for forecast preparation could be shifted downward, further freeing time at the WSFO.

Finally, Biedinger urged that we undertake a critical analysis of our products, eliminating those that aren't needed, and possibly redesigning others for easier preparation (possibly by computer). One attendee went so far as to recommend we perform the same analysis on our jobs!

Another attendee recommended that field forecaster achievements and constraints in the area of field-based research be documented (Dan---I will be following up on this item).

Bell (meteorologist - NMC Heavy Precipitation Branch) discussed HPB's threat score verification program. During the past two years, only winter season scores have improved (synoptic emphasis). Present work remains "seat of the pants" model corrections. Part of the summer season problem involves the "spotty" nature of precipitation patterns (i.e. mesoscale emphasis).

Subtle model errors can produce horrendous precipitation forecast errors. To improve guidance, NMC is leaning heavily toward LFM improvements using VAS input. Bell presented one case in which the LFM was run with and without VAS data. Initial analysis comparisons showed a 30m difference in eastern Pacific 700mb heights. This translated into a 90m error along the U.S. east coast in 48 hours. NGM implementation may also enhance HPB guidance. Recently, the NGM provided much improved guidance for the record-breaking January 1985 San Antonio snowstorm.

NMC's primary emphasis has been on longer ranges. Bell suggested creation of a national mesoscale QPF R & D effort, because of WSFO staff limitations.

Scotfield (meteorologist - NESDIS) emphasized the progress which has been made in heavy precipitation understanding, analysis, and forecasting. Satellites have played a significant role and the future promises further VISIONs for progress.

Scotfield defined the acronym thusly:

V - VAS data - improved and more frequent sounding analyses; tied to improving model performance; integration with NEXRAD and vertical profiler.

I  
S - Improved Satellite estimations - improvements on the Scotfield - Oliver technique, automatic estimation capabilities, apply moisture correction, correct for low-level inflow, overcome "warm-top" problem, etc.

I  
O - Improved Outlooks - possibly a satellite flash flood index.  
N - New Developments and finding the "Newton"'s (i.e. the people with scientific vision).

Sheridan (hydrologist - RFC Tulsa) emphasized the need for hydrometeorological cooperation between RFC's and WSFO's. Sheridan noted that the RFC has a role to play in the flash flood program, especially in assessing height of flood crest and site specific impact areas. Roles of hydrologists and meteorologists in the flash flood program were also discussed.

Sheridan also reiterated the problem of emphasizing severe weather at the expense of flooding. Several attendees noted instances in which a SELS severe weather watch issued during a flash flood watch event drew forecaster's attention away from the flooding threat. Anderson (Lubbock) suggested that SELS severe weather watches should explicitly reference existing flash flood watches.

Concern was raised about liability and credibility aspects of "missing" significant events. Belville noted that "mistakes" are not necessarily bad, provided we learn from them. "Negligence doesn't come because an event is missed; it comes from failing to learn from it".

Everyone knows drinking and driving don't mix. Neither do drinking and floods. All three together can be deadly. Sheridan noted alcohol was found in the blood of 8 of the 13 victims of the May 27, 1984 Tulsa flash flood.

Rogers (hydrologist/civil engineer - University of Houston) emphasized localized climatological applications to flooding. One approach involved studying radar and rainfall reports and flooding to evaluate the impact of changing land-use patterns. Rogers also noted the need for dam break studies in areas upstream from urban centers, and reservoir design/analysis studies. Rogers favored having NWS ask local

universities (especially those with civil engineering/hydrology departments) to get involved in demographic analyses of flood potential.

Steve Harned (MIC, WSO Houston) noted excellent cooperation between his WSO and users in developing their local flash flood plan. In particular, Harned noted community-based water management programs seem to be well-financed.

Berkowitz (meteorologist - NWSTC) discussed current and planned meteorologist training efforts. He emphasized the proposed meso-scale course, including its on-station pre-residence study approach, and follow-up on-station refresher training. NEXRAD and new-hires training was also mentioned.

Several attendees voiced strong support for on-station training efforts (both written/audiovisual and visits by training leaders). There was general feeling that field forecasters need to improve their analysis skills. NWSTC could benefit from more feedback on how its courses are satisfying needs and NWSTC could be more responsive in implementing changes.

Maddox (meteorologist - ERL) urged that we change the way we do business - decentralize (including appropriate NMC operations), decrease the chief/worker ratio, marry hydrologists and meteorologists, and elevate thinking to its proper place relative to observing. "The NWS needs to invest its diminished resources where opportunities to improve service are greatest", Maddox noted. He strongly encouraged universities to address "operationally-oriented" needs. Maddox also pointed out WSFO management holds the key to inspiring field "talent" to work on operational problems.

Another attendee questioned the disparate approaches in handling severe weather and flash flood watches. "If we have better resolution in forecasting severe weather, then why are severe weather watches issued with approximately 6 hours lead time, while flash flood watches have 12 - 24 hour lead times?"

Maddox also remarked our understanding of heavy precipitation events remains incomplete. Although we can recognize some large- and small-scale patterns, we too often find similar patterns yielding vastly different outcomes. Then, too, blind use of "pattern recognition" approaches can lead to high false alarms, an area in which little study has been

undertaken. Ken Howard (ERL) plans to conduct a validation study of his western U.S. synoptic climatology of heavy snow. He plans to evaluate 10 years of data to determine false alarm rate. "Improved understanding must precede improved forecast scores", according to Maddox.

Another approach involves use of "decision-trees". The concept was at the heart of the earlier Lubbock-based QPF program; it has since been expanded to dust-storms and heavy snow. Several offices now use various decision trees.

Jensen (meteorologist - Director, SRH) summarized many of the comments of previous panelists and emphasized a list of key words he had heard in the preceding discussions...REASONING, TRAINING, HYDROMETEOROLOGIST, TECHNOLOGY TRANSFER, LIABILITY, OVERCOMING DECLINING RESOURCES.

Jensen noted many forecasters use numerical and MOS guidance first, then try to adjust this to their meteorological feelings. Instead, Jensen suggested they need to get a handle on the weather situation and THEN look at guidance.

Training needs should be used to define training efforts and determine who should participate in the training (including management training and future planning) BEFORE training programs are set up! NWS needs to include outside contacts in solving our forecast problems. This means tapping universities, senior scientists within our agency and in sister agencies, and others.

Management holds the keys to successful operations. Some offices manage to inspire on-station studies; others don't. Some stations involve forecasters in decision-making, as well. The main objective, according to Jensen, is to "get the RIGHT product to the RIGHT user at the RIGHT time in the RIGHT form" (while making more efficient use of people and resources).

---

This summary was compiled by H. Michael Mogil, Southern Region SSD. Rapporteurs providing input were Steve Harned (WSO Houston), Chuck Kadin (NESDIS), Richard Hagan (WSO Brownsville), Lee Harrison (WSFO Little Rock), and Bob Stucky (RFC Slidell).

